Mechanisms of platelet inhibition by the selective serotonin reuptake inhibitor citalopram

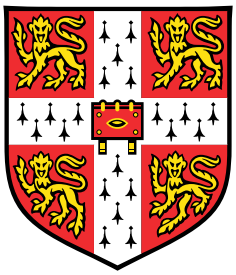

Harvey George Roweth

Supervisor: Dr Gavin E. Jarvis

Department of Physiology, Development and Neuroscience
University of Cambridge

This dissertation is submitted for the degree of
Doctor of Philosophy

Selwyn College November 2017

Declaration

This dissertation is the result of my own work and includes nothing which is the outcome of work done in collaboration except as declared in the Preface and specified in the text. It is not substantially the same as any that I have submitted, or, is being concurrently submitted for a degree or diploma or other qualification at the University of Cambridge or any other University or similar institution except as declared in the Preface and specified in the text. I further state that no substantial part of my dissertation has already been submitted, or, is being concurrently submitted for any such degree, diploma or other qualification at the University of Cambridge or any other University or similar institution except as declared in the Preface and specified in the text. This dissertation does not exceed 60,000 words, excluding bibliography, figures and appendices.

Harvey George Roweth
November 2017

Acknowledgements

First and foremost, I would like to thank my supervisor Dr Gavin Jarvis for giving me the opportunity to undergo this project. His support, guidance and patience were important if not essential to the completion of this thesis. I would also like to thank my co-supervisor, Dr Stewart Sage for his expertise and feedback, as well as the British Heart Foundation for their generous financial support over the last 3 years. Thanks also to Professor Richard Farndale, Professor Wolfgang Bergmeier, Dr Stephanie Jung, Dr Masaaki Moroi, Dr Matthew Harper, Dr Bonita Apta and Aaron Cook for their sharing of reagents or equipment, as well as their useful advice and feedback. Thank you mum and dad for always being a phone call away and for simply being there when needed. Importantly, I would like to thank Maddy for her patience, understanding and unwavering support. I promise to now start repaying the seemingly endless cups of coffee and cooked meals that have built up over the last few months.

Abstract

Background: Selective serotonin reuptake inhibitor (SSRI) antidepressants prevent serotonin (5-HT) uptake by the serotonin transporter (SERT). Since blood platelets express SERT, SSRIs may modify platelet function and the risk of cardiovascular disease. However, the beneficial or adverse effects of SSRIs on arterial thrombosis are poorly characterised and detailed *in vitro* experimental data is limited. The SSRI citalopram is a racemate, the (*S*)-isomer being the more potent SERT inhibitor. Although citalopram has been shown to inhibit platelets *in vitro*, it is unclear whether this is mediated via SERT blockade.

Aim: To determine if citalopram inhibits platelet function via SERT blockade, or through a novel mechanism of action.

Findings: 5-HT uptake into platelets was blocked by both citalopram isomers at concentrations that had no apparent effect on platelet function. Despite the (*S*)-citalopram isomer being the more potent SERT inhibitor, (*R*)-citalopram was equally potent at inhibiting other platelet functions. These findings strongly suggest that inhibition of platelet function by citalopram *in vitro* is not mediated by blocking SERT. Subsequent experiments identified two putative mechanisms for citalopram-mediated platelet inhibition: 1) citalopram did not inhibit calcium store release induced by the platelet agonist U46619, despite blocking subsequent Rap1 activation. A credible target for this inhibitory mechanism is the calcium and diacylglycerol guanine nucleotide exchange factor-1 (CalDAG-GEFI): 2) citalopram suppressed early protein phosphorylation within the GPVI pathway, resulting in the inhibition of subsequent platelet responses. Further experiments show that other commonly used antidepressants also inhibit platelets. As with citalopram, inhibition was only observed at concentrations above those required to block SERT, suggesting that alternative inhibitory mechanism(s) are responsible.

Conclusions: Data presented in this thesis support two novel putative mechanisms of citalopram-induced platelet inhibition. These findings demonstrate that citalopram and other antidepressants inhibit platelets independently of their ability to block SERT-dependent 5-HT transport. The identification of these mechanisms provides a pharmacological approach to develop novel antiplatelet agents based on current antidepressants.

Table of contents

List of figures

List of tables

Nomenclature

Abbreviations

4PL	Four-parameter logistic
5-HT	5-hydroxytryptamine, serotonin
5-HTP	5-hydroxy-L-tryptophan
A.U.	Arbitrary units
Abs	Absorbance
AC	Adenylate cyclase
ADAM10	A disintegrin and metalloproteinase domain-containing protein 10
ADP	Adenosine diphosphate
AM	Acetoxymethyl
ANOVA	Analysis of variance
APC	Allophycocyanin
ATP	Adenosine triphosphate
AUC	Area under the curve
BBB	Blood-brain barrier
BSA	Bovine serum albumin
Btk	Bruton's tyrosine kinase
$[Ca^{2+}]_{cyt}$	Cytosolic concentration of calcium
CalDAG-GEFI	Calcium and diacylglycerol guanine nucleotide exchange factor-1
cAMP	Cyclic adenosine monophosphate
CBD	Collagen-binding domain
CDC25	Cell division cycle 25
CD	Cluster of differentiation
CFT	Calcium-free Tyrode's
cGMP	Cyclic guanosine monophosphate
CLEC-2	C-type lectin-like receptor-2
CNS	Central nervous system
COX-1	Cyclooxygenase-1
CRACM1	Calcium-release activated calcium modulator-1
CRP	Collagen-related peptide
CRPXL	Cross-linked collagen-related peptide
Csk	C-terminal Src kinase
CVD	Cardiovascular disease

CYP	Cytochrome P
DAG	1,2-diacylglycerol
DAT	Dopamine transporter
DMSO	Dimethyl sulfoxide
DTS	Dense tubular system
ECL	Enhanced chemiluminescence
ECM	Extracellular matrix
EGTA	ethylene glycol-bis(β-aminoethyl)-N,N,N',N'-tetraacetic acid
ELISA	Enzyme-linked immunosorbent assay
ER	Endoplasmic reticulum
F.I.	Fluorescence intensity
FcγRIIA	Fc γ receptor IIA
Fc	Fragment crystallisable
FcRγ-chain	Fc receptor γ-chain
FDA	Food and Drug Administration
FITC	Fluorescein isothiocyanate
FSC	Forward scatter
GDP	Guanosine diphosphate
GDS	Guanine nucleotide dissociation stimulator
GFOGER	GPC-$[GPP]_5$-GFOGER-$[GPP]_5$-GPC
GI	Gastrointestinal
GPCR	G protein-coupled receptor
GPIb-IX-V	Glycoprotein Ib-IX-V
GPO	Gly-Pro-Hyp
GPP_{10}	GCP-$[GPP]_{10}$-GCPG
GPVI	Glycoprotein VI
GST	Glutathione S-transferase
GTP	Guanosine triphosphate
HPLC	High-pressure liquid chromatography
HRP	Horseradish peroxidase
ICAM	Intracellular adhesion molecule
Ig	Immunoglobulin
IFNγ	Interferon gamma
IL	Interleukin
IP_3	Inositol-1,4,5-trisphosphate

ITAM	Immunoreceptor tyrosine-based activation motif
ITC	Isothermal titration calorimetry
ITIM	Immunoreceptor tyrosine-based inhibition motif
ITSM	Immunoreceptor tyrosine-based switch motif
LAT	Linker of activated T cells
LBW	Lysis/binding/wash/buffer
LDH	Lactate dehydrogenase
LMWH	Low-molecular-weight heparin
LPS	Lipopolysaccharide
Mac-1	Macrophage-1 antigen
MAPK	Mitogen-activated protein kinase
MK	Megakaryocyte
MOPS	3-(N-morpholino)propanesulfonic acid
N/A	Not applicable
NAADP	Nicotinic acid adenine dinucleotide phosphate
NAD	Nicotinamide adenine dinucleotide
NCX3	Na^+/Ca^{2+} exchanger-3
NET	Norepinephrine transporter
nH	Hill coefficient
NO	Nitric oxide
NOS	Nitric oxide synthase
NP-40	Nonyl phenoxypolyethoxylethanol
OD	Optical density
PAF	Platelet-activating factor
PAGE	Polyacrylamide gel electrophoresis
PAO	Phenylarsine oxide
PAR	Protease-activated receptor
PBS	Phosphate-buffered saline
PDE3	Phosphodiesterase-3
PECAM-1	Platelet endothelial cell adhesion molecule-1
PE	Phycoerythrin
PerCP	Peridinin chlorophyll protein complex
PGE_1	Prostaglandin E_1
PGG_2	Prostaglandin G_2
PGH_2	Prostaglandin H_2

PGI_2	Prostaglandin I_2, prostacyclin
PH	Pleckstrin homology
PI3K	Phosphatidylinositol 3-kinase
PIP_2	Phosphatidylinositol-4,5-bisphosphate
PIP_3	Phosphatidylinositol-3,4,5-trisphosphate
PKA	Protein kinase A
PKB	Protein kinase B
PKC	Protein kinase C
PKG	Protein kinase G
PLCβ	Phospholipase Cβ
PLCγ2	Phospholipase Cγ2
PMA	Phorbol 12-myristate 13-acetate
PMCA	Plasma membrane calcium ATPase
pNPP	p-nitrophenyl phosphate
PPP	Platelet-poor plasma
PRP	Platelet-rich plasma
RBC	Red blood cell
PS	Phosphatidylserine
PVDF	Polyvinylidene fluoride
Rap1	Ras-related protein-1
RASA-3	Ras GTPase-activating protein-3
RBD	Rap-binding domain
REM	Ras exchange motif
RGD	Arg-Gly-Asp
RIAM	Rap1-GTP–interacting adaptor molecule
RT	Room temperature
SDS	Sodium dodecyl sulfate
SEM	Standard error of the mean
SERCA	Sarcoplasmic/endoplasmic reticulum calcium ATPase
SERT	Serotonin transporter
VMAT	Vesicular monoamine transporter
sGC	Soluble guanylyl cyclase
SFK	Src family kinase
SH2	Src homology-2
SH3	Src homology-3

SHIP	Phosphatidylinositol-3,4,5-trisphosphate 5-phosphatase
SHP	Src homology region 2 domain-containing phosphatase
SLP-76	SH2 domain-containing leukocyte phosphoprotein of 76 kDa
SNRI	Serotonin-norepinephrine reuptake inhibitor
SOCE	Store-operated calcium entry
SSC	Side scatter
SSRI	Selective serotonin reuptake inhibitor
STIM1	Stromal interaction molecule-1
Syk	Spleen tyrosine kinase
TBS-T	Tris-buffered saline with Tween
TCA	Tricyclic antidepressant
TG	Transglutaminase
TNFα	Tumour necrosis factor alpha
TPC	Two-pore channel
TPH	Tryptophan hydroxylase
TP	Thromboxane receptor
TxA_2	Thromboxane A_2
UFH	Unfractionated heparin
UTP	Uridine triphosphate
VASP	Vasodilator-stimulated phosphoprotein
vWF	von Willebrand factor
WB	Whole blood
WP	Washed platelet

Greek Symbols

α	alpha
β	beta
Δ	Delta
δ	delta
γ	gamma
ρ	rho
σ	sigma

Chapter 1
Introduction

1.1 An introduction to platelets

Blood platelets are small (approximately 1-3 μm) anucleate cells, derived from megakaryocytes primarily within the bone marrow. Platelets have long been known to play important roles in haemostasis and thrombosis, and have more recently been recognised to influence inflammation, wound repair, and cancer metastasis (Smyth et al., 2009, Gay and Felding-Habermann, 2011). Platelets predominantly regulate such processes through their activation, which is initiated by the binding of various ligands to surface receptors. Activated platelets undergo distinct morphological changes and adhere to either the lining of blood vessels or other cells within the blood. Platelets undergoing activation also release the contents of specialised granules, which stimulate adjacent platelets, other blood cells, and the endothelium.

1.1.1 The role of platelets in haemostasis and thrombosis

Impaired platelet activation or production is commonly associated with spontaneous and prolonged bleeding. This observation highlights the fundamental role of platelets to haemostasis, a physiological process that preserves vascular integrity and prevents blood loss upon blood vessel damage. Haemostasis is broadly separated into the early formation of a platelet plug, followed by thrombin-mediated fibrin formation, which leads to a stable clot. This section will first outline the steps required for platelet plug formation (Figure 1.1), before describing in more detail the roles of important ligands and receptors that govern platelet activation (Figure 1.2). Blood coagulation will be discussed briefly but is less relevant to the work of this thesis.

Upon vascular injury, extracellular matrix (ECM) proteins, including collagen, laminin, fibronectin, and von Willebrand factor (vWF), are exposed to flowing blood. In the arterial circulation, initial platelet interactions with the ECM are mediated by vWF, which binds both collagen and the platelet glycoprotein (GP)Ib-IX-V complex. vWF-GPIb-IX-V bonds do not support stable platelet adhesion and undergo rapid dissociation, resulting in platelet translocation or “rolling” over the exposed ECM (Fredrickson et al., 1998). Platelet activation through collagen binding to platelet glycoprotein VI (GPVI) then supports

firm adhesion to the ECM, through aiding the conversion of a second collagen receptor, integrin $\alpha_2\beta_1$, to a high-affinity state (Saelman et al., 1994, Gibbins, 2004). Activated platelets undertake a range of functional responses, mediated through secondary messengers, such as calcium (Ca^{2+}). Stimulated platelets undergo rapid rearrangements in their cytoskeleton, changing from quiescent disc-shaped cells to filopodia-protruding spheres, which then extend sheet-like lamellipodia (Deranleau et al., 1982, Aslan et al., 2012). These cytoskeletal changes mediate spreading over the damaged vasculature and increase contact points with the ECM and other platelets. Activated platelets also play an essential role in the initiation and propagation of blood coagulation by providing a phosphatidylserine-rich surface for the tenase and prothrombinase complexes to assemble, leading to thrombin generation and fibrin formation (Heemskerk et al., 2002). Activated platelets are able to cross-link through integrin $\alpha_{IIb}\beta_3$-fibrin(ogen)-$\alpha_{IIb}\beta_3$ interactions, forming a platelet aggregate, which, with fibrin, covers the site of vascular injury. Activated platelets release more than 300 proteins and small compounds into the blood (Coppinger et al., 2004). Many of these proteins derive from alpha granules, which store adhesive proteins, immune mediators, growth factors and proteins which integrate into the plasma membrane upon granule release (Berman et al., 1986, Harrison and Cramer, 1993). In contrast, platelet dense granules contain an important platelet agonist, adenosine diphosphate (ADP), as well as adenosine triphosphate (ATP), Ca^{2+}, magnesium (Mg^{2+}) and serotonin (5-HT). Overall, granule release potentiates platelet activation through the release of secondary agonists and increasing the surface expression of adhesion molecules.

Physiological platelet plug formation and the development of a blood clot (also referred to as a thrombus) are coordinated and regulated processes, isolated to a site of vascular injury. Uncontrolled and excessive platelet activation can produce thrombi that occlude blood vessels, referred to as thrombosis. Vessel occlusion by thrombosis is a key feature of atherosclerosis, a chronic inflammatory disease where fatty and fibrous lesions called atheromas develop within the tunica intima of arteries (Geng and Libby, 2002). These lesions are highly unstable and contain a collagen-rich fibrous cap. Atherogenesis narrows the vascular lumen, increasing shear rates and the possibility of plaque rupture. Upon plaque rupture, platelets adhere and aggregate to exposed collagen, further narrowing or occluding the vessel lumen. Impaired blood flow downstream of narrowed or occluded vessels causes tissue ischaemia and necrosis, which in the carotid or coronary arteries manifests as ischaemic stroke or myocardial infarction, respectively. Understanding

the mechanisms controlling platelet activation is therefore important for the continued development of drugs that effectively target atherothrombosis (Chapter 1.1.6).

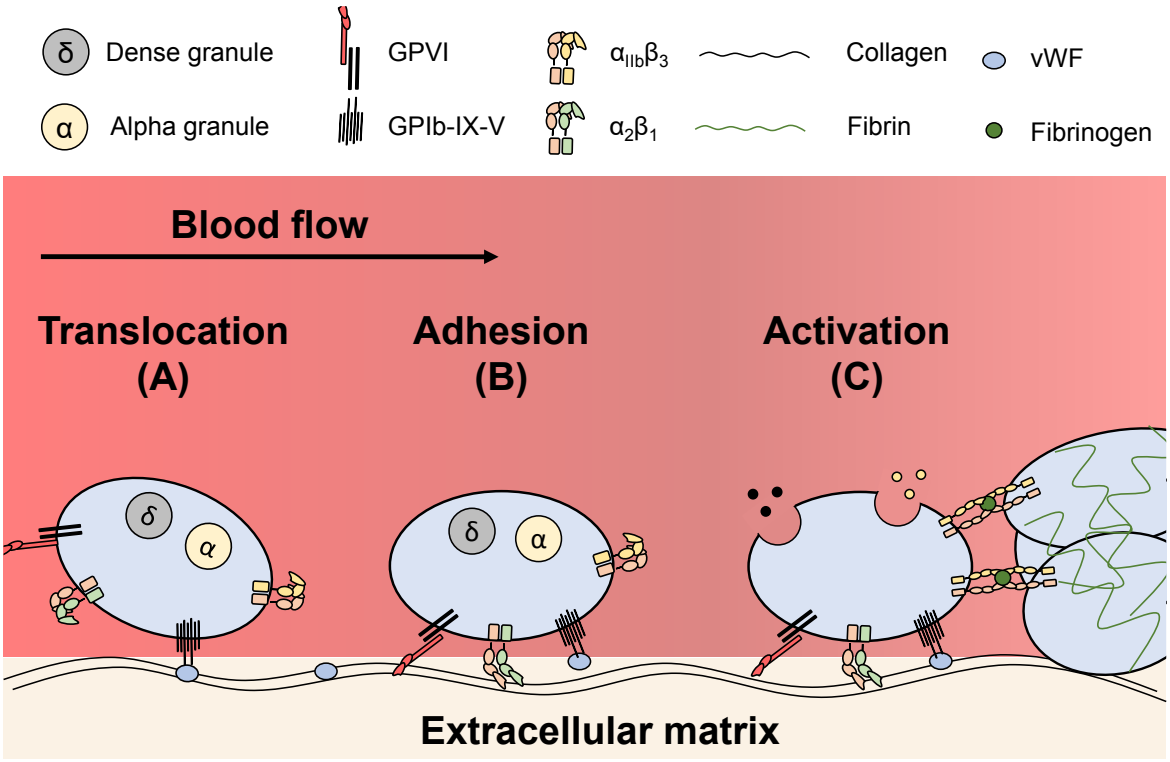

Figure. 1.1 Platelet plug formation is an early and important step of haemostasis. Platelets adhere to sub-endothelial extracellular matrix (ECM) proteins, exposed following endothelial breach or denudation. **(A)** Initial interactions are mediated through platelet glycoprotein (GP)Ib-IX-V and collagen-bound von Willebrand factor (vWF), exposed on the sub-endothelium. GPIb-IX-V-vWF interactions have a rapid on-off rate, allowing platelets to translocate over the ECM. **(B)** Integrin $\alpha_2\beta_1$ and GPVI bind collagen, providing stable adhesion to the vascular wall. **(C)** ECM-receptor interactions initiate intracellular signal transduction pathways that coordinate the release of alpha (α) and dense (δ) granules. Secondary platelet agonists from these granules recruit and potentiate the activation of adjacent platelets. Activated platelets also cross-link and aggregate via $\alpha_{\mathrm{IIb}}\beta_3$-fibrin(ogen)-$\alpha_{\mathrm{IIb}}\beta_3$ interactions. Platelet activation is essential to subsequent coagulation, where a clotting factor activation cascade results in thrombin generation, which mediates the conversion of fibrinogen to fibrin, stabilising the blood clot. This is an original image.

1.1.2 Platelet activation: ITAM-associated receptors

There are three glycoprotein receptors on human platelets that either contain or are non-covalently attached to immunoreceptor tyrosine-based activation motifs (ITAMs) (Boulaftali et al., 2014). These include GPVI, Fc γ receptor IIA (FcγRIIA), and the C-type lectin-like receptor-2 (CLEC-2). The ITAM is a highly-conserved cytoplasmic domain

(Tyrxx(Leu/Ile)x6-8Tyrxx(Leu/Ile), where x represents any amino acid) and plays an important role in receptor-mediated intracellular signal transduction (Underhill and Goodridge, 2007). Phosphorylation of tyrosine residues within the ITAM allow the binding of Src homology-2 (SH2)-containing tyrosine kinases, including spleen tyrosine kinase (Syk) and ZAP-70, resulting in the downstream activation of phospholipase Cγ2 (PLCγ2) (discussed further in Chapter 5).

GPVI

GPVI is associated with the ITAM-containing Fc receptor γ-chain (FcRγ-chain) homodimer and mediates platelet activation upon binding to collagen or laminin (Gibbins et al., 1997, Inoue et al., 2006). Collagen-binding induces receptor clustering and phosphorylation of the FcRγ-chain ITAM via the Src family kinases (SFKs) Fyn and Lyn (Poulter et al., 2017, Ezumi et al., 1998). The phosphorylated ITAM recruits and activates Syk, resulting in a downstream phosphorylation cascade which induces granule release and PLCγ2-mediated increases in cytosolic calcium concentration ($[Ca^{2+}]_{cyt}$) (Gibbins, 2004). Although less studied, GPVI binding to laminin initiates integrin $\alpha_6\beta_1$-dependent lamellipodia formation and platelet spreading (Inoue et al., 2006, Mangin et al., 2003). The structure, function, and signal transduction of GPVI are discussed further in Chapter 5.

FcγRIIA

Human platelets express FcγRIIA, a low-affinity receptor for the Fc region of immunoglobulin (Ig) immune complexes (Qiao et al., 2015). Like the FcRγ-chain, FcγRIIA mediates platelet activation through the binding of Syk to its phosphorylated ITAM (Yanaga et al., 1995). Binding of antibody Fc regions in immune complexes to FcγRIIA allow platelets to respond to infectious agents and mediate inflammatory processes. However, auto-antibody binding can also activate the FcγRIIA receptor and contribute to several immune-mediated thrombocytopenia and thrombosis syndromes, including heparin-induced thrombocytopenia and thrombosis (Davoren and Aster, 2006).

CLEC-2

CLEC-2 is a hemi-ITAM receptor, containing a single TyrxxLeu sequence (Suzuki-Inoue et al., 2006, Fuller et al., 2007). Its physiological ligand, podoplanin, mediates ITAM phosphorylation and downstream PLCγ2 activation (Suzuki-Inoue et al., 2006, 2007). Impaired CLEC-2 function inhibits platelet aggregation and causes defective ferric-chloride-induced thrombus formation (May et al., 2009, Haining et al., 2017). However, platelets

from transgenic mice where the CLEC-2 hemi-ITAM tyrosine residue has been substituted for alanine (p.(Tyr7Ala)) still aggregate and form occlusive thrombi in response to various platelet agonists or mechanical injury, respectively (Haining et al., 2017). Such findings suggest tyrosine phosphorylation of the CLEC-2 hemi-ITAM is not required for platelet activation, although alternative mechanisms have yet to be identified.

1.1.3 Platelet activation: integrins

Integrins are heterodimeric (α and β) transmembrane glycoproteins that connect the cytoskeleton to the ECM. Such connections are regulated through integrin transition from a low-affinity to a high-affinity state that permits ligand binding. Platelets express several integrins, including $\alpha_{\mathrm{IIb}}\beta_3$, $\alpha_{\mathrm{V}}\beta_3$, $\alpha_2\beta_1$, $\alpha_5\beta_1$ and $\alpha_6\beta_1$ (Hynes, 2002), of which $\alpha_{\mathrm{IIb}}\beta_3$ and $\alpha_2\beta_1$ play important roles in platelet aggregation and adhesion, respectively. In unstimulated platelets, integrins are maintained in a low-affinity state, with the N-terminal domain in a 'closed' confirmation. Platelet stimulation with various agonists initiates intracellular signal transduction, which converts the integrin to a high-affinity ligand-binding state. This process is often referred to as inside-out signalling (Nieswandt et al., 2009). Ligand-bound integrins also initiate 'outside-in' intracellular signal transduction, which drives the cytoskeletal rearrangements required for platelet spreading and subsequent blood clot stabilisation (Durrant et al., 2017). Integrins are therefore important bidirectional signalling receptors that play various important roles in platelet function.

$\underline{\alpha_{\mathrm{IIb}}\beta_3}$

Integrin $\alpha_{\mathrm{IIb}}\beta_3$ (also known as GPIIb-IIIa) is the most abundant platelet receptor ($\approx$ 80,000-120,000 per platelet) (Wagner et al., 1996). Patients with Glanzmann thrombasthenia lack functional $\alpha_{\mathrm{IIb}}\beta_3$ and often present with a severe bleeding phenotype, demonstrating a critical role for $\alpha_{\mathrm{IIb}}\beta_3$ in haemostasis (Phillips and Agin, 1977a). Upon platelet activation, $\alpha_{\mathrm{IIb}}\beta_3$ switches to a high-affinity state and binds fibrinogen, fibrin, vWF or fibronectin through their conserved Arg-Gly-Asp (RGD) motif (Pytela et al., 1986). Such interactions allow activated platelets to form $\alpha_{\mathrm{IIb}}\beta_3$-fibrin(ogen)-$\alpha_{\mathrm{IIb}}\beta_3$ cross-links, which are essential for platelet aggregation.

$\underline{\alpha_2\beta_1}$

Upon transition to a high-affinity state, integrin $\alpha_2\beta_1$ (also known as GPIa-IIa or VLA-2) demonstrates increased binding to collagen (I, II, III, IV & VI), establishing stable adhesive interactions with the ECM (Staatz et al., 1990, Saelman et al., 1994). Collagen-induced

outside-in signalling through $\alpha_2\beta_1$ is also thought to synergise platelet activation (Jarvis et al., 2002, 2012), and adhesion to the $\alpha_2\beta_1$-selective ligand GFOGER induces similar tyrosine phosphorylation patterns to GPVI agonists (Moroi et al., 1989, Inoue et al., 2003).

1.1.4 Platelet activation: G protein-coupled receptors

G protein-coupled receptors (GPCRs) are the largest family of protein receptors, consisting of an extracellular N-terminus, seven transmembrane domains, and an intracellular C-terminus (Rosenbaum et al., 2009). Ligand-binding initiates a conformational change in the GPCR intracellular domains, which are associated with heterotrimeric G$\alpha\beta\gamma$ proteins. Intracellular rearrangement of the GPCR mediates the exchange of guanosine diphosphate (GDP) for the 10-fold more abundant guanosine triphosphate (GTP) (Traut, 1994) on the G protein α subunit, which dissociates from the β and γ subunits. In platelets, activation of GPCRs initiates several intracellular signalling cascades through Gα and G$\beta\gamma$ isotypes, which play important roles in aggregation, adhesion, secretion, inside-out signalling, and shape change (Offermanns, 2006).

P2Y receptors

Purinoceptors (also known as purinergic receptors) are a large family of receptors that bind purine-based nucleosides and nucleotides (Abbracchio and Burnstock, 1994). P2Y purinoceptors are GPCRs that selectively bind ATP, ADP and uridine triphosphate (UTP) (von Kügelgen, 2006), with the platelet ADP receptors P2Y1 and P2Y12 coupled to either $G\alpha_q$ or $G\alpha_{12/13}$, and $G\alpha_i$, respectively (Hollopeter et al., 2001). P2Y1-mediated activation of $G\alpha_q$ increases $[Ca^{2+}]_{cyt}$ and protein kinase C (PKC) activity through activation of phospholipase Cβ (Léon et al., 1999) (discussed further in Chapter 4.1.1). $G\alpha_{12/13}$ induces the Rho-mediated cytoskeletal reorganisations required for platelet shape change (Klages et al., 1999). P2Y12-mediated activation of $G\alpha_i$ inhibits adenylate cyclase (AC), reducing production of the negative regulator, cyclic adenosine monophosphate (cAMP) (Hollopeter et al., 2001). Upon dissociation from $G\alpha_i$, the β and γ subunits activate phosphatidylinositol 3-kinase (PI3K), leading the downstream activation of PKC and protein kinase B (PKB) (Cantley, 2002). P2Y1 receptor activation causes rapid and transient platelet aggregation, whereas P2Y12 is required for a sustained response (Jarvis et al., 2000).

Thromboxane receptors

The thromboxane receptor (TP) is a $G\alpha_q/G\alpha_{12/13}$-coupled GPCR, which like P2Y1, mediates increases in $[Ca^{2+}]_{cyt}$, PKC activation, and platelet shape change (Shenker et al.,

1991, Offermanns et al., 1994). There are two TP splice variants, TPα and TPβ, although TPα is the predominant isoform expressed in platelets (Habib et al., 1999). TP ligands include several members of the prostanoid family of lipids, including thromboxane A_2 (TxA_2). Platelets synthesise TxA_2 through the conversion of arachidonic acid to PGH_2 to TxA_2 by cyclooxygenase-1 (COX-1) and TxA_2 synthase, respectively. Activated platelets upregulate TxA_2 synthesis, which plays an important role in potentiating platelet activation through TP receptors (FitzGerald, 1991). Due to its half-life of approximately 30 seconds (Hamberg et al., 1975), a stable analogue of TxA_2 (U46619) is commonly used to investigate TP signalling in platelets.

Protease-activated receptors

Protease-activated receptors (PARs) also couple to $G\alpha_q/G\alpha_{12/13}$ proteins, and mediate similar signalling events to P2Y1 and TP receptors (Coughlin, 2000). PARs 1 and 4 are expressed in human platelets (Kahn et al., 1998, 1999) and share a distinctive mechanism of thrombin-mediated activation, where partial N-terminal cleavage exposes a secondary N-terminal sequence that interacts with the second extracellular loop to stimulate intracellular GTP binding (Vu et al., 1991). PAR-specific agonists have demonstrated that PAR1 is the high-affinity thrombin receptor, whereas higher thrombin concentrations are required to activate PAR4 (Kahn et al., 1999).

Adrenergic receptors

The α_{2A} adrenergic receptor is expressed on platelets (Kobilka et al., 1987), yet little is known about its role or relevance in platelet function. The receptor putatively couples to $G\alpha_z$, a member of the $G\alpha_i$ family, which upon epinephrine binding inhibits cAMP production (Yang et al., 2000). Unlike ADP, TxA_2 or thrombin, platelet stimulation with epinephrine only induces platelet aggregation *in vitro* upon co-administration with additional platelet agonists, such as ADP (Thompson et al., 1986, Steen et al., 1993).

Serotonin receptors

Fourteen 5-HT receptor subtypes have been identified, including thirteen GPCRs and one ligand-gated ion channel (5-HT_3) (McCorvy and Roth, 2015). Platelets express 5-HT_{2A}, which is coupled to $G\alpha_q$ (de Clerck et al., 1984). Stimulation of platelets with 5-HT alone does not however induce platelet aggregation (Thompson et al., 1986, Lin et al., 2014). 5-HT_{2A} receptors act to augment platelet activation in response to sub-threshold concentrations of other platelet agonists, such as ADP (Thompson et al., 1986, Lin et al.,

2014, Adams et al., 2008). 5-HT_3 receptors have also been putatively identified in platelets (Stratz et al., 2008). However, the inability of SR 57227A (5-HT_3 agonist) to counteract the inhibitory effects of ondansetron (5-HT_3 competitive antagonist) on collagen-induced aggregation suggests the contribution of 5-HT_3 towards platelet activation is minimal (Liu et al., 2012). Indeed, the authors of this study attribute the antiplatelet effects of ondansetron to attenuated inositol-1,4,5-trisphosphate (IP_3) production and reduced mitogen-activated protein kinase (MAPK) phosphorylation, as opposed to inhibition of 5-HT_3. In addition to 5-HT receptors, platelets also store 5-HT within dense granules, which is released upon activation and provides the only substantial source of blood 5-HT for receptor stimulation (Hergovich et al., 2000, Maurer-Spurej et al., 2004).

1.1.5 Physiological platelet inhibition

Platelets become activated through numerous signalling pathways, often relying on positive feedback loops and secondary mediators to potentiate their activation. Platelets therefore also require stringent counterbalancing mechanisms to prevent spontaneous or excessive activation. Such safeguards localise the thrombus and prevent it spreading beyond the site of vascular injury.

The endothelium

Nitric oxide (NO) and prostacyclin (PGI_2) are important endothelium-derived regulators of platelet activation and thrombus formation. NO is synthesised from L-arginine by nitric oxide synthases (NOS) and released continuously by the endothelium, but due to its half-life of several milliseconds in the circulation (Liu et al., 1998), NO directly acts within a localised environment. Spatial NO signalling limits platelet adhesion and activation to sites of exposed ECM, where functional endothelial cells are lacking. NO diffuses across the platelet plasma membrane and binds soluble guanylyl cyclase (sGC), increasing levels of cyclic guanosine monophosphate (cGMP) (Katsuki et al., 1977). cGMP activates protein kinase G (PKG). PKG and PKA phosphorylate several proteins, including the IP_3 receptor (Teryshnikova et al., 1998) and the vasodilator-stimulated phosphoprotein (VASP) (Aszódi et al., 1999), preventing store-derived increases in $Ca^{2+}{}_{cyt}$ and cytoskeletal rearrangements, respectively. Platelets have also controversially been reported to express NOS isoforms and increase NO production upon activation, providing a putative mechanism of autoregulation (Freedman et al., 1997).

PGI_2 is another negative regulator of platelet activation, derived from endothelial arachidonic acid (Moncada et al., 1977). Like most prostanoids, PGI_2 has a short half-life

of several seconds, and when released has no prolonged circulatory effects, binding instead to $G\alpha_s$-coupled IP receptors on nearby platelets. Contrary to $G\alpha_i$, $G\alpha_s$ activates AC, increasing cAMP levels which in turn activate PKA (Nambal et al., 1994, Neves et al., 2002).

Ectonucleotidases

Extracellular ATP and ADP can bind and activate the P2X Ca^{2+} channel (discussed further in Chapter 4.1.1) and P2Y receptors respectively. Basal P2X and P2Y receptor stimulation is prevented through hydrolysis of ATP and ADP to AMP by leukocyte- or endothelial-derived ectonucleoside triphosphate diphosphohydrolase-1 and 5'-nucleotidase, retaining low ATP and ADP plasma concentrations in the absence of platelet dense granule release (Marcus et al., 1997, Kawashima et al., 2000).

ITIM-containing receptors

Unlike NO, PGI_2, and ectonucleotidases, immunoreceptor tyrosine-based inhibition motif (ITIM)-containing receptors selectively counteract the downstream effects of ITAM phosphorylation. As with the ITAM, the ITIM sequence (Ile/Val/LeuxTyrxxLeu/Val) undergoes tyrosine phosphorylation, providing a docking site for phosphatases that contain SH2 domains. Important ITIM-binding phosphatases include Src homology region 2 domain-containing phosphatase-1 (SHP-1), SHP-2, and phosphatidylinositol 3,4,5-trisphosphate 5-phosphatase-1 (SHIP-1) (Coxon et al., 2017). These phosphatases offset kinase-mediated signal transduction initiated by the stimulation of ITAM-associated receptors (Chapter 1.1.2).

Platelet endothelial cell adhesion molecule-1 (PECAM-1) is a cell surface glycoprotein, and the first identified ITIM-containing receptor on platelets (Newman et al., 1990, Ohto et al., 1985). PECAM-1 binds and signals through homophilic and heterophilic interactions with adjacent platelets and endothelial cells (Sun et al., 1996). Receptor clustering and platelet activation mediate phosphorylation of the PECAM-1 ITIM, leading to the recruitment of SHP-1 and SHP-2 (Hua et al., 1998). Platelets from PECAM-1-deficient mice display increased sensitivity to collagen stimulation and form larger thrombi *ex vivo* (Jones et al., 2001, Patil et al., 2001). Thrombosis models *in vivo* also suggest a physiological role for PECAM-1 in limiting thrombus size following vascular injury (Falati et al., 2006).

G6b is an ITIM-containing member of the Ig superfamily, whose expression is restricted to platelets and megakaryocytes (Senis et al., 2007, Coxon et al., 2017). The B isoform, (G6b-B) is a transmembrane receptor, containing both an ITIM and an Immunoreceptor tyrosine-based switch motif (ITSM, ThrxTyrxxVal/Ile), which mediates both

inhibitory and activatory responses (Mazharian et al., 2012). G6b-B ITIM phosphorylation recruits SHP-1 and SHP-2 and inhibits GPVI and CLEC-2 signalling through regulating ITAM-mediated signal transduction (Mori et al., 2008, Coxon et al., 2012b). Mice lacking G6b-B display macrothrombocytopenia, attributed to platelet pre-activation and clearance from the blood, in addition to reduced platelet production (Mazharian et al., 2012). Other ITIM-associated receptors identified in platelets include TREM-like transcript-1, paired immunoglobulin-like receptor-B, and leukocyte-associated immunoglobulin-like receptor-1 (Coxon et al., 2017).

1.1.6 Pharmacological platelet inhibition

Pathological platelet activation can result in thrombosis, which is central to arterial occlusion and the development of acute cardiovascular pathologies, particularly ischaemic stroke and myocardial infarction. Statistics published by the British Heart Foundation state that cardiovascular diseases (CVDs) in 2015 were responsible for more than a quarter of deaths in the U.K. (≈160,000), with more than 7 million people estimated to be living with CVD (British Heart Foundation, 2016). The annual healthcare cost of CVD in the U.K. is estimated at 9 billion pounds, with the total economic cost valued closer to 19 billion pounds (Wilkins et al., 2017). The discovery and development of drugs that reduce the risk of CVD are therefore important, and drugs which target thrombosis by suppressing platelet activation are routinely prescribed to high-risk patients (Antithrombotic Trialists Collaboration, 2002). However, by impairing platelet activation, drugs that reduce the risk of end stage thrombosis routinely disrupt physiological haemostasis, increasing the risk of prolonged and spontaneous haemorrhage. Such side effects often limit the dosage of antiplatelet medications and complicate surgical procedures (Harder et al., 2004). The development of novel agents that prevent pathological thrombosis while preserving physiological haemostasis is therefore the principal goal for future antiplatelet drug discovery.

Cyclooxygenase inhibitors

Although the antiplatelet effects of aspirin (also known as acetylsalicylic acid) were identified over 60 years ago (Craven, 1950, Miner and Hoffhines, 2007, Patrono and Rocca, 2009) it remains the most commonly prescribed antiplatelet medication in England, with over 26 million items dispensed in 2016 (National Statistics, 2017). Chronic oral administration of low-dose aspirin (50-100 mg day^{-1}) is associated with a reduced risk of thrombotic events (Patrono et al., 2005), but increases the risk of gastrointestinal (GI) bleeding (Sørensen et al., 2000). Aspirin blocks prostaglandin synthesis through the irreversible acetylation

of COX (Roth et al., 1975). In platelets, inhibition of COX-1 prevents the conversion of arachidonic acid to PGH_2, which impairs subsequent TxA_2 synthesis, blocking a major positive feedback loop for platelet activation (Hamberg et al., 1975). Due to the irreversible inhibition of COX-1, aspirin's antiplatelet effects persist throughout the platelet life span of approximately 8-9 days (Roth and Majerus, 1975, Leeksma and Cohen, 1956). In contrast, COX-1 inhibition by ibuprofen is reversible (Nishizawa and Wynalda, 1981, Parks et al., 1981) and has little antiplatelet effect (Gladding et al., 2008). Aspirin also inhibits endothelial COX-1, preventing the synthesis of inhibitory PGI_2 (Jaffe and Weksler, 1979). However, unlike anucleate platelets, protein turnover in endothelial cells restores prostaglandin synthesis as plasma concentrations of aspirin decrease (Jaffe and Weksler, 1979).

P2Y12 receptor antagonists

Clopidogrel and ticlopidine are thienopyridine prodrugs, which upon hepatic metabolism generate an active metabolite that irreversibly and covalently binds to P2Y12, blocking the ADP binding site (Puri et al., 1992, Savi et al., 2000). Like aspirin, clopidogrel and ticlopidine can be orally administered and are commonly prescribed alongside aspirin as a dual antiplatelet therapy (Mehta et al., 2001). However, the slow onset of clopidogrel and ticlopidine *in vivo* led to the development of prasugrel and ticagrelor. Prasugrel is another thienopyridine prodrug, with a higher metabolic conversion rate and more consistent metabolite levels than clopidogrel (Sugidachi et al., 2007). Ticagrelor is an orally administered non-competitive cyclopentyltrizolopyrimidine-type direct P2Y12 inhibitor, providing rapid and reversible platelet inhibition (Storey et al., 2007, van Giezen et al., 2009). The ATP analogue cangrelor is an intravenously administered P2Y12 inhibitor, whose short half-life of approximately 3.3 minutes leads to the restoration of platelet function 60-90 minutes after administration and has been approved for patients undergoing percutaneous coronary intervention (Ferreiro et al., 2009, Akers et al., 2010).

Protease-activated receptor antagonists

Vorapaxar is the first and only PAR inhibitor approved for clinical use. Vorapaxar is an orally administered, selective and potent PAR1 antagonist, used as an adjunctive antiplatelet therapy for the treatment of acute coronary syndromes (Chackalamannil et al., 2005, Tricoci et al., 2012). However, increased intracranial bleeding risks and severe bleeding side effects have been reported (Tricoci et al., 2012). Atopaxar is another PAR-1 antagonist, yet compared with vorapaxar has a slow onset of action, and short half-life (Leonardi et al., 2010). Peptides mimetics of PAR intracellular loops 1 and 3, called pepducins, suppress

G protein transduction and block PAR-mediated platelet activation (O'Callaghan et al., 2012). The PAR1 pepducin PZ-128 has rapid, reversible and specific effects and is currently under investigation as a novel antiplatelet agent (Gurbel et al., 2016). PAR-4 antagonists are also in development, including BMS-986141, which has entered a phase II clinical trial (Wong et al., 2017).

Integrin $\alpha_{IIb}\beta_3$ blockers

The monoclonal F(ab')$_2$ fragment abciximab can be administered for patients undergoing percutaneous coronary intervention and irreversibly binds $\alpha_{IIb}\beta_3$, directly impairing platelet aggregation (Coller et al., 1983). However, the major limitations of intravenous administration and bleeding side effects limit the use of abciximab as an antiplatelet medication (Gammie et al., 1998). Eptifibatide is a heptapeptide $\alpha_{IIb}\beta_3$ inhibitor that is orally-available, yet has a short half-life, low efficacy, and increases the risk of bleeding (Scarborough et al., 1999, Goa and Noble, 1999). As such, eptifibatide has not undergone further clinical investigation. The small molecule inhibitor, tirofiban is a clinically-approved and selective $\alpha_{IIb}\beta_3$ antagonist. However, a rapid off rate, short half-life, and increased risk of both bleeding and thrombocytopenia are current limitations associated with its clinical use (Barrett et al., 1994, Bougie et al., 2002).

Phosphodiesterase inhibitors

Compounds that block platelet PDEs increase levels of inhibitory cAMP and cGMP. Dipyridamole is a long-established antiplatelet medication, which inhibits PDE5 and PDE3, increases endothelial PGI_2 synthesis, and potentiates the effects of NO (Elkeles et al., 1968, Sakuma et al., 1990). Dipyridamole also inhibits platelet aggregation by blocking adenosine uptake into red blood cells (Gresele et al., 1986). However, dipyridamole shows low therapeutic efficacy as an antithrombotic agent (Gibbs and Lip, 1998). The quinolinone-derivative cilostazol specifically targets the PDE3 isoform and unlike many antiplatelet medications does not significantly prolong bleeding time, suggesting it may have minimal bleeding risk (Wilhite et al., 2003). However, clinical trials demonstrate minor antithrombotic effects of cilostazol treatment (Reilly and Mohler, 2001).

In summary, various antiplatelet drugs have been developed which reduce the risk of end stage pathological thrombosis. However, by suppressing platelet activation, all of the aforementioned compounds can inherently disrupt haemostasis, which often compromises vascular integrity.

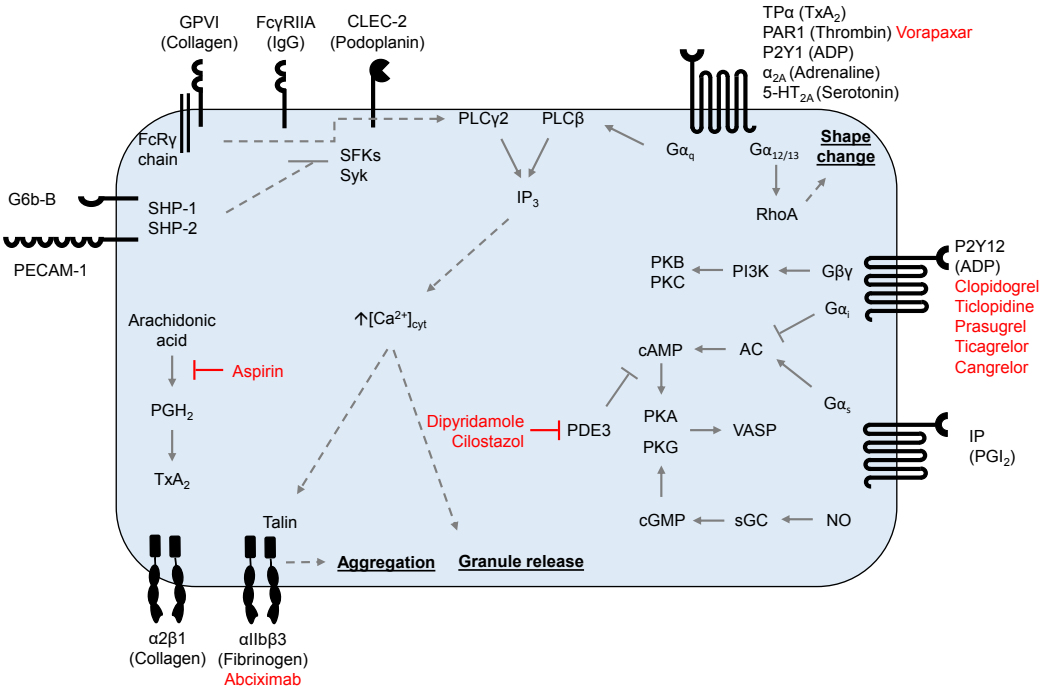

Figure. 1.2 Overview of platelet activation. Platelet activation is initiated by the binding of extracellular ligands to surface receptors. Glycoprotein VI (GPVI), Fc γ receptor IIA (FcγRIIA) and C-type lectin-like receptor 2 (CLEC-2) either contain or are associated with immunoreceptor tyrosine-based activation motifs (ITAMs), which mediate downstream activation of phospholipase C (PLC)γ2. In contrast, Gα_q-coupled receptors activate downstream PLCβ. Both PLC isoforms generate inositol-1,4,5-trisphosphate (IP_3), which binds the IP_3 receptor, causing increases in $[Ca^{2+}]_{cyt}$ through the release of intracellular Ca^{2+} stores. Ca^{2+} is an important secondary mediator for many platelet functional responses, including integrin $\alpha_{IIb}\beta_3$-mediated aggregation and granule release. G$\alpha_{12/13}$-coupled receptors activate RhoA, resulting in the cytoskeletal rearrangements required for platelet shape change. Gα_i-coupled receptors inhibit adenylate cyclase (AC), preventing the formation of regulatory cyclic adenosine monophosphate (cAMP), which is also inhibited by phosphodiesterase-3 (PDE3). G$\beta\gamma$ subunits activate phosphoinositide 3-kinase (PI3K), which phosphorylates positive regulators protein kinase B and (PKB) and protein kinase C (PKC). Activated platelets also synthesise the platelet agonist thromboxane A_2 (TxA_2) through the liberation of arachidonic acid. Physiological inhibitory signals counterbalance platelet activation and prevent spontaneous platelet stimulation. Immunoreceptor tyrosine-based inhibitory motif (ITIM)-containing receptors, including platelet endothelial cell adhesion molecule-1 (PECAM-1) and G6b-B, offset the stimulatory effects of ITAM-associated receptors. Gα_s-coupled prostanoid IP receptors activate AC, increasing cAMP levels. Nitric oxide (NO) activates soluble guanylyl cyclase (sGC), increasing inhibitory cyclic guanosine monophosphate levels. cAMP and cGMP activate negative platelet regulators protein kinase A (PKA) and protein kinase G (PKG), respectively. Receptor agonists are mentioned within brackets. Clinically-prescribed antiplatelet drugs are shown in red. Grey dashed lines indicate multiple intermediate steps. This is an original figure.

1.2 The role and regulation of peripheral serotonin

Previous research has characterised in detail how the stimulation or suppression of immunoglobin-type receptors (GPVI, CLEC-2), integrins ($\alpha_{IIb}\beta_3$) and GPCRs (P2Y1, P2Y12, TPα, PAR1, PAR4) modulate platelet activation and affect haemostasis. Such studies have led to the development of several antiplatelet drugs, which target and block the function of receptors that contribute towards pathological platelet activation. However, comparatively few studies have investigated the importance of peripheral 5-HT and 5-HT receptors in platelet functional responses. Indeed, the transport, storage and release of 5-HT from platelets is often overlooked with regards to platelet activation.

1.2.1 Serotonin

Serotonin (5-hydroxytryptamine, 5-HT) was first identified in the gastric mucosa of rabbits and therefore named enteramine (Ersparmer and Viallu, 1937). In 1948, Rapport and colleagues extracted a vasoconstrictive amine from bovine serum, which was thus named serotonin (Rapport et al., 1948a,b). Both compounds were subsequently identified as the same chemical structure, 5-hydroxytryptamine (5-HT) (Erspamer and Asero, 1952). 5-HT is synthesised from the essential amino acid L-tryptophan. The rate-limiting enzyme, tryptophan hydroxylase (TPH, EC 1.14.16.4), catalyses the hydroxylation of L-tryptophan to 5-hydroxy-L-tryptophan (5-HTP) in the presence of oxygen, iron (Fe^{2+}), and tetrahydrobiopterin. 5-HTP is then converted to 5-HT by 5-HT decarboxylase (also known as aromatic-L-amino acid decarboxylase, EC 4.1.1.28) (Bowsher and Henry, 1986). There are two TPH isoforms, TPH1 and TPH2. TPH1 mediates peripheral 5-HT synthesis and is predominantly expressed in the duodenum, pineal gland, thymus and spleen, whereas TPH2 is largely expressed in the mesencephalic tegmentum, striatum and hippocampus of the central nervous system (CNS) (Walther and Bader, 2003, Zhang et al., 2004, Sakowski et al., 2006).

The majority of mammalian 5-HT is synthesised, stored and released from enterochromaffin cells in the intestinal mucosa (Barter and Everson Pearse, 1955). These cells release 5-HT basally into the interstitial space of the lamina propria, where binding to 5-HT receptors on enteric neurons mediates several GI functions, including secretion, vasodilation, pain perception, nausea, and peristalsis (Gershon, 2004, Mawe and Hoffman, 2013). Following its secretion, 5-HT is either transported back into the gut epithelia and the enterochromaffin cells, or enters the circulation via the portal venous system, where it

is transported into platelets by the serotonin transporter (SERT) (Hergovich et al., 2000, Carneiro et al., 2008, Erspamer and Testini, 1959). Cytosolic 5-HT is carried across platelet dense granule membranes by a vesicular monoamine transporter (VMAT), driven by an ATPase-generated proton gradient (Fishkes and Rudnick, 1982). 5-HT is metabolised to 5-hydroxylindole acetic acid by monoamine oxidases (MAOs) A and B. Both MAO-A and MAO-B are expressed in neurons, whereas platelets only express the B isoform. 5-HT within circulation is passed through the liver via the portal vein, which upon metabolism is excreted within urine (Jonnakuty and Gragnoli, 2008).

Virtually all circulating 5-HT is stored within platelet dense granules, which act as a sink, maintaining plasma concentrations below 1 nM (Brenner et al., 2007). Upon activation and degranulation, platelets release 5-HT into the blood, where it binds platelet 5-HT_{2A} receptors and potentiates platelet activation (Thompson et al., 1986, Lin et al., 2014). Of note, haemostasis is impaired in TPH1-deficient mice, despite normal aggregation in response to collagen, U46619 (a TxA_2 analogue), or thrombin (Walther et al., 2003). 5-HT has also been shown to accelerate the conversion of fibrinogen to fibrin in whole blood (Milne and Cohn, 1957). These observations suggest that 5-HT is more likely to modulate haemostasis through mechanisms distinct from platelet aggregation, such as coagulation and vasoconstriction.

5-HT also modulates the activity of other cell types within the cardiovascular system. For example, 5-HT_1-like and 5-HT_2 receptor stimulation on smooth muscle cells induces vasoconstriction (Rapport et al., 1948a, Kaumann et al., 1993), whereas 5-HT_{1B} receptors on endothelial cells mediate the synthesis and release of the endothelium-derived relaxing factor, NO (Cocks and Angus, 1983, Elhusseiny and Hamel, 2001). Platelet-derived 5-HT binding to 5-HT_{2B} receptors on fibroblasts induces ECM synthesis, which can contribute to pathological tissue fibrosis (Dees et al., 2011). 5-HT also upregulates inflammation by stimulating neutrophils and lymphocytes (Mössner and Lesch, 1998, Duerschmied et al., 2013) (discussed further in Chapter 7). For the reasons described above, the sequestration and coordinated release of 5-HT by platelets is an important feature of cardiovascular physiology.

1.2.2 The serotonin transporter

The serotonin transporter (SERT, also known as 5-HTT) is a Na^+/Cl^--dependent monoamine transporter and the principal mediator of 5-HT uptake into cells (Blakely et al., 1991). SERT (*SLC6A4*) belongs to the neurotransmitter sodium symporter family, which includes the dopamine and norepinephrine transporters (DAT and NET, respectively) (Chen et al.,

2004). DAT can also transport 5-HT and may act as a compensation mechanism for dysfunctional SERT (Zhou et al., 2002). An 'alternating access model' for 5-HT uptake by SERT was first proposed in 1966 (Jardetzky, 1966). The model suggests that transmembrane ion gradients induce the alternate exposure of the 5-HT binding site to intra- and extracellular environments. Simultaneous binding of 5-HT, Na^+, and Cl^- on the extracellular side induces a conformational change in SERT, exposing the binding site to the cytoplasm. 5-HT, Na^+, and Cl^- then dissociate, allowing K^+ to bind SERT, initiating a second conformational change which exposes the binding site to the extracellular environment. K^+ subsequently dissociates, completing the cycle (Rudnick, 2006).

Until recently, the structure of SERT had largely been predicted through crystallographic experiments on the bacterial orthologue LeuT (Yamashita et al., 2005) and Drosophila DAT (Penmatsa et al., 2013, 2015). This was due to previously unsuccessful crystallography studies on human SERT as a result of protein instability following membrane extraction. However, Coleman et al. (2016) recently identified several mutations which increased thermal stability. Their crystallography data confirm that SERT is a 12-transmembrane domain transporter, with a large extracellular domain consisting of extracellular loop regions 2, 4, and 6, with intracellular loops 1, 5 and the C-terminal helix forming the majority of its cytoplasmic domain.

Neuronal SERT is predominantly expressed at pre-synaptic terminals within Raphe nuclei of the brainstem (Qian et al., 1995, Lanzenberger et al., 2012), where it mediates the reuptake of synaptic 5-HT, preventing continuous serotonergic signal transduction (Iversen, 2005). In contrast, peripheral SERT is highly expressed on enterochromaffin and epithelial cells of the gut (Wheatcroft et al., 2005, Gershon and Tack, 2007) and on platelets (Lesch et al., 1993, Qian et al., 1995, Brenner et al., 2007). SERT expression has also been suggested on lymphocytes (Faraj et al., 1994). However, its functional role and relevance are believed to be minimal (Beikmann et al., 2013).

The majority of functional SERT is located within the plasma membrane (Carneiro and Blakely, 2006), where is it thought to form homodimers and tetramers through sialylated N-glycans (Kilic and Rudnick, 2000). 5-HT binding to receptors mediates SERT redistribution to the plasma membrane, increasing 5-HT uptake (Carneiro and Blakely, 2006). 5-HT is believed to self-regulate its own uptake in a biphasic manner, where SERT surface expression initially increases with plasma 5-HT levels, but is then reduced at high 5-HT concentrations (Brenner et al., 2007, Mercado and Kilic, 2010). PKG signalling in SERT-transfected cell lines also increases SERT activity and trafficking to the plasma membrane (Zhu et al., 2004). In platelets, the C-terminal of SERT directly interacts with integrin $\alpha_{\mathrm{IIb}}\beta_3$

and SERT activity increases upon fibrinogen binding to $\alpha_{IIb}\beta_3$ (Carneiro et al., 2008). In contrast, platelet SERT activity is downregulated by stimulation with phorbol 12-myristate 13-acetate (PMA), which activates PKC and relocates SERT to the cytoskeleton (Carneiro and Blakely, 2006). Interactions with the adaptor protein Hic-5, are then thought to mediate internalisation of the transporter (Carneiro and Blakely, 2006). The non-receptor tyrosine kinase Src has also been shown to mediate SERT phosphorylation, the extent of which positively correlates with transporter activity (Zarpellon et al., 2008). Despite such findings, the detailed mechanisms underlying the expression, localisation and activity of SERT remain largely unknown.

1.2.3 Pharmacological inhibition of the serotonin transporter

Owing to its diverse expression throughout the body, drugs that block SERT-mediated 5-HT uptake influence serotonergic signalling within the CNS, the gut and the blood. There are three major clinically useful classes of SERT-inhibiting compound: tricyclic antidepressants (TCAs), serotonin-norepinephrine reuptake inhibitors (SNRIs) and selective serotonin reuptake inhibitors (SSRIs). Both TCAs and SNRIs will be discussed further in Chapter 6.

Selective serotonin reuptake inhibitors

SSRIs lodge within the 5-HT binding site on SERT, directly blocking 5-HT uptake (Coleman et al., 2016). Specifically, SSRIs bind SERT between transmembrane helices 1, 3, 6, 8, and 10, locking the transporter in an outward-open conformation (Coleman et al., 2016). SSRIs selectively bind SERT at nanomolar concentrations, whereas micromolar concentrations of SSRIs also bind DAT, NET, alpha-1 adrenergic receptors, muscarinic acetylcholine receptor M1 and the histamine H_1 receptor (Owens et al., 2001). The first clinically-approved SSRI was Zimelidine in 1982, but has since been withdrawn (Caillé et al., 1983). Over the following 35 years, seven SSRIs have been approved by the Food and Drug Administration (FDA), including fluoxetine (Prozac®), citalopram (Celexa®), escitalopram (Lexapro®), fluvoxamine (Luvox®), paroxetine (Paxil®), sertraline (Zoloft®), and vilazodone (Viibryd®).

Citalopram

In 2016, citalopram was the most commonly dispensed antidepressant and the 15th most widely dispensed medication in England (National Statistics, 2017). Although other SSRIs, including paroxetine, fluoxetine, and sertraline are more potent inhibitors of SERT, citalopram shows greater SERT selectivity over DAT and NET (Owens et al., 2001). Citalopram is

a 50:50 racemic (*RS*) combination of two enantiomeric isomers, (*R*)-citalopram and (*S*)-citalopram, the latter of which is approximately 30-fold more potent for blocking neuronal SERT (Owens et al., 2001). (*S*)-Citalopram is therefore predominantly responsible for the clinical effects of racemic (*RS*)-citalopram, leading to its isolation and commercialisation as escitalopram, a second-generation SSRI (Montgomery et al., 2001, Burke et al., 2002). Compared to other SSRIs, (*S*)-citalopram shows the highest selectivity for binding SERT, compared to DAT and NET (Owens et al., 2001).

Like all SSRIs, citalopram is orally administered and enters the portal circulation via the GI tract. Circulating citalopram has a plasma half-life of approximately 33 hours (Kragh-Sørensen et al., 1981), with around 50% bound to plasma proteins (Milne and Goa, 1991). Citalopram is also highly lipophilic (log $P = 3.6$), resulting in a bioavailability of approximately 80% (Madsen et al., 2003, Joffe et al., 1998). Both citalopram isomers are metabolised to demethylcitalopram by hepatic cytochrome P (CYP) 450 enzymes CYP2C19, CYP3A4 and CYP2D6 (Rochat et al., 1997, von Moltke et al., 1999), with an additional N-demethylation by CYP2D6 to didesmethylcitalopram (Olesen and Linnet, 1999). The contribution of demethylcitalopram and didesmethylcitalopram to the pharmacological effects of citalopram is negligible (Hyttel, 1977).

Blocking neuronal SERT with SSRIs

SSRIs are best known for their effects on serotonergic signalling within the CNS, and are typically prescribed as antidepressants. By blocking SERT on presynaptic neurons, SSRIs increase synaptic 5-HT concentrations, which augment and prolong serotonergic signal transduction. This mechanism has been putatively associated with reducing symptoms of depression and is commonly referred to as the monoamine hypothesis of depression (Owens, 2004). Despite the clear clinical benefits for depressed patients taking SSRIs, the monoamine hypothesis of depression does not explain how SSRIs can also be used as effective treatments for anxiety or obsessive-compulsive disorder (Rocca et al., 1997, Owens, 2004, Soomro et al., 2009). In addition, monoamine depletion through a tryptophan-free diet does not induce depression in healthy subjects (Benkelfat et al., 1994), nor does it worsen the symptoms of depressed patients (Delgado et al., 1994). Further studies are therefore required to understand the exact mechanism underling the clinical benefits of SSRIs, and to determine whether impaired serotonergic signalling is indeed the cause of clinical depression (Anderson, 1998, Geddes et al., 2006).

Blocking peripheral SERT with SSRIs

SSRIs prescribed as antidepressants to block neuronal SERT also inhibit peripheral SERT in both the gut and circulating blood cells. Blocking SERT on endothelial and enterochromaffin cells of the GI tract increases 5-HT binding to enteric neurons, which can propagate contractions associated with abdominal cramping and reduced peristaltic activity (Coates et al., 2006, Gershon and Tack, 2007). Within the blood, prolonged SSRI treatment blocks 5-HT uptake into platelets, gradually depleting dense granule stores (Hergovich et al., 2000, Maurer-Spurej et al., 2004, Bismuth-Evenzal et al., 2012). Both murine platelets deficient in SERT and the platelets from human patients chronically dosed with SSRIs demonstrate reduced aggregation responses to ADP, collagen or epinephrine, but not thrombin or arachidonic acid (Hergovich et al., 2000, Maurer-Spurej et al., 2004, Flöck et al., 2010, Carneiro et al., 2008, Bismuth-Evenzal et al., 2012). Sustained SSRI administration also reduces 5-HT_{2A} surface expression, preventing synergistic platelet activation by 5-HT and ADP (Oliver et al., 2016). These studies suggest the antiplatelet effects associated with chronic SSRI treatment are due to impaired platelet 5-HT_{2A} receptor signalling, following the release of dense granules devoid of 5-HT.

Blocking platelet SERT over two weeks with fluoxetine reduces plasma 5-HT concentrations from 4.5 ± 2.5 nM to 1.3 ± 0.4 nM (Alvarez et al., 1999). SSRIs which target SERT may consequently also modulate the function of vascular and immune cells that express 5-HT receptors, particularly those which respond to 5-HT released from activated platelets. The indirect effects of SSRIs on other such cell types is therefore an important consideration to pathologies beyond thrombosis and is discussed further in Chapter 7.

1.2.4 SSRIs and cardiovascular disease

Sustained SSRI treatment depletes dense granule 5-HT stores, and reduces agonist-induced platelet aggregation (Chapter 1.2.3). SSRIs prescribed as antidepressants may, therefore, modulate haemostasis and reduce the risk of thrombosis. Long-term SSRI treatment has been associated with a reduced risk of myocardial infarction (Sauer et al., 2001, Schlienger et al., 2004, Kimmel et al., 2011) and an increased risk of intracranial or GI haemorrhage (de Abajo et al., 1999, van Walraven et al., 2001, Dalton et al., 2003, Opatrny et al., 2008, Dall et al., 2009, Hackam and Mrkobrada, 2012). GI bleeding induced by SSRIs is thought to vary from 1/100 to 1/1,000 patients, with the highest risk in elderly patients (de Abajo et al., 2006). These reported effects on haemostasis and thrombosis have led some to suggest that SSRIs could be used to manage thrombotic disease (Galan et al., 2009, Pizzi et al., 2011), particularly in depressed patients, which often present with a pro-

thrombotic phenotype (Musselman et al., 2000, Serebruany et al., 2003). However, some studies have associated SSRI treatment with an unexplained increased risk of myocardial infarction (Tata et al., 2005, Blanchette et al., 2008), whilst others describe no association between SSRI treatment and cardiovascular outcomes (MacDonald et al., 1996, Cohen et al., 2000, Meier et al., 2001).

The conflicting findings described above suggest a more complicated association between SSRIs and CVD (de Abajo, 2011). For example, many of these studies do not acknowledge the role of depression as a risk factor for CVD (Hippisley-Cox et al., 1998, Musselman et al., 1998). Both morbidity and mortality in patients with depression and CVD are higher than in patients with CVD who are not depressed (Stewart et al., 2003). Depression and its severity are therefore an often-overlooked confounding factor. Several of these studies also fail to document patients undergoing conventional antiplatelet therapy with agents such as aspirin or clopidogrel, which are likely to mask or exaggerate the effects mediated by SSRIs. Various physiological mechanisms associating depression with CVD have been suggested, which include not only hyperactive platelets (Musselman et al., 2000, Serebruany et al., 2003), but also increased inflammation (Kop et al., 2002), oxidative stress (Yager et al., 2010) and hyperactivity of the hypothalamic-pituitary-adrenal axis (Jokinen and Nordström, 2009). Future studies investigating the effects of SSRI treatment on cardiovascular outcomes should take such mechanisms into consideration, and not merely focus on their putative antiplatelet effects.

1.2.5 The *in vitro* effects of SSRIs on platelets

Investigating the *in vitro* effects of SSRIs on platelets could provide mechanistic detail into their complicated association with haemostasis and CVD. However, despite the putative link between SSRIs, platelets and CVD, few studies show direct *in vitro* effects of SSRIs on platelet activation. Among those that do, reduced platelet aggregation to ADP or collagen was reported following pre-treatment with citalopram, fluoxetine or sertraline (Galan et al., 2009, Tseng et al., 2010, 2013, Carneiro et al., 2008). However, fluoxetine has also been shown to augment PAR-mediated platelet aggregation (Dilks and Flaumenhaft, 2008) and potentiate ADP-induced calcium signalling (Harper et al., 2009). Another study contradicts this, describing no effect of fluoxetine treatment on ADP-induced or PAR-mediated aggregation (Bampalis et al., 2010). Notably, SSRI pre-incubation times in these studies range from 2-10 minutes, suggesting effects may not be due to the gradual depletion of intra-platelet 5-HT stores, as observed following long-term SSRI administration (Hergovich et al., 2000, Maurer-Spurej et al., 2004, Oliver et al., 2016).

Another important consideration is that platelet inhibition in these *in vitro* studies was only observed at micromolar SSRI concentrations, despite citalopram (K_i = 9.6 ± 0.5 nM), fluoxetine (K_i = 5.7 ± 0.6 nM) and sertraline (K_i = 2.8 ± 0.8 nM) inhibiting SERT with nanomolar potencies (Owens et al., 2001). SSRIs may, therefore, affect platelet function through an alternative mechanism of action, which is independent of SERT-mediated 5-HT uptake. However, few studies have addressed the importance of functioning SERT during platelet activation (Carneiro et al., 2008), and none have explored the concept of SERT-independent platelet inhibition by SSRIs.

1.3 Aims, objectives and hypothesis

This thesis aims to identify the mechanisms responsible for *in vitro* platelet inhibition by the SSRI citalopram. This goal will be met through the following objectives:

1. Characterising the inhibitory effects of citalopram on platelets.
2. Determining whether citalopram inhibits platelets through blocking SERT.
3. Identifying the molecular mechanisms by which citalopram influences platelet activation.
4. Comparing the antiplatelet effects of citalopram to structurally distinct SERT-inhibiting compounds.

Experiments will follow the guidelines of pharmacological methodology, using a range of citalopram concentrations to determine its inhibitory potencies on various aspects of platelet function. My hypothesis is that citalopram will inhibit platelet function through a novel and unidentified mechanism of action that is distinct from its known effects on SERT-mediated 5-HT uptake.

Chapter 2
Materials and methods

Reagent	Source	Catalogue number	Diluent
(*R*)-citalopram oxalate	Insight Biotechnology	sc-219751	PBS
Citalopram hydrobromide	Cambridge Bioscience	C3477	PBS
Collagen III	Sigma	C4407	Acetic acid (10 mM)
CRP	RWF*	N/A	Acetic acid (10 mM)
CRPXL	RWF*	N/A	Acetic acid (10 mM)
Escitalopram oxalate	Cambridge Bioscience	E7209	PBS
Fibrinogen	Sigma	F4883	Saline
Fluoxetine hydrochloride	Cambridge Bioscience	F4780	DMSO
GFOGER	RWF*	N/A	Acetic acid (10 mM)
GR144053	Tocris	1263	PBS
Horm collagen®	Takeda	1130630	Acetic acid (10 mM)
Imipramine hydrochloride	Alfa Aesar	J63723	PBS
Ionomycin	Sigma	I0634	DMSO
Indomethacin	Sigma	I7378	DMSO
Milnacipran hydrochloride	Stratech Scientific	S3140	PBS
Platelet-activating factor	Cayman Chemical	60900	DMSO
Paroxetine hydrochloride	Sigma	P9623	DMSO
Prostaglandin E_1 (PGE_1)	Sigma	P-5515	Ethanol
Sertraline hydrochloride	Cambridge Bioscience	S1971	DMSO
Thrombin	Sigma	T4648	Saline
U46619	Sigma	D8174	DMSO

Table 2.1 Platelet agonists and antagonists used in this project. PGE_1, Prostaglandin E_1; PBS, phosphate-buffered saline; CRP, collagen-related peptide (GCO-$[GPO]_{10}$-GCOG, where O = hydroxyproline); CRPXL, cross-linked collagen-related peptide; GFOGER, GPC-$[GPP]_5$-GFOGER-$[GPP]_5$-GPC; DMSO, dimethyl sulfoxide; N/A, not applicable. Horm collagen® was dissolved in 10 mM acetic acid, containing 0.1% [w/v] fatty acid-free bovine serum albumin (Sigma, E8875). RWF* indicates reagents supplied by the laboratory of Professor Richard Farndale, University of Cambridge.

Analyte	Column temp (°C)	Flow rate (mL min^{-1})	A	B	Min	(A:B)
Serotonin (5-HT)	40	1	18.4 mM citric acid, 83.2 mM K_2HPO_4; pH 6.6	Acetonitrile	0.00	(94:6)
					6.00	(94:6)
Adenine nucleotides (ATP/ADP)	30	1.7	2.2 mM K_2HPO_4, 47.8 mM KH_2PO_4; pH 5.45	Acetonitrile	0.00	(100:0)
					1.50	(100:0)
					1.51	(98.5:1.5)
					2.70	(98.5:1.5)
					4.20	(91:9)
					5.70	(91:9)
					5.80	(25:75)
					6.80	(75:25)
					6.81	(100:0)

Table 2.2 High-pressure liquid chromatography methods for mobile phases. 5-HT, 5-hydroxytryptamine; ATP, adenosine triphosphate; ADP, adenosine diphosphate

Reagent	Source	Catalogue number	Working concentration	Application(s)
2-mercaptoethanol	British Drug Houses	441432A	5% [v/v]	Western blot; Rap1 pulldown
Acetylcholinesterase tracer	Cayman Chemical	10005064	1x	TxA_2 synthesis
Acetic acid	Sigma	33209	10 mM	Adhesion
Adenosine diphosphate	Sigma	A2383	Various	Nucleotide release
Adenosine triphosphate	Sigma	1930	Various	Nucleotide release
APC-annexin V	Thermofisher Scientific	BMS306APC	1:63	Flow cytometry
BODIPY-FL-GDP	Fisher Scientific	G22360	0.1 μM	Rap1 activity
Bovine serum albumin	GE Healthcare	K41-001	0.1-5.0% [w/v]	Adhesion; Western blot
Calcium chloride	Fisher Scientific	C/1280/53	10 mM	Monitoring calcium
Citric acid	Sigma	C0759	28.55 mM	Adhesion; 5-HT uptake
Dimethyl sulfoxide	Sigma	D5879	Various	Various
Dextran-500	Sigma	31392	1% [w/v]	Neutrophil preparation
EGTA	Calbiochem	324626	1 mM; 5 mM	Various
Ellman's reagent	Cayman Chemical	400050	1x	TxA_2 synthesis
ECL reagent	GE Healthcare	RPN2232	Various	Western blot
Fura-2-acetoxymethyl ester	TEFLabs	103	2.5 μM	Monitoring calcium
Glutathione agarose beads	Thermofisher Scientific	16120	50% [w/v]	Rap1 pulldown
Glycerol	Sigma	G9012	2% [v/v]; 5% [v/v]	Western blot; Rap1 pulldown
GPP_{10}	RWF*	N/A	10 μg mL^{-1}	Adhesion
GST-RalGDS-RBD	Thermofisher Scientific	16120	20 μg	Rap1 pulldown
NP-40	Thermofisher Scientific	N-6507	1% [v/v]	Rap1 pulldown
Paraformaldehyde	Alfa Aesar	J61899	2% [v/v]	Flow cytometry
Percoll®	Sigma	P1644	Various	Neutrophil preparation
Phosphate buffered saline	Oxoid	BR0014G	1x	Various
p-nitrophenyl phosphate	Sigma	P4744	3.53 mM	Adhesion
Potassium phosphate dibasic	Sigma	BCBP7848V	83.2 mM	5-HT uptake
Precision Plus Protein™ blue	Bio-Rad Laboratories	1610374	5 μL	Western blot
Precision Plus Protein™ dual colour	Bio-Rad Laboratories	1610373	5 μL	Western blot
Serotonin hydrochloride	Alfa Aesar	B21263	1 μM	5-HT uptake
Sodium azide	Sigma	71290	0.01% [w/v]	Western blot
Sodium dodecyl sulfate	Fisher Scientific	S/5200/53	Various	Western blot
Tris base	Sigma	T6066	Various	Various
Trisodium citrate	Sigma	C8532	11 mM; 71.4 mM	Phlebotomy; adhesion
Triton X-100	Sigma	T9284	0.1% [v/v]	Calcium; adhesion
Tween-20	Sigma	P9416	0.1% [v/v]	Western blot
TxB_2 monoclonal antibody	Cayman Chemical	10005065	1x	TxA_2 synthesis
TxB_2 standards	Cayman Chemical	10005066	Various	TxA_2 synthesis
Wright's stain, modified	Sigma	WS16	N/A	Neutrophil preparation

Table 2.3 Key reagents used in the project. TxA_2, Thromboxane A_2; APC, allophycocyanin; GDP, guanosine diphosphate; 5-HT, 5-hydroxytryptamine; EGTA, ethylene glycol-bis(β-aminoethyl)-N,N,N',N'-tetraacetic acid; ECL, Enhanced chemiluminescence; GPP_{10}, GCP-$[GPP]_{10}$-GCPG; GST-RalGDS-RBD, glutathione S-transferase-Ral guanine nucleotide dissociation stimulator-Rap-binding domain; NP-40, nonyl phenoxypolyethoxylethanol; PAF, platelet-activating factor. RWF* indicates reagents supplied by the laboratory of Professor Richard Farndale, University of Cambridge.

Buffer	Constituents	pH	Applications
Calcium-free Tyrode's	137 mM NaCl, 11.9 mM $NaHCO_3$, 0.4 mM NaH_2PO_4, 2.7 mM KCl, 1.1 mM $MgCl_2$, 5.6 mM glucose	7.40	Platelet preparation; neutrophil preparation
ELISA buffer	100 mM phosphate, 0.1% [w/v] BSA, 400 mM NaCl,1 mM EDTA, 0.01% [w/v] sodium azide	N/A	Thromboxane A_2 synthesis
Citrate lysis buffer	3.53 mM p-nitrophenyl phosphate, 71.4 mM trisodium citrate, 28.55 mM citric acid, 0.1% [v/v] Triton X-100	5.40	Static adhesion
Phosphate buffer	2.2 mM K_2HPO_4, 47.8 mM KH_2PO_4	5.45	Dense granule release (HPLC)
Lysis/binding/ wash buffer	25 mM Tris HCl, 150 mM NaCl, 5 mM $MgCl_2$, 1% [v/v] NP-40, 5% [v/v] glycerol	7.20	Rap1-GTP pulldown
Reaction buffer	20 mM Tris base, 150 mM NaCl, 5 mM $MgCl_2$, 2 mM dithiothreitol, 10% [v/v] glycerol, 0.08% [v/v] NP-40, 1 μM Rap1B, 0.1 μM BODIPY-FL-GDP	7.50	Rap1B nucleotide exchange
MOPS SDS running buffer	50 mM MOPS, 50 mM Tris base, 0.1% [w/v] SDS, 1 mM EDTA, 0.25% [v/v] NuPAGE® antioxidant	7.70	Western blot
Tris-buffered saline with tween	20 mM Tris base, 137 mM NaCl, 0.1% [v/v] Tween-20	7.60	Western blot

Table 2.4 Buffers used in the project. ELISA, enzyme-linked immunosorbent assay; Rap1, Ras-related protein-1; EDTA, Ethylenediaminetetraacetic acid; HPLC, high-pressure liquid chromatography; MOPS, 3-(N-morpholino)propanesulfonic acid; SDS, sodium dodecyl sulfate; N/A, not applicable

Antibody	Manufacturer	Catalogue number	Working concentration	Application
Src	Cell Signalling Technology	2108S	1:1000	Western blot
SFKs (Tyr-416)	Cell Signalling Technology	2101S	1:1000	Western blot
LAT	Millipore	06-807	1:1000	Western blot
LAT (Tyr-200)	Abcam	Ab68139	1:1000	Western blot
PLCγ2	Santa Cruz	sc-407	1:1000	Western blot
PLCγ2 (Tyr-1217)	Cell Signalling Technology	3871P	1:1000	Western blot
Rap1	Thermo Scientific	16120	1:1000	Western blot
Phosphotyrosine (4G10)	Millipore	05-321	1:1000	Western blot
Goat anti-mouse (HRP-conjugated)	Dako	P0447	1:5000	Western blot
Goat anti-rabbit (HRP-conjugated)	Dako	P0048	1:5000	Western blot
CD15 (FITC-conjugated)	eBioscience	11-0159-42	1:50	Flow cytometry
CD41a (PE-conjugated)	eBioscience	12-0419-42	1:100	Flow cytometry
CD45 (PerCP-conjugated)	eBioscience	45-0459-42	1:100	Flow cytometry
CD11b (APC-conjugated)	eBioscience	17-0113-42	1:100	Flow cytometry
$IgG_{2a}\kappa$ (isotype control)	Biolegend	400202	5 μg mL^{-1}	Flow cytometry
Fab	SMJ*	SMJ*	10 μg mL^{-1}	Flow cytometry
HY-101	SMJ*	SMJ*	5 μg mL^{-1}	Flow cytometry
204-11 Fab	SMJ*	SMJ*	10 μg mL^{-1}	Flow cytometry
$F(ab)_2$ (Alexa-488–conjugated)	Jackson ImmunoResearch	115-546-072	50 μg mL^{-1}	Flow cytometry

Table 2.5 Antibodies used in the project. SFKs, Src family kinases; LAT, linker of activated T cells; PLCγ2, phospholipase Cγ2; Rap1, Ras-related protein-1; Tyr, tyrosine residue; HRP, horseradish peroxidase; CD, cluster of differentiation; FITC, fluorescein isothiocyanate; PE, phycoerythrin; PerCP, peridinin chlorophyll protein complex; APC, Allophycocyanin. SMJ* indicates antibodies supplied by the laboratory of Dr Stephanie Jung, University of Cambridge.

2.1 Blood cell preparation

2.1.1 Phlebotomy

Fresh blood was obtained by venepuncture from healthy, drug-free, consenting human donors. Blood donation was approved by the University of Cambridge Human Biology Research Ethics Committee (Ref: HBREC.2015.18). Blood was drawn using a 21-gauge blood collection set (Greiner Bio-One, Stonehouse, U.K.) into 60 mL syringes containing the anticoagulant trisodium citrate (110 mM) in a 9:1 volume ratio (final citrate concentration = 11 mM).

2.1.2 Preparation of washed platelets

Citrated whole blood (WB) was centrifuged (520 x g, 5 minutes), using a Mistral 3000 centrifuge (MSE, London, UK) to obtain platelet-rich plasma (PRP). PRP was centrifuged further (150 x g, 5 minutes) to isolate and remove any residual red blood cells (RBCs). PRP was treated with prostaglandin E_1 (PGE_1, final concentration = 1 μM), to prevent subsequent platelet activation. Centrifugation (930 x g, 15 minutes) produced a platelet pellet and plasma was discarded. The pellet was resuspended in a modified calcium-free Tyrode's buffer (CFT: 137 mM NaCl, 11.9 mM $NaHCO_3$, 0.4 mM NaH_2PO_4, 2.7 mM KCl, 1.1 mM $MgCl_2$, 5.6 mM glucose; pH 7.4) (Figure 2.1). Experiments were performed 1 hour after platelet resuspension, allowing the restoration of basal intracellular signalling following PGE_1 addition. Platelet counts were adjusted using a Z2 Coulter particle counter (Beckman Coulter, High Wycombe, U.K.) with a 50 μm aperture, which recorded particles with a diameter between 1.79-3.86 μm.

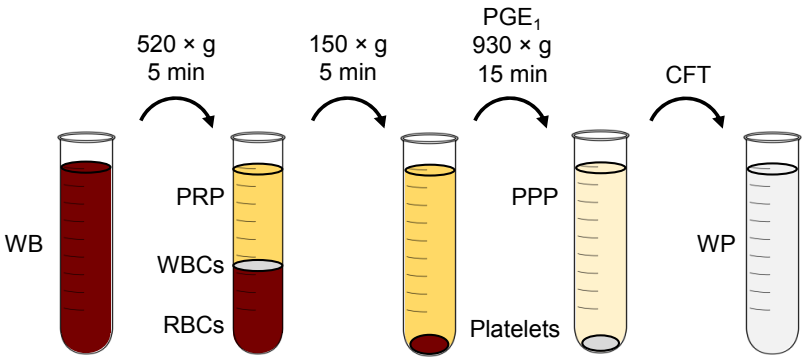

Figure. 2.1 Preparation of washed platelets. Whole blood (WB) containing trisodium citrate (final concentration 11 mM) was centrifuged (520 x g, 5 minutes) to obtain platelet-rich plasma (PRP). PRP was centrifuged further (150 x g, 5 minutes) to isolate and remove residual red blood cells (RBCs). Isolated PRP was treated with Prostaglandin E_1 (PGE_1), before further centrifugation (930 x g, 15 minutes) to attain a platelet pellet. Platelet-poor plasma (PPP) was discarded and the platelet pellet resuspended in a modified calcium-free Tyrode's buffer (CFT).

2.1.3 Preparation of neutrophils

Per 15 mL tube, 10 mL of citrated WB was added to 5 mL of saline, containing dextran-500 (final concentration 1% [w/v]). Tubes were mixed and left for 30 minutes to allow dextran-accelerated RBC sedimentation, whilst retaining white blood cells within the PRP. Pooled PRP samples (typically 12 mL) were aspirated with a pastette and layered over a discontinuous density gradient of Percoll® (1.5 mL of 1.110 g mL^{-1}, 1.5 mL of 1.088 g mL^{-1}). Percoll® densities were prepared by mixing Percoll® (1.130 g mL^{-1}) with 1.5 M NaCl (1.058 g mL^{-1}), each made up to 3 mL with distilled water (Table 2.6). The following equation was used to calculate the required volumes of Percoll®, NaCl and water:

$$V_0 = V\frac{\rho - 0.1_{\rho 10} - 0.9}{\rho_0 - 1}$$

Where: V_0 = volume of undiluted Percoll® required (mL); V = desired volume of final working solution (mL); ρ = desired density of final working solution (g mL^{-1}); ρ_0 = density of undiluted Percoll® (1.130 g mL^{-1}); ρ_{10} = density of 1.5 M NaCl (1.058 g mL^{-1}).

Desired density (g mL^{-1})	Percoll® (mL)	1.5 M NaCl (mL)	Water (mL)
1.110	2.405	0.300	0.295
1.088	1.897	0.300	0.803

Table 2.6 Volumes of undiluted Percoll®, NaCl and water required to make desired densities.

Samples were centrifuged (600 x g, 20 minutes) to separate granulocytes from the comparatively low density platelets, lymphocytes and monocytes. The isolated granulocyte band was aspirated, washed with phosphate-buffered saline (PBS), centrifuged (300 x g, 5 minutes) and resuspended in CFT (Figure 2.2A). To confirm the composition of the granulocyte-rich isolate, aliquots were fixed and stained with a modified Wright's stain and examined using light microscopy (Figure 2.2B). The cell concentration was adjusted accordingly using a Z2 Coulter particle counter, with an aperture diameter of 50 μm. Events were recorded with a diameter between 8.00-16.00 μm.

Neutrophil preparations used to measure integrin $\alpha_M\beta_2$ activation (Chapter 2.2.9) were further assessed for platelet and non-neutrophil leucocyte contamination, and cell viability as follows. Neutrophils (100 μL, 1.00 x 10^6 mL^{-1}) were incubated in the dark (5 minutes, 4°C) with fluorophore-conjugated antibodies for the active epitope of integrin α_M (CD11b) (Chapter 2.2.9), 3-fucosyl-N-acetyllactosamine (CD15) and either integrin α_{IIb} (CD41a), or leukocyte common antigen (CD45) (Table 2.5). CD41a and CD15 are exclusively expressed on the surface of platelets/megakaryocytes and neutrophils, respectively, whereas CD45 is expressed on all leucocytes. For each blood donor, a neutrophil sample was diluted 1:10 in CFT containing 2 mM $CaCl_2$ and 1:40 recombinant allophycocyanin (APC)-conjugated annexin V, which binds the apoptotic surface marker, phosphatidylserine. Samples were fixed with 2% [v/v] paraformaldehyde and the fluorescence intensity (F.I.), forward scatter (FSC), and side scatter (SSC) quantified using an Accuri^{TM} C6 flow cytometer (BD Bioscience, Oxford, U.K.). 30,000 events were recorded per sample and gated for neutrophils ($CD15^+/CD41a^-$ or $CD15^+/CD45^+$), platelets ($CD15^-/CD41a^+$), and non-neutrophil leukocytes ($CD15^-/CD45^+$) (Figure 2.2C-D). The percentage of annexin V^+ events within the neutrophil population was also quantified to assess cell viability (Figure 2.2E) (Hodge et al., 1999).

In summary, $CD15^+/CD45^+$ or $CD15^+/CD41a^-$ events (neutrophils) were 68.81 ± 2.08%, (N = 79 test samples, 6 blood donors, mean ± SEM), $CD15^-/CD41a^+$ events were 4.45 ± 0.48%, (N = 73 test samples, 6 blood donors, mean ± SEM) and $CD15^-/CD45^+$ events were 1.17 ± 0.31% (N = 6 test samples from separate blood donors, mean ± SEM) (Figure 2.2F). The remainder of the sampled population (≈25%) includes events with low F.I., FSC and SSC, which were considered acellular debris. Annexin V^+ events within the neutrophil population were (10.00 ± 1.32%, N = 6 blood donors) (Figure 2.2F).

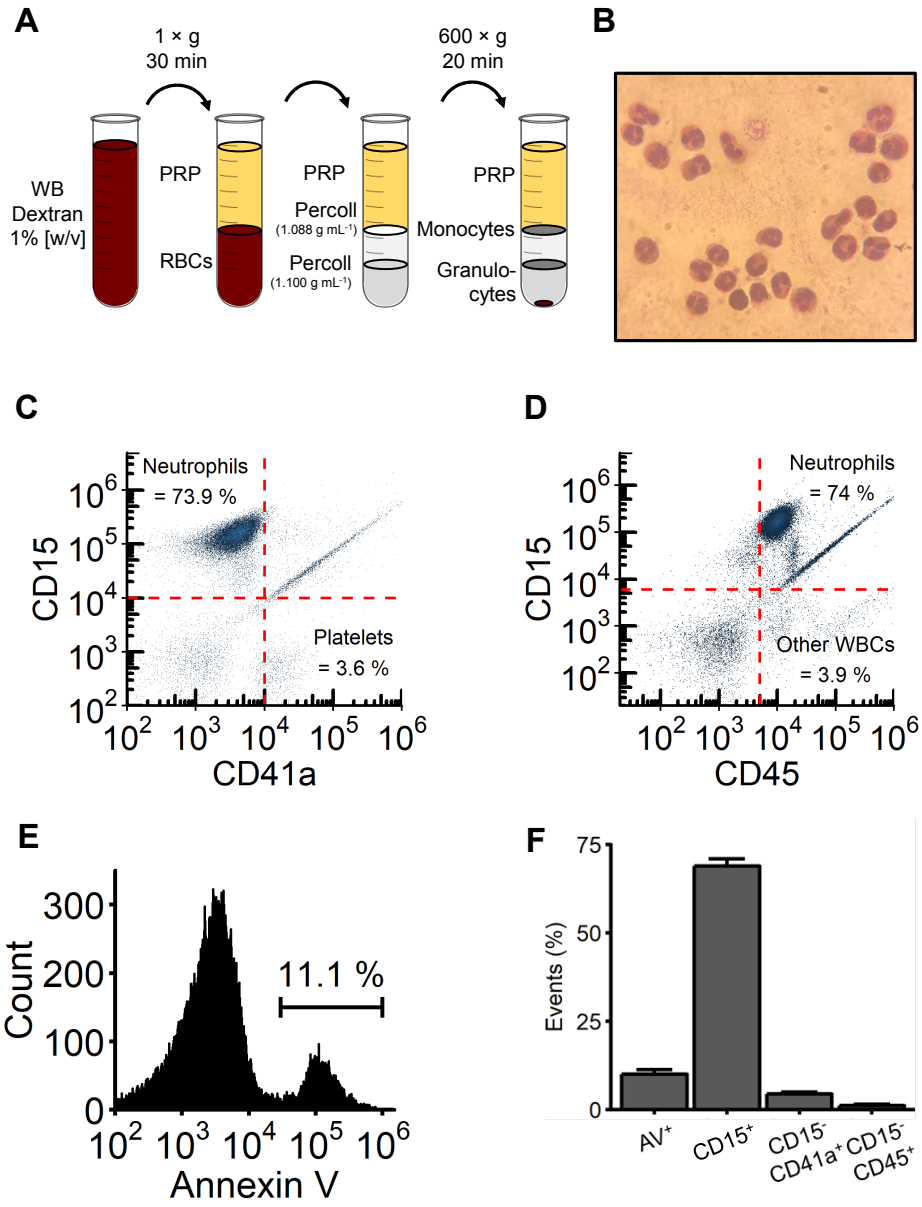

Figure. 2.2 Preparation of neutrophils. **(A)** Schematic representation of the process of neutrophil isolation. Whole blood (WB) was mixed with saline containing dextran-500 (final concentration 1% [w/v]). Tubes were left for 30 minutes to allow red blood cell (RBC) sedimentation, while retaining white blood cells within Platelet-rich plasma (PRP). Pooled PRP samples (typically 12 mL) were aspirated and layered over a discontinuous density gradient of Percoll® (1.5 mL of 1.100 g mL^{-1}, 1.5 mL of 1.088 g mL^{-1}). Samples were centrifuged (600 x g, 20 minutes) to separate granulocytes based on their density. Granulocytes were aspirated, washed with PBS, centrifuged (300 x g, 5 minutes) and resuspended in CFT. **(B)** Aliquots from the granulocyte-rich band were fixed and stained with a modified Wright's Stain and examined using light microscopy (optical lens 10x, objective lens 100x). **(C-F)** Flow cytometry was used to assess the purity and viability of samples used for integrin $\alpha_M\beta_2$ experiments. Fluorescence-based gates (red lines) determined the proportion of **(C)** platelets ($CD15^-/CD41a^+$), and **(D)** non-neutrophil leukocytes ($CD15^-/CD45^+$) and **(C-D)** neutrophils ($CD15^+/CD41a^-$ or $CD15^+/CD45^+$, respectively). **(E)** Annexin V^+ events within neutrophil populations were also quantified to determine cell viability. In **(F)**, neutrophil populations are collectively referred to as $CD15^+$.

2.2 Experiments

2.2.1 Serotonin uptake

Platelet serotonin transporter (SERT) activity was quantified by monitoring the reduction in extracellular serotonin (5-HT) concentration. Following 5-HT addition to WP (2.00 x 10^8 mL^{-1}), aliquots of WP were removed at various intervals (typically 5 minutes), and subsequent 5-HT uptake minimised by adding 5 mM ethylene glycol-bis(β-aminoethyl)-N,N,N',N'-tetraacetic acid (EGTA) and 16.6 μM indomethacin (final concentrations). Samples were then immediately centrifuged (8,000 x g, 1 minute) using a Micro Centaur (MSE, London, UK), and the supernatants frozen (-20°C).

Supernatant 5-HT concentrations were quantified using high-pressure liquid chromatography (HPLC). A Waters 2795 separations module (Waters, Hertfordshire, U.K.) fitted with a reversed phase C18 column (Kinetex®: 250 x 4.6 mm, 5 μm beads, 100 Å pore size) (Product code 00G-4601-E0, Phenomenex, Cheshire, U.K.) was used to separate the 5-HT using an isocratic method (mobile phase: 94% [v/v] phosphate buffer (18.4 mM citric acid, 83.2 mM K_2HPO_4; pH 6.6) and 6% [v/v] acetonitrile; column temperature = 40°C; flow rate = 1 mL min^{-1} (Table 2.2). A Waters 2487 Dual λ Absorbance Detector set to 276 nm was used to detect 5-HT, which appeared as a peak with a retention time of 4.2 minutes, (Figure 2.3A). Chromatograms were analysed using N2000 Chromatography Data System (Tianjin University, China). The area under the curve (AUC) of 5-HT standards dissolved in CFT were measured on each experimental day to determine supernatant concentrations of 5-HT (Figure 2.3B).

The 5-HT concentration decreases following its addition to WP (Figure 2.3C) and follows a first order pattern (Figure 2.3D). The natural log of 5-HT concentrations (μM) were fitted over time (minutes) using the LINEST function in Microsoft Excel, with the sum of squared residuals minimised using least squares to estimate a single rate constant for uptake (k_u) (Figure 2.3D). Rate constants were derived using the following equation:

$$C_t = C_0 e^{-k_u t}$$

Where: C_t = [5-HT] (μM) at time t (min); t = time from addition of 5-HT (min); C_0 = [5-HT] (μM) when t = 0; k_u = rate constant for 5-HT uptake (min^{-1}). Rate constants represent the probability of 5-HT uptake per unit time and therefore directly measure levels of active SERT.

During method development, the rate and extent of supernatant 5-HT decline were recorded with several 5-HT concentrations (0.5, 1 & 2 μM) (Figure 2.3D).Complete uptake of 0.5 & 1 μM 5-HT was achieved over 1 hour. Experiments in the results (Chapter 3.3.1) were therefore performed using 1 μM 5-HT.

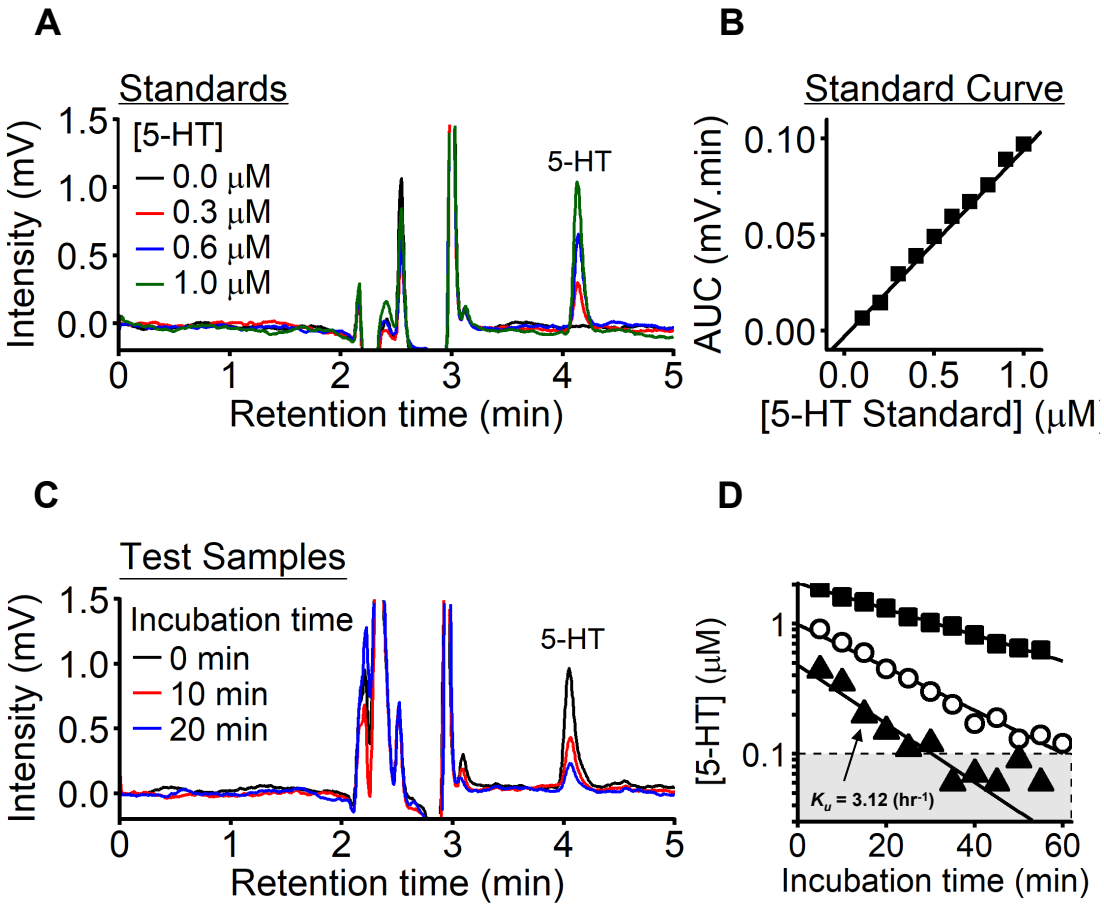

Figure. 2.3 Monitoring serotonin uptake into platelets. **(A)** Example high-pressure liquid chromatography (HPLC) chromatograms from serotonin (5-HT) standards. 5-HT (0, 0.3, 0.6 & 1 μM) was added to calcium-free Tyrode's (CFT) and the area under the curve (AUC) quantified for the peak at retention time 4.2 minutes. Deviations in voltage intensity between 2 and 3 minutes were undefined but did not affect 5-HT quantification. **(B)** Standard curves were created, using the AUC from chromatograms of 5-HT standards. **(C)** Example chromatogram traces, demonstrating the time-dependent reduction in platelet supernatant concentrations of 1 μM 5-HT following its exogenous addition to washed platelet (WP) samples. **(D)** Decreases in exogenous supernatant 5-HT (0.5, 1 & 2 μM) demonstrate the uptake of 5-HT into platelets over 60 minutes. An example rate constant (k_u) for 5-HT uptake is shown and represents the level of SERT activity following the addition of 0.5 μM 5-HT. Concentrations of 5-HT below the assay sensitivity of $\approx$ 0.1 μM (black dashed line, grey area) were not included in the fitting of rate constants.

2.2.2 Turbidimetric platelet aggregometry

Platelet aggregation was measured using turbidimetric aggregometry (Born, 1962, Jarvis et al., 2000), with two Aggregation Remote Analyzer Modules (AggRAM) and HemoRAM software (v1.2) (Helena Biosciences, Newcastle, U.K.). AggRAM modules recorded changes in optical density (OD) prior to and following the addition of platelet agonists. As platelets aggregate, the translucent WP suspension clarifies, reducing the OD. The extent of aggregation for each sample was calibrated using unactivated WP (high OD, 0% aggregation) and a platelet-free CFT (low OD, 100% aggregation). WP (247.5 μL, 2.00 x 10^8 mL^{-1}) were aliquoted into glass cuvettes, containing magnetic stir bars and placed into AggRAM modules (37°C, 1,000 rpm). 2.5 μL agonist was added and aggregation recorded at 37°C with a stirring speed of 1,000 rpm. After agonist addition, aggregation was recorded for at least 6 minutes and the maximum extent and rate of aggregation during this period were subsequently determined (Figure 2.4).

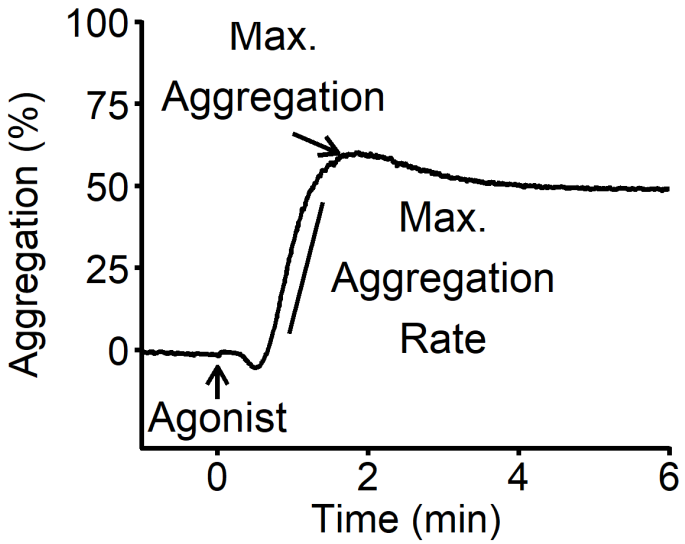

Figure. 2.4 Example aggregation trace. Aggregation was recorded for 6 minutes, following the addition of a platelet agonist. The maximum extent of aggregation (Max. Aggregation) and the maximum rate of aggregation (Max. Aggregation Rate) were recorded in every experiment. Max. Aggregation was typically used to describe platelet aggregation. The brief increase in optical density immediately after agonist addition is associated with platelet shape change.

2.2.3 Thromboxane A_2 synthesis

A Cayman TxB_2 Express ELISA kit (Cambridge Bioscience, Cambridge, U.K., product code: 10004023) was used to indirectly measure thromboxane A_2 (TxA_2) synthesis by quantifying concentrations of its stable metabolite, TxB_2. This assay is based on the competitive binding of TxB_2 in the platelet supernatant and a TxB_2-acetylcholinesterase conjugate (TxB_2 tracer) to anti-TxB_2 monoclonal antibodies that are bound to goat polyclonal anti-mouse IgG, which coats wells of a 96 well plate. Unbound supernatant/tracer TxB_2 is removed by washing the wells, before the addition of Ellman's Reagent, which contains Acetylcholine and 5,5'-dithio-bis-(2-Nitrobenzoic Acid). Hydrolysis of acetylcholine by the remaining antibody-bound TxB_2 tracer produces thiocholine, which reacts non-enzymatically with 5,5'-dithio-bis-(2-Nitrobenzoic Acid) to produce 5-thio-2-Nitrobenzoic Acid, which optimally absorbs light between 405-412 nm. The absorption intensity is therefore proportional to the amount of TxB_2 tracer bound to wells, which can be used to calculate the amount of TxB_2 within the platelet supernatant.

WP (247.5 μL, 2.00 x 10^8 mL^{-1}) were activated as for aggregometry (Chapter 2.2.2), with 5 mM EGTA and 16.6 μM indomethacin added 6 minutes after agonist addition, to minimise subsequent TxB_2 generation. Samples were immediately centrifuged (8,000 x g, 2 minutes), and the supernatants frozen (-80°C). Samples were later thawed and diluted 1:40 or 1:200 in ELISA buffer (100 mM phosphate, 0.1% [w/v] bovine serum albumin (BSA), 400 mM NaCl, 1 mM EDTA, 0.01% [w/v] sodium azide) and 50 μL added to wells of the polyclonal goat anti-mouse IgG-coated plate. 50 μL of TxB_2 standards were aliquoted to determine the relationship between absorbance and TxB_2 concentration. 50 μL of acetylcholinesterase tracer and 50 μL of anti-TxB_2 monoclonal antibody were added to each well and incubated for 2 hours at RT on an optical shaker. Wells were washed 4 times with wash buffer and incubated with 200 μL Ellman's reagent under dark conditions. Absorbance at 405 nm was checked periodically using a Sunrise^{TM} plate reader (Tecan, Reading, U.K.) until the absorbance of wells containing no supernatant TxB_2 were in the range of 0.3-1.5 absorbance units. Absorbance values for TxB_2 standards were fitted to a four-parameter logistic (4PL) model (Chapter 2.3), and the inverse function used to determine TxB_2 concentrations (Figure: 2.5). Samples were excluded from analysis if the calculated TxB_2 concentration fell outside the assay sensitivity range (1.6-1,000 pg mL^{-1}).

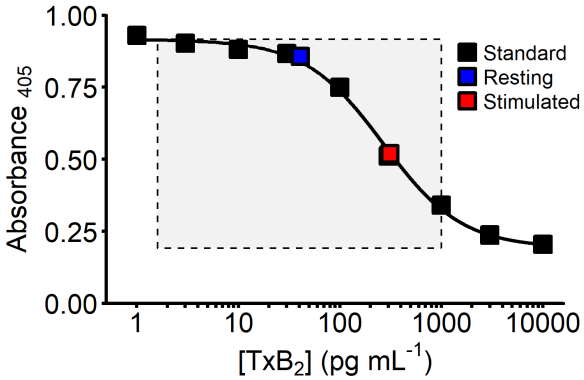

Figure. 2.5 Competitive enzyme-linked immunosorbent assay to measure thromboxane B_2. Absorbance values for thromboxane B_2 (TxB_2) standards were fitted to a four-parameter logistic (4PL) model. Absorbance values from diluted (1:200) supernatants of either unstimulated (blue) or collagen-stimulated (1 μg mL^{-1}, red) washed platelets were used to determine TxB_2 concentrations, using the 4PL fit generated from standards. Platelet samples were excluded from analysis if the calculated TxB_2 value fell outside the assay sensitivity range (grey shaded area within black dashed box).

2.2.4 Static adhesion

The adhesion of platelets or neutrophils to diverse ligands under static conditions was quantified by indirectly measuring levels of cell-derived acid phosphatase (EC 3.1.3.2) (Jarvis et al., 2012, Bellavite et al., 1994). Lysing adherent cells releases acid phosphatase, which, under appropriate conditions converts p-nitrophenyl phosphate (pNPP) to p-nitrophenol. Increasing the pH inhibits acid phosphatase and catalyses the change of p-nitrophenol to p-nitrophenolate, which absorbs light at 405 nm. The absorbance is therefore proportional to the levels of acid phosphatase and the extent of cell adhesion.

Immulon-2HB 96 flat-bottom well plates (Thermo Fisher Scientific, Loughborough, U.K.) were incubated overnight at 4°C with 100 μL of either BSA, GPP_{10}, Horm® collagen, collagen III, collagen-related peptide (CRP), fibrinogen, GFOGER, or thrombin (10 μg mL^{-1} in saline or 0.01 M acetic acid) (Tables 2.3 & 2.1). The excess ligand was discarded, and wells blocked with 175 μL BSA (5% [w/v] in CFT) for 1 hour. Wells were then washed three times with BSA (0.1% [w/v] in CFT). 50 μL of either WP (1.25×10^8 mL^{-1}) or isolated neutrophils (4.00×10^6 mL^{-1}) were added to wells and left for 1 hour at RT. Samples were discarded, and the wells washed as before, followed by the addition of 150 μL of citrate lysis buffer (3.53 mM pNPP, 71.4 mM trisodium citrate, 28.55 mM citric acid, 0.1% [v/v] Triton X-100; pH 5.4) to each well. After 1 hour, 100 μL of 2 M NaOH was added to each

well and absorbance measured at 405 nm, using either an ELx808 (Biotek, Swindon, U.K.) or a Sunrise^{TM} (Tecan, Reading, U.K.) plate reader.

2.2.5 Cell cytotoxicity

A Pierce LDH Cytotoxicity Assay Kit (Thermo Fisher Scientific, Loughborough, U.K., product code: 88953) was used to measure lactate dehydrogenase (LDH, EC 1.1.1.27) released from platelets or neutrophils as a result of cell lysis or damage induced by high drug concentrations. LDH is a cytosolic enzyme, and its detection in the supernatant of cellular suspensions is commonly used to assess membrane integrity and cell cytotoxicity. LDH catalyses the conversion of lactate to pyruvate, reducing nicotinamide adenine dinucleotide $(NAD)^+$ to NADH. Diaphorase (EC 1.6.99.1) uses NADH to reduce a tetrazolium salt to a red formazan product, which absorbs light at 490 nm.

250 μL of either WP (2.00 x 10^8 mL^{-1}) or isolated neutrophils (1.00 x 10^6 mL^{-1}) were placed within AggRAM modules (1,000 rpm, 10 minutes, 37°C). For positive controls, 10 μL of 10 x Lysis Buffer (proprietary, Thermo Fisher, product code: 1862876) was added to induce cytolysis. Supernatants were isolated following centrifugation (8,000 x g, 1 minute) using a Micro Centaur (MSE, London, UK) and 50 μL aliquoted into wells of an Immulon-2HB 96-well flat-bottom plate. For negative controls, 50 μL CFT alone was added to wells. 50 μL of reaction mixture (proprietary, Thermo Fisher, product code: 1862887) was added to each well for 30 minutes. 50 μL of a STOP solution (proprietary, Thermo Fisher, product code: 1862880) was added, and background absorbance at 680 nm subtracted from the absorbance at 490 nm. Measurements were taken using a Sunrise^{TM} plate reader (Tecan, Reading, U.K.).

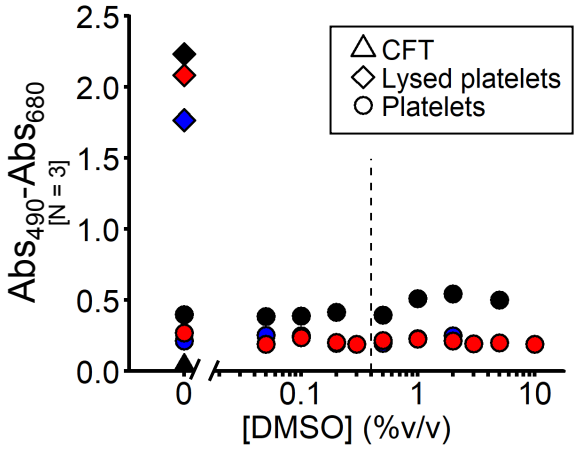

Figure. 2.6 Example data, showing how lactate dehydrogenase (LDH) levels were measured from the supernatants of washed platelets (WPs). In this example, platelets were treated with increasing concentrations of dimethyl sulfoxide (DMSO), which did not increase LDH levels up to concentrations of 10% [v/v]. Lysed platelets (diamonds) or calcium-free Tyrode's (CFT, triangles) were used as positive and negative controls, respectively. Three blood donors were used on separate occasions, which are represented as different colours. The highest DMSO concentration used during this project (0.4% [v/v]) is depicted by the vertical black line and did not cause LDH release. These data show that the concentrations of DMSO used in Chapter 6 did not cause cytotoxicity.

2.2.6 Monitoring cytosolic calcium concentration

Fluctuations in the concentration of cytosolic calcium ($[Ca^{2+}]_{cyt}$) were monitored using the ratiometric Ca^{2+} indicator, Fura-2. Excitation of Fura-2 at 340 and 380 nm excites Ca^{2+}-bound and Ca^{2+}-free Fura-2, respectively. Excited Fura-2 has a peak emission of 500 nm. PRP or isolated neutrophils were loaded with Fura-2 by incubation with acetoxymethyl ester (final concentration 2.5 μM, 30 minutes, 37°C). The acetoxymethyl (AM) ester groups of Fura-2AM allow membrane permeability before subsequent cleavage by intracellular esterases, trapping Fura-2 within the cytoplasm. In the case of PRP, WP preparation (2.00 x 10^8 mL^{-1}) was then continued (Chapter 2.1.2). Fura-2-loaded neutrophils were centrifuged (300 x g, 5 minutes) and resuspended in fresh CFT to 1.00 x 10^6 mL^{-1}. Fura-2 fluorescence was measured using a Cairn Optoscan Spectrophotometer (Cairn Research, Faversham, U.K.). 1.2 mL samples were aliquoted into cuvettes containing magnetic stir bars and placed into the chamber (stirring conditions, 37°C). Light from the high-intensity arc lamp was passed through a monochromator to provide excitation wavelengths of 340 and 380 nm and the emission of light at 500 nm was selected using a filter slider. Fluorescence was recorded using Acquisition Engine 1.1.7 (Cairn Research, Faversham,

U.K.). Extracellular Ca^{2+} was chelated 30 seconds after recording began by adding EGTA (10 mM), before the addition of agonist at 60 seconds.

On each experimental day, the F.I. of Fura-2 in the presence of high and low $[Ca^{2+}]$ was used to calibrate and quantify changes in $[Ca^{2+}]_{cyt}$ during experiments. 1.2 mL of cell suspension was incubated with Ca^{2+} (1 mM) and lysed with Triton X-100 (0.1% [v/v]), causing Ca^{2+} saturation of Fura-2 (F_{380min}, R_{max}). The addition of EGTA (10 mM) chelated Ca^{2+}, resulting in Ca^{2+}-free Fura-2 (F_{380max}, R_{min}). The protons liberated by EGTA were quenched with 20 mM Tris base (Figure 2.7). The following calculation, initially described by Grynkiewicz et al. (1985) was then used to determine $[Ca^{2+}]_{cyt}$ in experimental samples:

$$[Ca^{2+}]_{cyt} = K_d(\frac{F_{380max}}{F_{380min}})(\frac{R - R_{min}}{R_{max} - R})$$

Where: $[Ca^{2+}]_{cyt}$ = concentration of cytosolic calcium (nM); K_d = dissociation constant of Fura-2 (224 nM at 37°C); F_{380max} = maximum fluorescence at 380 nm; F_{380min} = minimum fluorescence at 380 nm; R = ratio of 340/380 nm; R_{max} = R under Ca^{2+}-saturating conditions; R_{min} = R under Ca^{2+}-free conditions (Figure 2.7).

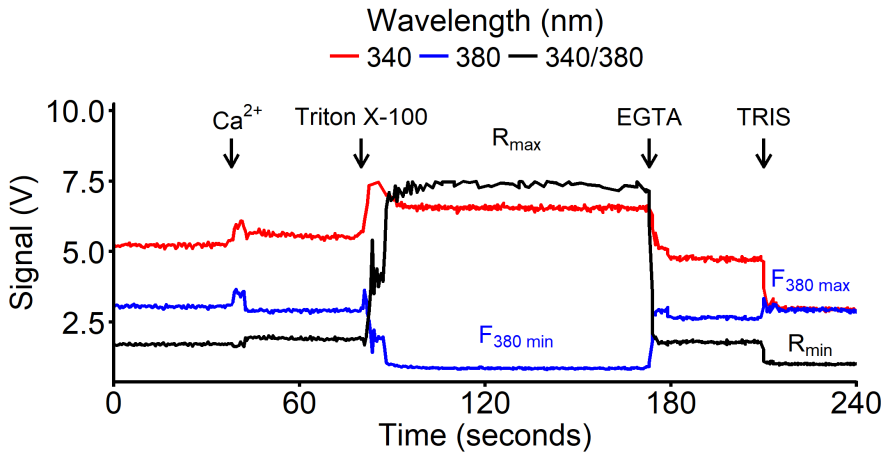

Figure. 2.7 Representative fluorescence (F) traces used to calibrate cytosolic calcium concentrations ($[Ca^{2+}]_{cyt}$). The signal produced by Fura-2 excitation at 340 (Ca^{2+}-bound) and 380 (Ca^{2+}-free) nm was monitored over time and used to calculate the fluorescence ratio (R, 340/380 nm). Ca^{2+} was added prior to cell lysis with Triton X-100, allowing full Ca^{2+} saturation of Fura-2 (F_{380min}, R_{max}). EGTA was added to chelate Ca^{2+} and the subsequent free protons quenched with Tris base (TRIS), resulting in no Ca^{2+}-bound Fura-2 (F_{380max}, R_{min}).

2.2.7 SDS PAGE and Western blot analysis

Cell lysates used for quantifying Rap1-GTP (Chapter 2.2.8) and protein tyrosine phosphorylation were separated by sodium dodecyl sulphate polyacrylamide gel electrophoresis (SDS PAGE), transferred to polyvinylidene fluoride (PVDF) membranes and detected with specific antibodies (Table 2.5).

250 μL WP (2.00 x 10^8 mL^{-1}) or neutrophils (1.00 x 10^6 mL^{-1}) were either stimulated in aggregometers (1,000 rpm, 37°C) or under non-stirring conditions at RT, respectively. Platelet samples were pre-incubated with the integrin $\alpha_{IIb}\beta_3$ antagonist GR 144053 (2 μM) to prevent aggregation. Following stimulation, samples assessed for protein tyrosine phosphorylation were diluted 5:1 in Laemmli sample buffer (final concentrations: 25 mM Tris HCl, 0.4% [v/v] glycerol, 0.8% [w/v] SDS, 1% [v/v] mercaptoethanol, 0.01% [w/v] brilliant blue). Total Rap1 and Rap1-GTP pulldown samples were prepared as described in Chapter 2.2.8. Samples were heated for 10 minutes at approximately 100°C. 20 μL of protein sample lysates were assigned and added to lanes of a 4-12% pre-cast NuPAGE® Bis-Tris gel (Invitrogen, Paisley, U.K.). 5 μL of Precision Plus Protein™ dual colour or all blue standards (Bio-Rad Laboratories, Hertfordshire, U.K.) were typically added to lanes 1 and 10, respectively. Gels were run at 200 volts for 1-1.5 hours in 1 x NuPAGE® MOPS SDS running buffer (50 mM MOPS, 50 mM Tris base, 0.1% [w/v] SDS, 1 mM EDTA, 0.25% [v/v] NuPAGE® antioxidant, pH 7.7). The gel and a PVDF membrane (Millipore, Watford, U.K.) were sandwiched between filter papers, assembled into a transfer cassette and immersed in transfer buffer (25 mM Tris base, 192 mM glycine, 0.5% [w/v] SDS, 17% [v/v] methanol). Transfers were completed (20 volts, overnight, 4°C) and transfer efficiency tested by staining gels with Coomassie stain (10% [v/v] glacial acetic acid, 45% [v/v] distilled water, 45% [v/v] methanol, 0.25% [w/v] brilliant blue), which confirmed complete protein post-transfer in all cases. Non-specific antibody binding minimised by incubating membranes with blocking buffer (10% [w/v] BSA, 20 mM Tris base, 137 mM NaCl, 0.1 % [v/v] Tween-20, pH 7.6) for 1 hour at RT. Membranes were agitated for 2 hours in BSA (5% [w/v], 0.01% [w/v] sodium azide, in Tris-buffered saline with Tween (TBS-T)), containing various primary antibodies (Tables 2.4 & 2.5). Membranes were washed 3 x 15 minutes in TBS-T, before 1 hour incubation with horseradish peroxidase (HRP)-conjugated secondary antibodies (Table 2.5). Membranes were washed as before, treated with enhanced chemiluminescence (ECL) reagent and exposed under dark conditions to hyperfilm® (GE Healthcare, Buckinghamshire, U.K.), allowing the detection of protein bands. X-ray films were developed using a medical film processor (Fuji, Bedford, U.K.).

Different film exposure times were used for each blot and those generating the greatest contrast between bands were selected for subsequent quantification. Membranes were agitated in Coomassie stain for approximately 30 minutes, to confirm similar protein concentrations between samples.

Developed X-ray films were scanned using a Xerox WorkCentre 7855 photocopier (Settings: greyscale; default for brightness, sharpness and saturation; 100% zoom; 600 dpi) to generate JPEG image files. Unprocessed image files were opened into ImageJ (v1.50) and no adjustments (e.g., brightness, sharpness or saturation) were made. Protein bands were quantified as follows: identical areas (height (100) x width (150) = 15,000 pixels) were drawn around each protein band and the density of all pixels (scale 0 – 255 each) summed. The integrated density of each area was therefore quantified on a scale from 0 (totally black) to 3,825,000 (totally white). Values are presented as % black. Background density levels were determined (≈ 45-48% black), representing no protein signal.

2.2.8 Rap1-GTP pulldown

An active Rap1 Pull-Down and Detection Kit (Thermofisher Scientific, Loughborough, U.K., product number: 16120) was used to isolate activated Rap1 (Rap1-GTP). Platelet lysates were incubated with a glutathione S-transferase (GST)-tagged Ral guanine nucleotide dissociation stimulator Ras-binding domain (RalGDS-RBD) fusion protein, which binds both glutathione and Rap1-GTP via GST and RBD, respectively. Glutathione was attached to cross-linked agarose, preventing the passage of GST-RalGDS-RBD and associated Rap1-GTP through membrane-incorporated spin cups (Figure 2.8).

250 μL of either WP (2.00×10^8 mL^{-1}) or neutrophils (1.00×10^6 mL^{-1}) were stimulated as for aggregometry for 1 minute. Reactions were terminated with 1:1 Lysis/binding/wash buffer (LBW: 25 mM Tris HCl, 150 mM NaCl, 5 mM $MgCl_2$, 1% [v/v] NP-40, 5% [v/v] glycerol, pH 7.2). Lysates were put on ice for 5 minutes, followed by centrifugation (8,000 x g, 1 minute) using a Micro Centaur (MSE, London, UK). For total Rap1 quantification, 20 μL of each sample lysate was aliquoted into 1:1 Laemmli buffer (final concentrations: 62.5 mM Tris HCl, 1% [v/v] glycerol, 2% [w/v] SDS, 2.5% [v/v] mercaptoethanol, 0.025% [w/v] brilliant blue). For some samples, lysates were incubated with 10 mM EGTA and 0.1 mM guanosine 5'-O-[gamma-thio]triphosphate (GTPγS) (30 minutes, 30°C), a non-hydrolysable analogue of GTP which can be used as an optional positive control (Figure A.2 in Appendix A). For Rap1-GTP quantification, the remaining 480 μL sample was aliquoted into spin cups, containing 100 μL of 50% glutathione-agarose beads and 20 μg of GST-RalGDS-RBD. Samples were briefly vortexed and incubated with gentle rocking (1 hour,

4°C). Samples were centrifuged (8,000 x g, 1 minute) using a Micro Centaur (MSE, London, UK) and washed 3 times with 400 μL LBW, before the addition of 50 μL Laemmli buffer. Samples were centrifuged (8,000 x g, 2 minutes) into tubes using a Micro Centaur (MSE, London, UK). Total Rap1 and Rap1-GTP samples underwent SDS PAGE and Western blot analysis (Chapter 2.2.7). Samples were probed with a Rap1 primary antibody (Table 2.5).

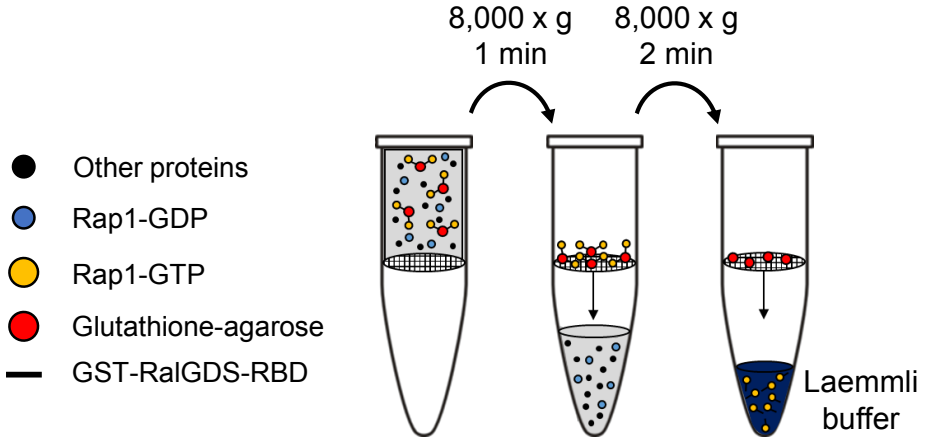

Figure. 2.8 Schematic illustration of the Rap1-GTP pulldown assay. Lysates were incubated with a glutathione S-transferase (GST)-tagged Ral guanine nucleotide dissociation stimulator Ras-binding domain (RalGDS-RBD) fusion protein, which indirectly links Rap1-GTP with glutathione-agarose beads. Proteins not linked to glutathione-agarose beads were passed through a membrane filter by centrifugation (8,000 x g, 1 minute), and the supernatant discarded. The addition of Laemmli sample buffer breaks GST-glutathione links, allowing Rap1-GTP to pass through the membrane filter upon centrifugation (8,000 x g, 2 minutes). This is an original image.

2.2.9 Neutrophil integrin $\alpha_M\beta_2$ activation

Neutrophil integrin $\alpha_M\beta_2$ (Mac-1, CD11b/CD18) activation was measured using an allophycocyanin (APC)-conjugated monoclonal antibody, which binds the activated epitope of integrin α_M (CD11b) (Table 2.5). Neutrophils (100 μL, 1.00 x 10^6 mL^{-1}) were incubated with the active CD11b antibody in the absence of light (5 minutes, 4°C). Various combinations of CD15, CD41a and CD45 antibodies were co-incubated to assess sample purity (Chapter 2.1.3). Samples were fixed with 2% [v/v] paraformaldehyde and the F.I., FSC and SSC of 30,000 sampled events quantified using an Accuri^{TM} C6 flow cytometer (BD Bioscience, Oxford, U.K.).

2.2.10 Rap1B nucleotide exchange activity

The rate and extent of Rap1B nucleotide exchange was measured using a fluorescence-based *in vitro* enzyme assay (Lozano et al., 2016, Ren et al., 2016). This assay uses the fluorophore BODIPY-FL, which exhibits similar spectral characteristics to fluorescein isothiocyanate (FITC) and is attached to either the 2' or 3' position of the guanosine diphosphate (GDP) ribose ring (BODIPY-FL-GDP). The F.I. of BODIPY-FL-GDP increases upon binding to Rap1. In this assay, the exchange of BODIPY-FL-GDP for non-fluorescent GDP on Rap1B was monitored by measuring increases in sample F.I. over time (Figure 2.9B). The addition of calcium and diacylglycerol guanine nucleotide exchange factor-1 (CalDAG-GEFI) increases the rate of nucleotide exchange and BODIPY-FL-GDP binding to Rap1, therefore increasing F.I. (Figure 2.9B).

100 μL of reaction buffer (20 mM Tris base, 150 mM NaCl, 5 mM $MgCl_2$, 2 mM dithiothreitol, 10% [v/v] glycerol, 0.08% [v/v] NP-40, 1 μM Rap1B, 0.1 μM BODIPY-FL-GDP, pH 7.5) was aliquoted into wells of a Nunc F96 well, black, flat-bottomed plate and the baseline F.I. recorded (Ex 485 nm, Em 520 nm) for 3 minutes with a Fluostar Optima plate reader (BMG Labtech, Aylesbury, U.K.). Measurements were halted for 105 seconds, allowing the addition of CalDAG-GEFI (0.3 μM) and recording resumed for 20 minutes. The average F.I. prior to CalDAG-GEFI addition was subtracted from the final F.I. after 20 minutes (ΔF.I.) and used to quantify CalDAG-GEFI-mediated Rap1B nucleotide exchange.

Recombinant Rap1B and CalDAG-GEFI were generous donations from Professor Wolfgang Bergmeier and Aaron Cook, from the University of North Carolina. Aaron Cook cloned Rap1B and CalDAG-GEFI from human genes into a protein expression vector p15LIC2 6xHis, which was purified in *E. coli*. Catalytically active and inactive CalDAG-GEFI protein variants were provided, which all contained a C-terminal truncation p.(Ala552_Leu609del), which "removed disordered regions to improve stability during the purification process, while leaving all the functional domains intact" (personal communication from Aaron Cook). Rap1B also contained a C-terminal truncation (p.(Lys168_Leu184del)) for the same reason. Catalytically inactive CalDAG-GEFI variants contained either an additional deletion (p.(Arg387_Pro404del)), or a glycine-tryptophan substitution at position 248 (p.(Gly248Trp)) (Lozano et al., 2016, Canault et al., 2014). CalDAG-GEFI variants p.(Arg387_Pro404del) and p.(Gly248Trp) did not increase the rate of Rap1B nucleotide exchange when compared to samples lacking CalDAG-GEFI (Figure 2.9B) and were thus used as negative controls. Protein sequences for both CalDAG-GEFI and Rap1B variants are shown in Figure B.1 of Appendix B.

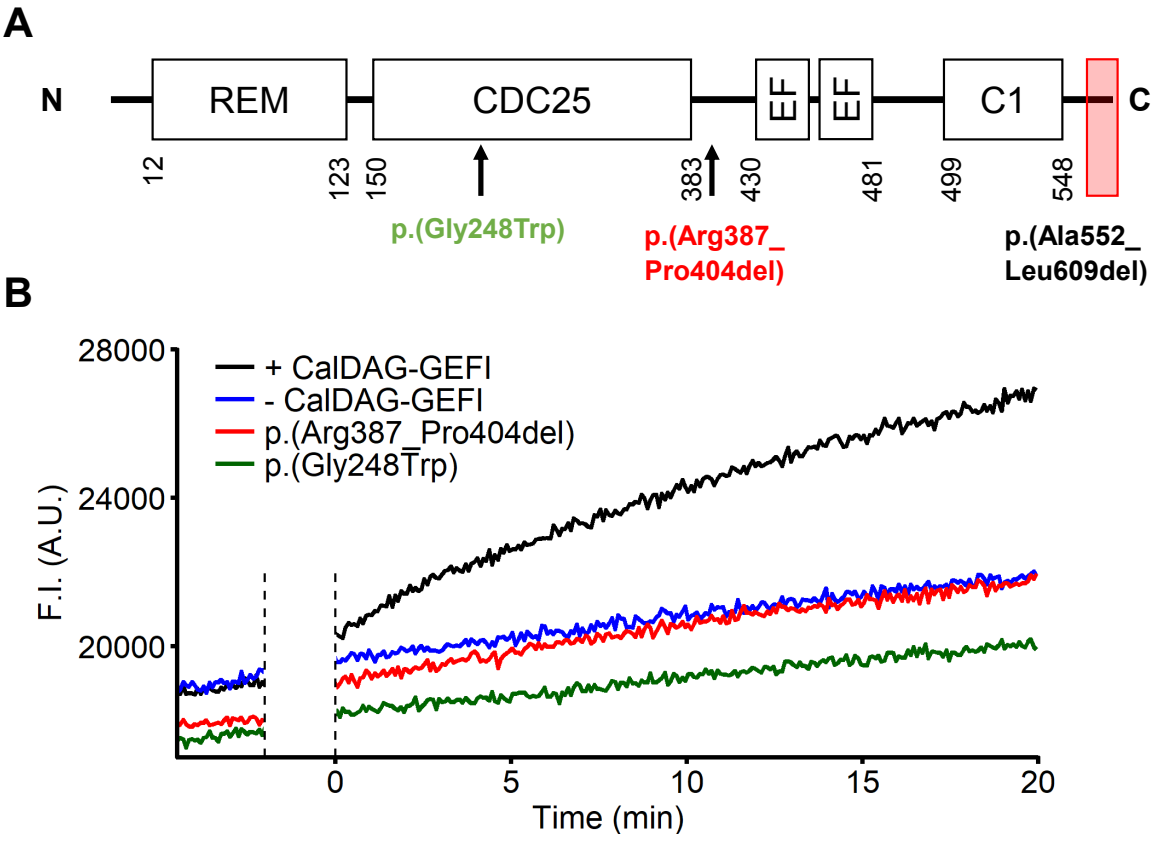

Figure. 2.9 Monitoring Rap1B nucleotide exchange. **(A)** Domain structure of the calcium and diacylglycerol guanine nucleotide exchange factor-1 (CalDAG-GEFI) (Westbury et al., 2017). Arrows demonstrate the locations of a glycine-tryptophan substitution at residue 248 (p.(Gly248Trp)) within the cell division cycle 25 (CDC25) domain, and an 18 residue deletion (p.(Arg387_Pro404del)) between the CDC25 and EF hand domains. CalDAG-GEFI variants all contained a C-terminal deletion (p.(Ala552_Leu609del)), represented by the red outlined box. **(B)** A BODIPY-FL fluorescence-based assay was used to monitor the nucleotide exchange activity of Rap1B in the presence or absence of CalDAG-GEFI. Fluorescence intensity (F.I.) traces demonstrate the intrinsic dissociation of non-fluorescent guanosine diphosphate (GDP) from Rap1B and the subsequent binding of BODIPY-FL-GDP in the absence of CalDAG-GEFI (blue line), which gradually increases sample fluorescence. Catalytically active (black line) or inactive (red line is p.(Arg387_Pro404del); green line is p.(Gly248Trp)) CalDAG-GEFI was added to wells containing Rap1B and BODIPY-FL-GDP during the period indicated by the white segment enclosed by black dashed lines. CalDAG-GEFI variants and Rap1B were provided by Professor Wolfgang Bergmeier and Aaron Cook, from the University of North Carolina.

2.2.11 Glycoprotein VI antibody binding

The binding of antibodies to dimeric or total (dimeric and monomeric) platelet glycoprotein VI (GPVI) was quantified using the GPVI-specific antibodies, 204-11 Fab and HY-101, respectively (Table 2.5). WP (2.50 x 10^7 mL^{-1}) were incubated for 10 minutes with either HY-101 (5 μg mL^{-1}) or 204-11 Fab (10 μg mL^{-1}). Murine IgG1 (5 μg mL^{-1}) or Fab (10 μg mL^{-1}) were used as corresponding isotype controls, respectively (Table 2.5). Alexa488-conjugated anti-mouse $F(ab)_2$ (5 μg mL^{-1}) was subsequently added and incubated for 10 minutes. Samples were diluted 1:8 in CFT and the F.I. measured using an Accuri^{TM} C6 flow cytometer (BD Bioscience, Oxford, U.K.).

2.2.12 Dense granule release

Supernatant concentrations of adenosine triphosphate (ATP) and adenosine diphosphate (ADP) were used to measure platelet dense granule release. WP (247.5 μL, 2.00 x 10^8 mL^{-1}) were activated as for aggregometry for 6 minutes (Chapter 2.2.2). 5 mM EGTA and 16.6 μM indomethacin were added 6 minutes after the addition of agonist, to minimise further nucleotide release. Samples were immediately centrifuged (8,000 x g, 1 minute) using a Micro Centaur (MSE, London, UK), the supernatants collected and frozen (-20°C). HPLC was used to quantify supernatant concentrations of ATP and ADP. Nucleotides were separated using a gradient method on a reversed phase C18 column with polar end-capping to tolerate a 100% aqueous phase (Synergi^{TM} Hydro-RP: 250 x 4.6 mm, 4 μm beads, 80 Å pore size) (Product code 00G-4375-E0, Phenomenex, Cheshire, U.K.). Two mobile phases were used, a phosphate buffer (2.2 mM K_2HPO_4, 47.8 mM KH_2PO_4; pH 5.45) and acetonitrile. Nucleotides were separated over 6 minutes at 30°C, with a constant flow rate of 1.7 mL min^{-1}. Details of the mobile phase method are in Table 2.2. Peaks for ATP and ADP were detected at 254 nm, with retention times of 3.4 and 4.5 minutes, respectively (Figure: 2.10A). Chromatograms were analysed using N2000 Chromatography Data System (Tianjin University, China). For each experimental day, ATP and ADP concentrations were determined using the AUC from peaks of known standards, which were used to construct linear standard curves (Figure: 2.10B). The limit of detection for ATP and ADP in the platelet supernatant was approximately 0.1 μM.

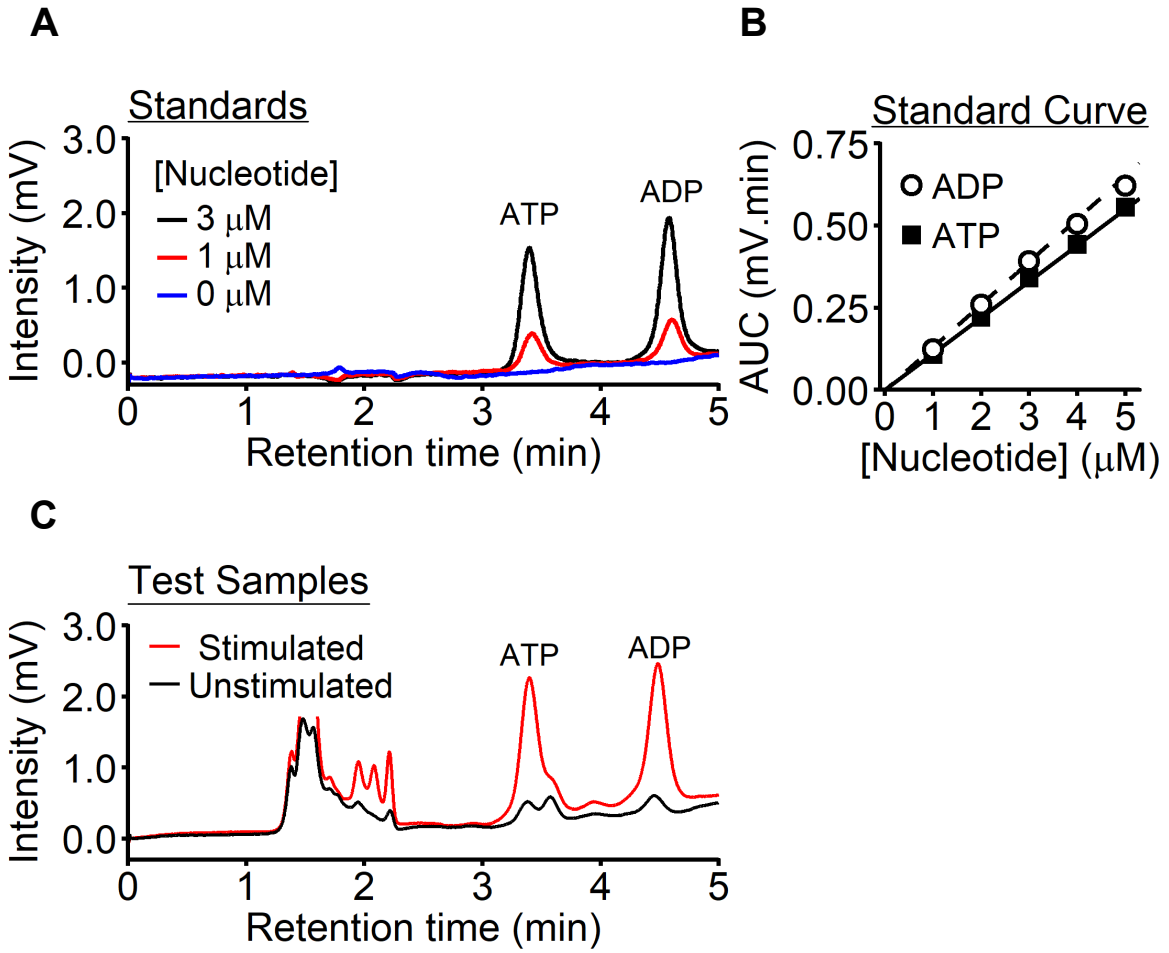

Figure. 2.10 Measuring platelet dense granule release. **(A)** Exogenous concentrations of adenosine triphosphate (ATP) and adenosine diphosphate (ADP) (0, 1, 3 μM) were added to calcium-free Tyrode's (CFT) and the area under the curve (AUC) of peaks at retention times 3.4 and 4.5 recorded. **(B)** Standard curves describing the relationship between AUC and nucleotide concentration were created for each experimental day, to determine ATP and ADP concentrations in platelet supernatants. **(C)** Example chromatograms for the supernatant of stimulated (red line) and unstimulated (black line) platelets. Undefined peaks between 1.2 and 2.2 minutes were not a consequence of platelet activation and did not disrupt the quantification of ATP or ADP.

2.3 Statistics and analysis

Concentration-response curves were modelled using a four-parameter logistic (4PL) equation (DeLean et al., 1978, Jarvis et al., 2000):

$$R_{PRED} = \frac{Min - Max}{1 + (\frac{[A]}{10^{-pA_{50}}})^{n_H}} + Max$$

Where: R_{PRED} = predicted response (dependent variable); $[A]$ = agent concentration (independent variable); Min = response when $[A] = 0$; Max = response when $[A] = \infty$; pA_{50} = -log $[A]$ when $R_{PRED} = (Max + Min)/2$; n_H = Hill coefficient. When A is an inhibitor, the pA_{50} is the pIC_{50}.

Parameter values were estimated by fitting the data to the 4PL model using the Solver Tool in Microsoft Excel to minimise the sum of the squares of the residuals (Figure 2.3A). For 5-HT uptake experiments (Chapter 3.2.1) and neutrophil adhesion to fibrinogen (Chapter 4.2.7), a naïve pooled approach (Mould and Upton, 2012) was adopted using GraphPad Prism 7.03 (CA, U.S.A.). In this approach, data from separate experiments was grouped and averaged as if it were from one experiment, which was then used to determine the four parameters and model plot fits (Figure 2.3B). For all other experiments, summary parameters were derived using a 'two-stage' approach (Steimer et al., 1984, Mould and Upton, 2012), in which parameter estimates were obtained for each individual experiment (usually per blood donor). These were then averaged and used to model the final fit shown in figures. Average data point values were printed over model fits, ± the standard error of the mean (SEM) (Figure 2.3B). Average pIC_{50} or pEC_{50} values were used to describe the concentration-dependent loss or gain in response, respectively. This approach was chosen over describing IC_{50} or EC_{50} values, as biological response data typically suit a log-normal distribution (Hancock et al., 1988). Likewise, the geometric mean of Hill coefficients (nH) was chosen over the arithmetic mean. R 3.3.2 (The R Foundation for Statistical Computing, Vienna, Austria) was used to generate figures and conduct analysis of variance (ANOVA).

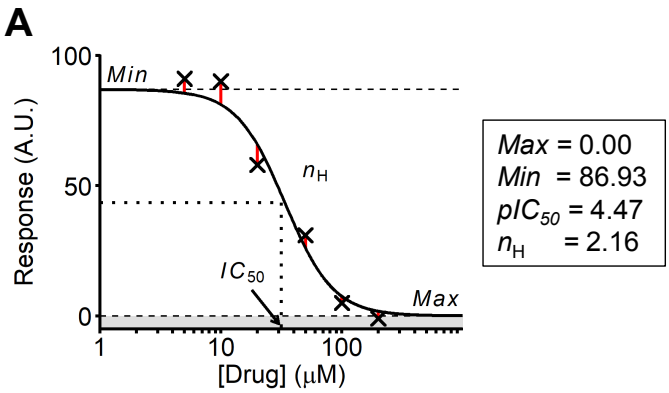

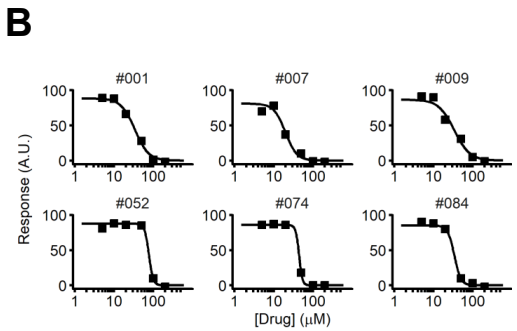

Naïve pooled approach

[Drug] (μM)	5	10	20	50	100	200
Average	84.50	86.50	68.83	30.33	3.00	-1.50
SEM	3.25	1.74	7.85	11.51	1.65	0.34

Average Parameter	*Min*	*Max*	pIC_{50}	n_H
	0.00	86.27	4.43	2.55

Two-stage approach

Donor	*Min*	*Max*	pIC_{50}	n_H
#001	88.38	0.00	4.47	2.48
#007	81.27	0.00	4.71	2.94
#009	86.93	0.00	4.47	2.17
#052	87.65	0.00	4.11	7.98
#074	85.77	0.00	4.36	10.34
#084	85.17	0.00	4.47	5.18
Average	0.00	85.87	4.43	4.35
SEM	0.00	1.04	0.08	1.37

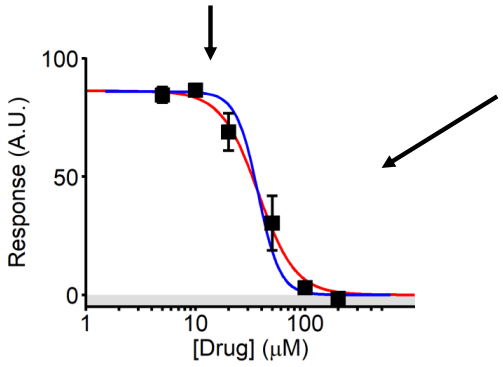

Figure. 2.11 Modelling concentration-response curves. **(A)** Description of the four-parameter logistic (4PL) model. The four parameters: Max, Min, pA_{50} and n_H were used to model concentration-response curves. In this example, a pIC_{50} value was used, due to the loss in response with increased drug concentration. Parameter values were optimised by minimising the sum of the squared residuals (red lines are residuals). **(B)** Example data from 6 blood donors demonstrates how results were analysed using either the naïve pooled approach or the two-stage approach. In this thesis, the two-stage approach was typically adopted, where parameter values from individual experiments were averaged and used to model the final plot fit. Average data points (± SEM) were printed over the fit.

Chapter 3
Citalopram inhibits platelets through a SERT-independent mechanism

3.1 Background

Citalopram is a selective serotonin reuptake inhibitor (SSRI) that suppresses platelet activation *in vitro* (Carneiro et al., 2008, Tseng et al., 2010, 2013). Citalopram's antiplatelet effects *in vitro* may be mediated through blocking the platelet serotonin transporter (SERT), preventing the uptake of serotonin (5-HT). Blocking platelet SERT *in vivo* with prolonged SSRI treatment gradually depletes dense granule stores of 5-HT, impairing 5-HT-enhanced platelet activation (Hergovich et al., 2000). However, citalopram incubations of only 3-10 minutes have been reported to inhibit platelet functions *in vitro* (Carneiro et al., 2008, Tseng et al., 2010, 2013). Furthermore, micromolar concentrations of citalopram were used in these studies, which are approximately three orders of magnitude greater than the nanomolar concentrations (K_i = 9.6 ± 0.5 nM) required to block SERT (Owens et al., 2001). These observations suggest that the *in vitro* antiplatelet effects of citalopram may not be a direct consequence of SERT inhibition.

3.1.1 Citalopram's stereochemistry

Citalopram is a 50:50 racemic (*RS*) mixture of two stereoisomers, (*R*)- and (*S*)-citalopram (Figure 3.1, Chapter 1.2.3). (*S*)-Citalopram (K_i = 2.5 ± 0.4 nM) is approximately 30-fold more potent than (*R*)-citalopram (K_i = 67.0 ± 8.0 nM) at inhibiting SERT-mediated 5-HT uptake (Owens et al., 2001), which equates to a eudysmic ratio of approximately 30. Previous *in vitro* studies have only investigated the effects of racemic (*RS*)- or (*S*)-citalopram on platelets (Atar et al., 2007, Carneiro et al., 2008, Tseng et al., 2010, 2013), with no attention given to the individual (*R*)-isomer. If citalopram suppresses *in vitro* platelet activation through blocking SERT, then any inhibitory effects will predominantly be mediated by (*S*)-citalopram. Similarly, (*R*)-citalopram, which has a lower affinity for binding and blocking SERT should be approximately 30-fold less potent at inhibiting platelet functions.

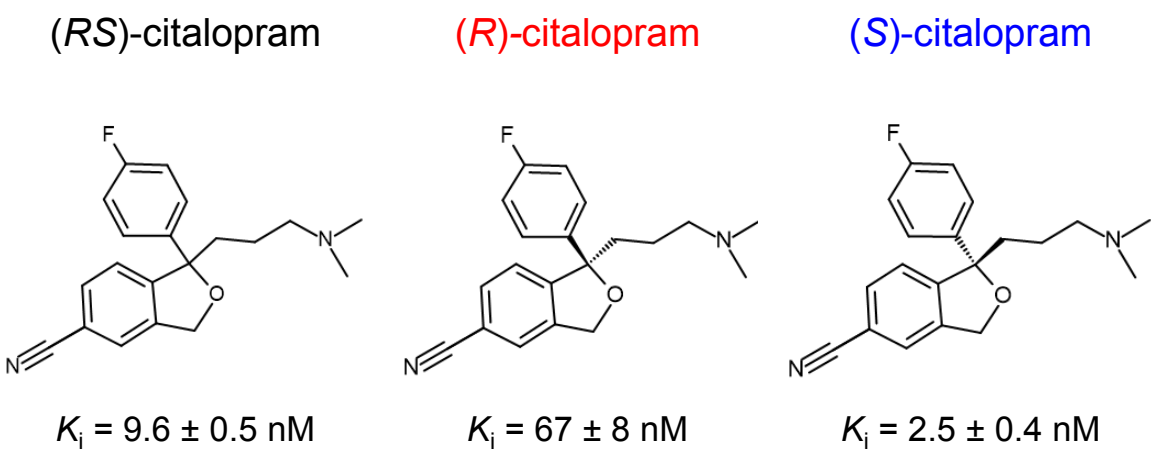

Figure. 3.1 Chemical structures of citalopram and its stereoisomers. Racemic (*RS*)-citalopram consists of a 50:50 mixture of (*R*) and (*S*) stereoisomers. (*RS*)-citalopram has one stereocentre, to which a 4-fluorophenyl group and an N,N-dimethyl-3-aminopropyl group are attached. The geometric differences between (*R*)-citalopram and (*S*)-citalopram isomers account for their discrepancy in both binding the serotonin transporter (SERT) and inhibiting SERT-mediated serotonin (5-HT) uptake. K_i values for 5-HT uptake (mean ± SEM) are from previously published data (Owens et al., 2001), derived from competition-binding assays between citalopram and radiolabelled 5-HT on human neurons of the frontal and parietal cortex. Chemical structures were constructed using BIOVIA Draw 2016 version 5.1.0.22 (Dassault Systèmes, Vélizy-Villacoublay, France).

3.1.2 Aims

Experiments performed within this chapter aim to:

1. Characterise the effects of citalopram on platelet functional responses *in vitro*.
2. Determine whether citalopram's effects are mediated through its known mechanism of action, i.e. inhibition of SERT.

To achieve these aims, the inhibitory potencies of (*RS*)-, (*R*)- and (*S*)-citalopram were compared for both platelet 5-HT uptake and several platelet functional responses, including aggregation, thromboxane A_2 (TxA_2) synthesis and adhesion. By using the same protocol for platelet preparation, direct comparisons can be made between inhibition of SERT and inhibition of platelet functional responses. Quantifying the time-dependent reduction in supernatant 5-HT (Chapter 2.2.1) also produced rate constants for 5-HT uptake, which are a more suitable index for SERT activity than previously published data on the competitive binding of citalopram and 5-HT (Owens et al., 2001).

3.2 Results

3.2.1 Citalopram blocks 5-HT uptake into platelets

Pre-incubating platelets with (*RS*)-citalopram (100 nM) prevented the uptake of 5-HT (1 μM) from the supernatant into platelets (Figure 3.2A). Rate constants for platelet 5-HT uptake (k_u) were obtained following pre-incubation for approximately 5 minutes with a range of (*RS*)-, (*R*)- and (*S*)-citalopram concentrations (Figure 3.2B). Owing to logistical constraints, it was not possible to collect data for all conditions on each experimental day to generate concentration-response curves. Therefore, a naïve pooled approach (Figure 2.11) was used to analyse data. In total, 76 rate constants from 11 blood donors were obtained on 14 separate occasions across a range of citalopram concentrations. Data from one blood donor (comprising of 4 rate constants) were excluded from the analysis as a hyper-functional outlier, lying more than 3 standard deviations beyond the basal range. The mean ± SEM basal rate constant for 5-HT uptake (no citalopram) was 4.60 ± 0.24 hr^{-1}. (*RS*)-, (*R*)- and (*S*)-citalopram blocked 5-HT uptake at nanomolar concentrations (Figure 3.2C) (N = 4-6 values per data point, n = 13 donors). The citalopram isomers had different inhibitory potencies: (*S*)-citalopram (pIC_{50} = 8.60 ± 0.13) was approximately 17-fold more potent than (*R*)-citalopram (pIC_{50} = 7.36 ± 0.19) and (*RS*)-citalopram (pIC_{50} = 8.33 ± 0.11) was approximately 1.8-fold less potent than (*S*)-citalopram. These results suggest that platelet 5-HT uptake inhibition by (*RS*)-citalopram is predominantly mediated by the (*S*)-citalopram isomer.

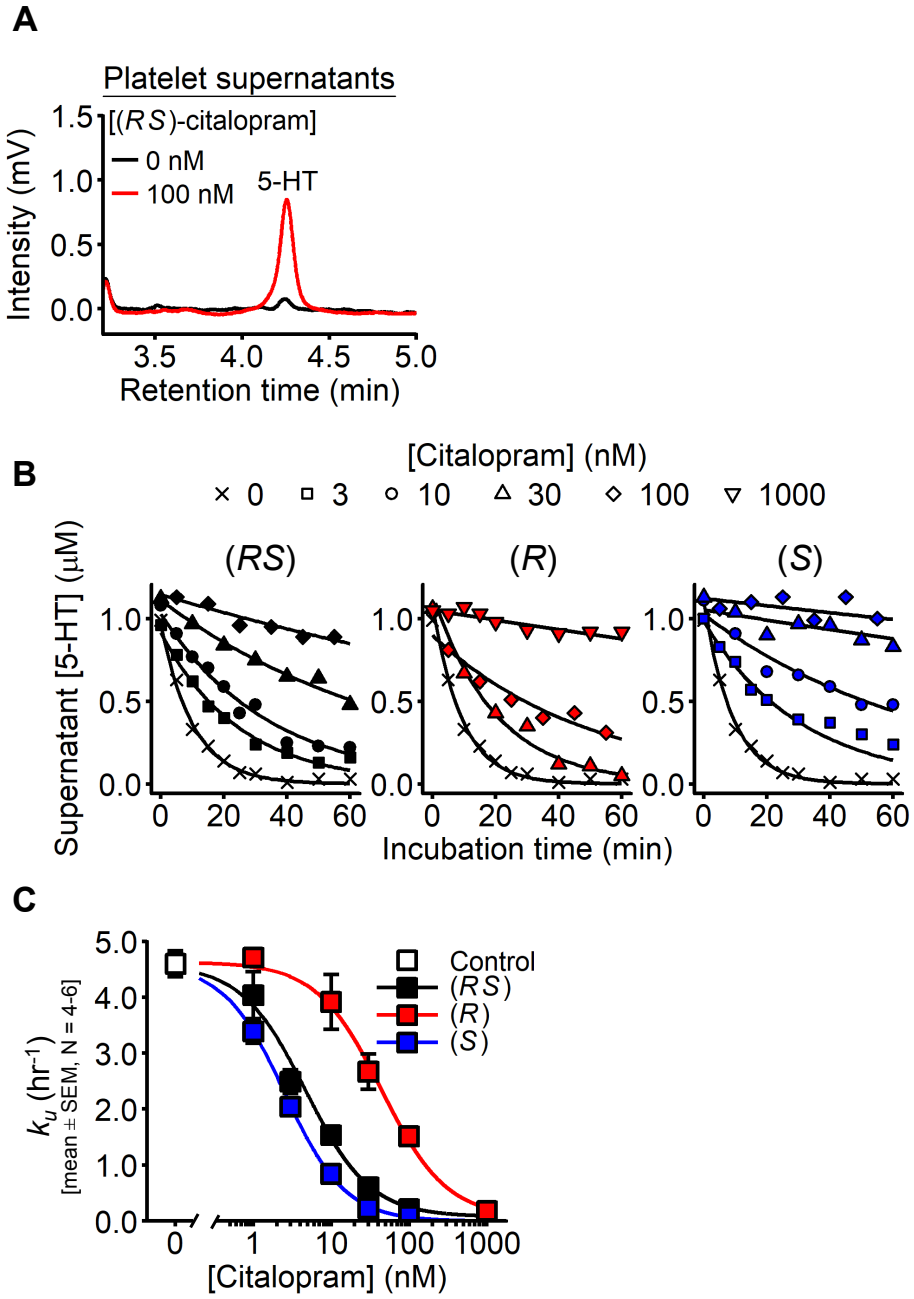

Figure. 3.2 Citalopram blocks 5-HT uptake into platelets. **(A)** Example high-pressure liquid chromatography (HPLC) chromatograms of platelet supernatants, isolated 30 minutes after the addition of 1 μM serotonin (5-HT). Before the addition of 5-HT, platelets were either untreated (black line) or pre-incubated with 100 nM (*RS*)-citalopram (red line) for approximately 5 minutes. **(B)** Example kinetic profiles, showing the reduction in supernatant 5-HT over time. Uptake was blocked by increasing concentrations of (*RS*)-, (*R*)- and (*S*)-citalopram (black, red and blue lines, respectively). Kinetic profiles were used to determine rate constants of uptake (k_u). **(C)** The inhibitory effect of (*RS*)-, (*R*)- and (*S*)-citalopram (0, 1, 3, 10, 30, 100 & 1,000 nM) on the rate constant of uptake were fitted to the four-parameter logistic (4PL) model using the naïve pooled approach (N = 4-6 replicates per data point, n = 13 separate blood donors).

3.2.2 Citalopram inhibits platelet aggregation

Previous results confirm (*S*)-citalopram is the more potent inhibitor of platelet 5-HT uptake (Chapter 3.2.1). The inhibitory potencies of (*RS*)-, (*R*)- and (*S*)-citalopram were also tested on several platelet functional responses and later compared with inhibitory potencies for 5-HT uptake, to determine if any effects were mediated through SERT blockade.

Preliminary experiments show (*RS*)-citalopram (100 μM) inhibited collagen-induced platelet aggregation (Figure 3.3). Inhibition was observed following short (*RS*)-citalopram pre-incubation times (30, 60 seconds) or in conjunction with the addition of collagen (0 seconds). Subsequent experiments were designed to quantify and compare the inhibitory potencies (i.e., the pIC_{50} values) of (*RS*)-, (*R*)- and (*S*)-citalopram on collagen- and U46619-induced platelet aggregation. Agonist concentration-response curves were obtained at 0, 20, 50 & 100 μM citalopram for collagen, and 0, 50, 100 & 200 μM citalopram for U46619. Unless otherwise stated, collagen refers to Horm® collagen. Treatment conditions were randomised, with citalopram simultaneously added to all washed platelet samples in advance of the first measurements. Therefore, some samples were incubated for longer periods of time, up to 3 hours. Collagen and U46619 experiments were conducted on the same donors (N = 7), but on separate occasions. Collagen- and U46619-induced aggregation were inhibited by (*RS*)-, (*R*)- and (*S*)-citalopram in a concentration-dependent manner (Figure 3.4). Responses to a fixed concentration of collagen (1 μg mL^{-1}) or U46619 (0.2 μM), which induced near-maximal aggregation under control conditions, were fitted to the four-parameter logistic (4PL) model with the Max parameter constrained to zero (Figure 3.4C). pIC_{50} values are shown in Table 3.1 and Figure 3.8. U46619 data from one experimental day was excluded, as the 4PL model failed to converge on a meaningful solution. 3-way ANOVA (Effect 1 (fixed) = citalopram {(*RS*), (*R*), (*S*)}; Effect 2 (fixed) = agonist {collagen, U46619}; Effect 3 (random) = donor {N = 7 (collagen), N = 6 (U46619)}) indicated no difference in inhibitory potency between (*RS*)-, (*R*)- and (*S*)-citalopram (P = 0.57, F = 0.57, df = 2, 27. H_0: μ_{RS}=μ_R=μ_S; H_1: $\mu_{RS} \neq \mu_R \neq \mu_S$).

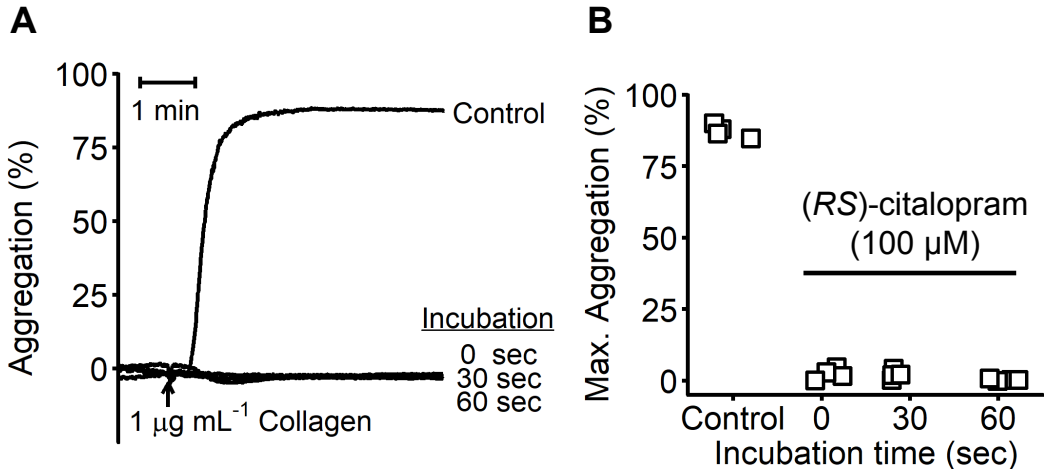

Figure. 3.3 Instantaneous platelet inhibition by citalopram. **(A)** Representative aggregation traces for either untreated platelets, or platelets pre-incubated with 100 μM (*RS*)-citalopram for either 30 or 60 seconds before stimulation with collagen (1 μg mL^{-1}). 0 seconds represents co-administration of both (*RS*)-citalopram (100 μM) and collagen (1 μg mL^{-1}). **(B)** Following collagen addition, the maximum extent of aggregation over 6 minutes (Max. Aggregation) was quantified (N = 4 blood donors).

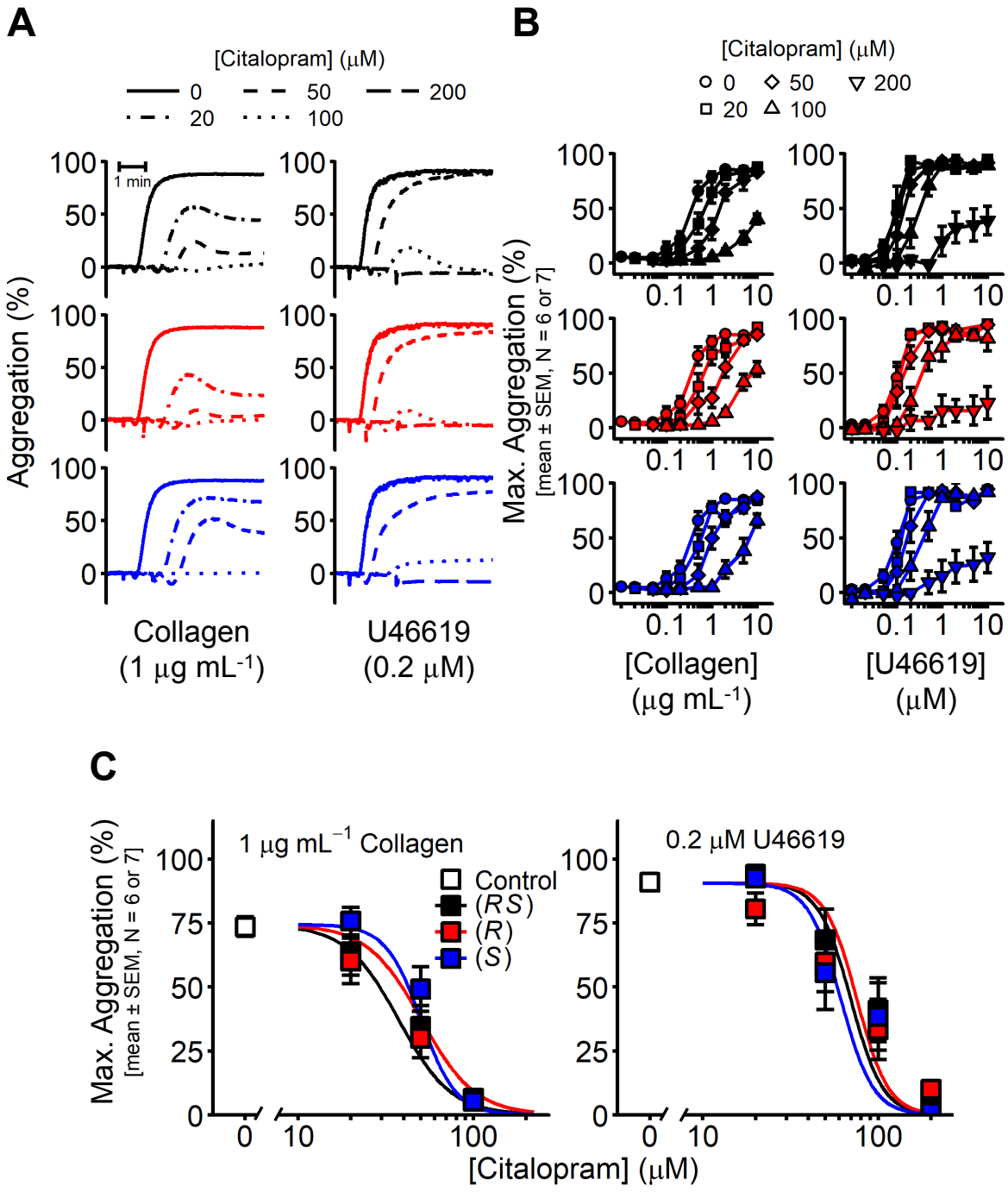

Figure. 3.4 Citalopram inhibits platelet aggregation. **(A)** Representative aggregation traces, illustrating concentration-dependent inhibition of collagen-induced or U46619-induced platelet aggregation by (*RS*)-, (*R*)- and (*S*)-citalopram (black, red and blue lines, respectively). **(B)** Collagen and U46619 agonist-response curves, reporting the maximum extent of aggregation (Max. Aggregation) of platelets pre-incubated with (*RS*)-, (*R*)- and (*S*)-citalopram (0, 20, 50, 100 & 200 μM). **(C)** Effects of (*RS*)-, (*R*)- and (*S*)-citalopram on Max. Aggregation induced by a fixed concentration of either collagen (1 μg mL^{-1}) or U46619 (0.2 μM) were fitted according to the four-parameter logistic (4PL) model (collagen: N = 7 blood donors, U46619: N = 6 blood donors).

3.2.3 Citalopram inhibits thromboxane A_2 synthesis

TxA_2 synthesis was indirectly measured by quantifying the generation of its stable metabolite, TxB_2. Platelets were pre-incubated with various (*RS*)-, (*R*)- and (*S*)-citalopram concentrations (0, 5, 10, 20, 50, 100 & 200 μM) for approximately 5 minutes before stimulation with 1 μg mL^{-1} collagen. pIC_{50} values are shown in Table 3.1 and Figure 3.8. (*RS*)-, (*R*)- and (*S*)-citalopram all inhibited TxB_2 generation at micromolar concentrations (Figure 3.5). 2-way ANOVA (Effect 1 (fixed) = citalopram {(*RS*), (*R*), (*S*)}; Effect 2 (random) = donor {N = 6}) indicated no difference in the pIC_{50} values of the three citalopram preparations ($P = 0.60$, F = 0.54, df = 2, 10. H_0: $\mu_{RS}=\mu_R=\mu_S$; H_1: $\mu_{RS} \neq \mu_R \neq \mu_S$). Aggregometry data obtained from these experiments provided independent replicates for inhibition of collagen-induced aggregation, which match previous results in Chapter 3.4: $pIC_{50(RS)}$ = 4.43 ± 0.08; $pIC_{50(R)}$ = 4.48 ± 0.07; $pIC_{50(S)}$ = 4.33 ± 0.06.

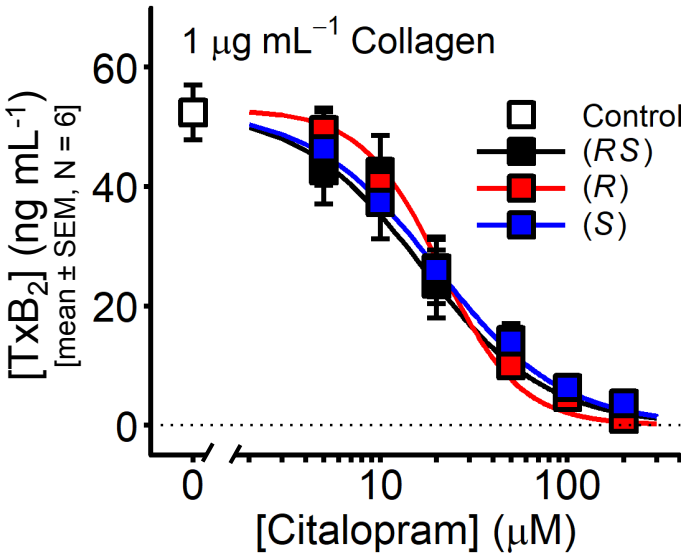

Figure. 3.5 Thromboxane A_2 (TxA_2) synthesis was measured by quantifying supernatant levels of its stable metabolite, TxB_2. Platelets were stimulated with collagen (1 μg mL^{-1}) for 6 minutes under aggregometry conditions (37°C, 1,000 rpm) and supernatants isolated. Full concentration-response curves were obtained from platelets pre-incubated for approximately 5 minutes with (*RS*)-, (*R*)- or (*S*)-citalopram (0, 5, 10, 20, 50, 100 & 200 μM) (N = 6 blood donors).

3.2.4 Citalopram inhibits static platelet adhesion

The effect of (*RS*)-, (*R*)- and (*S*)-citalopram on platelet adhesion to different adhesive ligands was determined under static conditions. Full concentration-response curves were obtained using 0, 10, 30, 50, 100, 200 & 300 μM citalopram for six adhesive ligands: Horm® collagen; collagen III; collagen-related peptide (CRP); fibrinogen; GFOGER (a peptide sequence, which is a integrin $\alpha_2\beta_1$-selective ligand, (Knight et al., 2000)) and thrombin. For negative controls, adhesion to bovine serum albumin (BSA) and GPP_{10} peptides (Smethurst et al., 2006) was also measured (Figure 3.6). Due to logistical constraints, all conditions could not be measured in a single blood donor. Hence, in seven donors (*RS*)-citalopram was tested, in two donors (*R*)- and (*S*)-citalopram were tested, and in two donors (*RS*)-, (*R*)- and (*S*)-citalopram were tested.

(*RS*)-, (*R*)- and (*S*)-citalopram inhibited platelet adhesion to every ligand tested. Inhibition was observed at micromolar concentrations (Figure 3.6). Concentration-response curves were fitted to the 4PL model and the pIC_{50} values recorded (Table 3.1 & Figure 3.8). 3-way ANOVA (Effect 1 (fixed) = citalopram {(*RS*), (*R*), (*S*)}; Effect 2 (fixed) = ligand {Horm® collagen, collagen III, CRP, fibrinogen, GFOGER, thrombin}; Effect 3 (random) = donor {N = 8-9 (*RS*) and N = 4 (*R*), (*S*)}) suggested there was a slight difference in inhibitory potency between (*RS*)-, (*R*)- and (*S*)-citalopram ($P = 0.058$).

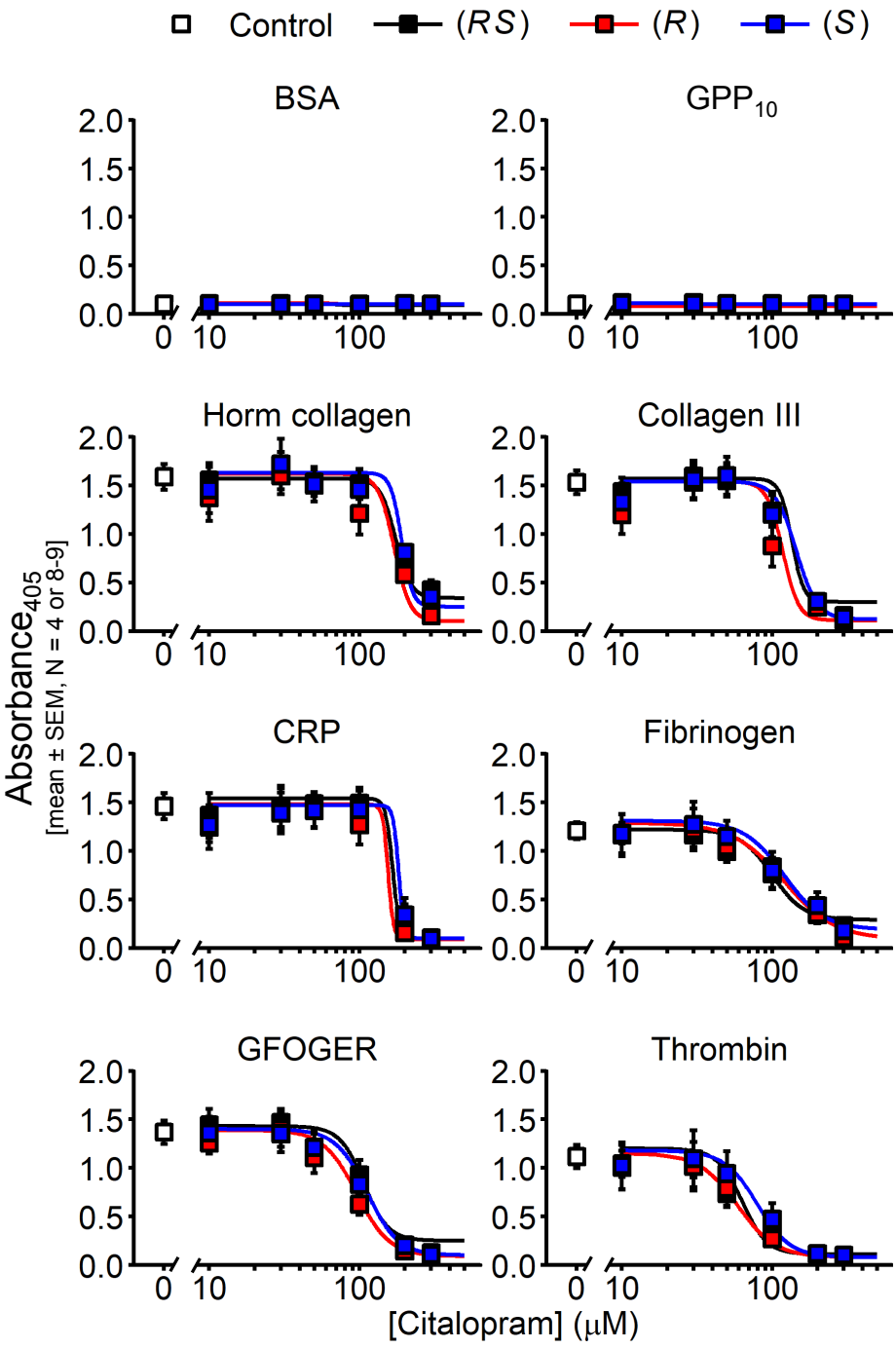

Figure. 3.6 Static adhesion of platelets to Horm® collagen, collagen III, collagen-related peptide (CRP), fibrinogen, GFOGER and thrombin was determined by measuring absorbance at 405 nm, which is proportional to acid phosphatase levels of the adherent cell population. Bovine serum albumin (BSA) and GPP_{10} were used as negative controls. Full concentration-response curves were obtained from platelets pre-incubated for approximately 5 minutes with (*RS*)-, (*R*)- or (*S*)-citalopram (0, 10, 30, 50, 100, 200 & 300 μM). For each ligand, (*R*) and (*S*): N = 4 blood donors, (*RS*): N = 8-9 blood donors.

3.2.5 Micromolar citalopram concentrations do not cause cytotoxicity

(*RS*)-, (*R*)- and (*S*)-citalopram inhibited every platelet function tested with similar potencies and at micromolar concentrations. An experiment was therefore designed to determine whether the citalopram concentrations used in these experiments were mediating their effects through cell cytotoxicity. Platelets were pre-incubated for 10 minutes with (*RS*)-citalopram (0, 10, 20, 50, 100 & 200 μM), before quantifying the levels of supernatant lactate dehydrogenase (LDH). (*RS*)-citalopram did not cause LDH release at any concentration tested (Figure 3.7).

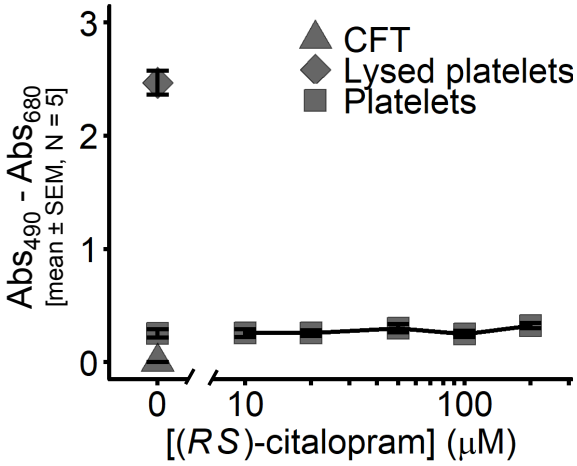

Figure. 3.7 Cell cytotoxicity was measured by quantifying supernatant levels of lactate dehydrogenase (LDH). Platelets were pre-incubated for 10 minutes with (*RS*)-citalopram (0, 10, 20, 50, 100 & 200 μM). Calcium-free Tyrode's (CFT) and lysed platelets were used as negative and positive controls, respectively (N = 5 blood donors). Absorbance ($Abs_{490} - Abs_{680}$) was used to indirectly measure levels of LDH.

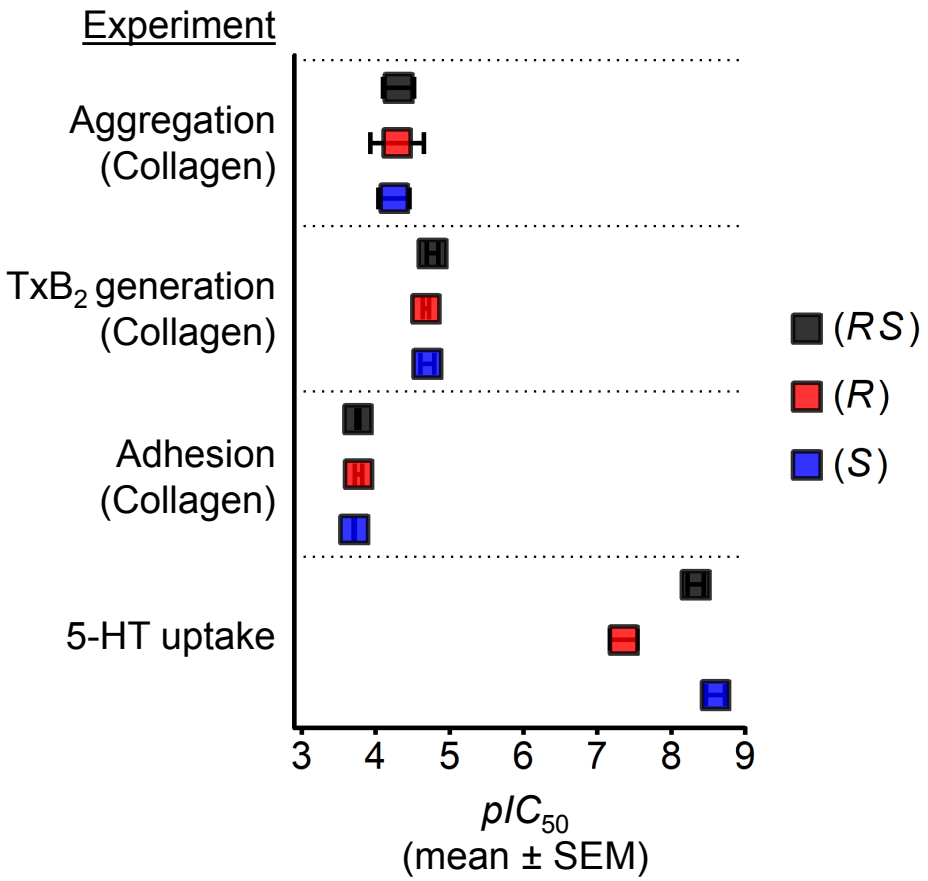

Figure. 3.8 Summary figure, demonstrating the differing inhibitory potencies (pIC_{50} values, mean ± SEM) between 5-HT uptake by (*RS*)-, (*R*)- and (*S*)-citalopram (Figure 3.2) and platelet aggregation (Figure 3.4), thromboxane B_2 (TxB_2) generation (Figure 3.5) and adhesion to Horm® collagen (Figure 3.6). Unobserved error bars lie within the symbols. The agonist used to induce a functional response is mentioned in brackets underneath each experiment.

		pIC_{50} mean ± SEM (N)			
Function	**Agonist/ligand**	**(*RS*)**	**(*R*)**	**(*S*)**	**Eudysmic ratio**
5-HT uptake	5-HT	8.33 ± 0.11 (13)	7.36 ± 0.19 (13)	8.60 ± 0.13 (13)	17.37
Aggregation	Horm® collagen	4.31 ± 0.21 (7)	4.29 ± 0.36 (7)	4.25 ± 0.21 (7)	0.91
	U46619	4.15 ± 0.27 (6)	4.12 ± 0.22 (6)	4.20 ± 0.29 (6)	1.20
TxB_2 generation	Horm® collagen	4.77 ± 0.08 (6)	4.68 ± 0.04 (6)	4.70 ± 0.09 (6)	1.05
Static adhesion	Horm® collagen	3.76 ± 0.02 (9)	3.77 ± 0.05 (4)	3.72 ± 0.01 (4)	0.89
	Collagen III	3.87 ± 0.04 (9)	3.93 ± 0.06 (4)	3.84 ± 0.02 (4)	0.81
	CRP	3.78 ± 0.04 (8)	3.81 ± 0.05 (4)	3.74 ± 0.01 (4)	0.85
	GFOGER	3.97 ± 0.03 (9)	4.02 ± 0.05 (4)	3.95 ± 0.03 (4)	0.85
	Fibrinogen	4.00 ± 0.07 (9)	3.92 ± 0.04 (4)	3.92 ± 0.05 (4)	1.00
	Thrombin	4.20 ± 0.05 (9)	4.23 ± 0.07 (4)	4.10 ± 0.06 (4)	0.63

Table 3.1 Summary pIC_{50} values (mean ± SEM (N)) for (*RS*)-, (*R*)- and (*S*)-citalopram on platelet aggregation, thromboxane B_2 (TxB_2) generation, static adhesion and 5-HT uptake. To calculate the eudysmic ratio of citalopram isomers, pIC_{50} values were converted to IC_{50} values and the molar concentration of (*R*)-citalopram divided by the molar concentration of (*S*)-citalopram.

3.3 Discussion

3.3.1 Overview

The aims of this chapter were to characterise the effects of citalopram on *in vitro* platelet functional responses, and determine if these effects are mediated through inhibition of SERT. Results presented in this chapter demonstrate that *in vitro* inhibition of SERT-mediated 5-HT uptake by citalopram does not correlate with inhibition of other platelet functional responses. Citalopram had a eudysmic (*R*)/(*S*) potency ratio of approximately 17 for blocking SERT-mediated 5-HT uptake, whereas the (*S*)- and (*R*)-citalopram isomers inhibited platelet aggregation, TxA_2 synthesis and adhesion with similar potencies (Table 3.1 and Figure 3.8). Furthermore, nanomolar concentrations of (*RS*)-, (*R*)- and (*S*)-citalopram inhibited 5-HT uptake, but did not affect other platelet functions, which were only inhibited at micromolar concentrations. Based on the evidence presented in this chapter, it is concluded that *in vitro* platelet inhibition by citalopram is not dependent on the inhibition of SERT and that other mechanisms must be identified to explain citalopram's antiplatelet effects.

3.3.2 Allosteric inhibition of serotonin uptake by citalopram

Citalopram has previously been described as an allosteric serotonin reuptake inhibitor (Zhong et al., 2012). A complex mechanism of action has been proposed, involving both a distinct primary binding site and an alternative allosteric binding site on SERT. It has been suggested that binding of either (*R*)- or (*S*)-citalopram to the allosteric site has differential effects on the affinity of the compounds at the primary binding site (Sánchez, 2006). This proposal provides a mechanistic explanation for the more rapid onset of action of (*S*)-citalopram in animal models of depression (Montgomery et al., 2001), and greater potency in clinical trials (Moore et al., 2005). However, both (*R*)- and (*S*)-citalopram slow the dissociation of [^{3}H]-(*S*)-citalopram from SERT at concentrations ranging between 1-200 μM (Plenge et al., 2007, Jacobsen et al., 2014). Such levels are well in excess of plasma concentrations of citalopram (120-600 nM), of which about 50-80% is bound to plasma proteins (Milne and Goa, 1991, Parker and Brown, 2000). Therefore, clinical plasma concentrations of either (*RS*)-citalopram or (*S*)-citalopram that block 5-HT uptake will have neither the proposed allosteric effect on SERT, nor the antiplatelet effects reported in this and other chapters (discussed further in Chapter 7). By contrast, results in this chapter are consistent with a simple mechanism of action, in which both (*R*)- and (*S*)-isomers

bind to a single primary site on SERT, but with differing affinities. Hill coefficients of unity support this hypothesis, suggesting that non-cooperative binding of citalopram to SERT inhibits 5-HT uptake.

3.3.3 SERT-independent platelet inhibition

The low (*R*) and high (*S*) isomer inhibitory potencies of (*RS*)-citalopram for 5-HT uptake provided a previously untested approach to evaluate the importance of functional SERT during platelet activation. Results in this chapter are the first to demonstrate the inhibitory effects of (*R*)-citalopram on platelets, and confirm the differing inhibitory potencies between citalopram isomers for 5-HT uptake into platelets (Figure 3.2). However, there was no difference in the inhibitory potencies of (*R*)-citalopram and (*S*)-citalopram for either platelet aggregation, TxA_2 synthesis or adhesion. Furthermore, 5-HT uptake was blocked by both isomers at nanomolar concentrations, whereas there was little if any functional platelet inhibition. The onset of (*RS*)-citalopram-induced inhibition of platelet aggregation was also instantaneous (Figure 3.3), contrary to patients taking daily doses of paroxetine, where platelet inhibition was only observed after 7-14 days (Hergovich et al., 2000). These findings suggest that unlike the effects observed with long-term *ex vivo* studies, citalopram-mediated platelet inhibition *in vitro* cannot be explained by the gradual depletion of 5-HT stores following SERT blockade.

Previous studies have reported antiplatelet effects of (*RS*)-citalopram *in vitro*, following incubation times of 3-10 minutes (Carneiro et al., 2008, Tseng et al., 2010, 2013). The authors from these studies suggest that citalopram binding to SERT suppresses platelet activation through a mechanism distinct from gradual 5-HT store depletion. In this putative mechanism, SERT blockade prior to platelet activation prevents the rapid uptake of 5-HT released from dense granules. Such increases in cytoplasmic 5-HT have been associated with augmenting platelet aggregation and alpha granule release through the covalent attachment of 5-HT to small GTPases, a process referred to as serotonylation (Walther et al., 2003). By binding SERT and blocking rapid 5-HT uptake, citalopram could, therefore, suppress *in vitro* platelet activation through impaired serotonylation. However, serotonylation does not explain how in this chapter, citalopram only inhibited platelet functions beyond the nanomolar concentrations required to inhibit SERT-mediated 5-HT uptake. On the contrary, results from this chapter conclude that *in vitro* platelet inhibition by citalopram is mediated through an unidentified SERT-independent mechanism.

(*RS*)-citalopram has previously been reported to specifically inhibit several collagen-induced platelet functional responses, including aggregation, granule release and TxA_2

synthesis (Tseng et al., 2010). Results in this chapter show citalopram also inhibits both U46619-induced aggregation and adhesion to the $\alpha_2\beta_1$-selective ligand, GFOGER. These observations suggest that citalopram inhibits a mutual factor, downstream of multiple platelet receptors. Inhibitory effects of (*RS*)-citalopram on platelet-rich plasma (PRP) support this hypothesis, citing impaired phosphoinositide 3-kinase (PI3K) activation, following stimulation of the P2Y12 receptor (Tseng et al., 2013). Chapters 4 and 5 of this thesis investigate the effects of citalopram on intracellular signal transduction pathways, subsequent to the stimulation of major platelet receptors.

It is important to note that with the exception of platelet aggregation, all the experiments performed in this chapter and several in upcoming chapters measure the platelet response to agonists at a single fixed time point. Further studies that make numerous recordings over a given period of time could provide more detailed information regarding the effects of citalopram on the kinetics of platelet activation. For example, live cell imaging of platelets undergoing activation could determine the effects of citalopram on filopodia and lamellipodia formation.

This chapter concludes that *in vitro* platelet inhibition by citalopram is not due to its conventional mechanism of blocking SERT-mediated 5-HT uptake.

Chapter 4
The effects of citalopram on calcium signalling

4.1 Background

Citalopram inhibits several platelet functions, including aggregation, thromboxane A_2 (TxA_2) synthesis and adhesion (Chapter 3). These functions are all mediated by increasing the cytosolic concentration of calcium ($[Ca^{2+}]_{cyt}$). This chapter examines the effects of citalopram on the $[Ca^{2+}]_{cyt}$, Ca^{2+}-dependent signalling processes and downstream cellular functions.

4.1.1 Calcium homeostasis

Ca^{2+} is an important second messenger in various cells, and many platelet agonists induce increases in $[Ca^{2+}]_{cyt}$. Elevated $[Ca^{2+}]_{cyt}$ is vital to platelet activation, mediating cytoskeletal reorganisation, granule release, integrin $\alpha_{IIb}\beta_3$ activation and TxA_2 synthesis (Varga-Szabo et al., 2009, Bergmeier and Stefanini, 2009). $[Ca^{2+}]_{cyt}$ increases in platelets are mediated through three distinct mechanisms: 1) The intracellular release of Ca^{2+} from the dense tubular system (DTS) or acidic stores, 2) extracellular Ca^{2+} entry across the plasma membrane following Ca^{2+} release from the DTS, known as store-operated calcium entry (SOCE), and 3) store-independent Ca^{2+} entry across the plasma membrane (non-SOCE) (Figure 4.1).

Intracellular Ca^{2+} release, SOCE and some forms of non-SOCE are initiated by agonists that bind cell surface receptors, activating downstream phospholipase C (PLC). There are two PLC isoforms that predominantly mediate platelet activation: PLCγ2, which is activated via tyrosine phosphorylation signalling pathways, including glycoprotein VI (GPVI), and PLCβ, which is activated via Gα_q-coupled receptors, such as the TxA_2 receptor (Varga-Szabo et al., 2009). Both PLC isoforms hydrolyse membrane-associated phosphatidylinositol-4,5-bisphosphate (PIP_2) to inositol-1,4,5-trisphosphate (IP_3) and 1,2-diacylglycerol (DAG). IP_3 and DAG increase $[Ca^{2+}]_{cyt}$ through two distinct pathways. IP_3 binds to IP_3 receptors, which are tetrameric ligand-gated Ca^{2+} channels, present on the platelet DTS. On binding IP_3, the IP_3 receptor channel opens, allowing Ca^{2+} efflux

from DTS stores into the cytosol (O'Rourke et al., 1985). Ca^{2+} release from the DTS causes Ca^{2+} dissociation from the intraluminal EF domains of stromal interaction molecule-1 (STIM1) (Grosse et al., 2007). STIM1 subsequently mediates a conformational change in the calcium-release activated calcium modulator-1 (CRACM1/Orai1) pore subunits of the CRAC channel, permitting SOCE (Zhang et al., 2005, Navarro-Borelly et al., 2008).

Acidic compartments within lysosomes and dense granules provide an additional source of intracellular Ca^{2+} (López et al., 2006, Rosado, 2011). Thrombin or collagen-related-peptide (CRP) increase levels of nicotinic acid adenine dinucleotide phosphate (NAADP), which mediates Ca^{2+} release through putative binding to two-pore channel 2 (TPC2) on dense granules (Coxon et al., 2012a, Ambrosio et al., 2015). However, comparative to the DTS, acidic store release is small and its underlying mechanism undetermined.

Non-SOCE is principally mediated by DAG and extracellular adenosine triphosphate (ATP), which bind and open either the transient receptor potential cation channel, subfamily C, member 6 (TRPC6) or the purinergic receptor ligand-gated ion channel 1 (P2X1), respectively (MacKenzie et al., 1996, Hassock et al., 2002).

In unstimulated platelets, Ca^{2+} entry into the cytosol across plasma and store membranes is counteracted by plasma membrane calcium ATPases (PMCAs) and sarcoplasmic/endoplasmic reticulum calcium ATPases (SERCAs), respectively (Redondo et al., 2005), maintaining a basal $[Ca^{2+}]_{cyt}$ between 40-80 nM (Vicari et al., 1994). Basal $[Ca^{2+}]_{cyt}$ are thought to be restored following agonist-induced Ca^{2+} signalling by the plasma membrane-bound Na^+/Ca^{2+} exchanger-3 (NCX3) (Roberts et al., 2012).

To summarise, agonist-induced Ca^{2+} store release and Ca^{2+} entry are mediated through various cell surface receptors and intracellular signal transduction pathways (Figure 4.1). The resulting increase in $[Ca^{2+}]_{cyt}$ is essential for platelet activation.

4.1.2 Rap1 and its regulation

$[Ca^{2+}]_{cyt}$ regulates Ras-related protein 1 (Rap1), a small GTPase. The two Rap1 isoforms, Rap1A (≈125,000 per platelet) and Rap1B (≈300,000 per platelet), are the most abundant small GTPases in platelets (Burkhart et al., 2012, 2014), and are also found in other cells, including leukocytes and endothelial cells (Wittchen et al., 2005, Fujita et al., 2005).

Rap1 exists in three interchangeable forms: inactive unbound Rap1, inactive guanosine diphosphate (GDP)-bound Rap1 and active guanosine triphosphate (GTP)-bound Rap1. Intrinsic GDP/GTP dissociation from Rap1 typically results in the subsequent binding of the 10-fold more abundant GTP (Traut, 1994, Stefanini and Bergmeier, 2016). However, in resting platelets, GDP/GTP dissociation from Rap1 is a slow process and Rap1 hydrolysis

of GTP to GDP is upregulated by the Ras GTPase-activating protein-3 (RASA-3, also known as *GAPIII*). This results in the majority of Rap1 in resting platelets existing in the inactive GDP-bound state (Stefanini et al., 2015).

During platelet activation, increases in $[Ca^{2+}]_{cyt}$ activate the calcium- and diacylglycerol-regulated guanine nucleotide exchange factor 1 (CalDAG-GEFI, also known as *RASGRP2*) (Figure 4.1). CalDAG-GEFI binds Ca^{2+} through a pair of EF domains within its C-terminal (Figure 2.9), inducing a conformational change which is essential to its activity (Vicari et al., 1994, Kawasaki et al., 1998). The C1 domain of CalDAG-GEFI has a very weak affinity (K_d = 2.89 ± 0.24 μM) for binding DAG analogues, and thus DAG is not believed to mediate CalDAG-GEFI activation (Czikora et al., 2016). Activated CalDAG-GEFI catalyses GDP dissociation from Rap1, enhancing the rate of Rap1 association with the more abundant GTP (Lienhard, 1973, Bos et al., 2007). This increases the amount of Rap1-GTP, despite the GTPase enhancing the activity of RASA-3. Rap1-GTP associates with the Rap1-GTP–interacting adaptor molecule (RIAM), forming a Rap1-RIAM-talin complex, which relocates talin to the plasma membrane (Lee et al., 2009). Relocalisation of Rap1-RIAM-talin to the plasma membrane allows talin to outcompete the α integrin subunit tail for binding to the β integrin subunit tail. Separation of the α and β integrin tails induces a conformational change in the integrin complex, increasing extracellular ligand-binding affinity (Moser et al., 2009). Murine platelets lacking Rap1B show reduced binding and spreading on immobilised fibrinogen, indicating impaired inside-out signalling through integrin $\alpha_{IIb}\beta_3$. This deficiency also suppresses platelet aggregation, prolongs tail bleeding times and reduces arterial thrombus formation (Chrzanowska-Wodnicka et al., 2005). Blocking Rap1 activation is associated with reduced granule secretion and impaired clot retraction (Stefanini et al., 2012). CalDAG-GEFI deficient mice have a similar platelet phenotype to Rap1 knockout models, with defects in aggregation, $\alpha_{IIb}\beta_3$ activation, and thrombus formation under flow (Crittenden et al., 2004, Bernardi et al., 2006). Despite prolonged tail bleeding times, CalDAG-GEFI knockout mice do not present with spontaneous haemorrhage or undergo collagen-induced thrombosis (Crittenden et al., 2004). Recent studies identified patients with CalDAG-GEFI mutations, which result in either loss of protein function or expression (Canault et al., 2014, Kato et al., 2016, Lozano et al., 2016, Bermejo et al., 2017, Sevivas et al., 2017, Westbury et al., 2017). These patients present with bleeding diathesis, as well as reduced Rap1 activation, integrin $\alpha_{IIb}\beta_3$ activation, platelet aggregation and *in vitro* thrombus formation, despite typical agonist-induced increases in $[Ca^{2+}]_{cyt}$. Taken together, the studies described above demonstrate that both CalDAG-GEFI and Rap1 are key orchestrators of Ca^{2+}-mediated platelet activation.

4.1.3 Calcium signalling in neutrophils

CalDAG-GEFI, Rap1 and PLCβ are also expressed in neutrophils, which exhibit similar activation pathways to platelets (M'Rabet et al., 1998, Crittenden et al., 2004, Bergmeier et al., 2007). Platelet-activating factor (PAF) activates the neutrophil PLCβ isoform downstream of the PAF receptor (PAF-R), causing increases in the $[Ca^{2+}]_{cyt}$, CalDAG-GEFI-dependent Rap1-GTP formation and the transition of integrins to a high-affinity binding state (M'Rabet et al., 1998, Bergmeier et al., 2007). High-affinity integrin $\alpha_M\beta_2$ (Macrophage-1 antigen (Mac-1), CD11b/18) binds endothelial intracellular adhesion molecules (ICAM)-1/2, contributing towards neutrophil adhesion and crawling in search of sites for extravasation (Halai et al., 2014). High-affinity $\alpha_M\beta_2$ also binds and adheres to fibrinogen, which plays an important role in innate antimicrobial responses (Flick et al., 2004, Bergmeier et al., 2007). Neutrophils from humans with loss-of-function CalDAG-GEFI mutations and from CalDAG-GEFI knockout mice display normal increases in $[Ca^{2+}]_{cyt}$ in response to agonists, despite impaired Rap1 activation, diminished adhesion or binding to blood vessels or fibrinogen, respectively, and reduced extravasation into inflammatory sites (Bergmeier et al., 2007, Lozano et al., 2016, Sevivas et al., 2017).

Taken together, these studies demonstrate that as with platelets, increasing the $[Ca^{2+}]_{cyt}$ in neutrophils mediates the conversion of integrins to a high-affinity binding state. This integrin transition promotes cell adhesion and is largely driven by increasing the levels of active, GTP-bound Rap1, via the Ca^{2+}-dependent CalDAG-GEFI.

4.1.4 Aims

Experiments in this chapter aim to:

1. Investigate the effects of racemic (*RS*) citalopram on Ca^{2+} signalling during platelet and neutrophil activation by measuring agonist-induced increases in $[Ca^{2+}]_{cyt}$ derived from intracellular stores and subsequent Rap1 activation.

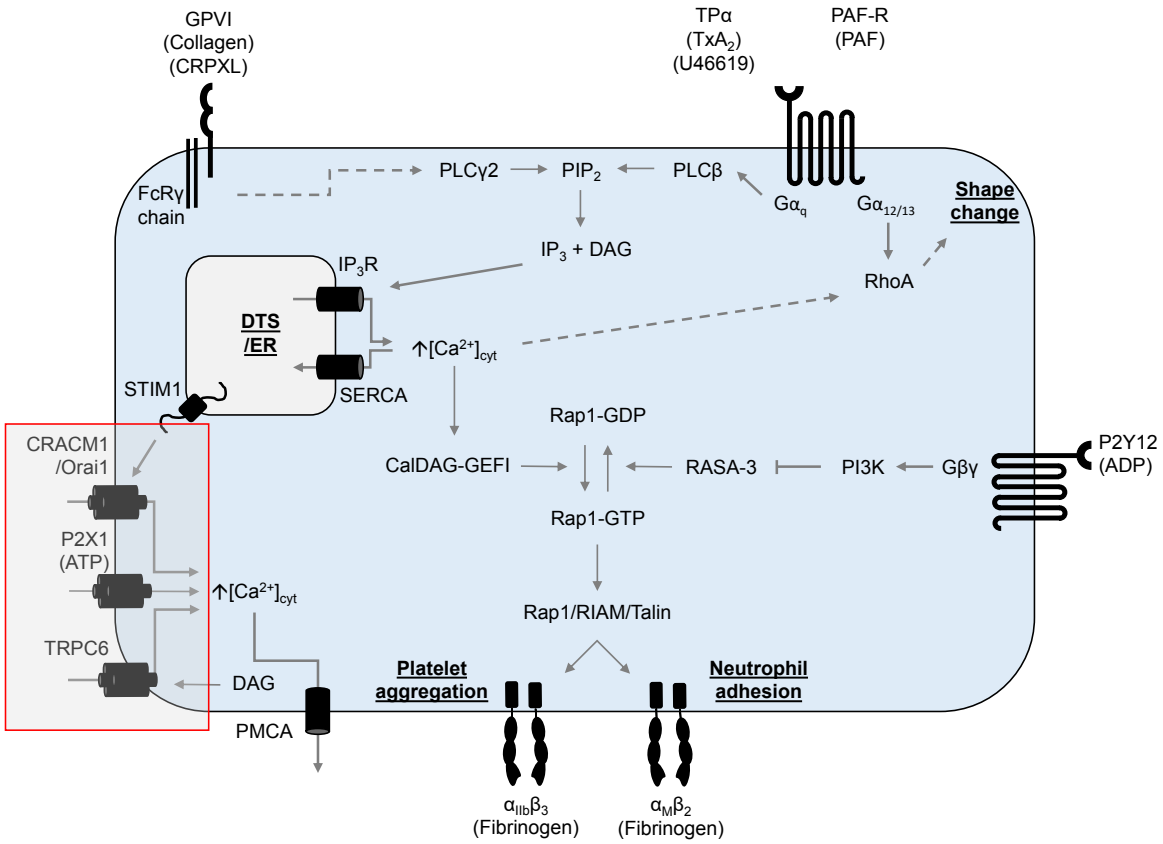

Figure. 4.1 Calcium signalling in platelets and neutrophils. Increases in cytosolic calcium concentration ($[Ca^{2+}]_{cyt}$) are initially mediated through the binding of extracellular ligands to surface receptors. Glycoprotein VI (GPVI), is associated with the Fc receptor γ-chain (FcRγ-chain), which upon stimulation with either collagen or cross-linked collagen-related peptide (CRPXL) mediates downstream activation of phospholipase C (PLC)γ2. The Gα_q-coupled thromboxane A_2 (TxA_2) receptor (TPα) is activated by either TxA_2, or its synthetic analogue U46619. The Gα_q-coupled platelet-activating factor receptor (PAF-R) is activated by PAF. Ligand-binding to TPα or PAF-R results in downstream activation of PLCβ. Both PLC isoforms hydrolyse phosphoinositide-4,5-bisphosphate (PIP_2) into inositol-1,4,5-trisphosphate (IP_3) and 1,2-diacylglycerol (DAG). IP_3 binds IP_3 receptors (IP_3R) on the platelet dense tubular system (DTS) or the neutrophil endoplasmic reticulum (ER), causing the release of intracellular Ca^{2+} stores into the cytosol. Store depletion mediates store-operated Ca^{2+} entry (SOCE) through interactions between stromal interaction molecule 1 (STIM1) and the calcium-release activated calcium modulator 1 (CRACM1/Orai1) pore subunits. SOCE and non-SOCE via P2X1 and the transient receptor potential cation channel, subfamily C, member 6 (TRPC6) are highlighted in red. This is due to the lack of extracellular Ca^{2+} in forthcoming experiments, where platelets and neutrophils were suspended in calcium-free Tyrode's (CFT). Increases in $[Ca^{2+}]_{cyt}$ activate the calcium- and diacylglycerol-regulated guanine nucleotide exchange factor 1 (CalDAG-GEFI), increasing Rap1-GTP formation. Rap1-GTP is also upregulated by P2Y12 stimulation, which activates phosphoinositide 3-kinase (PI3K), inhibiting Ras GTPase-activating protein 3 (RASA-3). Rap1-GTP complexes with Rap1-GTP–interacting adaptor molecule (RIAM) and talin, activating integrins $\alpha_{IIb}\beta_3$ or $\alpha_M\beta_2$ on platelets and neutrophils, respectively. Increases in $[Ca^{2+}]_{cyt}$ also indirectly mediate platelet shape change through RhoA. Ca^{2+} is removed from the cytosol by sarcoplasmic/endoplasmic reticulum calcium ATPases (SERCAs) and plasma membrane calcium ATPases (PMCAs) on the DTS/ER and plasma membrane, respectively. Receptor agonists are mentioned within brackets. Grey dashed lines indicate intermediate steps. This is an original image.

4.2 Results

4.2.1 Citalopram inhibits CRPXL-induced, but not U46619-induced calcium release from intracellular stores

Ca^{2+} is a common and well-recognised secondary mediator of intracellular signalling, and increasing the $[Ca^{2+}]_{cyt}$ in platelets is a key to their activation.

Preliminary experiments (N = 1 blood donor) identified concentrations of either the GPVI agonist, cross-linked collagen-related peptide (CRPXL, 0.5 μg ml^{-1}), or the TxA_2 mimetic, U46619 (0.2 μM) that induce near-maximal increases in $[Ca^{2+}]_{cyt}$ (Figure 4.2). Agonist-induced changes in $[Ca^{2+}]_{cyt}$ were then monitored in platelets pre-treated for approximately 5 minutes with a range of citalopram concentrations (0, 10, 20, 50, 100 & 200 μM) (Figure 4.3B,D). CRPXL (0.5 μg ml^{-1}) and U46619 (0.2 μM) induced a maximum increase in $[Ca^{2+}]_{cyt}$ of 199 ± 14 nM and 183 ± 16 nM, respectively (N = 7 blood donors). CRPXL-induced increases in $[Ca^{2+}]_{cyt}$ were abolished by citalopram pre-treatment (Figure 4.3A-B): pIC_{50} = 4.34 ± 0.09 (N = 7 blood donors). By contrast, citalopram had no effect on U46619-induced increases in $[Ca^{2+}]_{cyt}$ at concentrations up to 200 μM (Figure 4.3C-D) (N = 7 blood donors). On one separate occasion, U46619-induced aggregation was measured in the same preparation of Fura-2-loaded platelets that were used for Ca^{2+} measurements. Control platelets responded normally to 0.2 μM U46619 (Figure 4.3E). In platelets treated with citalopram (200 μM), aggregation was abolished, but the increase in $[Ca^{2+}]_{cyt}$ was unaffected. These data suggest that citalopram inhibits U46619-mediated platelet aggregation downstream of Ca^{2+} release from intracellular stores. Of note, although aggregation was inhibited, evidence of shape change remained. This observation was also made in previous experiments (Figures 3.3 & 3.4).

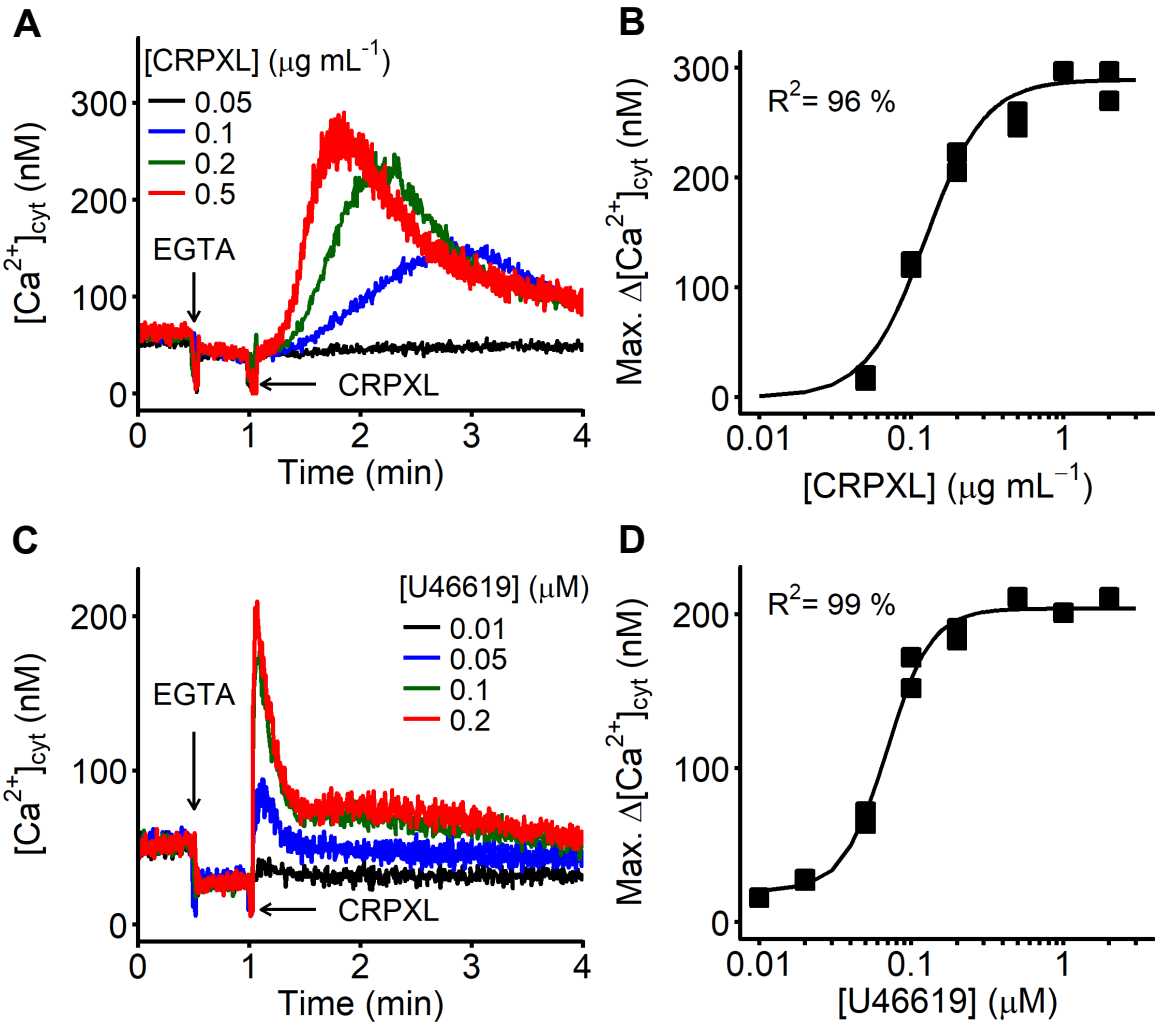

Figure. 4.2 Calcium (Ca^{2+}) release from intracellular stores was monitored in Fura-2-loaded platelets. Preliminary experiments (N = 1 blood donor) identified concentrations of **(A-B)** cross-linked collagen-related peptide (CRPXL) (0.5 μg ml^{-1}) or **(C-D)** U46619 (0.2 μM) which induce near-maximal increases in $[Ca^{2+}]_{cyt}$. After the addition of agonist, the $[Ca^{2+}]_{cyt}$ was recorded for 3 minutes. The maximum increase in $[Ca^{2+}]_{cyt}$ following agonist addition (Max. $\Delta[Ca^{2+}]_{cyt}$) was used to generate concentration-response curves, using the four-parameter logistic (4PL) model (N = 1 blood donor). R^2 represents the coefficient of determination.

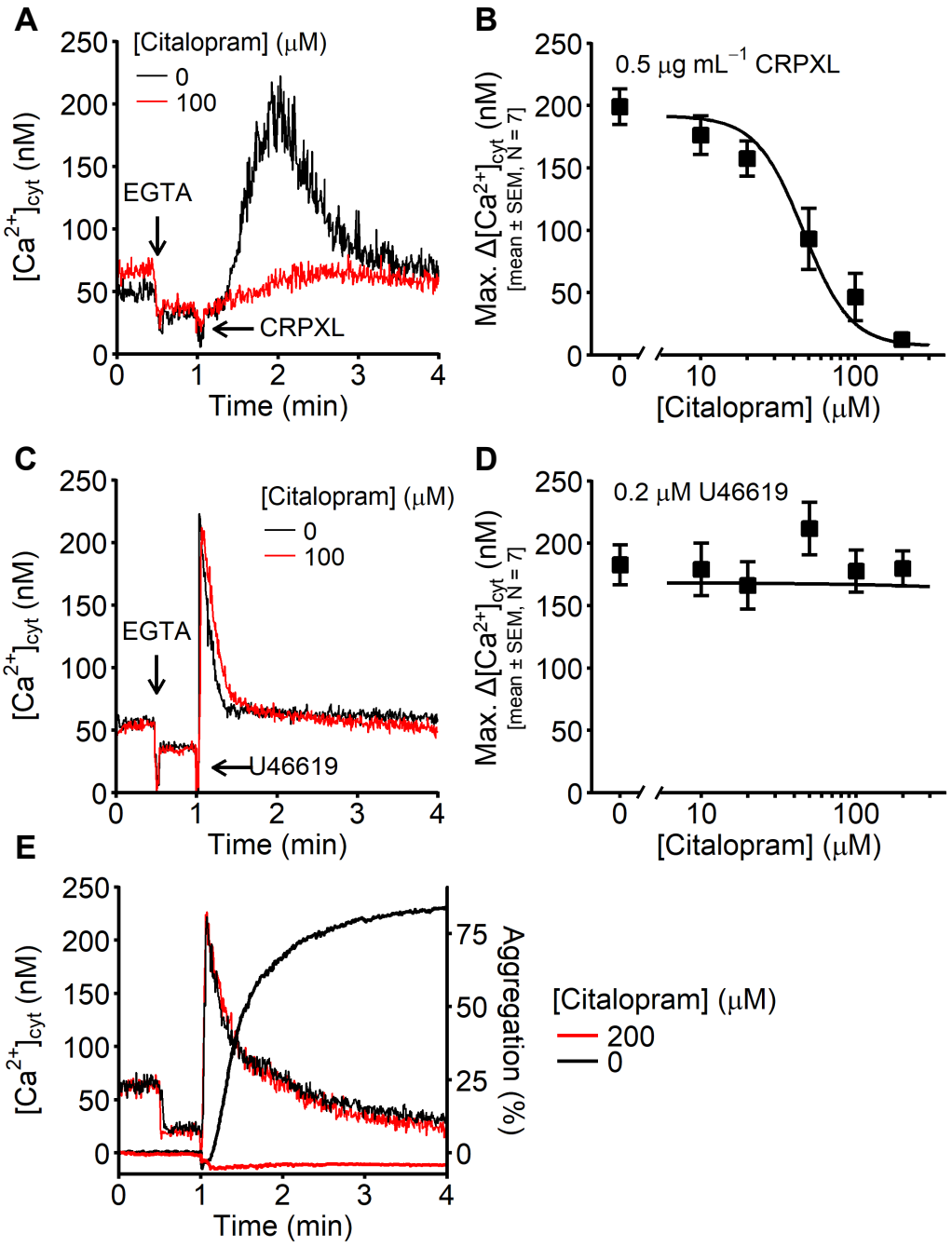

Figure. 4.3 Calcium (Ca^{2+}) release from intracellular stores in either untreated, or citalopram-treated platelets. Example traces are shown for both **(A)** cross-linked collagen-related peptide (CRPXL)-stimulated (0.5 μg ml^{-1}) and **(C)** U46619-stimulated (0.2 μM) platelets, either untreated or pre-treated with citalopram (100 μM) for approximately 5 minutes. After the addition of agonist, the $[Ca^{2+}]_{cyt}$ in platelets pre-incubated with citalopram (0, 10, 20, 50, 100 & 200 μM) was recorded for 3 minutes. **(B,D)** The maximum increase in $[Ca^{2+}]_{cyt}$ following agonist addition (Max. $\Delta[Ca^{2+}]_{cyt}$) was used to generate concentration-response curves, using the four-parameter logistic (4PL) model (N = 7 blood donors). **(E)** In a separate experiment, using platelets from the same blood donor on the same experimental day, $[Ca^{2+}]_{cyt}$ and aggregation were separately recorded following pre-incubation with or without citalopram (200 μM) and stimulation with U46619 (0.2 μM) (N = 1 blood donor).

4.2.2 Citalopram inhibits ionomycin-induced platelet aggregation

Further experiments were performed to confirm that citalopram could inhibit platelet aggregation downstream of Ca^{2+} store release, using the Ca^{2+} ionophore, ionomycin. Preliminary experiments (N = 1 blood donor) identified the concentration of ionomycin (0.5 μM) that induced near-maximal platelet aggregation (Figure 4.4A-B). Platelets were then pre-treated with citalopram (0, 50, 100 & 200 μM) for approximately 5 minutes, before stimulation with ionomycin (0.5 μM). Ionomycin-induced platelet aggregation was inhibited by citalopram in a concentration-dependent manner (Figure 4.4C-D): pIC_{50} = 3.98 ± 0.09 (N = 4 blood donors). This supports the previous hypothesis that citalopram can inhibit platelet aggregation downstream of intracellular Ca^{2+} store release.

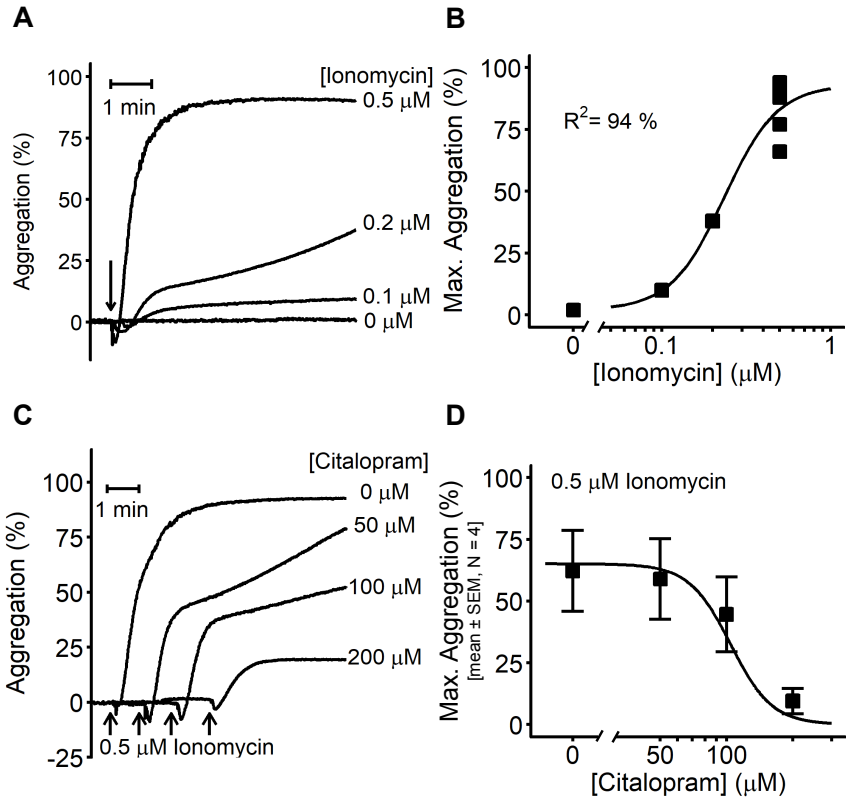

Figure. 4.4 Ionomycin-induced platelet aggregation. **(A-B)** Preliminary experiments (N = 1 blood donor) identified the concentration of ionomycin (0.5 μM) which induced near-maximal platelet aggregation. R^2 represents the coefficient of determination. **(C)** Example traces for ionomycin-induced aggregation in platelets pre-incubated with citalopram (ionomycin = 0.5 μM, citalopram = 0, 50, 100 & 200 μM) for approximately 5 minutes. Arrowheads indicate time points of ionomycin addition. The maximum extent of aggregation (Max. Aggregation) of platelets pre-incubated with a range of citalopram concentrations (0, 50, 100 & 200 μM) was used to generate concentration-response curves, using the four-parameter logistic (4PL) model, with the *Max* parameter constrained to zero (N = 4 blood donors).

4.2.3 Citalopram inhibits Rap1 activation in platelets

Rapid Rap1 activation is dependent on increasing the $[Ca^{2+}]_{cyt}$ and mediates downstream platelet aggregation. Platelets were pre-treated with citalopram (0 or 200 μM) for approximately 5 minutes, and either unstimulated or stimulated with CRPXL (0.5 μg mL^{-1}) or U46619 (0.2 μM). Levels of activated Rap1 were then isolated using a Rap1-GTP pulldown assay and subsequently quantified by Western blot (Figure 4.6). Densitometry data was analysed using a bespoke multiple linear regression model which incorporated the background density of X-ray film, levels of Rap1-GTP in unstimulated platelets, the effect of CRPXL and U46619 on Rap1-GTP levels, the effect of citalopram on Rap1-GTP levels in platelets stimulated with CRPXL or U46619 and random differences between donors (N = 4). Data were modelled as follows:

$$PRED_{\mathrm{i}} = \beta_0 + \beta_1 x_1 + \beta_2 x_2 + \beta_3 x_3 + \beta_4 x_4 + \beta_5 x_5 + \beta_6 x_6 + \beta_7 x_7 + \beta_8 x_8 + (-\beta_6 - \beta_7 - \beta_8) x_9 + \epsilon_{\mathrm{i}}$$

Where: $PRED_{\mathrm{i}}$ = predicted density; β_0 = background density of X-ray film; β_1 = density of unstimulated platelets; β_2 = CRPXL-induced effect above unstimulated platelets; β_3 = citalopram effect on CRPXL-stimulated platelets; β_4 = U46619-induced effect above unstimulated platelets; β_5 = citalopram effect on U46619-stimulated platelets; β_6 = difference between background density and donor 1; β_7 = difference between background density and donor 2; β_8 = difference between background density and donor 3; (-β_6 -β_7 -β_8) = difference between background density and donor 4; x_1 = 0 for background, 1 for platelet samples; x_2 = 1 for CRPXL, otherwise 0; x_3 = 1 for CRPXL and citalopram, otherwise 0; x_4 = 1 for U46619, otherwise 0; x_5 = 1 for U46619 and citalopram, otherwise 0; x_6 = 1 for donor 1, otherwise 0; x_7 = 1 for donor 2, otherwise 0; x_8 = 1 for donor 3, otherwise 0; x_9 = 1 for donor 4, otherwise 0; ϵ_{i} = residual error ($PRED_{\mathrm{i}}$ – dependent variable$_{\mathrm{i}}$).

The primary hypothesis (H_0: citalopram has no effect; H_1: citalopram does have an effect) was evaluated using an F-test by comparing the full model (9 parameters) with the partial model (7 parameters), where $\beta_3 = \beta_5 = 0$. Results from this analysis strongly suggest that citalopram altered both CRPXL- and U46619-induced levels of Rap1-GTP ($P = 7.48 \times 10^{-9}$, F = 83.40). These findings show that following U46619 stimulation, Rap1 activation is blocked by concentrations of citalopram that have no effect on Ca^{2+} release from intracellular stores.

4.2.4 Citalopram does not affect calcium release from neutrophil stores

Ca^{2+} signalling is highly homologous between platelets and neutrophils, both of which utilise Ca^{2+}-dependent Rap1 activation in response to exogenous agonists. Therefore, PAF-induced increases in $[Ca^{2+}]_{cyt}$ were measured in isolated neutrophils following citalopram treatment. Neutrophils were pre-incubated with citalopram (0, 10, 20, 50, 100, 200 & 500 μM) for approximately 5 minutes, before stimulation with PAF (1 μM). Citalopram pre-incubation did not affect PAF-induced increases in $[Ca^{2+}]_{cyt}$ (N = 6 blood donors) (Figure 4.5).

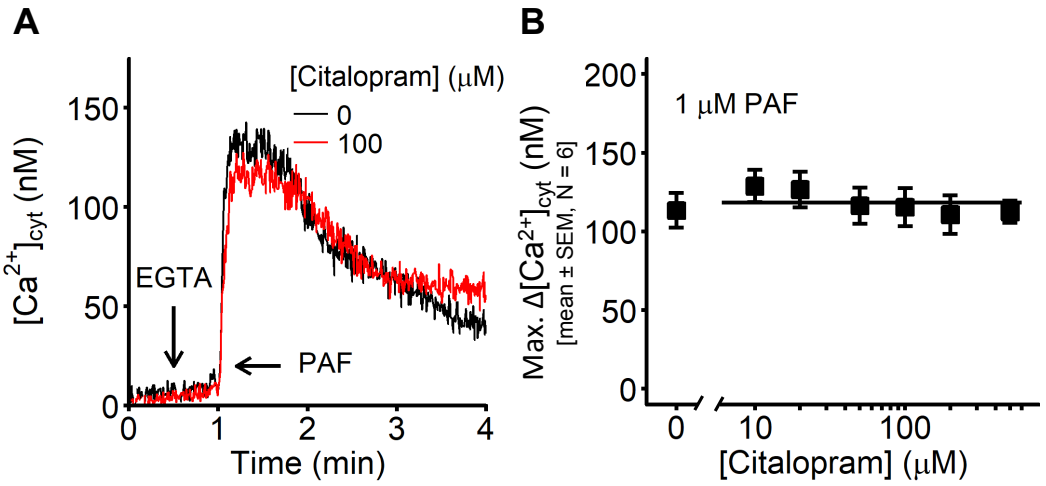

Figure. 4.5 Calcium (Ca^{2+}) store release was monitored in Fura-2-loaded neutrophils, stimulated with 1 μM platelet-activating factor (PAF). **(A)** Example traces demonstrate PAF-induced increases in $[Ca^{2+}]_{cyt}$. **(B)** Neutrophils were pre-incubated for approximately 5 minutes with citalopram (0, 10, 20, 50, 100, 200 & 500 μM) prior to the addition of PAF. The maximum increase in $[Ca^{2+}]_{cyt}$ following PAF addition (Max. $\Delta[Ca^{2+}]_{cyt}$) was used to produce a concentration-response curve, despite the four-parameter logistic (4PL) model failing to converge on a meaningful solution (N = 6 blood donors).

4.2.5 Citalopram inhibits Rap1 activation in neutrophils

Experiments were designed to determine if citalopram inhibits neutrophils downstream of Ca^{2+} store release, as observed in platelets stimulated with U46619. Therefore, the effects of citalopram (200 μM) on PAF-induced (1 μM) Rap1 activation were measured in neutrophils (Figure 4.7). Similar to previous results with platelets (Chapter 4.2.3), densitometry data was analysed using a bespoke multiple linear regression model which incorporated the background density of X-ray film, levels of Rap1-GTP in unstimulated neutrophils, the effect of citalopram on Rap1-GTP levels in unstimulated neutrophils, the effect of PAF on Rap1-GTP levels, the effect of citalopram on Rap1-GTP levels in PAF-stimulated neutrophils and random differences between donors (N = 4). Data were modelled as follows:

$$PRED_{\mathrm{i}} = \beta_0 + \beta_1 x_1 + \beta_2 x_2 + \beta_3 x_3 + \beta_4 x_4 + \beta_5 x_5 + \beta_6 x_6 + \beta_7 x_7 + (-\beta_5 - \beta_6 - \beta_7) x_8 + \epsilon_{\mathrm{i}}$$

Where: $PRED_{\mathrm{i}}$ = predicted density; β_0 = background density of X-ray film; β_1 = density of unstimulated neutrophils; β_2 = citalopram effect on unstimulated neutrophils; β_3 = PAF-induced effect; β_4 = citalopram effect on PAF-stimulated neutrophils; β_5 = difference between background and donor 1; β_6 = difference between background and donor 2; β_7 = difference between background and donor 3; (-β_5 -β_6 -β_7) = difference between background and donor 4; x_1 = 0 for background, 1 for neutrophil samples; x_2 = 1 for citalopram and no PAF, otherwise 0; x_3 = 1 for PAF and no citalopram, otherwise 0; x_4 = 1 for PAF and citalopram, otherwise 0; x_5 = 1 for donor 1, otherwise 0; x_6 = 1 for donor 2, otherwise 0; x_7 = 1 for donor 3, otherwise 0; x_8 = 1 for donor 4, otherwise 0; ϵ_{i} = residual error ($PRED_{\mathrm{i}}$ – dependent variable$_{\mathrm{i}}$).

The primary hypothesis (H_0: citalopram has no effect; H_1: citalopram does have an effect) was evaluated using an F-test by comparing the full model (8 parameters) with the partial model (6 parameters), where $\beta_2 = \beta_4 = 0$. Results from this analysis strongly suggest that citalopram altered Rap1-GTP levels in neutrophils stimulated with PAF (P = 5.88 x 10^{-6}, F = 38.65). These results demonstrate that as with platelets, citalopram also blocks Rap1 activation in neutrophils, despite typical Ca^{2+} release from intracellular stores.

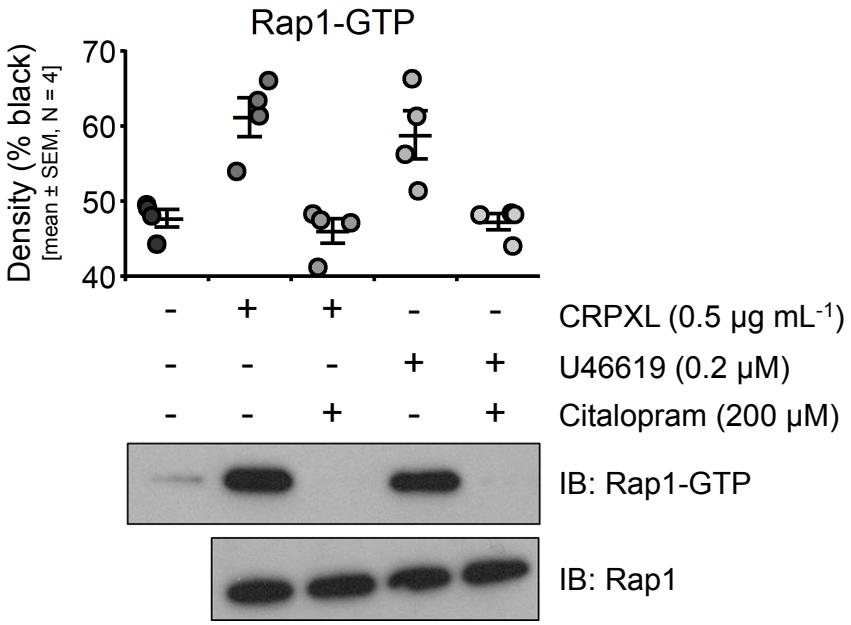

Figure. 4.6 Citalopram inhibits Rap1 activation in platelets. Platelets were pre-treated with (+) or without (-) citalopram (200 μM) for approximately 5 minutes, before stimulation for 1 minute with either CRPXL (0.5 μg mL^{-1}) or U46619 (0.2 μM). Rap1-GTP was isolated from unstimulated and stimulated platelets and quantified using densitometry. Total Rap1 levels were also measured (N = 4 blood donors). Uncropped images for each donor are shown in Figure A.1 of Appendix A.

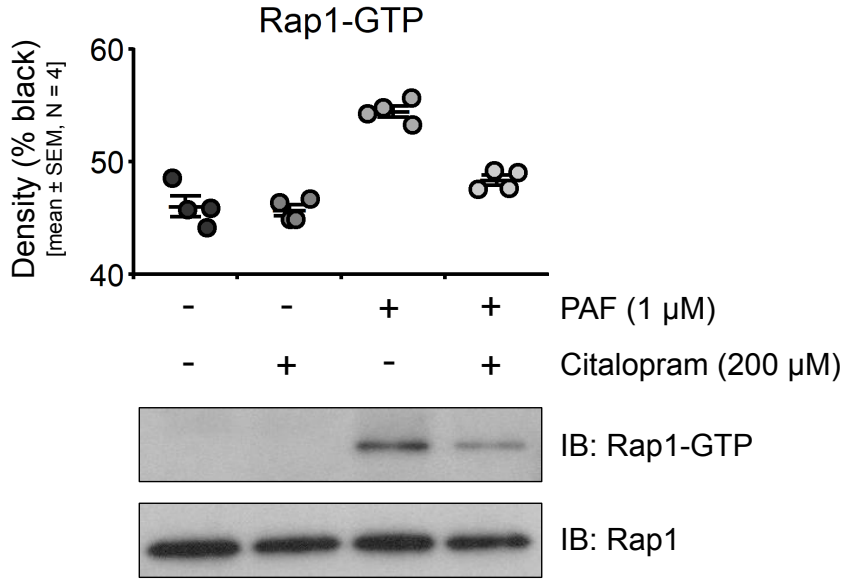

Figure. 4.7 Citalopram inhibits Rap1 activation in neutrophils. Neutrophils were pre-incubated with (+) or without (-) citalopram (200 μM) for approximately 5 minutes, followed by either no stimulation (-) or stimulation (+) with 1 μM platelet-activating factor (PAF) for 1 minute. Rap1-GTP was isolated and quantified using densitometry (N = 4 blood donors). Uncropped images for each donor are shown in Figure A.2 of Appendix A.

4.2.6 Citalopram inhibits integrin $\alpha_M\beta_2$ activation in neutrophils

Rap1-GTP plays an important role in the subsequent transition of β integrins to an active, high-affinity binding state. Therefore, the effects of citalopram on integrin $\alpha_M\beta_2$ activation were investigated in PAF-stimulated neutrophils. Neutrophils were pre-incubated with citalopram (0, 5, 10, 20, 50, 100, 200 & 500 μM) for approximately 5 minutes, followed by PAF stimulation (1 μM). The binding of a allophycocyanin (APC)-conjugated antibody to the active epitope of integrin α_M (CD11b) was measured in the neutrophil ($CD15^+/CD41a^-$ or $CD15^+/CD45^+$) population (Figure 2.2C-D). Representative histograms, (Figure 4.8A) demonstrate that citalopram inhibited PAF-induced integrin $\alpha_M\beta_2$ activation. Citalopram inhibited the median fluorescence intensity (F.I.) in a concentration-dependent manner (Figure 4.8B): pIC_{50} = 4.02 ± 0.15 (N = 6 blood donors). Of note, high concentrations of citalopram reduced integrin $\alpha_M\beta_2$ activation below that of unstimulated cells.

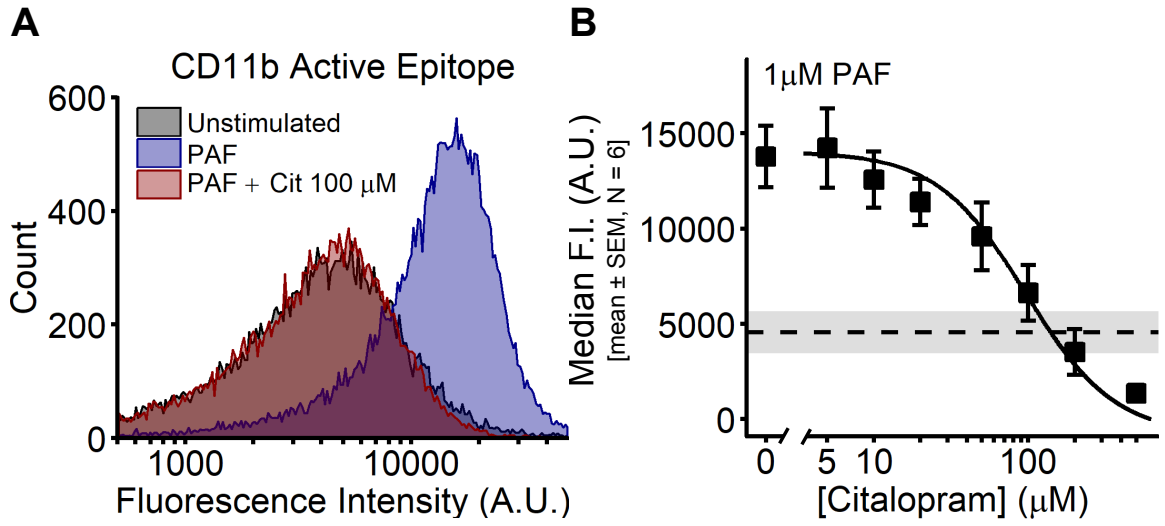

Figure. 4.8 Integrin $\alpha_M\beta_2$ activation on neutrophils stimulated with platelet-activating factor (PAF). **(A)** Representative histograms, measuring allophycocyanin (APC)-conjugated antibody binding to the active epitope of α_M (CD11b) in unstimulated (PAF = 0 μM) or PAF-stimulated neutrophils (citalopram = 0, 100 μM, PAF = 1 μM). **(B)** A range of citalopram concentrations (0, 5, 10, 20, 50, 100, 200 & 500 μM) were used to create concentration-response curves (N = 6 blood donors). Dashed line (mean) and grey area (± SEM) indicate $\alpha_M\beta_2$ activation in unstimulated neutrophils.

4.2.7 Citalopram inhibits neutrophil adhesion to fibrinogen

Experiments were designed to determine if impaired integrin $\alpha_M\beta_2$ activation by citalopram translated to a reduction in agonist-induced cell adhesion. Therefore, the adhesion of PAF-stimulated neutrophils to fibrinogen was investigated under static conditions, as described in Chapter 2.2.4. Citalopram inhibited neutrophil adhesion in a concentration-dependent manner, over a range of PAF concentrations (citalopram = 0, 10, 20, 50, 100, 200 & 500 μM, PAF = 0, 1, 10, 100, 1,000 & 10,000 nM). Agonist-response curves were generated (Figure 4.9A), and the absorbance values at a fixed PAF concentration (1 μM) used to fit the 4PL model (Figure 4.9B): pIC_{50} = 3.88 ± 0.04; (N = 6-10 blood donors).

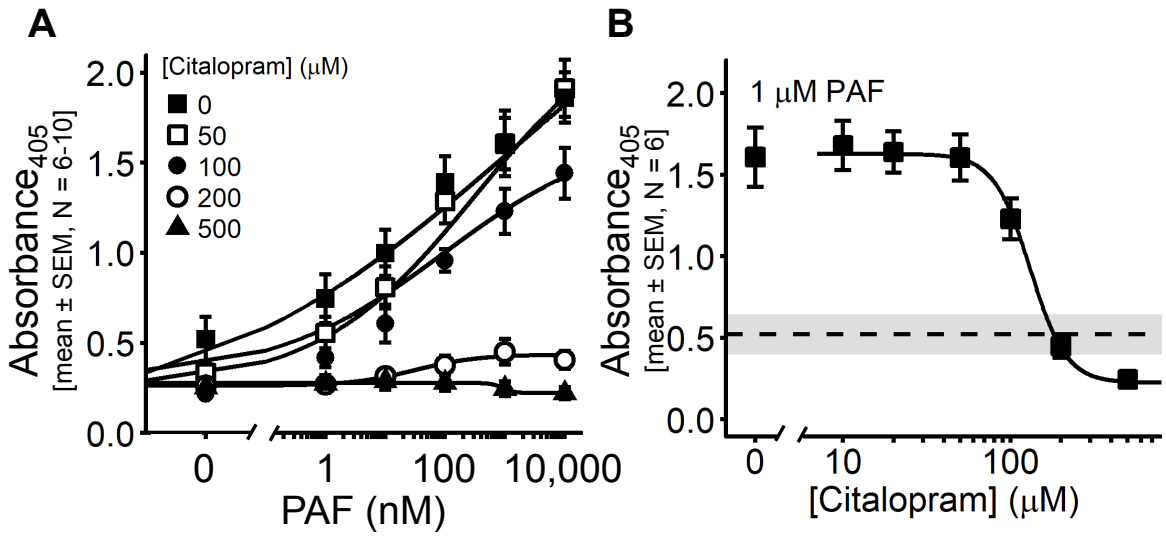

Figure. 4.9 Static adhesion of platelet-activating factor (PAF)-stimulated neutrophils to fibrinogen. **(A)** The adhesion of neutrophils pre-incubated with citalopram (0, 10, 20 , 50, 100, 200 & 500 μM) prior to PAF stimulation (0, 1, 10, 100, 1,000, & 10,000 nM) was used to create agonist-response curves. Citalopram concentrations 10 & 20 μM showed comparable absorbance to untreated neutrophils and were omitted for presentational purposes. **(B)** Neutrophil adhesion at a fixed PAF concentration (1 μM) was used to fit the four-parameter logistic (4PL) model (N = 6-10 blood donors).

4.2.8 Citalopram is not cytotoxic to neutrophils

The membrane integrity of neutrophils was assessed to check if impaired functional responses by citalopram were a result of cell cytotoxicity. Neutrophils (1.00×10^6 mL^{-1}) were incubated with citalopram for 10 minutes before measuring supernatant levels of lactate dehydrogenase (LDH). Calcium-free Tyrode's (CFT) and lysed neutrophils were used as negative and positive controls, respectively. Concentrations of citalopram used in previously described experiments (0, 10, 20, 50, 100, 200 & 500 μM) had no effect on LDH release (Figure 4.10) (N = 5 blood donors).

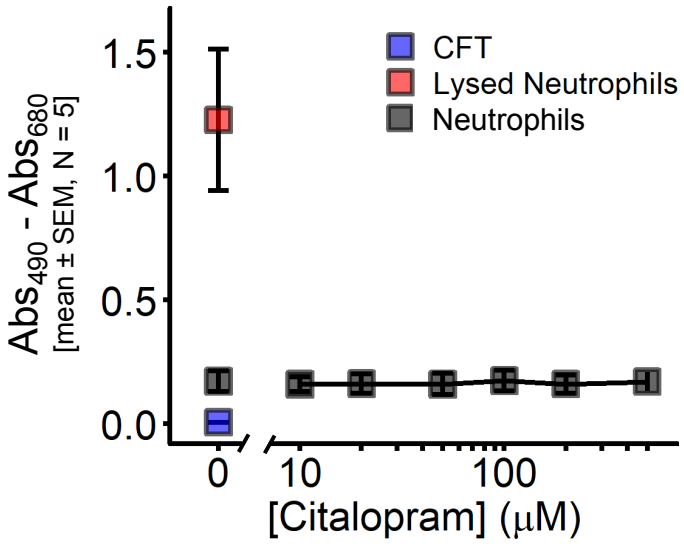

Figure. 4.10 Citalopram is not cytotoxic to neutrophils. Lactate dehydrogenase (LDH) release from neutrophils incubated for 10 minutes with various citalopram concentrations (0, 10, 20, 50, 100, 200 & 500 μM). Calcium-free Tyrode's (CFT) or lysed neutrophils were used as negative and positive controls, respectively (N = 5 blood donors). Non-visible error bars lie within the translucent symbols. Abs represents absorbance.

4.2.9 Citalopram inhibits the nucleotide exchange rate of Rap1B

Experiments conducted with both platelets and neutrophils suggest that citalopram inhibits Rap1 activation, despite having no effect on agonist-induced Ca^{2+} release from intracellular stores. Experiments were therefore designed to determine if citalopram suppresses the CalDAG-GEFI-mediated nucleotide exchange of Rap1B, which occurs downstream of Ca^{2+} store release. A BODIPY-FL fluorescence-based assay (Chapter 2.2.10) was used to determine if citalopram directly inhibits either CalDAG-GEFI or Rap1 activity. Citalopram inhibited the rate of CalDAG-GEFI-induced BODIPY-FL-GDP exchange onto Rap1B in a concentration-dependent manner (0, 1, 10, 100 & 1,000 μM). Peak increases in F.I. (ΔF.I.) were fitted to the 4PL model, with the Max parameter constrained to the basal ΔF.I. when no CalDAG-GEFI was added (Figure 4.11). The pIC_{50} value was 3.67 ± 0.32 (N = 4 experiments).

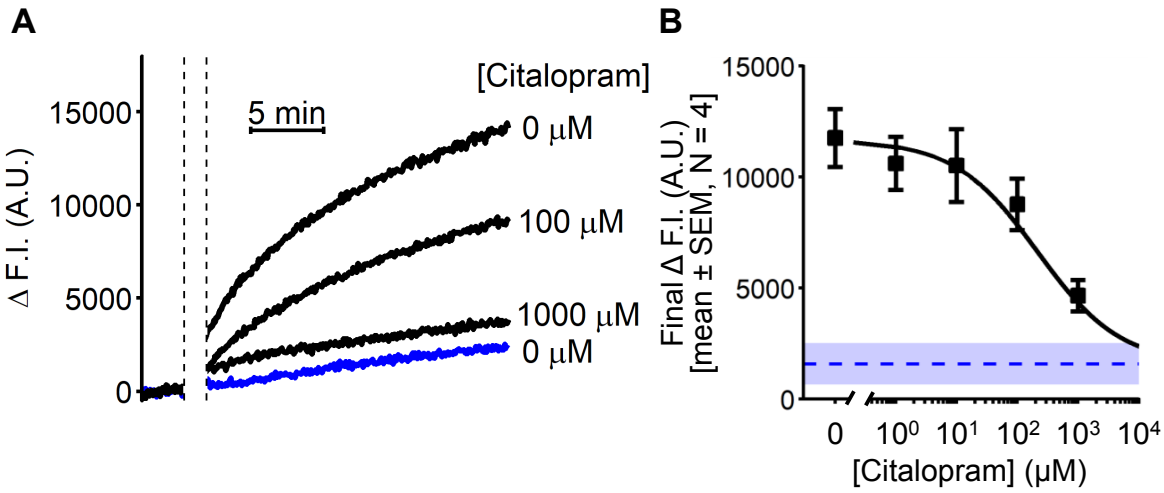

Figure. 4.11 A BODIPY-FL fluorescence-based assay was used to monitor the nucleotide exchange activity of Rap1B. **(A)** Example fluorescence traces, where CalDAG-GEFI was pre-incubated with citalopram (0, 100 & 1000 μM) for approximately 5 minutes before its addition to wells (white segment, black dashed lines) containing BODIPY-FL-GDP and Rap1B. Blue trace indicates fluorescence in the absence of CalDAG-GEFI. **(B)** Following CalDAG-GEFI pre-incubations with citalopram (0, 1, 10, 100 & 1000 μM), increases in fluorescence intensity (ΔF.I.) were recorded and the ΔF.I. 20 minutes after the addition of CalDAG-GEFI (Final ΔF.I.) used to create concentration-response curves. Blue dashed line (mean), and blue area (± SEM) show Final ΔF.I. in the absence of CalDAG-GEFI, which was used to constrain the Max parameter of the four-parameter logistic (4PL) model (N = 4 experiments).

4.3 Discussion

4.3.1 Overview

Results produced in this chapter have identified a putative, novel mechanism of platelet inhibition by citalopram. Citalopram inhibited Ca^{2+}-dependent Rap1 activation in U46619-stimulated platelets, despite having no effect on u46619-induced Ca^{2+} release from intracellular stores. These findings suggest that citalopram inhibits the guanine nucleotide exchange factor CalDAG-GEFI, which upregulates Rap1 activation in the presence of Ca^{2+}. Similar results were observed with PAF-stimulated neutrophils, which also express both Rap1 and CalDAG-GEFI, supporting the hypothesis that citalopram inhibits CalDAG-GEFI. Finally, pre-incubation of citalopram with CalDAG-GEFI reduced CalDAG-GEFI-mediated Rap1B nucleotide exchange.

Taken together, results from this chapter suggest two distinct, agonist-specific mechanisms of platelet inhibition by citalopram. 1) Inhibition of CRPXL-induced platelet activation upstream of Ca^{2+} release from intracellular stores. 2) Inhibition of U46619-induced platelet activation downstream of Ca^{2+} store release. This second mechanism is likely mediated through either inhibition of CalDAG-GEFI or direct blockade of Rap1-GTP formation. The mechanism underlying platelet inhibition by citalopram prior to Ca^{2+} store release will be investigated in Chapter 5.

4.3.2 Citalopram's effects on intracellular calcium levels

Citalopram inhibited CRPXL-induced Ca^{2+} release from intracellular stores (pIC_{50} = 4.33 ± 0.09) (Figure 4.3A-B). Such findings are likely to account for how, as shown in Chapter 3, citalopram inhibited collagen-induced platelet aggregation (pIC_{50} = 4.31 ± 0.21), thromboxane A_2 synthesis (pIC_{50} = 4.77 ± 0.08) and adhesion (pIC_{50} = 3.76 ± 0.02), as these processes are dependent on increasing the $[Ca^{2+}]_{cyt}$.

By contrast, citalopram did not affect U46619-induced Ca^{2+} store release, even at concentrations which inhibit platelet aggregation (Figure 4.3C-E). This suggests that unlike CRPXL-stimulated platelets, the inhibitory effects of citalopram on U46619-induced platelet aggregation reside downstream of Ca^{2+} release from intracellular stores. This hypothesis is supported by the observation that citalopram can also inhibit aggregation following Ca^{2+} store release by the ionophore, ionomycin (Figure 4.4). Contrary to CRPXL, which induces PLCγ2-mediated increases in $[Ca^{2+}]_{cyt}$ via GPVI signal transduction, U46619 induces PLCβ-mediated increases in $[Ca^{2+}]_{cyt}$ through binding to Gα_q-coupled

TPα receptors. Ca^{2+} store release was also preserved in PAF-stimulated neutrophils, which likewise mediate activation through Gα_q. Comparing the effects of citalopram on $[Ca^{2+}]_{cyt}$ increases by stimulating other Gα_q-coupled receptors, such as protease-activated receptors (PARs) or P2Y1 could establish if Gα_q-mediated Ca^{2+} store release is unaffected by citalopram.

4.3.3 Citalopram's effects on Rap1 activation

Despite normal Ca^{2+} store release, platelets pre-treated with citalopram (200 μM) did not aggregate in response to U46619 (Figure 4.3C-E). Activated Rap1 mediates platelet aggregation downstream of increases in $[Ca^{2+}]_{cyt}$ by aiding the transition of integrin $\alpha_{IIb}\beta_3$ to a high-affinity binding state (Lee et al., 2009, Moser et al., 2009, Chrzanowska-Wodnicka et al., 2005). Citalopram blocked Rap1 activation in platelets stimulated with CRPXL (Figure 4.6). This was expected, as rapid Rap1 activation is dependent on increases in $[Ca^{2+}]_{cyt}$, which were inhibited in CRPXL-stimulated platelets that were pre-treated with citalopram (Figure 4.3). However, in U46619-stimulated platelets, concentrations of citalopram which do not inhibit Ca^{2+} store release did block Rap1 activation (Figure 4.6). This finding suggests that citalopram inhibits CalDAG-GEFI, a guanine nucleotide exchange factor that upregulates Rap1 activation downstream of increases in $[Ca^{2+}]_{cyt}$ (Chapter 4.1.2). This hypothesis is supported by the fact that despite abolished aggregation in response to U46619, platelet shape change is preserved in both citalopram-treated platelets (Figures 3.4 & 4.3E), and platelets from CalDAG-GEFI knockout mice (Crittenden et al., 2004). These early cytoskeletal reorganisations are instead believed to be mediated by the Ca^{2+}-dependent small GTPase, Rho (Kimura et al., 1996, Klages et al., 1999).

To test the hypothesis that citalopram inhibits CalDAG-GEFI, Ca^{2+} store release and Rap1 activation were investigated in neutrophils, which also express Rap1 and CalDAG-GEFI (M'Rabet et al., 1998, Crittenden et al., 2004). As with U46619-stimulated platelets, citalopram had no effect on $[Ca^{2+}]_{cyt}$ increases in neutrophils stimulated with PAF, which like U46619 mediates $[Ca^{2+}]_{cyt}$ increases through PLCβ. Citalopram did, however, inhibit PAF-induced Rap1 activation, providing supportive evidence that citalopram inhibits CalDAG-GEFI. In neutrophils, Rap1-GTP mediates the downstream transition of integrin $\alpha_M\beta_2$ to an active, high-affinity state, allowing adhesion to endothelial adhesion molecules and fibrinogen (Flick et al., 2004, Bergmeier et al., 2007, Halai et al., 2014). Citalopram inhibited PAF-induced neutrophil $\alpha_M\beta_2$ activation and adhesion to fibrinogen, suggesting that citalopram also inhibits neutrophil functional responses. The effects of citalopram and other SSRIs on neutrophil function will be discussed further in Chapter 7.4.1.

4.3.4 Indirect inhibition of CalDAG-GEFI

Putative CalDAG-GEFI inhibition by citalopram could be mediated through either direct interactions, or through binding and regulating other proteins. CalDAG-GEFI phosphorylation by protein kinase A (PKA) (Ser-116, Ser-117, Ser-586) prevents Rap1 activation in platelets (Subramanian et al., 2013). However, CalDAG-GEFI phosphorylation by PKA at these same amino acid residues increases Rap1 activation in neurons of the striatum (Nagai et al., 2016), suggesting a complex and potentially cell-specific form of CalDAG-GEFI regulation. Levels of the PKA activator, cyclic adenosine monophosphate (cAMP) were unchanged in both unstimulated and ADP-stimulated platelets that were pre-incubated with or without 50 μM citalopram (Tseng et al., 2013). Although this suggests that citalopram does not increase PKA activity, the unclear effects of PKA-mediated CALDAG-GEFI phosphorylation on Rap1 activation imply that such observations should be interpreted with caution. Activated ERK1/2 also phosphorylate CalDAG-GEFI (Ser-391), which reduces CalDAG-GEFI nucleotide exchange activity and Rap1 activation (Ren et al., 2016). ERK1/2 activation is downstream of Rap1 activation and provides a putative negative-feedback loop to auto-regulate ERK1/2 signalling (Stefanini et al., 2009). However, citalopram inhibits initial Rap1 activation, suggesting that downstream ERK1/2 are not activated and are therefore unable to phosphorylate CalDAG-GEFI. Taken together, the studies described above suggest that citalopram is unlikely to inhibit CalDAG-GEFI through an indirect mechanism of action.

4.3.5 CalDAG-GEFI-independent mechanisms of Rap1 inhibition

In addition to CalDAG-GEFI, Rap1 activation is possible through inhibition of the GTPase activating protein, RASA-3. ADP-binding to Gα_i-coupled P2Y12 receptors activates PI3K, which inhibits RASA-3 (Stefanini et al., 2015). RASA-3 inhibition reduces the intrinsic GTPase activity of Rap1, causing a gradual increase in Rap1-GTP (Stefanini et al., 2009, 2012, 2015). In this chapter, Rap1 activity was recorded 1 minute after agonist addition. Rap1 activation over this time frame is predominantly mediated through the activation of CalDAG-GEFI as opposed to RASA-3 inhibition, which reportedly takes 5-10 minutes (Franke et al., 1997, Crittenden et al., 2004, Stefanini et al., 2009, 2015). This observation therefore strongly suggests that inhibition of U46619-induced aggregation by citalopram is not through preserved RASA-3 activity.

Theoretically, citalopram could prevent Rap1 activation by sequestering GTP. However, due to the high cytosolic concentrations of GTP ($\approx$300 μM) and its picomolar-nanomolar

affinity for small G proteins (Traut, 1994, Bos et al., 2007), this hypothesis seems highly unlikely. Furthermore, GTP is required for Rho-mediated platelet shape change (Klages et al., 1999), which is preserved in citalopram-treated platelets stimulated with U46619 (Figures 3.4 & 4.3E). Alternatively, citalopram may directly bind Rap1, preventing GTP loading irrespective of CalDAG-GEFI activity. Rap1B-deficient platelets undergo impaired but not ablated aggregation in response to various platelet agonists (Chrzanowska-Wodnicka et al., 2005). Determining if citalopram has any additional inhibitory effects in this mouse model and in platelets lacking the Rap1A isoform could help determine if citalopram inhibits U46619-mediated platelet aggregation through binding and inhibiting Rap1.

4.3.6 Direct inhibition of CalDAG-GEFI

To ascertain if citalopram directly inhibits CalDAG-GEFI, an *in vitro* CalDAG-GEFI activity assay was performed. In this assay, recombinant Rap1B was co-incubated with fluorophore-conjugated GDP (BODIPY-FL-GDP) (Lozano et al., 2016, Ren et al., 2016). The F.I. of BODIPY-FL increases upon its association with Rap1B, increasing sample F.I. (ΔF.I.). The addition of recombinant CalDAG-GEFI catalyses the rate of Rap1B nucleotide exchange, increasing BODIPY-FL-GDP binding to Rap1B and ΔF.I. (Figure 2.9B). This *in vitro* enzyme assay removed the complex spatial and temporal dynamics of the intracellular environment, as well as proteins that may bind to and affect CalDAG-GEFI or Rap1 activity, such as PKA and ERK1/2, or RASA-3, respectively. This reductionist approach allowed the direct interactions between isolated citalopram, CalDAG-GEFI and Rap1B to be investigated.

Citalopram reduced the extent of CalDAG-GEFI-mediated BODIPY-FL-GDP binding to Rap1B over a 20 minute period (Figure 4.11). This suggests that citalopram impairs Rap1B nucleotide exchange through either directly reducing CalDAG-GEFI activity or by blocking BODIPY-FL-GDP binding to Rap1B. The inhibitory potency for citalopram in this *in vitro* assay (pIC_{50} = 3.67 ± 0.32) does not match its effects on platelet function (U46619-induced aggregation: pIC_{50} = 4.15 ± 0.27). Possible explanations for this discrepancy include the acellular nature of the assay and the reaction buffer (Table 2.4), which differs from the intracellular environment. The proteins used in this assay also contrast from those in cellular experiments. Rap1B and CalDAG-GEFI contain C-terminal truncations (Figure B.1 in Appendix B). While anecdotal reports claim these truncations preserve protein activity and functional domains, the tertiary structure and unidentified C-terminal interactions with other proteins may be compromised. This assay also fails to identify if reduced BODIPY-FL-GDP binding to Rap1B was a consequence of citalopram binding to CalDAG-

GEFI, or to Rap1B itself. Additional experiments using isothermal titration calorimetry (ITC) could identify the direct binding target of citalopram. ITC is a technique commonly used to assess drug-protein interactions, providing information on enthalpy changes, binding affinity constants and stoichiometry (Damian, 2013). Unlike the binding assay conducted in this chapter, ITC also does not require conjugated fluorophores, which may interfere with normal protein function.

In conclusion, results in this chapter demonstrate that despite typical U46619-induced Ca^{2+} store release, citalopram blocked Rap1 activation in both platelets and neutrophils. Citalopram also reduced the rate of CalDAG-GEFI-mediated nucleotide exchange onto Rap1B. Taken together, these findings suggest citalopram either directly inhibits CalDAG-GEFI, or blocks nucleotide binding to Rap1. Either of these mechanisms could account for citalopram-mediated inhibition of both platelet and neutrophil functional responses.

Chapter 5
Citalopram inhibits glycoprotein VI-mediated signalling

5.1 Background

In Chapter 3, citalopram was shown to inhibit several collagen-induced platelet functions, including aggregation, thromboxane A_2 (TxA_2) synthesis and adhesion. Collagen initiates platelet activation by binding either integrin $\alpha_2\beta_1$ or the glycoprotein VI (GPVI) receptor, which mediates downstream increases in cytosolic calcium concentration ($[Ca^{2+}]_{cyt}$). In Chapter 4, it was shown that increases in $[Ca^{2+}]_{cyt}$ induced by the GPVI-selective agonist, cross-linked collagen-related peptide (CRPXL) were inhibited by citalopram (Figure 4.3). This suggests that citalopram inhibits early signalling events in GPVI-mediated platelet activation, prior to Ca^{2+} release from intracellular stores, resulting in the downstream inhibition of platelet functional responses.

5.1.1 The GPVI receptor

GPVI is a 58 kDa transmembrane receptor, belonging to the immunoglobin (Ig)-like superfamily and is only expressed in megakaryocytes and platelets (Phillips and Agin, 1977b, Lagrue-Lak-Hal et al., 2001, Jandrot-Perrus et al., 2000). The extracellular region of GPVI consists of two Ig-like domains (D1D2) and a heavily glycosylated Ser/Thr-rich stalk region (Miura et al., 2000, Horii et al., 2006). A positively-charged residue (Arg-272) within the transmembrane domain of GPVI mediates non-covalent linkage to the Fc receptor γ-chain (FcRγ-chain) (Zheng et al., 2001, Bori-Sanz et al., 2003, Tsuji et al., 1997). FcRγ-chain knockout mice do not express functional GPVI, and GPVI-FcRγ-chain complexes are essential for GPVI-mediated signal transduction (Nieswandt et al., 2000, Tsuji et al., 1997, Berlanga et al., 2002). The Src family kinases (SFKs) Fyn and Lyn constitutively bind to the Pro-rich cytoplasmic domain of GPVI via their Src homology-3 (SH3) domains (Suzuki-Inoue et al., 2002), priming the receptor for rapid signal transduction (Ezumi et al., 1998, Suzuki-Inoue et al., 2002, Schmaier et al., 2009). A basic amino acid-rich region proximal to the GPVI transmembrane domain binds calmodulin, which dissociates from GPVI upon agonist-induced signal transduction and activates a disintegrin and metallo-

proteinase domain-containing protein 10 (ADAM10) (Andrews et al., 2002, Gardiner et al., 2004). ADAM10 mediates the proteolytic cleavage of a soluble GPVI ectodomain fragment, causing irreversible inactivation of the receptor (Andrews et al., 2007, Qiao et al., 2010).

5.1.2 GPVI agonists

GPVI is the major collagen receptor involved in platelet activation (Nieswandt and Watson, 2003). X-ray crystallographic data suggest that the GPVI collagen-binding domain (CBD) is a shallow groove on the surface of the D1 domain (Horii et al., 2006). GPVI binds Gly-Pro-Hyp (GPO, where O = hydroxyproline) sequence repeats within the collagen triple helix, although other binding motifs certainly play a role (Jarvis et al., 2008). A collagen-related peptide (CRP), containing 10 GPO repeats initiates weak platelet aggregation and has been described as a partial agonist (Asselin et al., 1999). However, cross-linking CRP through cysteine residues at its N-terminus and C-terminus (CRPXL) produces a potent platelet agonist, which initiates rapid platelet aggregation (Morton et al., 1995, Knight et al., 1999). CRPXL- and collagen-stimulated platelets undergo a similar tyrosine phosphorylation cascade (Chapter 5.1.4) (Asselin et al., 1997). However, unlike collagen, CRPXL has no effect on GPVI-deficient platelets and does not bind the other collagen receptor, integrin $\alpha_2\beta_1$ (Morton et al., 1995, Knight et al., 1999), providing evidence that CRPXL is a GPVI-selective platelet agonist.

5.1.3 GPVI dimers and higher-order clustering

GPVI CBDs form back-to-back dimers in crystals, with parallel putative collagen-binding grooves that match the triple helices of fibrillar collagen (Horii et al., 2006). This structural orientation could explain why dimeric (D1D2-Fc)$_2$ GPVI has a higher collagen-binding affinity than monomeric D1D2 domains (Miura et al., 2002). Dimer-specific antibodies, such as 204-11 Fab, have demonstrated that dimeric GPVI (≈29% of total GPVI) is present on the surface of resting platelets, which may mediate initial collagen binding and collagen-induced activation (Berlanga et al., 2007, Jung et al., 2012, 2009). Platelet activation in turn increases dimer formation (Jung et al., 2012, Loyau et al., 2012). Experiments utilising super-resolution microscopy show collagen binding to dimeric GPVI coalesces the receptor into higher-order clusters, which increases collagen avidity and may colocalise intracellular proteins, initiating intracellular phosphorylation (Poulter et al., 2017).

5.1.4 GPVI-mediated signal transduction

GPVI signal transduction involves the coordinated phosphorylation of several intracellular proteins (Figure 5.1). GPVI itself has no intrinsic kinase activity and relies on SFKs to initiate the phosphorylation cascade. The SFKs Fyn/Lyn are constitutively associated with the GPVI-FcRγ-chain complex (Ezumi et al., 1998). GPVI-bound Lyn is phosphorylated within its activation loop (Tyr-396), which is thought to prime GPVI for rapid agonist-induced signal transduction (Schmaier et al., 2009). CD148 maintains the activity of GPVI-associated SFKs by reversing Csk-mediated phosphorylation of the SFK C-terminal (Senis et al., 2009, Ellison et al., 2010, Mori et al., 2012). Agonist-induced increases in GPVI dimerisation and clustering initiate trans-autophosphorylation of the Fyn/Lyn activation loop, and are thought to bring Fyn/Lyn within the vicinity of the intracellular immunoreceptor tyrosine-based activation motif (ITAM) of the FcRγ-chain (Suzuki-Inoue et al., 2002). Platelets deficient in both Fyn and Lyn demonstrate delayed and impaired responses to CRPXL, which are blocked by the SFK inhibitor, PP1 (Quek et al., 1998), suggesting other SFKs play an albeit small role in GPVI-mediated activation. Lyn/Fyn phosphorylate tandem tyrosine residues within the FcRγ-chain ITAM, allowing spleen tyrosine kinase (Syk) to bind the ITAM via its Src homology-2 (SH2) domains, which induces Syk auto-phosphorylation (Gibbins et al., 1996, Ezumi et al., 1998). Syk phosphorylates the linker of activated T cells (LAT) (Zhang et al., 1998), which becomes phosphorylated at multiple sites and recruits phospholipase Cγ2 (PLCγ2) and phosphatidylinositol 3-kinase (PI3K) within the proximity of their substrates via their SH2 domains (Gibbins et al., 1998, Gross et al., 1999, Pasquet et al., 1999). PI3K converts phosphatidylinositol-3,4-bisphosphate (PIP_2) to phosphatidylinositol-3,4,5-trisphosphate (PIP_3) (Leevers et al., 1999). PIP_3 recruits additional PLCγ2 and Bruton's tyrosine kinase (Btk) via their pleckstrin homology (PH) domains, allowing Btk to phosphorylate PLCγ2 at several tyrosine residues, including Tyr-1217 (Quek et al., 1998, Watanabe et al., 2001). Phosphorylated PLCγ2 mediates the hydrolysis of residual PIP_2 to inositol-1,4,5-trisphosphate (IP_3) and 1,2-diacylglycerol (DAG) (Wilde and Watson, 2001). IP_3 and DAG are key secondary messengers of platelet activation, responsible for the downstream release of Ca^{2+} from intracellular stores (Chapter 4.1.1 & Figure 4.1) and activation of protein kinase C (PKC), respectively (Gibbins, 2004).

To summarise, the coordinated signal transduction described above is essential for downstream platelet functional responses induced by GPVI stimulation, including granule release and platelet aggregation.

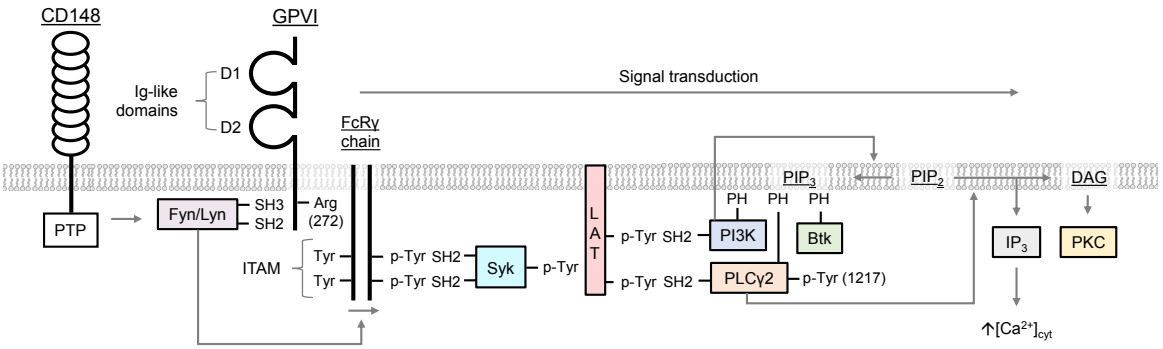

Figure. 5.1 Schematic summary of initial glycoprotein VI (GPVI)-mediated signalling during platelet activation. The extracellular region of GPVI consists of two immunoglobin (Ig)-like domains (D1D2) which bind collagen. GPVI binding to collagen mediates receptor clustering and tyrosine (Tyr) phosphorylation of the intracellular immunoreceptor tyrosine-based activation motif (ITAM) of the Fc receptor γ (FcRγ)-chain by the Src-family kinases Fyn and Lyn. CD148 maintains the activity of Fyn and Lyn by reversing Csk-mediated phosphorylation of the SFK C-terminal through its protein tyrosine phosphatase (PTP) domain. ITAM phosphorylation permits binding of spleen tyrosine kinase (Syk) through its Src homology-2 (SH2) domains, activating Syk through auto-phosphorylation, which results in the phosphorylation of the linker of activated T cells (LAT). Phosphoinositide 3-kinase (PI3K) is then recruited to LAT and phosphorylates phosphatidylinositol-4,5-bisphosphate (PIP_2) to phosphatidylinositol-3,4,5-trisphosphate (PIP_3). Bruton's tyrosine kinase (Btk) and Phospholipase Cγ2 (PLCγ2) are recruited to membrane-associated PIP_3 via their pleckstrin homology (PH) domains, allowing Btk to phosphorylate PLCγ2 at Tyr-1217, resulting in its activation. Activated PLCγ2 cleaves residual PIP_2 to produce inositol-1,4,5-trisphosphate (IP_3) and 1,2-diacylglycerol (DAG), which mediate downstream platelet activation through increasing the concentration of cytosolic calcium ($[Ca^{2+}]_{cyt}$) and activating protein kinase C (PKC), respectively. This is an original image.

5.1.5 Aims

Experiments in this chapter aim to:

1. Describe the inhibitory effects of citalopram on GPVI-mediated signal transduction.

2. Identify where citalopram exerts its effects in the GPVI signalling pathway.

Experiments will measure CRPXL-induced phosphorylation of the FcRγ-chain, SFKs, LAT and PLCγ2, as well as the binding of GPVI antibodies to the surface of resting platelets.

5.2 Results

5.2.1 Citalopram inhibits CRPXL-induced platelet aggregation

Collagen activates platelets through binding either GPVI or integrin $\alpha_2\beta_1$. The results presented in Chapter 3 show citalopram inhibits collagen-induced functional responses. In the case of GPVI, these effects are likely due to disrupted Ca^{2+} signalling, as shown using the GPVI-selective agonist, CRPXL (Figure 4.3). The effects of citalopram on platelet aggregation induced by CRPXL were therefore investigated to determine if citalopram inhibits platelet activation induced by a GPVI-selective agonist.

Citalopram inhibited CRPXL-induced platelet aggregation in a concentration-dependent manner (Figure 5.2). Figure 5.2B demonstrates the inhibitory effects of citalopram on the maximum extent of aggregation over 6 minutes. Pre-incubating platelets with 20 μM or 50 μM citalopram caused concentration-dependent 2.16-fold and 2.50-fold rightward shifts in agonist-response curves, respectively. In contrast, high concentrations of citalopram (100 μM) caused a 4.78-fold rightward shift in the agonist-response curve (Figure 5.2B). Schild analysis for citalopram concentrations between 5-50 μM gave a pA_2 value of 4.84 and a slope of 1.104, and thus displayed characteristics of competitive antagonism. However, incorporating higher concentrations of citalopram (100-200 μM) increased the slope to 1.800 (Figure 5.2C). These data suggest that at concentrations up to 50 μM, citalopram inhibits CRPXL-induced platelet aggregation through a seemingly competitive mechanism, yet this inhibition becomes non-competitive at concentrations exceeding 50 μM.

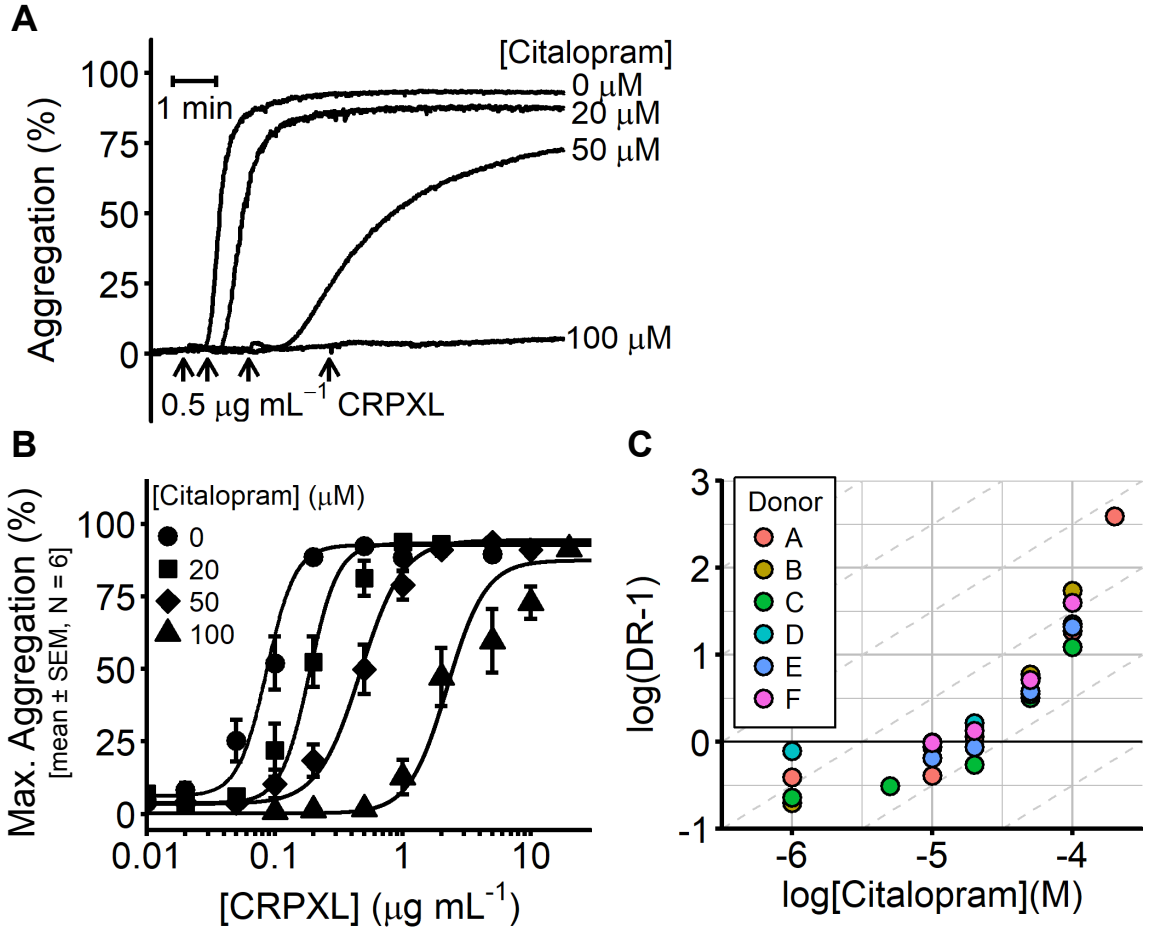

Figure. 5.2 Citalopram inhibits CRPXL-induced platelet aggregation **(A)** Example aggregation traces of platelets pre-incubated with citalopram (0, 20, 50, & 100 μM) for approximately 5 minutes, before stimulation with a fixed concentration of cross-linked collagen-related peptide (CRPXL, 0.5 μg mL^{-1}). Arrowheads indicate time points of CRPXL addition. **(B)** Agonist concentration-response curves demonstrate how the maximum extent of platelet aggregation (Max. Aggregation) to a range of CRPXL concentrations was inhibited by citalopram. Concentrations of citalopram below 20 μM demonstrate similar responses to untreated platelets and were omitted from the figure for presentational purposes. 5 μM and 200 μM citalopram were only tested in a single donor and was therefore also omitted from the figure. **(C)** Schild analysis was carried out on a range of citalopram concentrations (0, 1, 5, 10, 20, 50, 100, & 200 μM). Dashed grey lines indicate a slope of 1, which correlates to data expected from a competitive antagonist. DR represents the dose ratio (N = 6 blood donors).

5.2.2 Citalopram inhibits tyrosine phosphorylation of Src family kinases, LAT and PLCγ2

GPVI signal transduction prior to Ca^{2+} store release and platelet aggregation is mediated through a well-characterised tyrosine phosphorylation cascade (Chapter 5.1.4 & Figure 5.1). The effects of citalopram on CRPXL-induced protein phosphorylation were therefore investigated, to identify where in the GPVI signalling cascade citalopram may mediate its inhibitory effects.

In an initial unblinded experiment (Figure 5.3A) citalopram reduced whole cell lysate tyrosine phosphorylation (N = 2 donors, (4G10)) in platelets stimulated with CRPXL (5 μg mL^{-1}). Reduced tyrosine phosphorylation of the FcRγ-chain (kDa $\approx$ 15) (Gibbins et al., 1996) was also observed. Citalopram similarly reduced the site-specific tyrosine phosphorylation of SFKs (Tyr-416), LAT (Tyr-200) and PLCγ2 (Tyr-1217) (N = 1 donor).

Protein samples from subsequent experiments were randomly loaded into wells in a blinded fashion. For each donor, basal phosphorylation (CRPXL = 0) and CRPXL-induced phosphorylation of citalopram-treated platelets (CRPXL = 5 μg mL^{-1}; citalopram = 0, 1, 10, 20, 50, 100 & 200 μM) was quantified (Figure 5.3B). Uncropped images for Western blots used for densitometric quantification can be found in Figure A.3 & A.4 of Appendix A. Citalopram inhibited CRPXL-induced phosphorylation of PLCγ2, SFK and LAT in a concentration-dependent manner (Figure 5.3B). Citalopram-induced responses were fitted to the four-parameter logistic (4PL) model and the pIC_{50} values are as follows: (SFK (Tyr-416) = 4.26 ± 0.02, N = 4; LAT (Tyr-200) = 3.76 ± 0.06, N = 5; PLCγ2 (Tyr-1217) = 4.40 ± 0.77, N = 5 blood donors). Due to an incomplete concentration-response curve, the Max parameter for LAT (Tyr-200) was constrained to basal phosphorylation (CRPXL = 0).

In unstimulated platelets (CRPXL = 0), no LAT (Tyr-200) or PLCγ2 (Tyr-1217) phosphorylation was observed, but was detectable with SFK (Tyr-416) (Figure 5.3). Citalopram did not affect levels of Src ($P = 0.64$), LAT ($P = 0.43$) or PLCγ2 ($P = 0.30$) within protein lysates, as determined by 1-way ANOVA (Effect 1 (fixed) = parameter {*Max*, *Min*}; H_0: $Max = Min$; H_1: $Max \neq Min$). These data show that citalopram inhibits tyrosine phosphorylation of the FcRγ-chain, as well as the phosphorylation of SFKs, LAT and PLCγ2, at amino acid residues relating to their activity within the GPVI pathway.

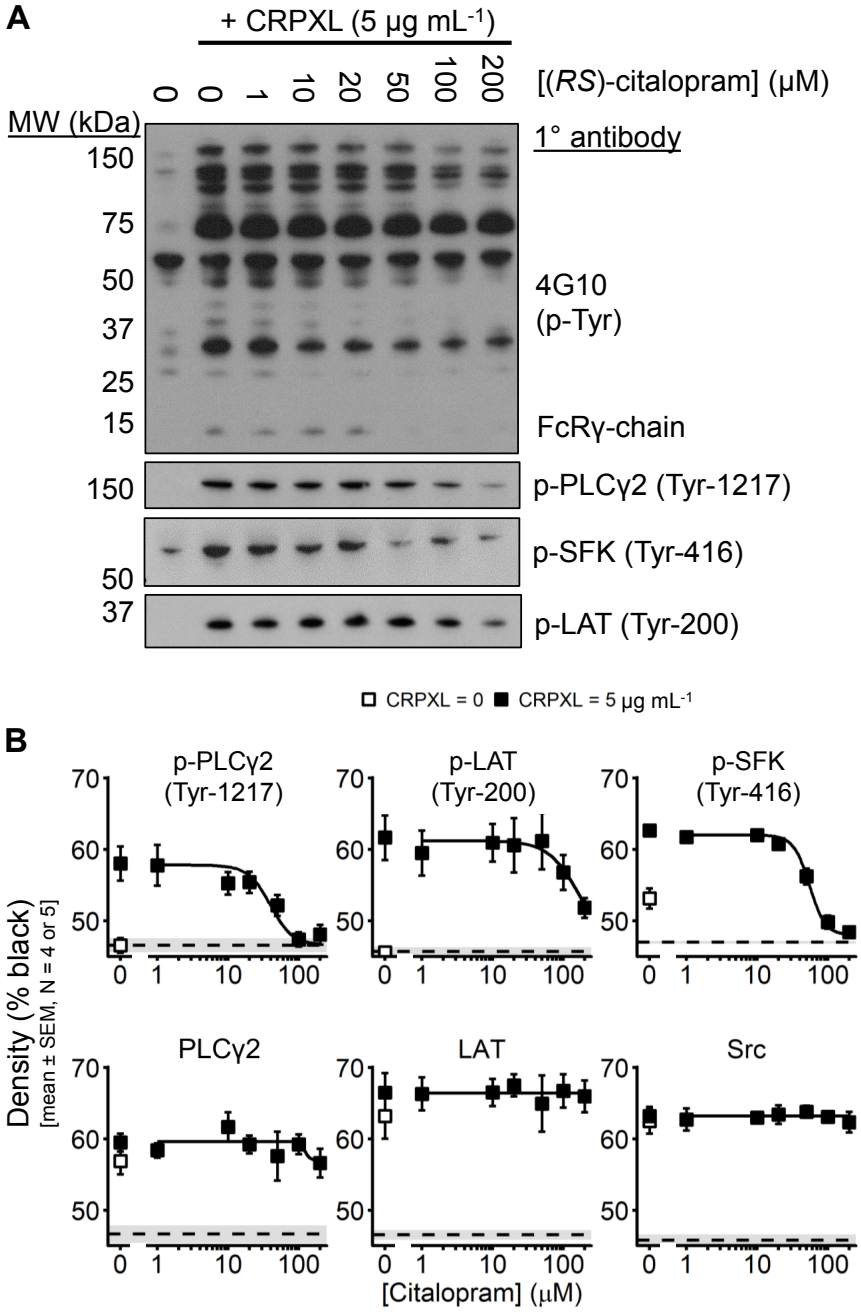

Figure. 5.3 Whole cell tyrosine phosphorylation (4G10) and site-specific phosphorylation of Src family kinases (SFK), linker of activated T cells (LAT) and phospholipase Cγ2 (PLCγ2). Platelets were stimulated with 5 μg mL^{-1} cross-linked collagen-related peptide (CRPXL) for 6 minutes under turbidimetric conditions, in the presence of the integrin $\alpha_{IIb}\beta_3$ inhibitor, GR144053 (2 μM). **(A)** Images from a non-blinded pilot study demonstrate the concentration-effect of citalopram both on whole cell tyrosine phosphorylation and the site-specific phosphorylation of SFKs (Tyr-416), LAT (Tyr-200) and PLCγ2 (Tyr-1217). **(B)** Densitometric quantification for unstimulated (white squares = 0 CRPXL) or stimulated platelets (black squares = 5 μg mL^{-1} CRPXL). Dashed lines (mean) and the grey area (± SEM) indicate background signal of developed X-ray films. Lower panels represent protein levels from the same samples used to assess phosphorylation (SFK (Tyr-416): N = 4 blood donors, LAT (Tyr-200) and PLCγ2 (Tyr-1217): N = 5 blood donors). Uncropped blot images for each donor can be found in Figure A.3 & A.4 of Appendix A.

5.2.3 Citalopram inhibits the binding of glycoprotein VI antibodies

Citalopram inhibits early protein phosphorylation within the GPVI signalling pathway. Such phosphorylation is likely initiated through clustering of the GPVI receptor upon agonist binding. Pre-existing GPVI dimers on resting platelets are also thought to mediate initial collagen binding and receptor clustering, which induces intracellular protein phosphorylation (Berlanga et al., 2007, Jung et al., 2009, 2012, Poulter et al., 2017, Loyau et al., 2012). The effects of citalopram on antibody binding to dimeric GPVI or total GPVI were therefore measured, to determine if citalopram inhibits platelets through reducing levels of dimeric GPVI, or total GPVI surface expression, respectively.

Pre-treatment for approximately 5 minutes with citalopram (200 μM) reduced the fluorescence intensity (F.I.) of platelets labelled with either dimeric (204-11 Fab) or total (HY-101) GPVI antibodies (Figure 5.4), which is indicative of reduced antibody binding. The inhibitory effect of citalopram on 204-11 Fab or HY-101 binding was concentration-dependent (citalopram = 0, 10, 20, 50, 100 & 200 μM). Median F.I. from platelet samples were fitted to the 4PL model, with Max constrained to the F.I. of the isotype control (Figure 5.4). pIC_{50} values were: (204-11 Fab = 4.16 ± 0.03; HY-101 = 3.93 ± 0.07; (N = 6 blood donors)). These data suggest citalopram either reduces both GPVI surface expression and dimer formation on resting platelets, or blocks the binding of GPVI antibodies.

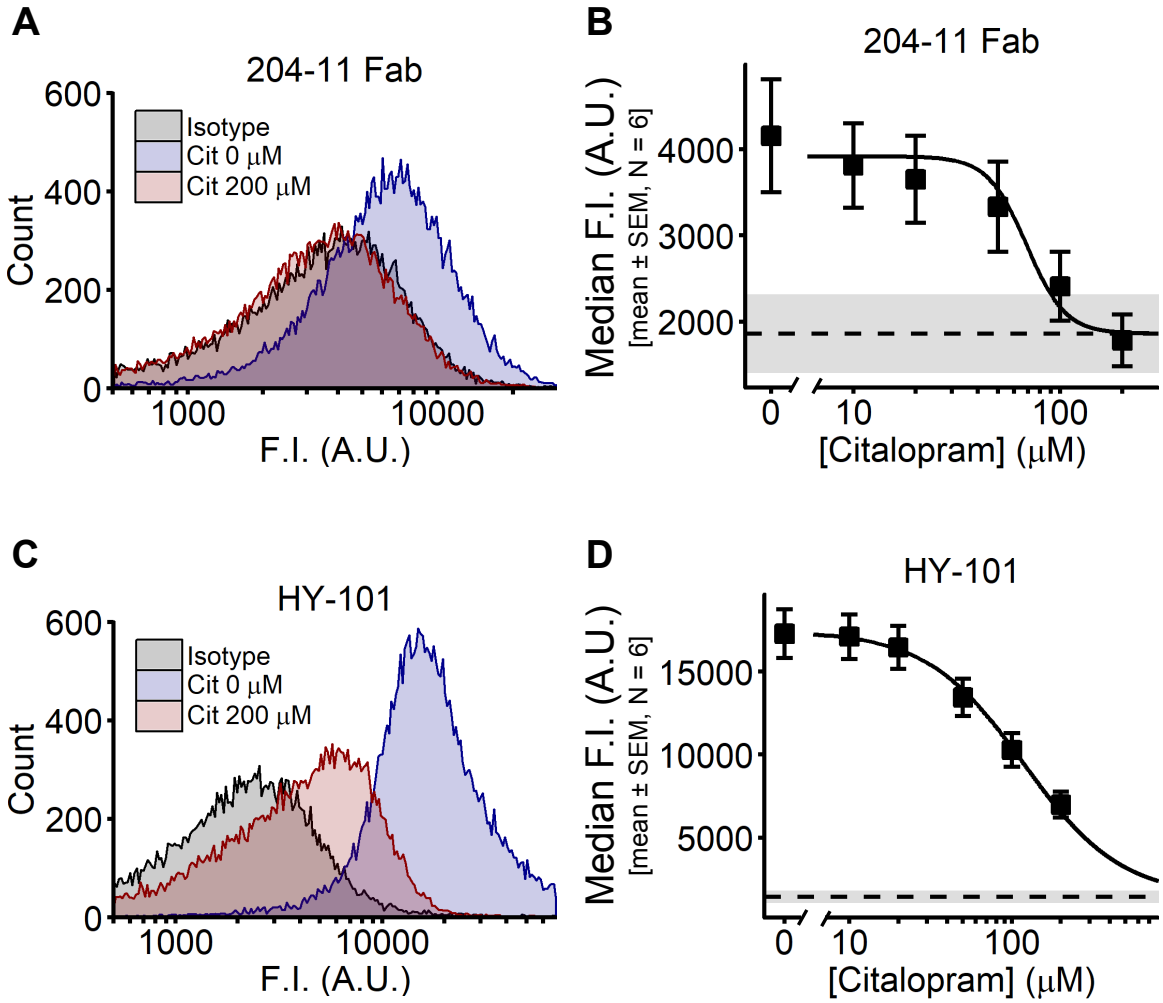

Figure. 5.4 Binding of dimeric glycoprotein VI (GPVI) (204-11 Fab) or total GPVI (HY-101) antibodies to unstimulated platelets. Control Fab or IgG2 were used as corresponding isotype controls for **(A-B)** 204-11 Fab and **(C-D)** HY-101, respectively. Example histograms represent the fluorescence intensity (F.I.) of platelets pre-incubated with either a GPVI-specific antibody (blue = 0 μM citalopram, red = 200 μM citalopram), or an isotype control (grey). Sample median F.I. was used to generate concentration-response curves, fitted to the four-parameter logistic (4PL) model. Dashed lines (mean) and grey space (± SEM) indicate F.I. of isotype controls, which were used to constrain the Max parameter of the 4PL model (N = 6 blood donors).

5.2.4 Citalopram inhibition is reversible

Impaired antibody binding to GPVI could be a consequence of reduced GPVI surface expression. For example, GPVI ectodomain cleavage or internalisation are irreversible mechanisms that reduce GPVI surface expression and could account for impaired antibody binding. An experiment was therefore designed to determine if platelet inhibition by citalopram was due an irreversible mechanism of action. Platelets were pre-incubated for approximately 5 minutes with citalopram, which was subsequently removed by pelleting and resuspending platelets in fresh calcium-free Tyrode's (CFT). Platelets were then stimulated with collagen under aggregometry conditions.

Consistent with previous results (Figure 3.4), citalopram inhibited collagen-induced platelet aggregation (citalopram = 100 μM, collagen = 0.05, 0.1, 0.2, 0.5, 1, 2, 5 & 10 μg mL^{-1}) 5.5A-B). Resuspension of platelets in fresh CFT partially restored collagen-induced aggregation, which was comparable to resuspended platelets with no prior citalopram treatment (Figure 5.5C-E). A second citalopram treatment (100 μM) to previously treated, pelleted and resuspended platelets again inhibited collagen-induced aggregation. Agonist concentration-response curves were fitted to the 4PL model and pEC_{50} values for the five different treatments (Figure 5.5F) are: (untreated = 6.53 ± 0.09; citalopram-treated = 5.19 ± 0.11; untreated resuspended = 5.93 ± 0.17; citalopram-treated resuspended = 5.90 ± 0.18; citalopram-treated, resuspended and citalopram-treated = 5.02 ± 0.08; (N = 6 blood donors)). Analysis by 2-way ANOVA (Effect 1 (fixed) = treatment {1,2,3,4,5}; Effect 2 (random) = donor {N = 6}) strongly suggested a difference between the pEC_{50} values of the five treatments ($P = 8.47 \times 10^{-9}$, F = 35.28, df = 4, 20). A post-hoc Tukey test strongly suggested that there was no difference between the pEC_{50} values of untreated and citalopram-treated platelets following resuspension ($P = 0.9998$). These data show the inhibitory effects of citalopram on collagen-induced platelet aggregation are reversible.

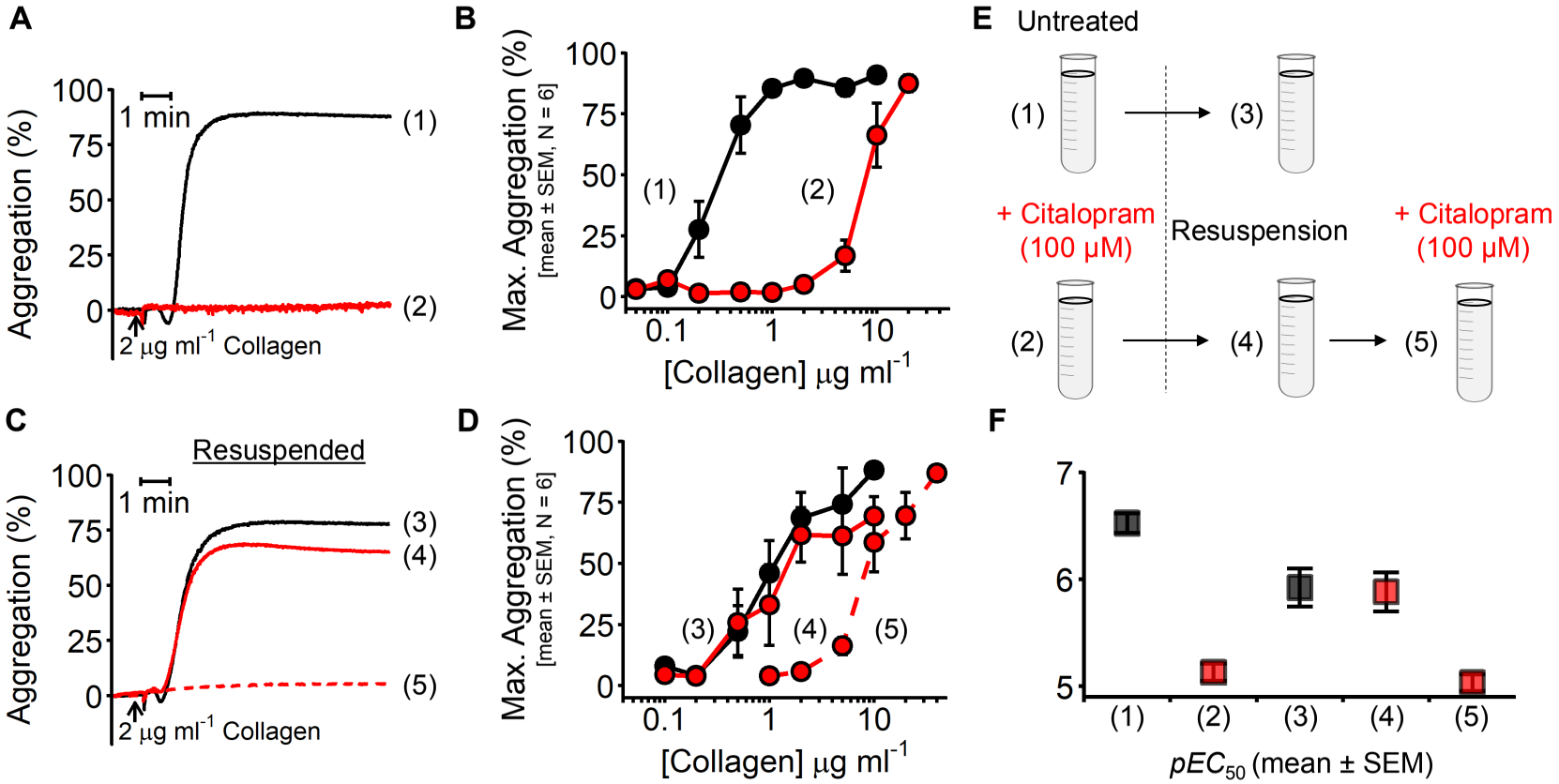

Figure. 5.5 Citalopram inhibition of collagen-induced platelet aggregation is reversible. **(A-B)** Two stocks of washed platelets were either untreated (1) or treated with 100 μM citalopram (2). Samples were aliquoted to measure collagen-induced aggregation. **(C-D)** Stocks (1) and (2) were then treated with PGE_1, centrifuged, pellets resuspended in fresh calcium-free Tyrode's (CFT) and left to rest for 1 hour. Platelet aggregation was then measured in untreated resuspended platelets (3), citalopram-treated resuspended platelets (4), and citalopram-treated resuspended platelets which received a second subsequent citalopram treatment of 100 μM (5). **(E)** Schematic outlining the experimental design to test the reversibility of platelet inhibition by citalopram. Resuspension indicates the removal of citalopram by resuspending platelets in fresh CFT. **(F)** pEC_{50} values, derived from the concentration-response curves of **(B,D)** (N = 6 blood donors).

5.3 Discussion

5.3.1 Overview

The experiments in this chapter aim to identify mechanisms of citalopram inhibition on the GPVI signalling pathway. Citalopram inhibited CRPXL-induced platelet aggregation, with Schild analysis suggesting citalopram shows characteristics of a competitive antagonist at concentrations up to 50 μM. Citalopram did, however, display characteristics of a non-competitive antagonist at concentrations exceeding 50 μM. Citalopram also inhibited the CRPXL-induced phosphorylation of SFKs, FcRγ-chain, LAT and PLCγ2. The binding of GPVI antibodies to resting platelets was also reduced following citalopram treatment, suggesting either a reduction in GPVI surface expression or disrupted antibody binding. Finally, inhibition of collagen-induced aggregation by citalopram was reversible, demonstrating that citalopram does not mediate its effects through reducing GPVI surface expression. Based on these results, the data in this chapter suggest a putative mechanism of platelet inhibition by citalopram, where direct and competitive interactions with the GPVI receptor prevent agonist binding and disrupt downstream signal transduction.

5.3.2 Inhibition of early GPVI signal transduction

Previous results show that citalopram inhibited CRPXL-induced increases in $[Ca^{2+}]_{cyt}$ (Figure 4.3). The effects of citalopram on GPVI signalling events upstream of $[Ca^{2+}]_{cyt}$ increases were therefore investigated, including the phosphorylation of SFKs, LAT and PLCγ2 at amino acid residues associated with signal transduction. Collagen binding to its other receptor $\alpha_2\beta_1$, induces integrin outside-in signalling, phosphorylating several proteins that are also involved in GPVI signal transduction, including Syk and PLCγ2 (Inoue et al., 2003, Jarvis et al., 2004). Therefore, to discriminate between citalopram's effects on GPVI and $\alpha_2\beta_1$ outside-in signalling, platelets were stimulated with the GPVI-selective agonist, CRPXL.

Citalopram inhibited CRPXL-induced phosphorylation of SFKs (Tyr-416), LAT (Tyr-200) and PLCγ2 (Tyr-1217) (Figure 5.3). Concentrations of citalopram at or above 100 μM abolished phosphorylation of SFKs and PLCγ2, despite residual LAT phosphorylation. Although functional LAT is required for optimal GPVI-mediated platelet activation, other adaptor proteins, including Src homology 2 domain-containing leukocyte phosphoprotein of 76 kDa (SLP-76) are thought to be of greater importance for downstream PLCγ2 phosphorylation and platelet aggregation (Judd et al., 2002). Citalopram may, there-

fore, suppress the activity of other adaptor proteins, such as SLP-76, while only partially impairing LAT phosphorylation.

Platelet lysates probed with 4G10 (which binds phosphorylated tyrosine residues) suggest that citalopram also inhibits FcRγ-chain phosphorylation (kDa $\approx$ 15) (Gibbins et al., 1996). The SFKs Lyn/Fyn phosphorylate the FcRγ-chain ITAM, resulting in downstream LAT and PLCγ2 phosphorylation (Chapter 5.1.4). Citalopram may, therefore, prevent Lyn/Fyn-mediated FcRγ-chain ITAM phosphorylation. The phospho-SFK (Tyr-416) antibody used in this chapter (Table 2.5) cross-reacts with the activation loop of Lyn (Tyr-396) and Fyn (Tyr-419), suggesting that citalopram reduces phosphorylation of the Fyn/Lyn activation loop. Citalopram also reduced SFK (Tyr-416) phosphorylation below basal (unstimulated) levels. In unstimulated platelets, the activation loop of GPVI-bound Lyn is phosphorylated, which is thought to prime platelets for rapid signal transduction upon receptor ligation and clustering (Schmaier et al., 2009). Citalopram could, therefore, prevent receptor priming by impairing basal phosphorylation of the Lyn activation loop. Lyn/Fyn activity is also controlled through C-terminal phosphorylation (Lyn = Tyr-507, Fyn = Tyr-530) by C-terminal Src kinase (Csk). Phosphorylation by Csk blocks the active site of Lyn/Fyn through interactions with their own SH2 domains, a process reversed by the receptor-type tyrosine-protein phosphatase J (also known as CD148 or DEP-1) (Senis et al., 2009, Ellison et al., 2010, Mori et al., 2012). Citalopram could theoretically prevent ITAM phosphorylation through the C-terminal phosphorylation of Fyn/Lyn, mediated by either upregulated Csk activity, or reduced CD148 activity. However, results from this chapter suggest inhibition of the Fyn/Lyn activation loop is the primary cause for impaired ITAM phosphorylation and downstream signal transduction.

5.3.3 The effects of citalopram on the GPVI receptor

Citalopram prevented early protein phosphorylation following CRPXL stimulation (Figure 5.3). Such phosphorylation is thought to be initiated by increased GPVI dimerisation and clustering upon agonist stimulation (Poulter et al., 2017, Jung et al., 2012, Loyau et al., 2012). GPVI dimers on unstimulated platelets provide high-affinity sites for collagen, priming platelets for increased dimer formation and receptor clustering upon collagen-binding (Jung et al., 2012, Poulter et al., 2017, Loyau et al., 2012). The binding of a dimeric GPVI antibody (204-11 fab) was reduced in unstimulated platelets pre-treated with citalopram, suggesting citalopram either reduced GPVI dimer levels or disrupted 204-11 Fab binding. Of note, reduced binding was also observed with HY-101, an antibody which binds both

monomeric and dimeric GPVI. These two findings suggest that citalopram either reduces total GPVI surface expression or blocks the binding of GPVI antibodies.

GPVI expression on the platelet surface can be reduced through two irreversible mechanisms: 1) Proteolytic cleavage of its extracellular domain, often referred to as "shedding" or 2) receptor internalisation (Rabie et al., 2007). GPVI shedding occurs within seconds of collagen-induced platelet activation, liberating a GPVI ectodomain fragment and retaining a $\approx$ 10 kDa portion within the plasma membrane (Gardiner et al., 2007). Ectodomain shedding is predominantly mediated by ADAM10 on the platelet surface, which is activated by calmodulin dissociation from GPVI (Andrews et al., 2002, Gardiner et al., 2007). The mechanisms underlying GPVI Internalisation are largely unknown. Cyclic adenosine monophosphate (cAMP) levels and GPVI signal transduction have separately been reported to induce GPVI internalisation *in vitro* and *in vivo*, respectively (Rabie et al., 2007, Takayama et al., 2008).

Experiments utilising platelet aggregometry were therefore conducted to test if citalopram inhibited platelets through an irreversible mechanism of action. The supernatant of platelets treated with citalopram was replaced with fresh CFT, with the assumption that if citalopram irreversibly inhibits GPVI-mediated activation, then removing citalopram from the supernatant would not restore responses to collagen. Removing citalopram did, however, restore collagen-induced platelet aggregation (Figure 5.5), suggesting that citalopram-induced inhibition of GPVI signalling is reversible and therefore unlikely to be a consequence of GPVI cleavage or internalisation. PLCγ2 and LAT phosphorylation was also not observed or impaired in either unstimulated or citalopram-treated CRPXL-stimulated platelets, respectively (Figure 5.3), and functional PLCγ2 and LAT are required for receptor shedding (Rabie et al., 2007). ADAM10-mediated cleavage of GPVI is also Ca^{2+}-dependent, and citalopram inhibits CRPXL-induced increases in $[Ca^{2+}]_{cyt}$ (Figure 4.3). These findings collectively suggest citalopram does not cause GPVI cleavage. Comparing platelet and supernatant levels of the GPVI ectodomain following citalopram treatment could reinforce this hypothesis (Gardiner et al., 2007).

5.3.4 Putative competitive binding of citalopram to GPVI

Despite its reversible effects, citalopram prevented the binding of GPVI antibodies, and impaired platelet activation by GPVI agonists. This suggests a putative inhibitory mechanism, whereby citalopram directly binds the GPVI receptor. This hypothesis is supported both by previous experiments, where simultaneous co-incubation of platelets with both citalopram and collagen prevented platelet aggregation (Figure 3.3), and from Schild

analysis from this chapter, which suggests citalopram inhibition displays characteristics of a competitive antagonist at concentrations up to 50 μM. Comparisons between this seemingly competitive mechanism and the non-competitive effects observed above 50 μM will be discussed further in Chapter 7.3.1. Further experiments, involving competition binding assays or surface plasmon resonance could help identify direct interactions between citalopram and GPVI.

Comparing the effects of citalopram between GPVI and a different receptor that shares initial steps in platelet activation, could establish if inhibition is solely mediated through binding GPVI. Fc γ receptor IIA (FcγRIIA)-mediated signal transduction, for example, is highly homologous to that of GPVI. The intracellular region of FcγRIIA contains an ITAM which is phosphorylated by Lyn/Fyn, mediating Syk auto-phosphorylation, downstream PLCγ2 activation and Ca^{2+} release from intracellular stores (Shen et al., 1994, Qiao et al., 2015). Therefore, if citalopram also inhibits FcγRIIA-mediated phosphorylation of SFKs, the FcγRIIA ITAM and PLCγ2, then its effects are unlikely through binding GPVI, but instead by suppressing the activity of downstream intracellular proteins that are important for platelet activation. The effects of citalopram treatment on FcγRIIA stimulation are however yet to be determined and could be investigated in future experiments. Similar experiments could also be designed to assess the inhibitory effects of citalopram on CLEC-2-mediated signal transduction.

In summary, the results presented in this chapter show that citalopram inhibits early signalling events of GPVI-mediated platelet activation. Citalopram also prevented the binding of GPVI antibodies, which was not a consequence of irreversible reductions in GPVI surface expression. These findings, in conjunction with the rapid and seemingly competitive nature of inhibition, suggest a putative mechanism in which citalopram binds GPVI, preventing the subsequent binding of antibodies and agonists. Whether citalopram inhibits GPVI signalling through direct binding to the receptor or by suppressing the activity of an intracellular target is, however, yet to be determined.

Chapter 6
Platelet inhibition by various antidepressants

6.1 Background

Data presented in earlier chapters demonstrates that the selective serotonin reuptake inhibitor (SSRI) citalopram inhibits platelet functional responses through at least two serotonin transporter (SERT)-independent mechanisms. In addition to citalopram, several other SSRIs have been reported to inhibit platelets *in vitro*, as have some serotonin and norepinephrine reuptake inhibitors (SNRIs) and tricyclic antidepressants (TCAs). However, unlike citalopram, the effects that other antidepressants have on platelets are inconsistent and a systemic investigation is required for comprehensive characterisation.

6.1.1 The effects of antidepressants on platelet function

In addition to citalopram, other SSRIs have been reported to mediate platelet function *in vitro*. Pre-treating platelets with 50 μM fluoxetine, sertraline or paroxetine inhibited platelet aggregation in response adenosine diphosphate (ADP) (Tseng et al., 2013). Paradoxically, 5 μM fluoxetine augmented protease-activated receptor (PAR)-mediated platelet aggregation (Dilks and Flaumenhaft, 2008), and 20 μM fluoxetine increased ADP- and thrombin-induced calcium (Ca^{2+}) release from intracellular stores (Harper et al., 2009). Fluoxetine (10 μM) has also been reported to have no effect on platelet aggregation initiated by PAR agonists, ADP or collagen (Bampalis et al., 2010). The varied agonists and platelet preparations in these studies, which include washed platelets (Dilks and Flaumenhaft, 2008, Harper et al., 2009), platelet-rich plasma (Tseng et al., 2013) and whole blood (Bampalis et al., 2010), could partially account for such conflicting findings. Previous experiments also use narrow or single antidepressant concentration ranges, making clear comparisons between SSRIs difficult.

SNRIs are another class of antidepressant that bind SERT, but also show some selectivity for the norepinephrine transporter (NET) (Owens et al., 1997, Bymaster et al., 2001, Vaishnavi et al., 2004). Platelets pre-treated with 90 μM of the SRNI, venlafaxine show reduced aggregation in response to ADP, epinephrine and arachidonic acid (Sarma and

Horne, 2006). Such concentrations exceed those required to inhibit either SERT (K_i = 102 ± 9 nM) or NET (K_i = 1,644 ± 84 nM) (Owens et al., 1997). However, lower concentrations of venlafaxine (3.6-360 nM) which dose-dependently block SERT did not inhibit platelet adhesion to either collagen or fibrinogen (Hallback et al., 2012). This suggests that as with SSRIs, any *in vitro* antiplatelet effects mediated by SNRIs occur at micromolar concentrations and are therefore likely to be independent of SERT inhibition.

TCAs such as imipramine and doxepin also bind and inhibit SERT at nanomolar concentrations (Owens et al., 1997, Tatsumi et al., 1997). These TCAs are however not selective for SERT, and bind to NET, 5-$HT_{1A/2A}$ receptors, histamine H_1 receptors, $\alpha_{1/2}$ adrenergic receptors and muscarinic receptors with nanomolar affinities (Owens et al., 1997, Vaishnavi et al., 2004). Doxepin has recently been shown to inhibit platelet activation *in vitro* (Geue et al., 2017). Pre-treating platelets with 5 μM doxepin inhibited glycoprotein VI (GPVI)-mediated inositol triphosphate (IP_3) production, increases in cytosolic calcium concentration ($[Ca^{2+}]_{cyt}$), granule release and platelet aggregation. This concentration of doxepin is approximately two orders of magnitude higher than the concentration required to bind SERT (K_i = 68 ± 1 nM) (Tatsumi et al., 1997), suggesting effects were not mediated through blocking the transporter. Indeed, the authors hypothesise a SERT-independent mechanism, where doxepin binding to histamine H_1 receptors impairs platelet activation (discussed further in Chapter 7).

To summarise, in addition to citalopram, several antidepressants that block SERT at nanomolar concentrations have previously been reported to inhibit platelets *in vitro*. However, in all cases, inhibition was only observed at micromolar concentrations, suggesting a SERT-independent mechanism of action. Although there are several reports on the effects of SSRIs, TCAs and SNRIs on platelet function *in vitro*, there have been no systematic studies, and experiments predominantly focus on platelet aggregation, with little data available on other functions, such as $[Ca^{2+}]_{cyt}$ or platelet granule release. The micromolar concentrations required to inhibit platelets could also induce cytotoxicity, a question not addressed in any of the aforementioned studies. Finally, the narrow or single antidepressant concentration ranges that have been used provide no information on the inhibitory potencies (e.g. pIC_{50} values) of these compounds. Such information could be compared between antidepressants to determine the most potent antiplatelet agents.

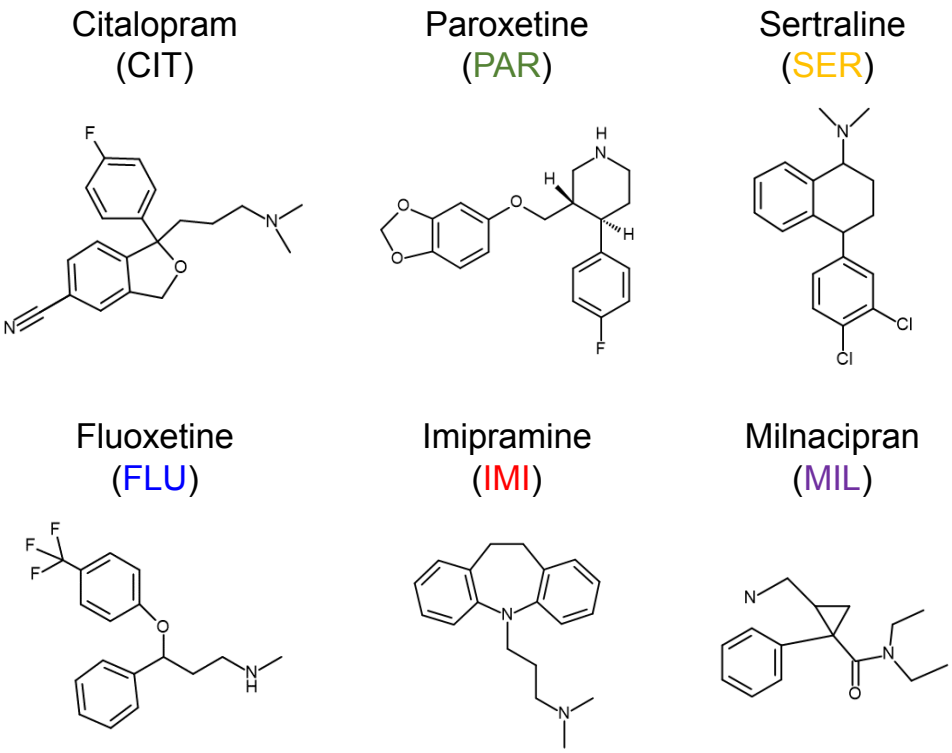

Figure. 6.1 Chemical structures of antidepressants used in this chapter. Citalopram, paroxetine, sertraline and fluoxetine are selective serotonin reuptake inhibitors (SSRIs), imipramine is a tricyclic antidepressant (TCA) and milnacipran is a serotonin and norepinephrine reuptake inhibitor (SNRI). Chiral centres and stereoisomers of citalopram, sertraline, fluoxetine and milnacipran are not depicted. The colour scheme used in compound abbreviations is used throughout the chapter. Chemical structures were constructed using BIOVIA Draw 2016 version 5.1.0.22 (Dassault Systèmes, Vélizy-Villacoublay, France).

6.1.2 Aims

Experiments in this chapter aim to comprehensively characterise the *in vitro* effects of commonly-prescribed antidepressants on platelets. This aim will be met by:

1. Using a wide range of antidepressant concentrations to determine and compare any inhibitory potencies on platelet functional responses, including aggregation, dense granule release and Ca^{2+} store release.

Six antidepressants were tested (Figure 6.1), including four SSRIs (citalopram; paroxetine; sertraline; fluoxetine), a TCA (imipramine) and a SNRI (milnacipran).

6.2 Results

6.2.1 Cell cytotoxicity

Supernatant levels of lactate dehydrogenase (LDH) were measured to test if micromolar antidepressant concentrations induced cytotoxicity. Platelets were incubated for 10 minutes with either citalopram, paroxetine, sertraline, fluoxetine, imipramine or milnacipran (2, 5, 10, 20, 50, 100 & 200 μM), before quantifying supernatant levels of LDH. Citalopram, imipramine and milnacipran did not induce LDH release at any concentration tested. However, paroxetine, sertraline and fluoxetine induced dose-dependent cytotoxicity at concentrations above 50 μM (Figure 6.2). Therefore, concentrations of sertraline, paroxetine and fluoxetine above 50 μM were not used in subsequent experiments.

6.2.2 Inhibition of platelet aggregation

Previous studies by others describe both inhibitory and potentiating effects of antidepressants on platelet aggregation (Chapter 6.1.1). These studies used various platelet preparations and agonists, as well as a limited range of antidepressant concentrations. Therefore, the effects of either citalopram, paroxetine, sertraline, fluoxetine, imipramine or milnacipran on collagen-induced platelet aggregation were quantified using a range of antidepressant concentrations. 1, 2, 5, 10, 20 & 50 μM were used for paroxetine, sertraline and fluoxetine. Due to its non-cytotoxic effects (Figure 6.2), the above concentrations were also used for imipramine, with an additional 100 μM treatment. An initial pilot experiment determined that higher concentrations of milnacipran would be required for inhibitory effects. As such, the milnacipran concentrations used in this experiment were 10, 20, 50, 100, 200 & 500 μM. Due to limited resources, and its previously determined inhibitory potency (Figure 3.4, $IC_{50} \approx 50$ μM) the range of citalopram concentrations was restricted to 5, 10, 20, 50, 100 & 200 μM. Platelets were pre-incubated with antidepressants for approximately 5 minutes, before stimulation with collagen (1 μg mL^{-1}).

Every antidepressant inhibited platelet aggregation in a concentration-dependent manner, but with differing potencies (Figure 6.3). pIC_{50} values for the maximum extent of aggregation over 6 minutes were: citalopram = 4.52 ± 0.09; paroxetine = 5.13 ± 0.11; sertraline = 4.99 ± 0.03; fluoxetine = 5.13 ± 0.11; imipramine = 4.96 ± 0.05; milnacipran = 3.72 ± 0.09 (N = 5 blood donors). Data for citalopram obtained from these experiments was comparable to previous results for inhibition of collagen-induced aggregation: pIC_{50} = 4.31 ± 0.21 (Table 3.1).

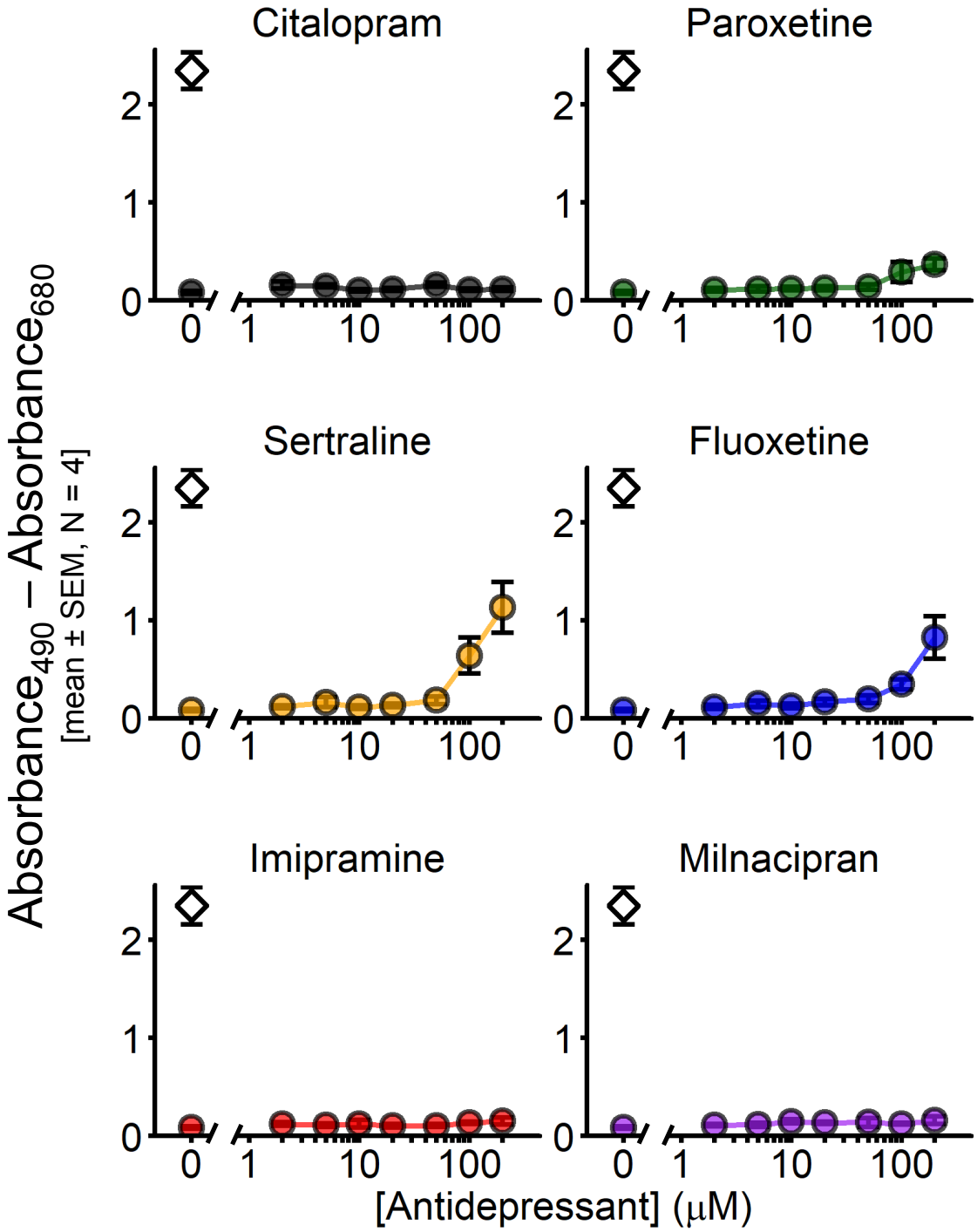

Figure. 6.2 Lactate dehydrogenase (LDH) release from platelets into the supernatant was used as a marker of cell cytotoxicity. Platelets were incubated for 10 minutes with either citalopram, paroxetine, sertraline, fluoxetine, imipramine or milnacipran. Levels of supernatant LDH were quantified by subtracting the absorbance at 680 nm from the absorbance at 490 nm. Lysed platelets (white diamonds) were used as positive controls. Unobserved error bars (SEM) reside within data points (N = 4 blood donors).

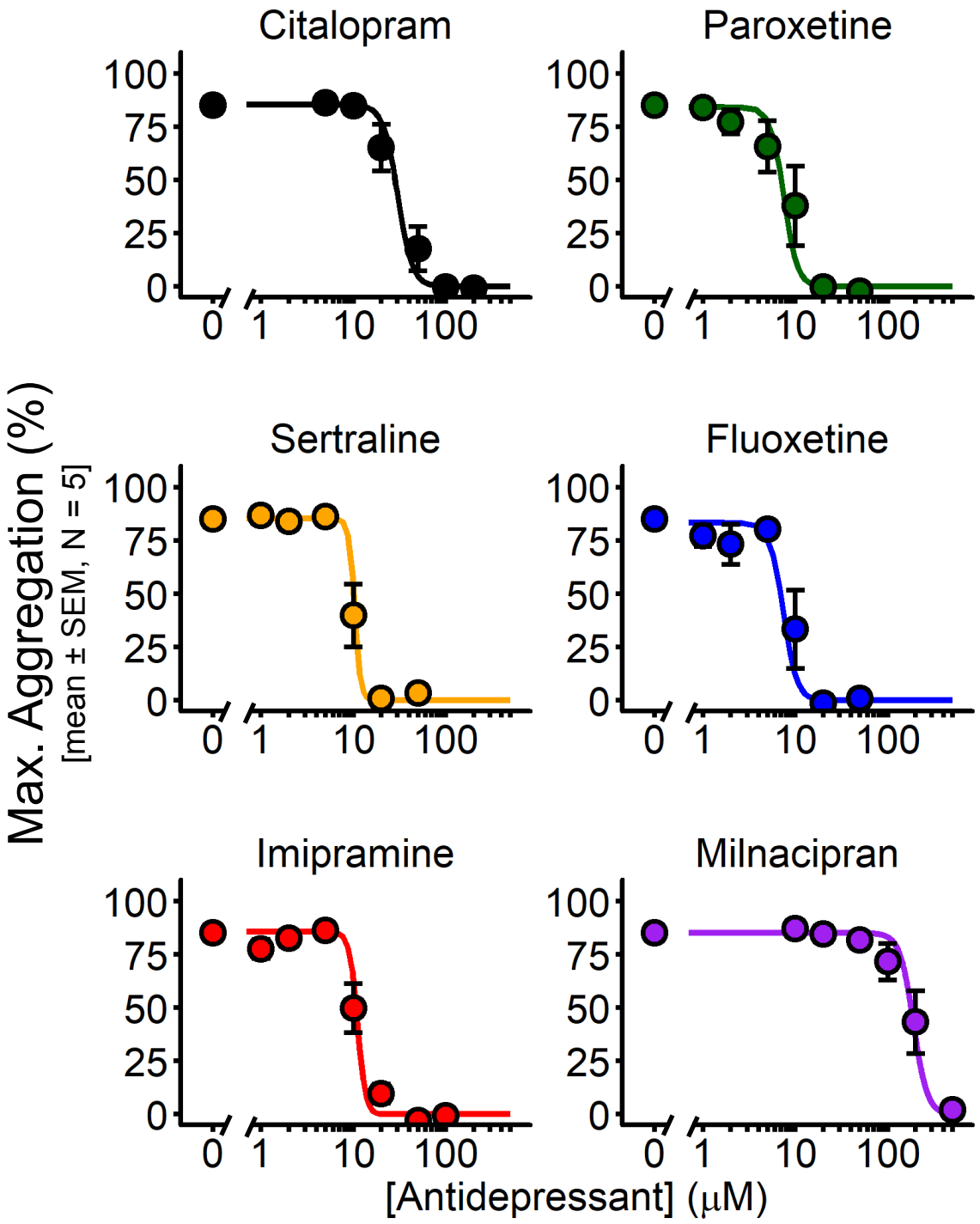

Figure. 6.3 Platelet aggregation was monitored following pre-incubation for approximately 5 minutes with either citalopram, paroxetine, sertraline, fluoxetine, imipramine or milnacipran. Platelet aggregation was induced by 1 μg mL^{-1} collagen, and the maximum extent of platelet aggregation (Max. Aggregation) was recorded over 6 minutes. Concentration-response curves were generated according to the four-parameter logistic (4PL) model, using various antidepressant concentrations. pIC_{50} values were used to compare inhibitory potencies (N = 5 blood donors).

6.2.3 Inhibition of platelet dense granule release

Dense granule release is an important feature of platelet activation, potentiating aggregation through secondary mediators, such as ADP and 5-HT. Antidepressants may, therefore, inhibit platelet aggregation by suppressing the release of platelet agonists from dense granules. However, with the exception of citalopram, which dose-dependently inhibited dense granule release at 5 and 50 μM (Tseng et al., 2010), the *in vitro* effects of antidepressants on dense granule release remain largely undocumented. Collagen-induced dense granule release was therefore quantified by measuring supernatant concentrations of adenosine triphosphate (ATP) from samples previously processed for aggregometry (Chapter 6.2.2). Every antidepressant inhibited ATP release into the supernatant in a concentration-dependent manner, with varied potencies (Figure 6.4). pIC_{50} values were: citalopram = 4.53 ± 0.06; paroxetine = 4.96 ± 0.12; sertraline = 5.04 ± 0.05; fluoxetine = 5.05 ± 0.12; imipramine = 4.84 ± 0.09; milnacipran = 3.75 ± 0.09 (N = 5 blood donors).

6.2.4 Inhibition of platelet calcium signalling

Ca^{2+} is an important secondary messenger in platelet signalling during activation, and increasing the $[Ca^{2+}]_{cyt}$ mediates subsequent dense granule release and platelet aggregation. Impaired Ca^{2+} signalling could, therefore, explain why antidepressants inhibit platelet aggregation (Figure 6.3) and dense granule secretion (Figure 6.4). This hypothesis is supported by previous results (Figure 4.3), where citalopram inhibited cross-linked collagen-related peptide (CRPXL)-induced increases in $[Ca^{2+}]_{cyt}$. However, a detailed account of the effects of other antidepressants on $[Ca^{2+}]_{cyt}$ is lacking. Therefore, CRPXL-induced (0.5 μg mL^{-1}) Ca^{2+} store release was measured in platelets pre-treated for approximately 5 minutes with antidepressants. A range of concentrations (5, 10, 20 & 50 μM) were used for paroxetine, sertraline and fluoxetine, with an additional 100 μM treatment included for imipramine. Due to limited resources, concentrations for citalopram (10, 20, 50, 100 & 200 μM) and milnacipran (100, 200, 500 & 1000 μM) were restricted.

Each antidepressant inhibited peak increases in $[Ca^{2+}]_{cyt}$ induced by CRPXL. Inhibition was concentration-dependent, but antidepressants inhibited responses with differing potencies (Figure 6.5). pIC_{50} values were: citalopram = 4.21 ± 0.13; paroxetine = 4.88 ± 0.08; sertraline = 5.08 ± 0.03; fluoxetine = 4.78 ± 0.06; imipramine = 4.74 ± 0.15; milnacipran = 3.48 ± 0.17 (N = 4 blood donors). The *Max* parameter was constrained to zero. Data for citalopram from these experiments was comparable to previous results for inhibition of CRPXL-induced increases in $[Ca^{2+}]_{cyt}$: pIC_{50} = 4.34 ± 0.09 (Chapter 4.3).

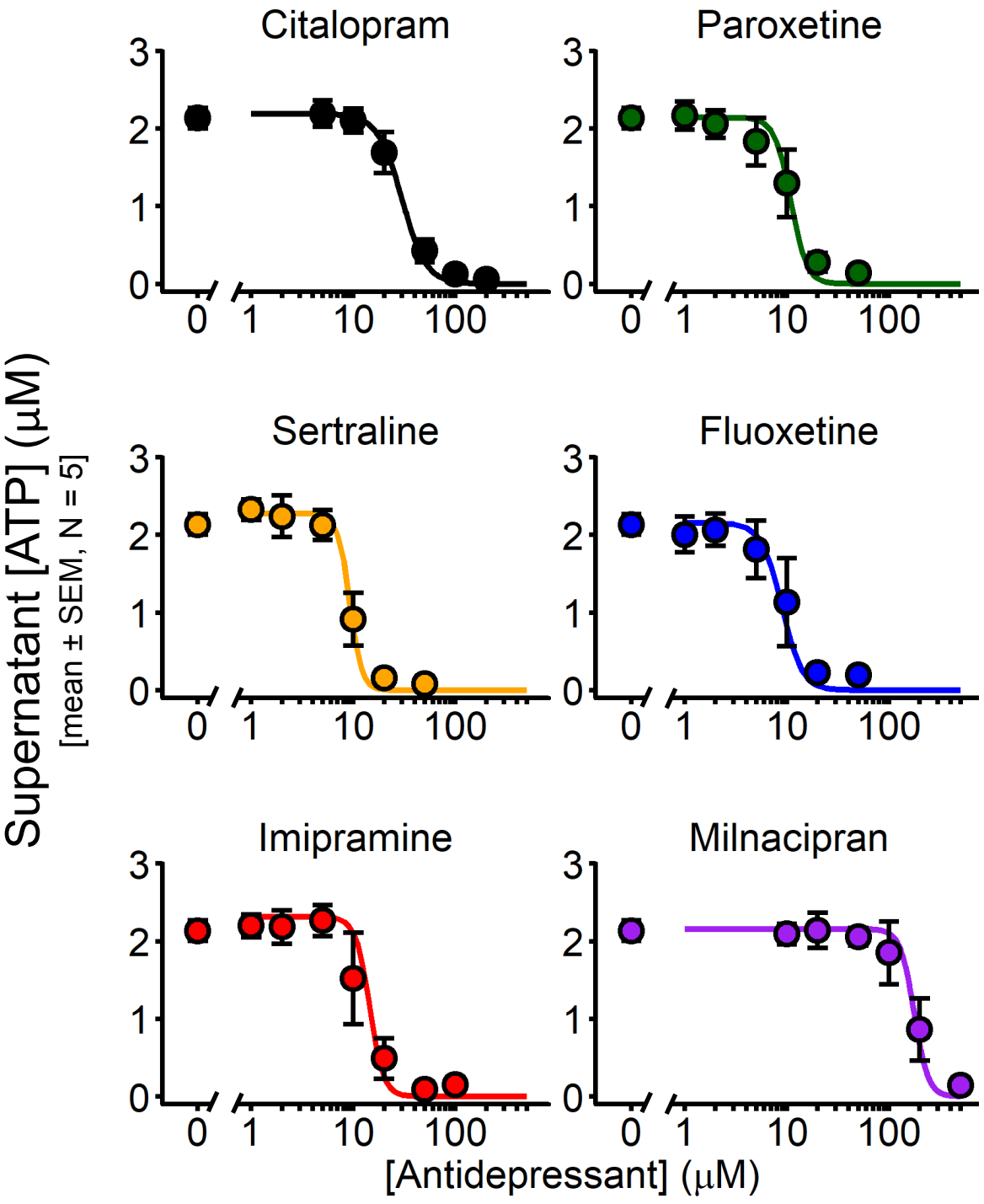

Figure. 6.4 Supernatant concentrations of adenosine triphosphate (ATP) were measured as a marker of dense granule release, using high-pressure liquid chromatography (HPLC). Prior to stimulation for 6 minutes with 1 μg mL^{-1} collagen, platelets were pre-incubated for approximately 5 minutes with either citalopram, paroxetine, sertraline, fluoxetine, imipramine or milnacipran. ATP concentration-response curves were generated from the supernatants of platelets pre-treated with various concentrations of each antidepressant. pIC_{50} values were used to compare the inhibitory potencies (N = 5 blood donors).

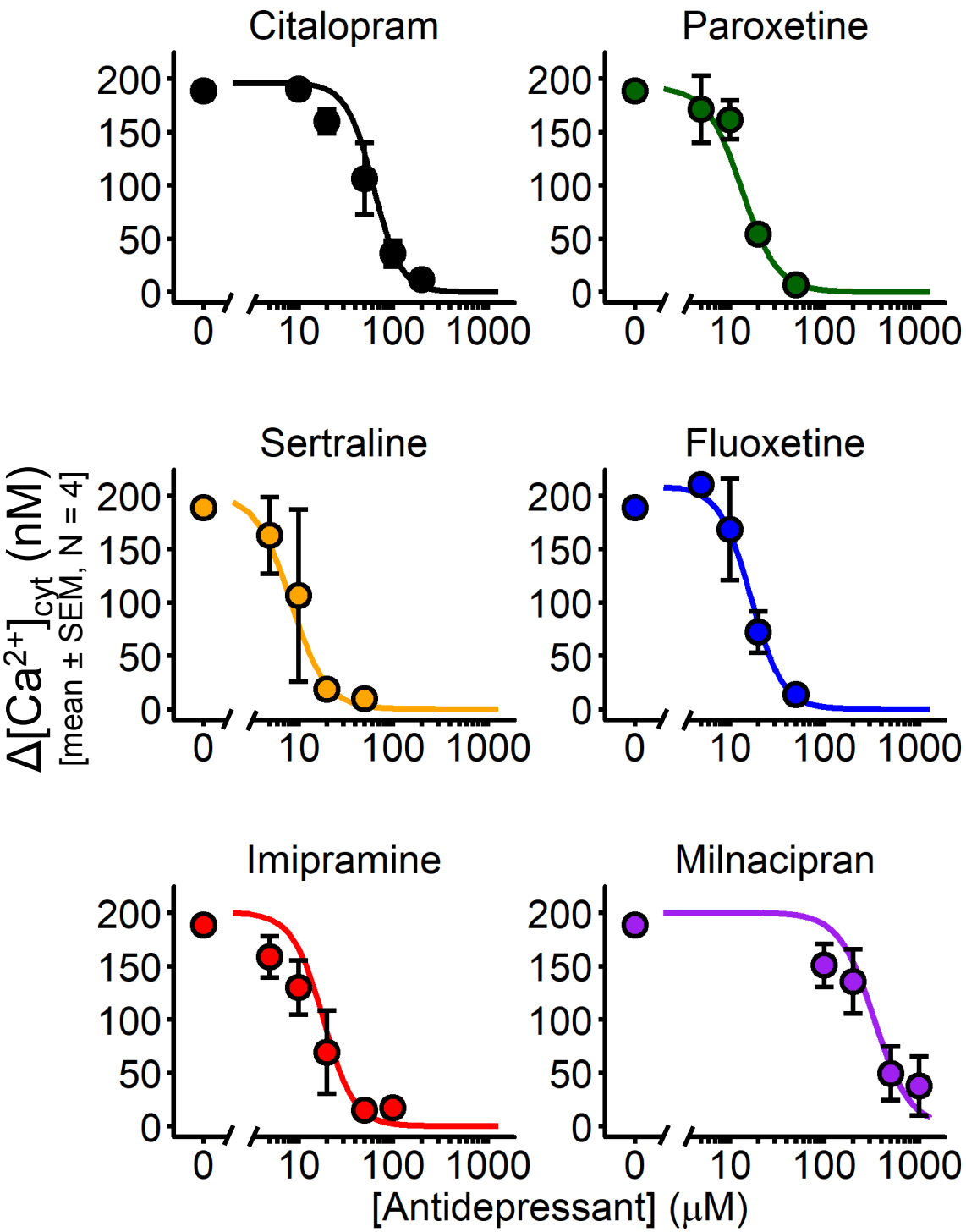

Figure. 6.5 The release of calcium (Ca^{2+}) from intracellular stores was measured using the Ca^{2+} indicator, Fura-2. Platelets were pre-incubated for approximately 5 minutes with either citalopram, paroxetine, sertraline, fluoxetine, imipramine or milnacipran. Cross-linked collagen-related peptide (CRPXL, 0.5 μg mL^{-1}) was added to increase the cytosolic concentration of Ca^{2+} ($[Ca^{2+}]_{cyt}$) and the maximum $[Ca^{2+}]_{cyt}$ was recorded over 3 minutes ($\Delta[Ca^{2+}]_{cyt}$). Various antidepressant concentrations were used to generate concentration-response curves. Inhibitory potencies were compared using pIC_{50} values (N = 4 blood donors).

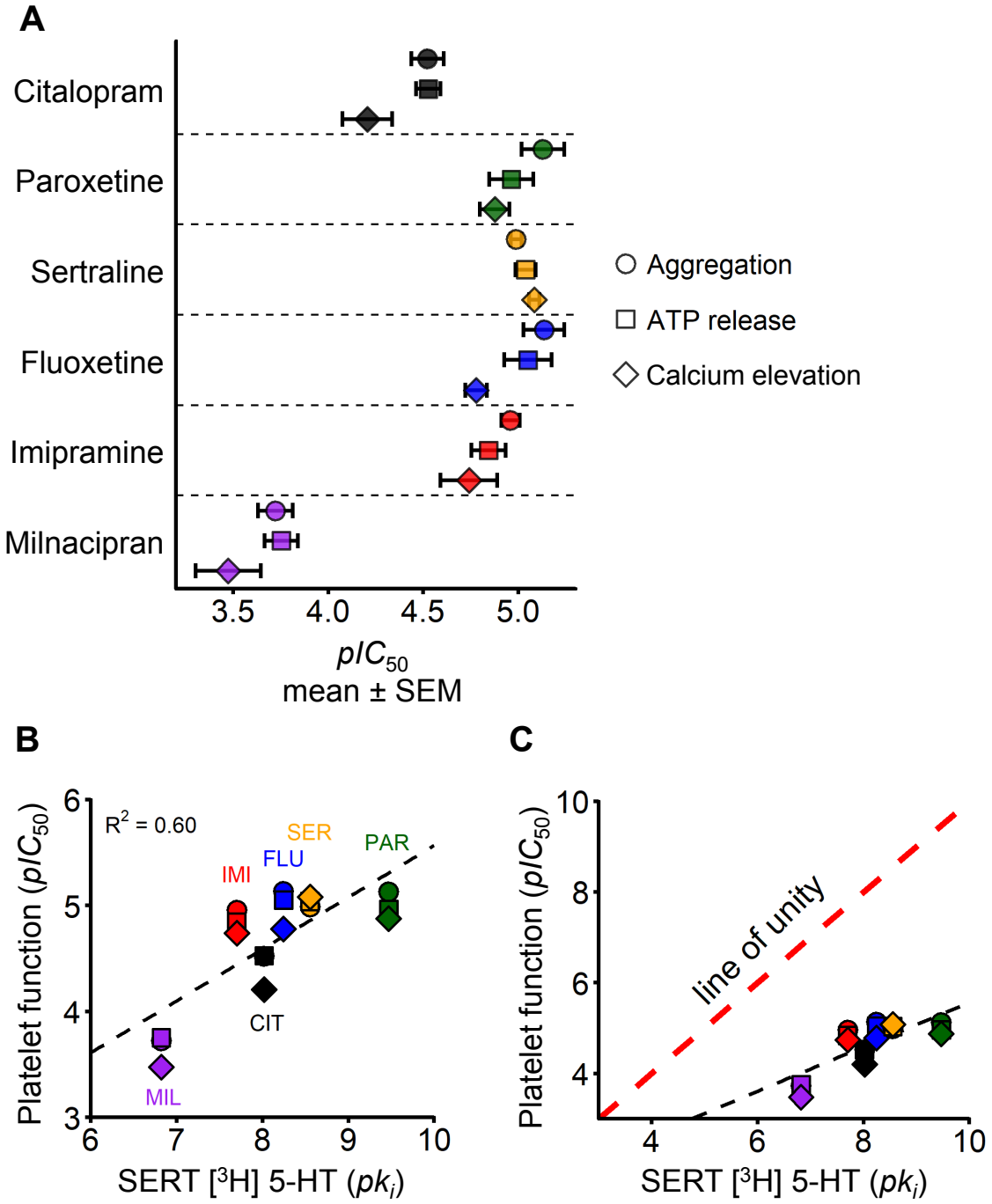

Figure. 6.6 Summary of platelet inhibition and SERT blockade by various antidepressants **(A)** Summary results from the chapter, comparing pIC_{50} values (mean ± SEM) between antidepressants, as well as between Max. Aggregation (Figure 6.3), adenosine triphosphate (ATP) release (Figure 6.4) and calcium release from intracellular stores (Figure 6.5). **(B)** Inhibitory pIC_{50} values for antidepressants were compared against previously published pK_i values for the binding of tritiated 5-HT ([^{3}H] 5-HT) to SERT, which is used as a marker for 5-HT uptake (Owens et al., 1997, 2001, Vaishnavi et al., 2004). The black, dashed line represents the fit for linear regression. **(C)** The line of unity (red, dashed line) indicates where data should reside if SERT blockade and platelet inhibition occurred at similar antidepressant concentrations.

6.3 Discussion

6.3.1 Overview

Results in this chapter show platelet inhibition by four SSRIs (citalopram, paroxetine, sertraline, fluoxetine), a TCA (imipramine) and a SNRI (milnacipran). Inhibition was concentration-dependent for each antidepressant and was only achieved at micromolar concentrations, unlike the nanomolar concentrations required to inhibit 5-HT uptake via SERT (Owens et al., 1997, 2001, Tatsumi et al., 1997, Vaishnavi et al., 2004). Every antidepressant tested inhibited platelet aggregation (Figure 6.3), dense granule release (Figure 6.4) and Ca^{2+} store release (Figure 6.5). Following agonist stimulation, early increases in $[Ca^{2+}]_{cyt}$ derived from intracellular stores are essential for subsequent platelet aggregation and dense granule release (Varga-Szabo et al., 2009). Therefore, the inability for antidepressant-treated platelets to aggregate and release dense granules following stimulation with collagen is likely due to impaired Ca^{2+} release from intracellular stores. Future studies should investigate whether these antidepressants inhibit GPVI-mediated signal transduction upstream from increases in $[Ca^{2+}]_{cyt}$, as observed with citalopram (Chapter 5).

6.3.2 Cytotoxicity

LDH is present in the cell cytosol, and supernatant concentrations are commonly measured as a marker for membrane permeability and cell cytotoxicity (Decker and Lohmann-Matthes, 1988, Fotakis and Timbrell, 2006). Paroxetine, sertraline and fluoxetine all induced LDH release at concentrations at or above 100 μM (Figure 6.2), suggesting these concentrations are cytotoxic to platelets. The highest working concentration of dimethyl sulfoxide (DMSO, 0.4% [v/v]) that was used as a diluent for paroxetine, sertraline and fluoxetine does not cause LDH release (Figure 2.6). Indeed, DMSO did not induce LDH release at concentrations up to 10% [v/v]. Therefore, the cytotoxicity observed is unlikely to be a result of DMSO and is more likely mediated by the SSRI compound itself. Paroxetine, sertraline and fluoxetine, but not citalopram have previously been reported to dose-dependently induce apoptosis between 10-100 μM in T lymphocytes (Gobin et al., 2013) (discussed further in Chapter 7.4.1). However, cell cytotoxicity and programmed cell death through apoptosis are two distinct mechanisms in which cell viability is reduced and should therefore not be directly compared. Lymphocyte apoptosis was also observed in cell culture after a 24 hour incubation, unlike experiments in this chapter, where platelets

were treated for 10 minutes under turbidimetric conditions. Determining the rate and cause of cell cytotoxicity induced by paroxetine, fluoxetine and sertraline are worthwhile considerations for future experiments.

6.3.3 Varied inhibitory potencies between antidepressants

One of the major limitations of previous studies was the narrow or singular range of concentration-responses to various antidepressants. By using a comprehensive range of antidepressant concentrations, experiments from this chapter provided inhibitory potencies (pIC_{50} values) for citalopram, paroxetine, sertraline, fluoxetine, imipramine and milnacipran, which can be used to directly compare their antiplatelet effects.

Every antidepressant inhibited platelet aggregation, dense granule release and Ca^{2+} release from intracellular stores, but with varied potencies (Figure 6.6). The most potent compounds for inhibiting platelet functions were paroxetine, sertraline, fluoxetine and imipramine, with IC_{50} values of approximately 5 μM. Plasma concentrations of paroxetine following chronic administration (30 mg per day) typically range between 100-200 nM, of which approximately 95% is bound to plasma proteins (Kaye et al., 1989). Therefore, the concentration of free paroxetine in the plasma (5-10 nM), would be enough to block SERT (K_i = 0.34 ± 0.03 nM) (Owens et al., 2001) but would not reach the micromolar concentrations required to inhibit platelets in the *in vitro* experiments presented in this chapter. The SNRI milnacipran demonstrated the lowest inhibitory potency for platelet functions, with effects only observed at concentrations above 50 μM. With the exception of milnacipran, citalopram was the least potent antidepressant tested, with IC_{50} values greater than 10 μM. Future experiments should investigate how the differing inhibitory potencies between antidepressants relate to their chemical structures (Figure 6.1).

6.3.4 Comparative effects to SERT inhibition

All the antidepressants tested inhibit platelet functional responses with micromolar potencies (Figure 6.6). However, nanomolar concentrations are required to inhibit SERT-mediated 5-HT uptake (Cheetham et al., 1993, Owens et al., 2001, Vaishnavi et al., 2004). If the antiplatelet effects of these antidepressants were mediated through SERT blockade, then the inhibitory potencies for platelet functions and 5-HT uptake would be equivalent and congregate along the line of unity (Figure 6.6C). Figure 6.6B shows the linear correlation between blocking SERT and inhibiting platelet functional responses is minimal (coefficient of determination (R^2) = 0.60), and influenced by the low inhibitory poten-

cies of milnacipran for both 5-HT uptake and platelet functional responses (R^2 = 0.18 without milnacipran). Taken together, these results show that like citalopram, other antidepressants including paroxetine, sertraline, fluoxetine, imipramine and milnacipran inhibit platelet functions through a SERT-independent mechanism. Future experiments should address whether such effects are mediated through common inhibitory mechanisms of action, such as the impaired Rap1 activation and reduced GPVI signal transduction described with citalopram in Chapters 4 and 5, respectively.

6.3.5 SERT-independent mechanisms for antidepressants

Micromolar concentrations of SSRIs, SNRIs and TCAs also bind other monoamine transporters and cell surface receptors, which may inhibit platelet functional responses. The micromolar concentrations of antidepressants used in these experiments also bind and block DAT, histamine H_1 receptors and 5-HT_{2A} receptors, which have all been either identified or suggested to be expressed on platelets (de Clerck et al., 1984, Mannaioni et al., 1990, Frankhauser et al., 2006). The consequences of antidepressants binding these receptors on platelets are discussed further in Chapter 7.

Take together, results from this chapter show several classes of antidepressant inhibit platelets *in vitro*, including 4 SSRIs (citalopram, paroxetine, sertraline, fluoxetine), a TCA (imipramine) and a SNRI (milnacipran). The inhibitory potencies for platelet functional responses varied between antidepressants and appear unrelated to their inhibitory potencies for SERT-dependent 5-HT uptake. As reported with citalopram in previous chapters, inhibition was observed following pre-incubation times of approximately 5 minutes and at micromolar concentrations, with platelet functions unaffected at concentrations known to block SERT. These findings suggest that like citalopram, the antidepressants tested in this chapter also inhibit platelets irrespective of 5-HT transport. Future experiments should investigate whether this inhibition is mediated through a common shared mechanism, such as those previously described with citalopram (Chapters 4 & 5). Determining the reasons for varied inhibitory potencies among antidepressants and how this may relate to their differing chemical structures is another prospective area for future research.

Chapter 7
Discussion and conclusions

7.1 Summary of results

The results presented in this thesis have characterised the *in vitro* inhibitory effects of citalopram and other selective serotonin reuptake inhibitors (SSRIs) on platelets. In Chapter 3, the effects of citalopram on various platelet functions were defined. In particular, the differential effects of (*R*) and (*S*) isomers of racemic (*RS*) citalopram were used to assess the contribution of SERT-mediated 5-HT transport to platelet activation. Despite (*S*)-citalopram being the more potent inhibitor of 5-HT uptake, both (*R*)-citalopram and (*S*)-citalopram showed similar inhibitory potencies for platelet aggregation, thromboxane A_2 (TxA_2) synthesis, and adhesion. Furthermore, platelet inhibition by (*R*)-citalopram and (*S*)-citalopram was only achieved at micromolar concentrations, despite both isomers blocking 5-HT uptake at nanomolar concentrations. It was therefore concluded that citalopram inhibits *in vitro* platelet functions through a SERT-independent mechanism.

The aims of Chapters 4 and 5 were to investigate and identify potential SERT-independent mechanisms of platelet inhibition by citalopram, through characterising the effects of citalopram on two distinct intracellular signalling processes: 1) calcium (Ca^{2+}) signalling and 2) signalling through tyrosine phosphorylation. In Chapter 4, the effects of citalopram on Ca^{2+} signalling are reported. Citalopram failed to inhibit Ca^{2+} release from intracellular stores induced by the TxA_2 mimetic, U46619, despite blocking subsequent Rap1 activation and platelet aggregation. Similar results were observed using human neutrophils stimulated with platelet-activating factor (PAF), which, like U46619, induces Ca^{2+} signalling and Rap1 activation via phospholipase Cβ (PLCβ). Notably, Ca^{2+}-dependent Rap1 activation in both platelets and neutrophils is mediated by the calcium and diacylglycerol guanine nucleotide exchange factor-1 (CalDAG-GEFI). Results from an *in vitro* binding assay show that citalopram inhibits CalDAG-GEFI-mediated nucleotide exchange of Rap1B, suggesting that citalopram binds directly to either CalDAG-GEFI or Rap1.

In Chapter 5, the effects of citalopram on glycoprotein VI (GPVI)-mediated signal transduction were investigated. Citalopram suppressed protein tyrosine phosphorylation throughout the GPVI signalling pathway, preventing downstream aggregation in

response to the GPVI-selective agonist, cross-linked collagen-related peptide (CRPXL). Schild analysis of the inhibition of CRPXL-induced aggregation by citalopram was consistent with a competitive mechanism of action at concentrations up to 50 μM, yet showed non-competitive characteristics at greater concentrations (discussed further in Chapter 7.2.3). Although citalopram reduced the binding of anti-GPVI antibodies to unstimulated platelets, the reversibility of the inhibition of collagen-induced platelet aggregation by citalopram suggests that impaired antibody binding was not due to a loss of surface receptor expression, but to a disruption of antibody binding. The observation that citalopram instantaneously inhibits collagen-induced platelet aggregation (Figure 3.3) suggests these inhibitory effects occur at the platelet surface. Taken together, these results are consistent with a putative mechanism where citalopram binds directly to GPVI, thereby preventing collagen- and CRPXL-induced platelet activation. However, additional experiments are required to test an alternative hypothesis, whereby citalopram inhibits GPVI-mediated platelet activation by blocking initial intracellular signal transduction.

Finally, Chapter 6 demonstrated that other commonly-prescribed antidepressants also inhibit platelets. Experiments were conducted using several antidepressants that block SERT with nanomolar affinity, including four SSRIs (citalopram, paroxetine, sertraline, fluoxetine), a tricyclic antidepressant (imipramine) and a serotonin and norepinephrine reuptake inhibitor (milnacipran). Every antidepressant tested inhibited platelet aggregation, dense granule release, and increases in cytosolic Ca^{2+} ($[Ca^{2+}]_{cyt}$), but only at concentrations greater than 2 μM, which are beyond the nanomolar concentrations required to block SERT. These antidepressants inhibited platelets with varied potencies, but with little correlation to their inhibitory potencies for SERT. This suggests that, as previously concluded with citalopram, alternative mechanisms of platelet inhibition are responsible. Whether the modes of action of these other antidepressants are similar to the putative inhibitory mechanisms of citalopram remains to be determined.

7.2 The *in vitro* effects of SSRIs on platelets

This thesis aims to investigate and determine the *in vitro* inhibitory effects of citalopram and other SSRIs on platelets. Several putative mechanisms for such inhibition exist, which are either dependent on or are distinct from blockade of SERT.

7.2.1 SERT-dependent effects of SSRIs on platelets

5-HT store depletion from dense granules

By blocking SERT on platelets, SSRIs prevent the uptake and storage of 5-HT within dense granules (Hergovich et al., 2000). SSRI administration over several weeks gradually depletes intraplatelet 5-HT stores, which can no longer augment platelet activation upon dense granule release (Hergovich et al., 2000, Maurer-Spurej et al., 2004). However, platelets treated with either citalopram, fluoxetine, or sertraline for 4 minutes *in vitro* still retain 5-HT within their dense granules (Maurer-Spurej et al., 2004). The typical SSRI incubation times for experiments in this thesis were approximately 5 minutes, and recorded times from previous *in vitro* studies range from 3-20 minutes (Galan et al., 2009, Tseng et al., 2010, 2013, Carneiro et al., 2008). Therefore, 5-HT store depletion is unlikely to occur in experiments from this thesis and previous *in vitro* studies. The concentrations of SSRIs required to inhibit various platelet functions also inhibit dense granule release (Chapter 6.4), implying that the intraplatelet concentration of 5-HT is of little consequence to the inhibitory effects observed in experiments from this thesis.

Serotonylation

By blocking SERT prior to platelet activation, SSRIs prevent rapid 5-HT reuptake following dense granule release. Such uptake increases cytosolic concentrations of 5-HT ($[5\text{-HT}]_{cyt}$), which has been proposed to potentiate platelet activation through a mechanism distinct from 5-HT receptors (Walther et al., 2003). This process, termed serotonylation, involves the transglutaminase (TG)-mediated covalent attachment of 5-HT to GTPases, rendering them constitutively active. Serotonylation of the GTPases RhoA and Rab4 has, for example, been associated with augmented aggregation and alpha granule release, respectively (Walther et al., 2003). Acute SERT blockade by SSRIs may, therefore, prevent rapid 5-HT uptake and increases in platelet $[5\text{-HT}]_{cyt}$ following dense granule release, thus preventing serotonylation-enhanced platelet activation. However, in results presented in this thesis, SSRIs only inhibited platelet responses at concentrations beyond those required to block SERT, suggesting that inhibition was not through preventing the rapid uptake of 5-HT. SSRIs also inhibited dense granule release (Chapter 6.4), suggesting a lack of extracellular 5-HT available for rapid uptake. TG also requires Ca^{2+} to covalently bind 5-HT to proteins (Walther et al., 2003) and CRPXL-induced increases in $[Ca^{2+}]_{cyt}$ were blocked by SSRIs (Chapter 6.5), suggesting that CRPXL-stimulation did not increase TG activity. Taken together, these three observations suggest that any effects of citalopram or other SSRIs on platelet function described in this thesis are unrelated to serotonylation.

7.2.2 SERT-independent effects of SSRIs on platelets

The principal aim of this thesis was to determine if the antiplatelet effects of citalopram are mediated through inhibition of SERT. Results from Chapter 3 demonstrate that platelet inhibition by citalopram is independent of SERT activity. Therefore, citalopram is likely to mediate its effects through binding and modulating the activity of an alternative target. Despite its classification as a SSRI, citalopram also binds several other transporters and cell surface receptors, which may account for its *in vitro* effects.

Dopamine and norepinephrine transporters

SSRIs bind the dopamine transporter (DAT) and citalopram binds DAT with micromolar affinity (K_i = 16.54 ± 3.80 μM) (Owens et al., 2001), suggesting that citalopram binds DAT at concentrations used in experiments presented in this thesis. However, whether DAT is expressed in platelets is unclear, with one study reporting its expression (Frankhauser et al., 2006), despite a proteomic study failing to detect DAT amid approximately 4,000 different proteins (Burkhart et al., 2012). Even if DAT is expressed is platelets, citalopram concentrations up to 100 μM have no effect on dopamine uptake into neurons (Owens et al., 2001). Citalopram binding to DAT is therefore unlikely to be of importance to experiments in this thesis. Citalopram also binds the norepinephrine transporter (NET, K_i = 6.19 ± 0.82 μM), preventing norepinephrine uptake (K_i = 5.03 ± 0.13 μM) (Owens et al., 2001). However, proteomic data suggest that NET is reportedly not expressed in platelets (Burkhart et al., 2012). Together, these studies suggest that citalopram is unlikely to exert its antiplatelet effects through binding either DAT or NET.

Serotonin receptors

Micromolar concentrations of citalopram bind 5-HT_{2A} receptors ($K_i \approx 1.7$ μM) (Leysen et al., 1982), preventing receptor stimulation (Hyttel, 1982, Leysen et al., 1982). In experiments presented in this thesis, citalopram had little effect on platelet activation at concentrations that inhibit 5-HT_{2A} receptors (1-10 μM), and at higher concentrations suppressed the release of 5-HT-enriched dense granules (Figure 6.4). Antagonism of platelet 5-HT_{2A} receptors marginally impairs platelet activation induced by sub-threshold concentrations of collagen (Thompson et al., 1986, Lin et al., 2014), and tryptophan hydroxylase 1-deficient mice which are devoid of peripheral 5-HT respond normally to either collagen or U46619 (Walther et al., 2003). Collectively, these observations suggest impaired serotonergic signalling was not the cause of platelet inhibition by citalopram.

Histamine receptors

In addition to 5-HT, human platelets have been reported to sequester and store another monoamine, histamine (Mannaioni et al., 1992, Masini et al., 1998), which is released upon platelet activation (Mannaioni et al., 1990, 1993, Masini et al., 1994, 1998). Histamine H_1 receptors may also be expressed on human platelets (Mannaioni et al., 1992), and nanomolar concentrations of SSRIs, including citalopram bind and inhibit H_1 receptors (K_i = 288 ± 20 nM) (Owens et al., 2001). Therefore, the micromolar concentrations of citalopram used in experiments in this thesis are likely to bind and inhibit putative platelet H_1 receptors. However, if citalopram inhibits platelets through impaired histamine signalling, then effects should first be observed at the nanomolar concentrations required to antagonise H_1 receptors. The lack of dense granule release from platelets inhibited by citalopram also suggests that even if H_1 receptors are inhibited, histamine itself is not released. It is also important to note that histamine levels in human platelets (12.2 ± 1.5 picomoles per 10^9 platelets) (Saxena et al., 2017) are negligible, and H_1 antagonists only inhibit platelet aggregation at concentrations at or exceeding 10 μM (Nosál et al., 2005, Masini et al., 1994), despite binding H_1 receptors at nanomolar concentrations (Janssens et al., 2005). Therefore, the role of histamine and H_1 receptors in platelet function is poorly understood and is likely to hold little physiological relevance. Taken together, the observations described in this section suggest the *in vitro* antiplatelet effects of citalopram are unlikely to be mediated through antagonism of histamine H_1 receptors.

Sigma-1 receptors

Murine neurons expressing citalopram-insensitive SERT (p.(Ile172Met)) displayed similar (*RS*)-citalopram-induced migration responses to neurons expressing wild type SERT. (*RS*)-citalopram also mediated its effects at 10 μM (Bonnin et al., 2012). Both of these observations suggest a SERT-independent mechanism of action, and citalopram's effects were indeed attributed to the (*R*)-isomer, which activated intracellular sigma-1 (σ1) receptors (Bonnin et al., 2012). In neurons, σ1 receptors respond to Ca^{2+} release from the endoplasmic reticulum, prolonging Ca^{2+} signalling into mitochondria through inositol-1,4,5-trisphosphate (IP_3) receptors, which ensures cell survival (Hayashi and Su, 2007). Despite proteomic analysis identifying σ1 receptors in platelets (Burkhart et al., 2012), the role of σ1 receptors in platelet function has not been investigated. Both citalopram (K_i = 292 nM) and fluvoxamine (K_i = 36 nM) bind σ1 receptors with nanomolar affinity and act as receptor agonists (Narita et al., 1996, Yagasaki et al., 2006, Ishikawa et al., 2007). However, platelet inhibition by SSRIs described in experiments presented in this thesis

was only observed at micromolar concentrations and is therefore unlikely to be due to the stimulation of $\sigma 1$ receptors.

In summary, the concentrations of citalopram and other SSRIs used in this project not only block SERT, but are also known to antagonise platelet 5-HT_{2A} and histamine H_1 receptors, and act as $\sigma 1$ receptor agonists. Platelet inhibition was, however, only observed beyond the nanomolar concentrations required to modulate the activity of these receptors. Therefore, the SERT-independent mechanisms of SSRIs demonstrated in this thesis are unlikely to be due to their effects on signal transduction through 5-HT_{2A}, histamine H_1, or $\sigma 1$ receptors. Given this conclusion and the unlikely relevance of serotonylation, the putative inhibitory mechanisms of suppressed Rap1 activation (Chapter 4) and competitive antagonism of GPVI (Chapter 5) provide a more plausible explanation for the antiplatelet effects of citalopram.

7.2.3 Putative concentration-dependent mechanisms of inhibition

In this thesis, I propose two novel and putative mechanisms of platelet inhibition by citalopram: 1) inhibition of CalDAG-GEFI-mediated Rap1 activation; and 2) competitive antagonism of the GPVI receptor. The concentration-dependent transition of citalopram from a competitive to a non-competitive pattern of inhibition (Figure 5.2) is consistent with these two inhibitory mechanisms exerting their effects at differing concentrations, and may also underlie the apparent differing potencies of citalopram against U46619- and collagen-induced platelet aggregation (Figure 3.4). Citalopram concentrations at or below 50 μM may inhibit platelets by binding to GPVI and competing with collagen or CRPXL, thereby impairing downstream protein phosphorylation, Ca^{2+} release from intracellular stores and functional responses (Figure 7.1). However, at concentrations above 50 μM, citalopram may exert additional inhibitory effects through preventing CalDAG-GEFI-mediated Rap1 activation, which is essential to platelet aggregation by GPVI agonists (Crittenden et al., 2004, Stefanini et al., 2015, Piatt et al., 2016). This inhibition would not be competitively overcome by increased concentrations of agonist and would therefore appear non-competitive. The observation that citalopram did not alter $[Ca^{2+}]_{cyt}$ increases in platelets stimulated with the TxA_2 mimetic U46619 (Figure 4.3), and that U46619-induced platelet aggregation was only inhibited by citalopram concentrations at or exceeding 50 μM (Figure 3.4) is consistent with this mechanistic model of dual inhibition. Citalopram may, therefore, solely inhibit U46619-induced platelet activation through impaired Rap1 activation, which only occurs at citalopram concentrations at or exceeding 50 μM.

Future experiments could test if increasing the concentration of CRPXL above the fixed concentration used in this study (0.5 μg mL^{-1}) counteracts the inhibitory effects of citalopram on Ca^{2+} release from intracellular stores. If citalopram is a competitive GPVI antagonist, then platelets treated with high concentrations of both CRPXL and citalopram should demonstrate Ca^{2+} store release. However, these platelets would also be expected to show impaired Rap1 activation and aggregation, due to citalopram's additional effects on either CalDAG-GEFI or Rap1 at high concentrations. Measuring Rap1 activation in U46619-stimulated platelets pre-treated with a range of citalopram concentrations could also establish the lowest concentration required to initiate this inhibitory mechanism of action, which should be approximately 50 μM.

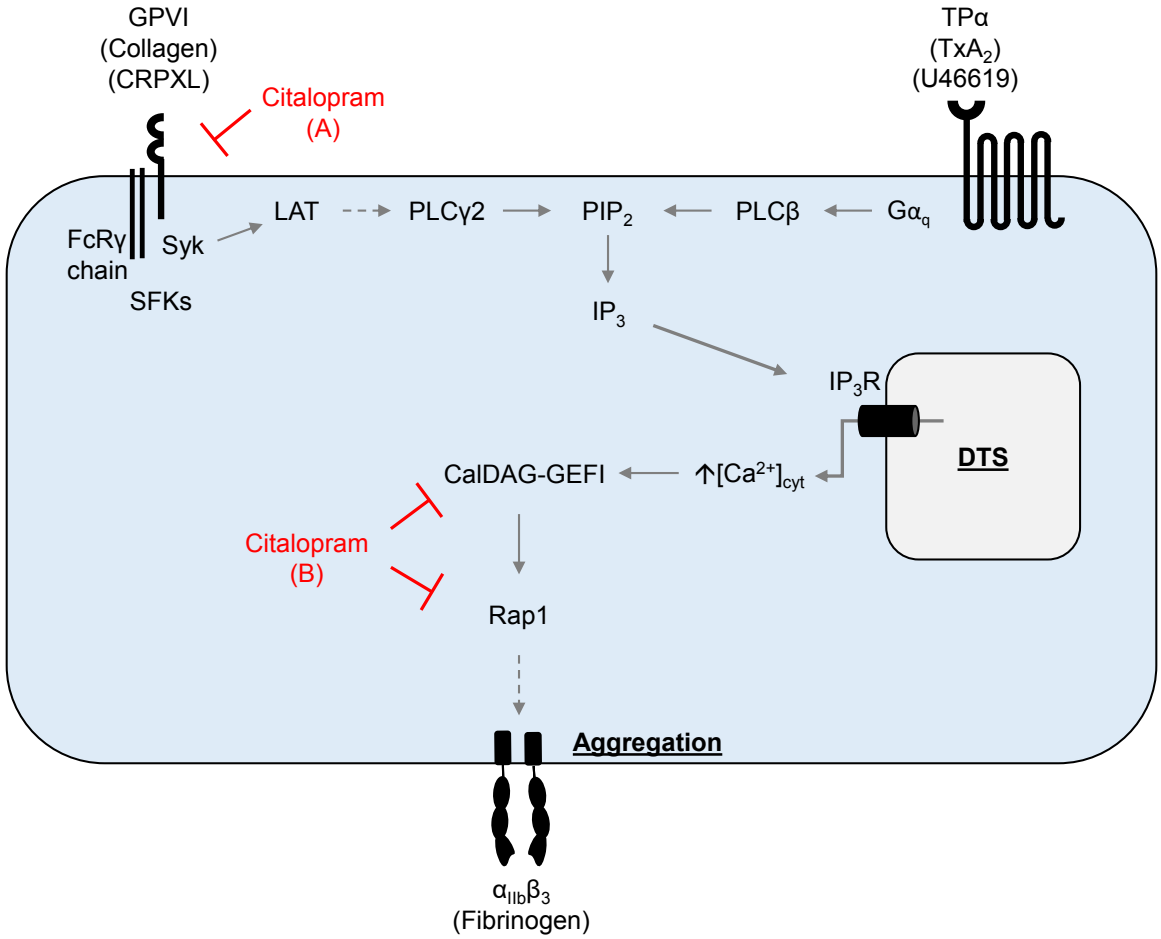

Figure. 7.1 Experiments presented in this thesis have identified two putative mechanisms for platelet inhibition by citalopram. **(A)** Citalopram suppressed early protein phosphorylation within the GPVI pathway, resulting in the inhibition of subsequent functional responses, such as calcium (Ca^{2+}) release from intracellular stores and platelet aggregation. Citalopram also impaired antibody binding, which was more likely due to a disruption of antibody binding than a loss of surface receptor expression. These observations suggest that citalopram binds GPVI and acts as a competitive antagonist to GPVI ligands. **(B)** In contrast, citalopram did not affect U46619-induced Ca^{2+} store release, despite blocking subsequent Rap1 activation. A valid target for this inhibitory mechanism is direct binding to the Ca^{2+}-dependent calcium and diacylglycerol guanine nucleotide exchange factor-1 (CalDAG-GEFI). This second mechanism appears to be less sensitive to the inhibitory effects of citalopram, as higher concentrations are required to inhibit U46619-induced aggregation compared to platelets stimulated with GPVI agonists. Receptor agonists are stated within brackets. Grey dashed lines indicate intermediate steps.

7.3 The potential use of SSRIs as antiplatelet medications

7.3.1 Clinical relevance of SSRIs

Repeated daily oral doses of 30-60 mg citalopram gives a steady-state plasma concentration of 120-600 nM, of which approximately 50-80% is bound to plasma proteins (Milne and Goa, 1991, Parker and Brown, 2000). The micromolar concentrations of citalopram required to inhibit platelets in experiments in this thesis are therefore far higher than clinically achievable doses. This suggests that the reported effects of SSRIs on haemostasis, which include increased risk of bleeding, are more likely through prolonged SERT blockade and the consequential disruption of 5-HT homeostasis, as opposed to the putative SERT-independent mechanisms identified in this thesis.

Increasing citalopram dosage in patients may provide the additional antiplatelet effects presented in this thesis. However, albeit rare, citalopram overdoses 30-100 times the recommended maximum dose of 60 mg a day have been associated with convulsions and tachycardia (Barbey and Roose, 1998). Citalopram overdose in combination with other sedative drugs or ethanol has also resulted in several fatalities (Barbey and Roose, 1998). In one fatal case, where citalopram was taken in isolation, blood concentrations were approximately 75-fold higher than therapeutic levels (Barbey and Roose, 1998), which equates to just under 50 μM. This concentration is similar to pIC_{50} values of citalopram reported in this thesis (Table 3.1). Therefore, the micromolar concentrations of citalopram required to inhibit platelets *in vitro* are unlikely to be tested in human subjects.

An alternative antiplatelet approach to increasing citalopram dosage would be to identify similar compounds with greater inhibitory potencies. For example, paroxetine, sertraline and fluoxetine all inhibit platelet functions with approximately 4-fold greater potency than citalopram (Figure 6.6). Whether paroxetine, sertraline and fluoxetine all inhibit platelet function through the same putative mechanisms as citalopram is an important question that should be addressed in future studies. The differing antiplatelet potencies for SSRIs described in this thesis should also encourage the screening of structurally similar compounds (Topiol et al., 2017). Such a screen could be based on a compound's ability to inhibit platelets as opposed to blocking SERT, which could lead to the identification of novel and potent antiplatelet agents.

Long-term administration of SSRIs at clinically relevant concentrations inhibits platelet SERT, depletes intra-platelet 5-HT stores and impairs agonist-induced platelet aggregation (Hergovich et al., 2000). SERT inhibition could, therefore, provide a novel

form of antiplatelet therapy. However, one of the major limitations of SSRIs as potential antiplatelet agents is their ability to cross the blood-brain barrier and inhibit 5-HT reuptake by pre-synaptic neurons within the central nervous system (CNS). The addition of a positively charged methyl group to a nitrogen atom on citalopram (N-methyl-citalopram) prevents transport across the BBB, while maintaining inhibitory potency for 5-HT uptake into platelets (Bismuth-Evenzal et al., 2010). The *in vitro* and *in vivo* antiplatelet effects of N-methyl-citalopram have yet to be tested, but could provide a novel approach to inhibit either peripheral SERT, or at micromolar concentrations SERT-independent platelet activation, without disrupting serotonergic signalling within the CNS. However, as with citalopram, N-methyl-citalopram is also likely to block peripheral SERT within the gut, which may disrupt serotonergic signalling of the enteric nervous system.

Despite minimal platelet inhibition following therapeutic SSRI dosage, SERT-inhibiting compounds such as citalopram may act synergistically with conventional antiplatelet drugs, such as low-dose aspirin and clopidogrel. Such effects may also apply for the *in vitro* models tested in this thesis and should be explored in further studies.

7.3.2 CalDAG-GEFI as an antithrombotic target

Results presented in Chapter 4 suggest that micromolar concentrations of citalopram prevent Rap1 activation, most likely through direct inhibition of CalDAG-GEFI or binding to and inhibiting Rap1. Murine platelets lacking CalDAG-GEFI show preserved haemostasis and are resistant to collagen-induced thrombosis, despite demonstrating prolonged tail bleeding times (Crittenden et al., 2004). Albeit rare, human loss-of-function CalDAG-GEFI mutations have been described in approximately 14 pedigrees (Canault et al., 2014, Kato et al., 2016, Lozano et al., 2016, Bermejo et al., 2017, Sevivas et al., 2017, Westbury et al., 2017). These patients display a non-syndromic recessive platelet function disorder, where the presence of a single normal allele is sufficient to prevent bleeding. Similar observations have been made in mice expressing approximately 10% of normal CalDAG-GEFI levels, which were protected from arterial thrombosis, with minimal impact on haemostasis (Piatt et al., 2016). Unlike for example cyclooxygenases, which are the target of aspirin, CalDAG-GEFI expression is limited to the haematopoietic lineage and a subpopulation of neurons within the basal ganglia (Kawasaki et al., 1998, Crittenden et al., 2004). Compounds that inhibit CalDAG-GEFI may, therefore, inhibit platelet function and have fewer off-target effects on other cell types. However, CalDAG-GEFI inhibitors are also likely to impair neutrophil function, as demonstrated by CalDAG-GEFI knockout mice, which represent a model for leukocyte adhesion deficiency type III (Bergmeier et al.,

2007). Nonetheless, the findings described in this section collectively suggest that partial inhibition of CalDAG-GEFI could provide a novel approach to antiplatelet therapy.

Despite suggestions that CalDAG-GEFI is a clinically-relevant antiplatelet target (Crittenden et al., 2004, Stefanini and Bergmeier, 2010), clear and viable inhibitors have yet to be identified. Phenylarsine oxide (PAO) reportedly inhibits platelet aggregation through putative binding to CalDAG-GEFI (Kuo et al., 2014). However, PAO is a highly toxic thiol-reactive agent, which binds cysteine residues and effects numerous cellular processes. For example, the concentrations of PAO reported to inhibit platelets (≥2 μM) also inhibit protein-tyrosine phosphatases, induce apoptosis and cause cell cytotoxicity (Garcia-Morales et al., 1990, Huang et al., 2017). In contrast, SSRIs retain a good safety profile (Kushboo and Sharma, 2017), are clinically prescribed and could potentially be restricted to peripheral circulation (Bismuth-Evenzal et al., 2010). However, further studies are required to test whether citalopram and other SSRIs directly inhibit CalDAG-GEFI, and indeed to what extent haemostasis is disrupted following pharmacological inhibition of CalDAG-GEFI .

7.3.3 GPVI as an antithrombotic target

Results presented in Chapter 5 demonstrate a second putative mechanism of platelet inhibition by citalopram, through preventing GPVI-mediated activation. Citalopram suppressed GPVI-mediated signal transduction (Figure 5.3) and prevented the binding of GPVI antibodies (Figure 5.4). Citalopram also rapidly inhibited collagen-induced platelet aggregation (Figure 3.3), which was recovered by washing citalopram from the supernatant (Figure 5.5). These findings collectively suggest that citalopram may directly bind the GPVI receptor, competitively reduce agonist binding and thereby inhibit platelet activation.

GPVI is only expressed in megakaryocytes and platelets (Phillips and Agin, 1977b, Jandrot-Perrus et al., 2000, Lagrue-Lak-Hal et al., 2001), implying that its inhibition could provide a selective approach to antithrombotic therapy. GPVI-deficient patients occasionally present a mild bleeding phenotype, suggesting a small but non-essential role for GPVI in haemostasis (Moroi et al., 1989, Arai et al., 1995, Dumont et al., 2009). In mice, pharmacological depletion of GPVI moderately increases bleeding, but completely protects against collagen-induced thromboembolism (Nieswandt et al., 2001). These studies and others have encouraged the ongoing development of GPVI inhibitors, some of which are discussed below.

Current approaches to blocking GPVI-mediated platelet activation can be split into three categories: 1) suppressing intracellular signalling downstream of GPVI, 2) occupying

GPVI-binding sites on collagen, and 3) directly binding GPVI, which either depletes the receptor or prevents agonist stimulation. Small molecule inhibitors targeting GPVI signal transduction are currently under investigation. BI1002494, for example, is an orally administered spleen tyrosine kinase (Syk) inhibitor, which protects mice from arterial thrombosis and ischaemic stroke (van Eeuwijk et al., 2016). However, the diverse role of kinases in most cell types remains the major limitation of such compounds. Syk, for instance, is important not only for immune receptor signalling in platelets, but also in lymphocytes and natural killer cells (Turner et al., 2000). The recombinant dimeric GPVI fusion protein Revacept binds collagen and outcompetes GPVI, which reduces collagen-induced aggregation while preserving haemostasis (Ungerer et al., 2011). A phase II clinical trial investigating the effects of Revacept on patients undergoing elective percutaneous coronary interventions is currently ongoing (European Union Clinical Trials Directive, 2017). The varying amounts of collagen exposed during atherosclerosis will, however, complicate a suitable dosage strategy. Antibodies that bind GPVI, including OM4 Fab (Li et al., 2007) and ACT017 (Lebozec et al., 2017) demonstrate high affinity, antithrombotic efficacy, and have little or no impact on bleeding. However, intravenous administration and immune recognition are common limitations of antibody therapy.

Small molecule inhibitors could provide an alternative approach to blocking GPVI-mediated platelet activation. Such compounds could be orally administered, without initiating immune responses. *In silico* docking models suggest losartan, an angiotensin II receptor type 1 antagonist, may interact with the collagen-binding domain (CBD) of GPVI (Taylor et al., 2014). However, despite inhibiting both CRPXL- and collagen-induced aggregation ($IC_{50} \approx$ 1-2 μM), losartan also inhibited U46619-induced aggregation ($IC_{50} \approx$ 20 μM) (Taylor et al., 2014), suggesting that like citalopram, GPVI-independent mechanisms must impair platelet activation through other receptors. The micromolar concentrations of losartan required to inhibit platelets *in vitro* are an order of magnitude higher than clinically achievable concentrations of approximately 120 nM (Yeung et al., 2000). Citalopram also inhibited GPVI-mediated platelet activation at micromolar concentrations (Chapter 5), and suppressed U46619-induced aggregation (Figure 3.4), making it a similarly undesirable candidate for selective GPVI inhibition. A direct comparison of citalopram-mediated platelet inhibition in the presence or absence of losartan could further address citalopram's putative mechanism of GPVI inhibition. Further studies should determine whether citalopram directly binds GPVI and if other SSRIs, such as those described in Chapter 6, show greater inhibitory potency.

7.4 SSRIs beyond haemostasis and thrombosis

A role for platelets has been proposed in numerous physiological and pathological processes other than haemostasis and thrombosis (Smyth et al., 2009, Gay and Felding-Habermann, 2011). Therefore, the antiplatelet effects of SSRIs may indirectly disrupt the function of other cell types that communicate with platelets, particularly cells that line the vasculature or mediate immune responses. SSRIs have also been reported to directly modulate functions of leukocytes and cancerous cell lines (Gobin et al., 2014), through either inhibition of SERT or via putative SERT-independent mechanisms.

7.4.1 SSRIs and the immune system

Innate immunity - neutrophils

The storage and release of 5-HT plays an important role in the innate immune system. During platelet activation, 5-HT released from dense granules upregulates von Willebrand factor (vWF) secretion from vascular endothelial cells, promoting neutrophil recruitment and adhesion to sites of inflammation (Palmer et al., 1994, Duerschmied et al., 2013). Blocking platelet SERT with fluoxetine depleted platelet 5-HT stores and reduced serum 5-HT concentrations, inhibiting leukocyte rolling and adhesion upon lipopolysaccharide (LPS) stimulation (Duerschmied et al., 2013). In contrast, acute fluoxetine treatment for two hours increased plasma 5-HT concentrations and LPS-induced leukocyte rolling (Herr et al., 2014).

Comparatively few studies have investigated the *in vitro* effects of SSRIs on neutrophil function. Fluoxetine treatment for 30 minutes at 10 μM inhibited PAF- and N-formylmethionyl-leucyl-phenylalanine-induced superoxide generation, and micromolar concentrations of fluoxetine also reduced cell viability (LD_{50} = 14 μM) (Strümper et al., 2003). In experiments in this thesis however, citalopram treatment for approximately 5 minutes at micromolar concentrations did not cause cell cytotoxicity (Figure 4.10) and suppressed neutrophil Rap1 activation, despite preserved increases in $[Ca^{2+}]_{cyt}$ (Figures 4.5 & 4.7). Downstream effects of Rap1 activation including the transition of integrin $\alpha_M\beta_2$ to a high-affinity binding state and neutrophil adherence to the $\alpha_M\beta_2$ ligand, fibrinogen, were also inhibited by citalopram (Figures 4.8 & 4.9). Unlike platelets, neutrophils do not express SERT (Tomazella et al., 2009). Therefore, these results reveal a direct and SERT-independent effect of citalopram on neutrophil function.

Adaptive immunity – lymphocytes

In addition to neutrophils, 5-HT and SSRIs have been reported to modulate cells of the adaptive immune system. Lymphocytes express SERT (Barkan et al., 2004). However, lymphocyte SERT function is thought to be minimal, with 5-HT uptake from the circulation predominantly mediated by platelets (Beikmann et al., 2013). Lymphocytes do, however, respond to 5-HT. For example, 5-HT stimulates lymphocyte 5-HT_{1A} receptors thereby increasing cell proliferation (Iken et al., 1995). Therefore, as with neutrophils, blocking platelet SERT may disrupt lymphocyte function through modulating plasma 5-HT levels.

Several studies report that SSRI concentrations beyond those required for SERT blockade directly inhibit lymphocyte functional responses to various agonists. Micromolar concentrations of citalopram, fluoxetine, paroxetine, fluvoxamine and sertraline reduced the proliferation of lymphocytes stimulated with anti-CD3/CD28 beads in a concentration-dependent manner (Gobin et al., 2013). Of note, paroxetine, fluoxetine and sertraline inhibited proliferation at concentrations below 10 μM, unlike citalopram, which only exhibited effects at 50 μM (Gobin et al., 2013). These differing inhibitory potencies are comparable to the antiplatelet effects observed in results presented in this thesis (Figure 6.6), suggesting a similar mechanism of action for both platelets and lymphocytes. Micromolar concentrations of paroxetine and sertraline also induced dose-dependent lymphocyte apoptosis and decreased cell viability (Taler et al., 2007, Gobin et al., 2013). Paroxetine and fluvoxamine concentrations above 10 μM arrested proliferation and induced apoptosis in both lymphoid and non-lymphoid cell lines, irrespective of SERT expression (Schuster et al., 2007). Acetylated paroxetine and fluvoxamine also failed to bind lymphocyte SERT, yet retained their antiproliferative and pro-apoptotic effects. These two observations lead the authors to suggest that both paroxetine and fluvoxamine modulate lymphocyte function through an unidentified, SERT-independent mechanism of action (Schuster et al., 2007).

Micromolar concentrations of SSRIs also inhibit lymphocyte cytokine secretions. Paroxetine and sertraline at or above 10 μM reduced tumour necrosis factor alpha (TNFα) secretion from CD3-activated T lymphocytes (Taler et al., 2007). Incubating T lymphocytes with citalopram (20 μM) also decreased LPS-induced secretion of interleukin (IL)-1β, IL-2, IL-6, TNFα, and interferon gamma (IFNγ) (Xia et al., 1996). Platelets store many of these pro-inflammatory cytokines within alpha granules, which are released upon their activation (Battinelli et al., 2014). The observation that citalopram (50 μM) inhibits collagen-induced alpha granule release *in vitro* (Tseng et al.,

2010) suggests that micromolar concentrations of SSRIs impair the secretion of inflammatory mediators from both platelets and lymphocytes.

The mechanism by which micromolar concentrations of SSRIs reduce lymphocyte proliferation, induce apoptosis, and inhibit cytokine release is currently unknown. Both fluoxetine (20 μM) and citalopram (20 μM) elevate cyclic adenosine monophosphate (cAMP) levels in stimulated T cells (Xia et al., 1996, Edgar et al., 1999). cAMP-mediated protein kinase A (PKA) activity is a key negative regulator of T cell activation (Tamir et al., 1996), and its upregulation by SSRIs is therefore a potential mechanism of inhibition. Increased cAMP production and PKA signalling are also important negative regulators in platelets, which could account for the inhibitory effects of SSRIs presented in the results of this thesis and of other *in vitro* studies. However, Tseng et al. (2013) did not observe any change in platelet cAMP levels following citalopram treatment (25, 50 μM), suggesting the effects of citalopram may vary dependent on cell type.

Taken together, SSRIs inhibit the *in vitro* functions of both neutrophils and lymphocytes at micromolar concentrations, which are comparable to the concentrations that inhibit platelets in the results presented in this thesis. These micromolar SSRI concentrations, alongside the lack of SERT expression on neutrophils and its minimal role in lymphocytes suggest that as with platelets, SSRIs are able to modulate immune cell functions through SERT-independent mechanisms.

7.4.2 SSRIs and cancer

Several conventional antithrombotic agents have been associated with impaired cancer growth and metastasis. For example, both unfractionated heparin (UFH) and low-molecular-weight heparin (LMWH) prevent the cancer cell-induced release of pro-angiogenic proteins from platelet alpha granules, which inhibits *in vitro* models of angiogenesis (Battinelli et al., 2014). UFH and LMWH are prescribed as anticoagulants for their ability to accelerate the activity of antithrombin III, which inactivates both thrombin and factor Xa (Griffith, 1982). The authors suggest this conventional mechanism of action prevented the generation and activation of thrombin derived from either platelets or cancer cells, which impaired subsequent platelet activation by protease activated receptors, inhibiting alpha granule release and angiogenesis (Battinelli et al., 2014). More recently, inhibition of platelet P2Y12 receptors with ticagrelor decreased cancer cell proliferation and increased apoptosis, as well as reducing the growth of murine ovarian tumours (Cho et al., 2017).

Collectively, these studies suggest that other compounds that inhibit platelets may, in doing so, also reduce the risk of cancer growth and metastasis. Despite numerous studies investigating the putative antiplatelet effects of SSRIs (Chapter 1.2.4), no studies have explored whether platelet inhibition by SSRIs in turn influences cancer development. SSRI treatment has previously been associated with a reduced risk of colorectal cancer (Xu et al., 2006, Coogan et al., 2009). However, the mechanisms underlying such effects are unknown and may not be a consequence of platelet inhibition.

Previous studies in both animal models and cancer cell lines have associated SSRI treatment with anticancer effects. Rats treated with fluoxetine for six weeks were less likely to develop colon cancer and displayed reduced epithelial proliferation and angiogenesis (Kannen et al., 2011). However, the effects of fluoxetine on tumorigenesis are controversial, with aged (19-23 month) mice treated with fluoxetine for two weeks more prone to experimental metastasis (Kubera et al., 2009). The prolonged exposure of fluoxetine at nanomolar concentrations described in these studies should not be directly compared to the *in vitro* antiplatelet effects of SSRIs presented in this thesis, which occur rapidly and at micromolar concentrations.

As with lymphocytes, SSRIs also modulate apoptosis and proliferation in several cancer cell lines at micromolar concentrations, suggesting a SERT-independent mechanism of action. For example, micromolar concentrations of sertraline and paroxetine dose-dependently inhibit proliferation and increase apoptosis in both malignant Jurkat T-cells (Amit et al., 2009) and two colorectal cell lines (HT29 and LS1034) (Gil Ad et al., 2008). Fluoxetine, paroxetine and citalopram also activate caspases and increase surface phosphatidylserine (PS) expression in Burkitt lymphoma cells (Serafeim et al., 2003), suggesting upregulated apoptosis. Despite SERT expression on Burkitt lymphoma cells, apoptotic effects were only observed at concentrations ranging from 1-100 μM, leading the authors to suggest inhibition was independent of SERT. Contrary to results presented in this thesis, fluoxetine, paroxetine, and citalopram increased $[Ca^{2+}]_{cyt}$ (Serafeim et al., 2003). These studies collectively support conclusions from Chapter 7.4.1, that SSRIs mediate various SERT-independent effects *in vitro*, which may vary depending on the cell type, the length of SSRI exposure, and the SSRI itself.

7.4.3 Potential effects of SSRIs along the platelet lineage

Platelets are derived from megakaryocytes (MKs), which predominantly reside within the bone marrow. Therefore, it is noteworthy that MKs also express 5-HT_{2A} receptors, whose stimulation is associated with anti-apoptotic and pro-mitogenic effects (Yang et al., 1996,

2007). MKs also express functional SERT, which is blocked *in vitro* by citalopram (Tytgat et al., 2002, Giannaccini et al., 2010). However, despite reported cases of escitalopram-mediated thrombocytopenia (Song et al., 2012), the effects of either prolonged or short-term SERT blockade on MK function are undocumented. The physiological relevance of SERT expression within the bone marrow is also unknown, as the vast majority of platelet 5-HT is derived from enterochromaffin cell secretions into the blood, which are transported into circulating platelets (Gershon and Tack, 2007, Mawe and Hoffman, 2013). This poses the question of whether MKs express SERT solely to package into platelets, or if the transporter mediates a distinct and undefined role in MK function.

Both platelets and MKs express CalDAG-GEFI, which upregulates Rap1-mediated integrin $\alpha_{\mathrm{IIb}}\beta_3$ activation (Eto et al., 2002, Crittenden et al., 2004). Activated $\alpha_{\mathrm{IIb}}\beta_3$ in mature MKs binds fibrinogen, which is associated with increased platelet production (Larson and Watson, 2006). In platelets, micromolar concentrations of citalopram inhibited both CalDAG-GEFI-mediated Rap1 activation (Figures 4.6, 4.7 & 4.11) and integrin $\alpha_{\mathrm{IIb}}\beta_3$ activation (Tseng et al., 2010). Similar SERT-independent effects might also be observed in MKs treated with citalopram, which could impair platelet production. Therefore, investigating the effects of citalopram on MKs should be considered for future investigation.

7.5 Conclusions and future directions

Understanding the inhibitory mechanisms of citalopram and other SSRIs on platelets may lead to either the discovery of similar compounds with greater antiplatelet potency, or the use of SSRIs as *in vitro* tools to investigate the mechanisms governing platelet activation. Results presented in this thesis provide compelling evidence that inhibition of platelet SERT by citalopram is not responsible for its functional inhibition of platelets. In addition, two putative mechanisms for SERT-independent platelet inhibition by citalopram have been proposed: 1) prevention of CalDAG-GEFI-dependent Rap1 activation and 2) competitive inhibition of the GPVI receptor. Both CalDAG-GEFI and GPVI are currently under investigation as novel targets to prevent thrombosis, and results from this thesis may contribute towards the identification and development of drugs that inhibit either of these proteins. Future studies should investigate if other SSRIs that inhibit platelets utilise the same putative inhibitory mechanisms as citalopram. Investigating the structure-activity relationships underlying platelet inhibition by different SSRIs is also recommended, and could lead to the targeted identification and development of novel antiplatelet agents.

References

Abbracchio, M. P. and Burnstock, G. (1994). Purinoceptors: Are there families of P2X and P2Y purinoceptors? *Pharmacology and Therapeutics*, 64(3):445–475.

Adams, J. W., Ramirez, J., Ortuno, D., Shi, Y., Thomsen, W., Richman, J. G., Morgan, M., Dosa, P., Teegarden, B. R., Al-Shamma, H., Behan, D. P., and Connolly, D. T. (2008). Anti-thrombotic and vascular effects of AR246686, a novel 5-HT_{2A} receptor antagonist. *European Journal of Pharmacology*, 586:234–243.

Akers, W. S., Oh, J. J., Oestreich, J. H., Ferraris, S., Wethington, M., and Steinhubl, S. R. (2010). Pharmacokinetics and pharmacodynamics of a bolus and infusion of cangrelor: a direct, parenteral P2Y12 receptor antagonist. *Journal of Clinical Pharmacology*, 50(1):27–35.

Alvarez, J. C., Gluck, N., Fallet, A., Grégoire, A., Chevalier, J. F., Advenier, C., and Spreux-Varoquaux, O. (1999). Plasma serotonin level after 1 day of fluoxetine treatment: a biological predictor for antidepressant response? *Psychopharmacology*, 143(1):97–101.

Ambrosio, A. L., Boyle, J. A., and Di Pietro, S. M. (2015). TPC2 mediates new mechanisms of platelet dense granule membrane dynamics through regulation of Ca^{2+} release. *Molecular Biology of the Cell*, 26(18):3263–3274.

Amit, B. H., Gil-Ad, I., Taler, M., Bar, M., Zolokov, A., and Weizman, A. (2009). Proapoptotic and chemosensitizing effects of selective serotonin reuptake inhibitors on T cell lymphoma/leukemia (Jurkat) *in vitro*. *European Neuropsychopharmacology*, 19(10):726–734.

Anderson, I. M. (1998). SSRIs versus tricyclic antidepressants in depressed inpatients: a meta-analysis of efficacy and tolerability. *Depression and Anxiety*, 7(1):11–17.

Andrews, R. K., Karunakaran, D., Gardiner, E. E., and Berndt, M. C. (2007). Platelet receptor proteolysis: a mechanism for downregulating platelet reactivity. *Thrombosis and Vascular Biology*, 27(7):1511–1520.

Andrews, R. K., Suzuki-inoue, K., Shen, Y., Tulasne, D., Watson, S. P., and Berndt, M. C. (2002). Interaction of calmodulin with the cytoplasmic domain of platelet glycoprotein VI. *Blood*, 99(11):4219–4221.

Antithrombotic Trialists Collaboration (2002). Collaborative meta-analysis of randomised trials of antiplatelet therapy for prevention of death, myocardial infarction, and stroke in high risk patients. *British Medical Journal*, 324:71–86.

Arai, M., Yamamoto, N., Moroi, M., Akamatsu, N., Fukutake, K., and Tanoue, K. (1995). Platelets with 10% of the normal amount of glycoprotein VI have an impaired response to collagen that results in a mild bleeding tendency. *British Journal of Haematology*, 89(1):124–130.

Aslan, J. E., Itakura, A., Gertz, J. M., and McCarty, O. J. T. (2012). Platelet shape change and spreading. In Gibbins, J. M. and Mahaut-Smith, M. P., editors, *Platelets and megakaryocytes. Methods in molecular biology (methods and protocols)*, pages 91–100. Springer, New York, NY.

Asselin, J., Gibbins, J. M., Achison, M., Lee, Y. H., Morton, L. F., Farndale, R. W., Barnes, M. J., and Watson, S. P. (1997). A collagen-like peptide stimulates tyrosine phosphorylation of syk and phospholipase Cγ2 in platelets independent of the integrin $\alpha_2\beta_1$. *Blood*, 89(4):1235–1242.

Asselin, J., Knight, C. G., Farndale, R. W., Barnes, M. J., and Watson, S. P. (1999). Monomeric (glycine-proline-hydoxyproline)10 repeat sequence is a partial agonist of the platelet collagen receptor glycoprotein VI. *Biochemical Journal*, 339:413–418.

Aszódi, A., Pfeifer, A., Ahmad, M., Glauner, M., Zhou, X. H., Ny, L., Andersson, K. E., Kehrel, B., Offermanns, S., and Fässler, R. (1999). The vasodilator-stimulated phosphoprotein (VASP) is involved in cGMP- and cAMP-mediated inhibition of agonist-induced platelet aggregation, but is dispensable for smooth muscle function. *EMBO Journal*, 18(1):37–48.

Atar, D., Malinin, A., Pokov, A., van Zyl, L., Frasure-Smith, N., Lesperance, F., and Serebruany, V. L. (2007). Antiplatelet properties of escitalopram in patients with the metabolic syndrome: a dose-ranging *in vitro* study. *Neuropsychopharmacology*, 32(11):2369–2374.

Bampalis, V. G., Khandoga, A. L., and Siess, W. (2010). Fluoxetine inhibition of 5-HT-potentiated platelet aggregation in whole blood. *Thrombosis and Haemostasis*, 104(6):1272–1274.

Barbey, J. T. and Roose, S. P. (1998). SSRI safety in overdose. *Journal of Clinical Psychiatry*, 59:42–48.

Barkan, T., Gurwitz, D., Levy, G., Weizman, A., and Rehavi, M. (2004). Biochemical and pharmacological characterization of the serotonin transporter in human peripheral blood lymphocytes. *European Neuropsychopharmacology*, 14(3):237–243.

Barrett, J. S., Murphy, G., Peerlinck, K., De Lepeleire, I., Gould, R. J., Panebianco, D., Hand, E., Deckmyn, H., Vermylen, J., and Arnout, J. (1994). Pharmacokinetics and pharmacodynamics of MK-383, a selective non-peptide platelet glycoprotein-IIb/IIIa receptor antagonist, in healthy men. *Clinical Pharmacology and Therapeutics*, 56:377–388.

Barter, R. and Everson Pearse, A. G. (1955). Mammalian enterochromaffin cells as the source of serotonin (5-hydroxytryptamine). *The Journal of Pathology*, 69(1):25–31.

Battinelli, E. M., Markens, B. A., Kulenthirarajan, R. A., Machlus, K. R., Flaumenhaft, R., and Italiano, J. E. (2014). Anticoagulation inhibits tumor cell mediated release of platelet angiogenic proteins and diminishes platelet angiogenic response. *Blood*, 123(1):101–113.

Beikmann, B. S., Tomlinson, I. D., Rosenthal, S. J., and Andrews, A. M. (2013). Serotonin uptake is largely mediated by platelets versus lymphocytes in peripheral blood cells. *ACS Chemical Neuroscience*, 4(1):161–170.

Bellavite, P., Andrioli, G., Guzzo, P., Arigliano, P., Chirumbolo, S., Manzato, F., and Santonastaso, C. (1994). A colorimetric method for the measurement of platelet adhesion in microtiter plates. *Analytical Chemistry*, 216:444–450.

Benkelfat, C., Ellenbogen, M. A., Dean, P., Palmour, R. M., and Young, S. N. (1994). Mood-lowering effect of tryptophan depletion. *Archives of General Psychiatry*, 51:687–697.

Bergmeier, W., Goerge, T., Wang, H. W., Crittenden, J. R., Baldwin, A. C. W., Cifuni, S. M., Housman, D. E., Graybiel, A. M., and Wagner, D. D. (2007). Mice lacking the signaling molecule CalDAG-GEFI represent a model for leukocyte adhesion deficiency type III. *The Journal of Clinical Investigation*, 117(6):1699–1707.

Bergmeier, W. and Stefanini, L. (2009). Novel molecules in calcium signaling in platelets. *Journal of Thrombosis and Haemostasis*, 7:187–190.

Berlanga, O., James, J. R., Frampton, J., Davis, S. J., and Tomlinson, M. G. (2007). Glycoprotein VI oligomerization in cell lines and platelets. *Journal of Thrombosis and Haemostasis*, 5:1026–1033.

Berlanga, O., Tulasne, D., Bori, T., Snell, D. C., Miura, Y., Jung, S. M., Moroi, M., Frampton, J., and Watson, S. P. (2002). The Fc receptor γ-chain is necessary and sufficient to initiate signalling through glycoprotein VI in transfected cells by the snake C-type lectin, convulxin. *European Journal of Biochemistry*, 269:2951–2960.

Berman, C. L., Yeo, E. L., Wencel-Drake, J. D., Furie, B. C., Ginsberg, M. H., and Furie, B. (1986). A platelet alpha granule membrane protein that is associated with the plasma membrane after activation. *The Journal of Clinical Investigation*, 78(1):130–137.

Bermejo, E., Alberto, M. F., Paul, D., Cook, A. A., Nurden, P., Sanchez Luceros, A., Nurden, A., and Berg (2017). Marked bleeding diathesis in patients with platelet dysfunction due to a novel mutation in RASGRP2, encoding CalDAG-GEFI (p.Gly305Asp). *Platelets*, 20:1–3.

Bernardi, B., Guidetti, G. F., Campus, F., Crittenden, J. R., Graybiel, A. M., Balduini, C., and Torti, M. (2006). The small GTPase Rap1b regulates the cross talk between platelet integrin $\alpha_2\beta_1$ and integrin $\alpha_{\mathrm{IIb}}\beta_3$. *Blood*, 107(7):2728–2736.

Bismuth-Evenzal, Y., Gonopolsky, Y., Gurwitz, D., Iancu, I., Weizman, A., and Rehavi, M. (2012). Decreased serotonin content and reduced agonist-induced aggregation in platelets of patients chronically medicated with SSRI drugs. *Journal of Affective Disorders*, 136:99–103.

Bismuth-Evenzal, Y., Roz, N., Gurwitz, D., and Rehavi, M. (2010). N-methyl-citalopram: a quaternary selective serotonin reuptake inhibitor. *Biochemical Pharmacology*, 80:1546–1552.

Blakely, R. D., Berson, H. E., Fremeau, R. T., Caron, M. G., Peek, M. M., Prince, H. K., and Bradley, C. C. (1991). Cloning and expression of a functional serotonin transporter from rat brain. *Nature*, 354:66–70.

Blanchette, C. M., Simoni-Wastila, L., Zuckerman, I. H., and Stuart, B. (2008). A secondary analysis of a duration response association between selective serotonin reuptake inhibitor use and the risk of acute myocardial infarction in the aging population. *Annals of Epidemiology*, 18(4):316–321.

Bonnin, A., Zhang, L., Blakely, R. D., and Levitt, P. (2012). The SSRI citalopram affects fetal thalamic axon responsiveness to netrin-1 *in vitro* independently of SERT antagonism. *Neuropsychopharmacology*, 37:1879–1884.

Bori-Sanz, T., Suzuki-Inoue, K., Berndt, M. C., Watson, S. P., and Tulasne, D. (2003). Delineation of the region in the glycoprotein VI tail required for association with the Fc receptor γ-chain. *The Journal of Biological Chemistry*, 278(38):35914–35922.

Born, G. V. R. (1962). Aggregation of blood platelets by adenosine diphosphate and its reversal. *Nature*, 194:927–929.

Bos, J., Rehmann, H., and Wittinghofer, A. (2007). GEFs and GAPs: critical elements in the control of small G proteins. *Cell*, 129:865–877.

Bougie, D. W., Wilker, P. R., Wuitschick, E. D., Curtis, B. R., Malik, M., Levine, S., Lind, R. N., Pereira, J., and Aster, R. H. (2002). Acute thrombocytopenia after treatment with tirofiban or eptifibatide is associated with antibodies specific for ligand-occupied GPIIb/IIIa. *Blood*, 100(6):2071–2076.

Boulaftali, Y., Hess, P. R., Kahn, M. L., and Bergmeier, W. (2014). Platelet immunoreceptor tyrosine-based activation motif (ITAM) and hemITAM signaling and vascular integrity in inflammation and development. *Circulation Research*, 114:1174–1184.

Bowsher, R. R. and Henry, D. P. (1986). Aromatic L-amino acid decarboxylase: biochemistry and functional significance. In Boulton, A. A., Baker, G. B., and Yu, P. H., editors, *Neurotransmitter Enzymes*, pages 33–78. Humana Press, Totowa, NJ.

Brenner, B., Harney, J. T., Ahmed, B. A., Jeffus, B. C., Unal, R., Mehta, J. L., and Kilic, F. (2007). Plasma serotonin levels and the platelet serotonin transporter. *Journal of Neurochemistry*, 102(1):206–215.

British Heart Foundation (2016). BHF CVD statistics factsheet - UK [pdf]. Available at: https://www.bhf.org.uk/research/heart-statistics. Accessed: 09/13/2017.

Burke, W. J., Gergel, I., and Bose, A. (2002). Fixed-dose trial of the single isomer SSRI escitalopram in depressed outpatients. *Journal of Clinical Psychiatry*, 63(4):331–336.

Burkhart, J. M., Gambaryan, S., Watson, S. P., Kerstin, J., Ulrich, W., Albert, S., Heemskerk, J. W., and Zahedi, R. P. (2014). What can proteomics tell us about platelets? *Circulation Research*, 114:1204–1219.

Burkhart, J. M., Vaudel, M., Gambaryan, S., Radau, S., Walter, U., Martens, L., Geiger, J., Sickmann, A., and Zahedi, R. P. (2012). The first comprehensive and quantitative analysis of human platelet protein composition allows the comparative analysis of structural and functional pathways. *Blood*, 120(15):e73–e82.

Bymaster, F. P., Dreshfield-Ahmad, L. J., Threlkeld, P. G., Shaw, J. L., Thompson, L., Nelson, D. L., Hemrick-Luecke, and Susan K. Wong, D. T. (2001). Comparative affinity of duloxetine and venlafaxine for serotonin and norepinephrine transporters *in vitro* and *in vivo*, human serotonin receptor subtypes, and other neuronal receptors. *Neuropsychopharmacology*, 25(6):871–880.

Caillé, G., Kouassi, E., and de Montigny, C. (1983). Pharmacokinetic study of zimelidine using a new GLC method. *Clinical Pharmacokinetics*, 8(6):530–540.

Canault, M., Ghalloussi, D., Grosdidier, C., Guinier, M., Perret, C., Chelghoum, N., Germain, M., Raslova, H., Peiretti, F., Morange, P. E., Saut, N., Pillois, X., Nurden, A. T., Cambien, F., Pierres, A., van den Berg, T. K., Kuijpers, T. W., Alessi, M. C., and Tregouet, D. A. (2014). Human CalDAG-GEFI gene (RASGRP2) mutation affects platelet function and causes severe bleeding. *The Journal of Experimental Medicine*, 211(7):1349–1362.

Cantley, L. (2002). The phosphoinositide 3-kinase pathway. *Science*, 296:1655–1657.

Carneiro, A. M. D. and Blakely, R. D. (2006). Serotonin-, protein kinase C-, and Hic-5-associated redistribution of the platelet serotonin transporter. *Journal of Biological Chemistry*, 281(34):24769–24780.

Carneiro, A. M. D., Cook, E. H., Murphy, D. L., and Blakely, R. D. (2008). Interactions between integrin $\alpha_{\mathrm{IIb}}\beta_3$ and the serotonin transporter regulate serotonin transport and platelet aggregation in mice and humans. *The Journal of Clinical Investigation*, 118(4):1544–1552.

Chackalamannil, S., Xia, Y., Greenlee, W. J., Clasby, M., Doller, D., Tsai, H., Asberom, T., Czarniecki, M., Ahn, H. S., Boykow, G., Foster, C., Agans-Fantuzzi, J., Bryant, M., Lau, J., and Chintala, M. (2005). Discovery of potent orally active thrombin receptor (protease activated receptor 1) antagonists as novel antithrombotic agents. *Journal of Medicinal Chemistry*, 48(19):5884–5887.

Cheetham, S. C., Viggers, J. A., Slater, N. A., Heal, D. J., and Buckett, W. R. (1993). [^{3}H]Paroxetine binding in rat frontal cortex strongly correlates with [^{3}H]5-HT uptake: effect of administration of various antidepressant treatments. *Neuropharmacology*, 32(8):737–743.

Chen, N. H., Reith, M. E. A., and Quick, M. W. (2004). Synaptic uptake and beyond: the sodium- and chloride-dependent neurotransmitter transporter family SLC6. *Pflugers Archiv European Journal of Physiology*, 447(5):519–531.

Cho, S. M., Noh, K., Haemmerle, M., Li, D., Park, H., Hu, Q., Hisamatsu, T., Mitamura, T., Ling Celia Mak, S., Kunapuli, S., Ma, Q., Sood, K., Afshar-Kharghan, V., and Sood, A. K. (2017). Role of ADP receptors on platelets in the growth of ovarian cancer. *Blood*, 130(10):1235–1243.

Chrzanowska-Wodnicka, M., Smyth, S. S., Schoenwaelder, S. M., Fischer, T. H., and White, G. C. (2005). Rap1b is required for normal platelet function and hemostasis in mice. *The Journal of Clinical Investigation*, 115(3):680–687.

Coates, M. D., Johnson, A. C., Greenwood-van Meerveld, B., and Mawe, G. M. (2006). Effects of serotonin transporter inhibition on gastrointestinal motility and colonic sensitivity in the mouse. *Neurogastroenterology and Motility*, 18(6):464–471.

Cocks, T. M. and Angus, J. A. (1983). Endothelium-dependent relaxation of coronary arteries by noradrenaline and serotonin. *Nature*, 305(13):627–629.

Cohen, H. W., Gibson, G., and Alderman, M. H. (2000). Excess risk of myocardial infarction in patients treated with antidepressant medications: Association with use of tricyclic agents. *American Journal of Medicine*, 108(1):2–8.

Coleman, J. A., Green, E. M., and Gouaux, E. (2016). X-ray structures and mechanism of the human serotonin transporter. *Nature*, 532:334–339.

Coller, B. S., Peerschke, E. I., Scudder, L. E., and Sullivan, C. A. (1983). A murine monoclonal antibody that completely blocks the binding of fibrinogen to platelets produces a thrombasthenic-like state in normal platelets and binds to glycoproteins IIb and/or IIIa. *The Journal of Clinical Investigation*, 72(1):325–338.

Coogan, P. F., Strom, B. L., and Rosenberg, L. (2009). Antidepressant use and colorectal cancer risk. *Pharmacoepidemiology and Drug Safety*, 18:1111–1114.

Coppinger, J. A., Cagney, G., Toomey, S., Kislinger, T., Belton, O., McRedmond, J. P., Cahill, D. J., Emili, A., Fitzgerald, D. J., and Maguire, P. B. (2004). Characterization of the proteins released from activated platelets leads to localization of novel platelet proteins in human atherosclerotic lesions. *Blood*, 103(6):2096–2104.

Coughlin, S. R. (2000). Thrombin signalling and protease-activated receptors. *Nature*, 407:258–264.

Coxon, C. H., Geer, M. J., and Senis, Y. A. (2017). ITIM receptors: more than just inhibitors of platelet activation. *Blood*, 129(26):3407–3418.

Coxon, C. H., Lewis, A. M., Sadler, A. J., Vasudevan, S. R., Thomas, A., Dundas, K. A., Taylor, L., Campbell, R. D., Gibbins, J. M., Churchill, G. C., and Tucker, K. L. (2012a). NAADP regulates human platelet function. *Biochemical Journal*, 441:435–442.

Coxon, C. H., Sadler, A. J., Huo, J., and Campbell, R. D. (2012b). An investigation of hierachical protein recruitment to the inhibitory platelet receptor, G6B-b. *PLoS ONE*, 7(11):e49543.

Craven, L. L. (1950). Acetylsalicylic acid, possible preventive of coronary thrombosis. *Annals of Western Medicine and Surgery*, 4(2):95.

Crittenden, J. R., Bergmeier, W., Zhang, Y., Piffath, C. L., Liang, Y., Wagner, D. D., Housman, D. E., and Graybiel, A. M. (2004). CalDAG-GEFI integrates signaling for platelet aggregation and thrombus formation. *Nature Medicine*, 10(9):982–986.

Czikora, A., Lundberg, D. J., Abramovitz, A., Lewin, N. E., Kedei, N., Peach, M. L., Zhou, X., Merritt, R. C., Craft, E. A., Braun, D. C., and Blumberg, P. M. (2016). Structural basis for the failure of the C1 domain of ras guanine nucleotide releasing protein 2 (RasGRP2) to bind phorbol ester with high affinity. *Journal of Biological Chemistry*, 291(21):11133–11147.

Dall, M., Schaffalitzky de Muckadell, O. B., Lassen, A. T., Hansen, J. M., and Hallas, J. (2009). An association between selective serotonin reuptake inhibitor use and serious upper gastrointestinal bleeding. *Clinical Gastroenterology and Hepatology*, 7(12):1314–1321.

Dalton, S. O., Johansen, C. J., Mellemkaer, L., Norgard, B., Sorenson, H. T., and Olsej, J. H. (2003). Use of selective serotonin reuptake inhibitors and risk of upper gastrointestinal tract bleeding. *Archives of Internal Medicine*, 163:59–64.

Damian, L. (2013). Isothermal titration calorimetry for studying protein-ligand interactions. In Williams, M. and Daviter, T., editors, *Protein-ligand interactions. methods in molecular biology (methods and protocols)*, pages 103–118. Humana Press, Totowa, NJ.

Davoren, A. and Aster, R. H. (2006). Heparin-induced thrombocytopenia and thrombosis. *American Journal of Hematology*, 81(1):36–44.

de Abajo, F. J. (2011). Effects of selective serotonin reuptake inhibitors on platelet function: mechanisms, clinical outcomes and implications for use in elderly patients. *Drugs and Aging*, 28(5):345–367.

de Abajo, F. J., García Rodríguez, L. A., and Montero, D. (1999). Association between selective serotonin reuptake inhibitors and upper gastrointestinal bleeding: population based case-control study. *British Medical Journal*, 319:1106–1109.

de Abajo, F. J., Montero, D., García Rodríguez, L. A., and Madurga, M. (2006). Antidepressants and risk of upper gastrointestinal bleeding. *Basic and Clinical Pharmacology and Toxicology*, 98(3):304–310.

de Clerck, F., Xhonneux, B., Leysen, J., and Janssen, P. (1984). Evidence for functional 5-HT_2 receptor sites on human blood platelets. *Biochemical Pharmacology*, 33(17):2807–2811.

Decker, T. and Lohmann-Matthes, M. L. (1988). A quick and simple method for the quantitation of lactate dehydrogenase release in measurements of cellular cytotoxicity and tumor necrosis factor (TNF) activity. *Journal of Immunological Methods*, 115(1):61–69.

Dees, C., Akhmetshina, A., Zerr, P., Reich, N., Palumbo, K., Horn, A., Jüngel, A., Beyer, C., Krönke, G., Zwerina, J., Reiter, R., Alenina, N., Maroteaux, L., Gay, S., Schett, G., Distler, O., and Distler, J. H. (2011). Platelet-derived serotonin links vascular disease and tissue fibrosis. *The Journal of Experimental Medicine*, 208(5):961–972.

DeLean, A., Munson, P. J., and Rodbard, D. (1978). Simultaneous analysis of families of sigmoidal curves: application to bioassay, radioligand assay, and physiological dose-response curves. *The American Journal of Physiology*, 235(2):97–102.

Delgado, P. L., Price, L. H., Miller, H. L., Salomon, R. M., Aghajanian, G. K., Heninger, G. R., and Charney, D. S. (1994). Serotonin and the neurobiology of depression: effects of tryptophan depletion in drug-free depressed patients. *Archives of General Psychiatry*, 51:865–874.

Deranleau, D. A., Dubler, D., Rothen, C., and Lüscher, E. F. (1982). Transient kinetics of the rapid shape change of unstirred human blood platelets stimulated with ADP. *Proceedings of the National Academy of Sciences of the United States of America*, 79(23):7297–7301.

Dilks, J. R. and Flaumenhaft, R. (2008). Fluoxetine (Prozac) augments platelet activation mediated through protease-activated receptors. *Journal of Thrombosis and Haemostasis*, 6(4):705–708.

Duerschmied, D., Suidan, G. L., Demers, M., Herr, N., Carbo, C., Brill, A., Cifuni, S. M., Mauler, M., Cicko, S., Bader, M., Idzko, M., Bode, C., and Wagner, D. D. (2013). Platelet serotonin promotes the recruitment of neutrophils to sites of acute inflammation in mice. *Blood*, 121(6):1008–1015.

Dumont, B., Lasne, D., Rothschild, C., Bouabdelli, M., Ollivier, V., Oudin, C., Ajzenberg, N., Grandchamp, B., and Jandrot-Perrus, M. (2009). Absence of collagen-induced platelet activation caused by compound heterozygous GPVI mutations. *Blood*, 114(9):1900–1903.

Durrant, T. N., van den Bosch, M. T., and Hers, I. (2017). Integrin $\alpha_{IIb}\beta_3$ outside-in signaling. *Blood*, Aug 9. pii: blood-2017-03-773614. doi: 10.1182/blood-2017-03-773614. [Epub ahead of print].

Edgar, V. A., Sterin-Borda, L., Cremaschi, G. A., and Genaro, A. M. (1999). Role of protein kinase C and cAMP in fluoxetine effects on human T-cell proliferation. *European Journal of Pharmacology*, 372(1):65–73.

Elhusseiny, A. and Hamel, E. (2001). Sumatriptan elicits both constriction and dilation in human and bovine brain intracortical arterioles. *British Journal of Pharmacology*, 132(1):55–62.

Elkeles, R. S., Hampton, J. R., Honour, A. J., Mitchell, J. R. A., and Prichard, J. S. (1968). Effect of a pyrimido-pyrimidine compound on platelet behaviour *in vitro* and *in vivo*. *Lancet*, 292:751–754.

Ellison, S., Mori, J., Barr, A. J., and Senis, Y. A. (2010). CD148 enhances platelet responsiveness to collagen by maintaining a pool of active Src family kinases. *Journal of Thrombosis and Haemostasis*, 8(7):1575–1583.

Erspamer, V. and Asero, B. (1952). Identification of enteramine, the specific hormone of the enterochromaffin cell system, as 5-Hydroxytryptamine. *Nature*, 169:800–801.

Erspamer, V. and Testini, A. (1959). Observations on the release and turnover rate of 5-hydroxytryptamine in the gastrointestinal tract. *Journal of Pharmacy and Pharmacology*, 11(1):618–623.

Ersparmer, V. and Viallu, M. (1937). Ricerche sul secreto delle cellule enterocromaffini. *Zeitschrift für Zellforschung und Mikroskopische Anatomie*, 27(1):81–99.

Eto, K., Murphy, R., Kerrigan, S. W., Bertoni, A., Stuhlmann, H., Nakano, T., Leavitt, A. D., and Shattil, S. J. (2002). Megakaryocytes derived from embryonic stem cells implicate CalDAG-GEFI in integrin signaling. *Proceedings of the National Academy of Sciences of the United States of America*, 99(20):12819–12824.

European Union Clinical Trials Directive (2017). Revacept, a novel inhibitor of platelet adhesion in patients with stable coronary artery disease undergoing elective percutaneous coronary interventions. EudraCT: 2015-000686-32. Available at: https://www.clinicaltrialsregister.eu/ctr-search/search?query=2015-000686-32. accessed: 30/10/2017.

Ezumi, Y., Shindoh, K., Tsuji, M., and Takayama, H. (1998). Physical and functional assoication of the Src family kinases Fyn and Lyn with the collagen receptor glycoprotein VI-Fc receptor γ chain complex on human platelets. *The Journal of Experimental Medicine*, 188(2):267–276.

Falati, S., Patil, S., Gross, P. L., Stapleton, M., Merrill-Skoloff, G., Barrett, N. E., Pixton, K. L., Weiler, H., Cooley, B., Newman, D. K., Newman, P. J., Furie, B. C., Furie, B., and Gibbins, J. M. (2006). Platelet PECAM-1 inhibits thrombus formation *in vivo* Platelet PECAM-1 inhibits thrombus formation *in vivo*. *Blood*, 107(2):535–541.

Faraj, B. A., Olkowski, Z. L., and Jackson, R. T. (1994). Expression of a high-affinity serotonin transporter in human lymphocytes. *International Journal of Immunopharmacology*, 16(7):561–567.

Ferreiro, J. L., Ueno, M., and Angiolillo, D. J. (2009). Cangrelor: a review on its mechanism of action and clinical development. *Expert Review of Cardiovascular Therapy*, 7(10):1195–1201.

Fishkes, H. and Rudnick, G. (1982). Bioenergetics of serotonin transport by membrane vesicles derived from platelet dense granules. *Journal of Biological Chemistry*, 257(10):5671–5677.

FitzGerald, G. A. (1991). Mechanisms of platelet activation: thromboxane A_2 as an amplifying signal for other agonists. *The American Journal of Cardiology*, 68(7):11–15.

Flick, M. J., Du, X., Witte, D. P., Jiroušková, M., Soloviev, D. A., Busuttil, S. J., Plow, E. F., and Degen, J. L. (2004). Leukocyte engagement of fibrin(ogen) via the integrin receptor $\alpha_M\beta_2$/Mac-1 is critical for host inflammatory response *in vivo*. *The Journal of Clinical Investigation*, 113(11):1596–1606.

Flöck, A., Zobel, A., Bauriedel, G., Tuleta, I., Hammerstingl, C., Höfels, S., Schuhmacher, A., Maier, W., Nickenig, G., and Skowasch, D. (2010). Antiplatelet effects of antidepressant treatment: a randomized comparison between escitalopram and nortriptyline. *Thrombosis Research*, 126(2):e83–e87.

Fotakis, G. and Timbrell, J. A. (2006). *In vitro* cytotoxicity assays: comparison of LDH, neutral red, MTT and protein assay in hepatoma cell lines following exposure to cadmium chloride. *Toxicology Letters*, 160(2):171–177.

Franke, B., Akkerman, J. W. N., and Bos, J. L. (1997). Rapid Ca^{2+}-mediated activation of Rap1 in human platelets. *EMBO Journal*, 16(2):252–259.

Frankhauser, P., Grimmer, Y., Bugert, P., Deuschle, M., Schmidt, M., and Schloss, P. (2006). Characterization of the neuronal dopamine transporter DAT in human blood platelets. *Neuroscience Letters*, 399(3):197–201.

Fredrickson, B. J., Dong, J. F., McIntire, L. V., and López, J. A. (1998). Shear-dependent rolling on von Willebrand factor of mammalian cells expressing the platelet glycoprotein Ib-IX-V complex. *Blood*, 92(10):3684–3693.

Freedman, J. E., Loscalzo, J., Barnard, M. R., Alpert, C., Keaney, J. F., and Michelson, A. D. (1997). Nitric oxide release from activated platelets inhibits platelet recruitment. *The Journal of Clinical Investigation*, 100:350–356.

Fujita, H., Fukuhara, S., Sakurai, A., Yamagishi, A., Kamioka, Y., Nakaoka, Y., Masuda, M., and Mochizuki, N. (2005). Local activation of Rap1 contributes to directional vascular endothelial cell migration accompanied by extension of microtubules on which RAPL, a Rap1-associating molecule, localizes. *Journal of Biological Chemistry*, 280(6):5022–5031.

Fuller, G. L., Williams, J. A., Tomlinson, M. G., Eble, J. A., Hanna, S. L., Pöhlmann, S., Suzuki-Inoue, K., Ozaki, Y., Watson, S. P., and Pearce, A. C. (2007). The C-type lectin receptors CLEC-2 and Dectin-1, but not DC-SIGN, signal via a novel YXXL-dependent signaling cascade. *Journal of Biological Chemistry*, 282(17):12397–12409.

Galan, A. M., Lopez-Vilchez, I., Diaz-Ricart, M., Navalon, F., Gomez, E., Gasto, C., and Escolar, G. (2009). Serotonergic mechanisms enhance platelet-mediated thrombogenicity. *Thrombosis and Haemostasis*, 102(3):511–519.

Gammie, J. S., Zenati, M., Kormos, R. L., Hattler, B. G., Wei, L. M., Pellegrini, R. V., Griffith, B. P., Dyke, C. M., Reopro, B. A., Lilly, E., and Lilly, E. (1998). Abciximab and excessive bleeding in patients undergoing emergency cardiac operations. *The Annals of Thoracic Surgery*, 65(2):465–469.

Garcia-Morales, P., Minami, Y., Luong, E., Klausner, R. D., and Samelson, L. E. (1990). Tyrosine phosphorylation in T cells is regulated by phosphatase activity: studies with phenylarsine oxide. *Proceedings of the National Academy of Sciences of the United States of America*, 87:9255–9259.

Gardiner, E. E., Arthur, J. F., Khan, M. L., Berndt, M. C., and Andrews, R. K. (2004). Regulation of platelet membrane levels of glycoprotein VI by a platelet-derived metalloproteinase. *Blood*, 104:3611–3617.

Gardiner, E. E., Karunakaran, D., Shen, Y., Arthur, J. F., Andrews, R. K., and Berndt, M. C. (2007). Controlled shedding of platelet glycoprotein (GP) VI and GPIb–IX–V by ADAM family metalloproteinases. *Journal of Thrombosis and Haemostasis*, 5:1530–1537.

Gay, L. J. and Felding-Habermann, B. (2011). Contribution of platelets to tumour metastasis. *Nature Reviews Cancer*, 11(2):123–134.

Geddes, J., Freemantle, N., Mason, J., Eccles, M., and Boynton, J. (2006). Selective serotonin reuptake inhibitors (SSRIs) versus other antidepressants for depression. *Cochrane database of systematic reviews*, 1(3):3–6.

Geng, Y. J. and Libby, P. (2002). Progression of atheroma: a struggle between death and procreation. *Arteriosclerosis, Thrombosis, and Vascular Biology*, 22(9):1370–1380.

Gershon, M. D. (2004). Serotonin receptors and transporters - roles in normal and abnormal gastrointestinal motility. *Alimentary Pharmacology and Therapeutics*, 20:3–14.

Gershon, M. D. and Tack, J. (2007). The serotonin signaling system: from basic understanding to drug development for functional GI disorders. *Gastroenterology*, 132:397–414.

Geue, S., Walker-Allgaier, B., Eißler, D., Tegtmeyer, R., Schaub, M., Lang, F., Gawaz, M., Borst, O., and Münzer, P. (2017). Doxepin inhibits GPVI-dependent platelet Ca^{2+} signaling and collagen-dependent thrombus formation. *American Journal of Physiology Cell Physiology*, 312:765–774.

Giannaccini, G., Betti, L., Palego, L., Schmid, L., Fabbrini, L., Pelosini, C., Gargini, C., Da Valle, Y., Lanza, M., Marsili, A., Maffei, M., Santini, F., Vitti, P., Pinchera, A., and Lucacchini, A. (2010). Human serotonin transporter expression during megakaryocytic differentiation of MEG-01 cells. *Neurochemical Research*, 35(4):628–635.

Gibbins, J. M. (2004). Platelet adhesion signalling and the regulation of thrombus formation. *Journal of Cell Science*, 117(16):3415–3425.

Gibbins, J. M., Asselin, J., Farndale W, R., Barnes, M., Law, C. L., and Watson, S. P. (1996). Tyrosine phosphorylation of the Fc receptor γ-chain in collagen-stimulated platelets. *Journal of Biological Chemistry*, 271(30):18095–18099.

Gibbins, J. M., Briddon, S., Shutes, A., Vugt, M. J. V., van de Winkel, J. G. J., Saito, T., and Watson, S. P. (1998). The p85 Subunit of phosphatidylinositol 3-kinase associates with the Fc receptor γ-chain and linker for activitor of T cells (LAT) in platelets stimulated by collagen and convulxin. *Journal of Biological Chemistry*, 273(51):34437–34443.

Gibbins, J. M., Okuma, M., Farndale, R. W., Barnes, M., and Watson, S. P. (1997). Glycoprotein VI is the collagen receptor in platelets which underlies tyrosine phosphorylation of the Fc receptor gamma-chain. *FEBS Letters*, 413(2):255–259.

Gibbs, C. R. and Lip, G. Y. H. (1998). Do we still need dipryidamole? *British Journal of Clinical Pharmacology*, 45:323–328.

Gil Ad, I., Zolokov, A., Lomnitski, L., Taler, M., Bar, M., Luria, D., Ram, E., and Weizman, A. (2008). Evaluation of the potential anti-cancer activity of the antidepressant sertraline in human colon cancer cell lines and in colorectal cancer-xenografted mice. *International Journal of Oncology*, 33:277–286.

Gladding, P. A., Webster, M. W. I., Farrell, H. B., Zeng, I. S. L., Park, R., and Ruijne, N. (2008). The antiplatelet effect of six non-steroidal anti-inflammatory drugs and their pharmacodynamic interaction with aspirin in healthy volunteers. *American Journal of Cardiology*, 101(7):1060–1063.

Goa, K. L. and Noble, S. (1999). Eptifibatide: a review of its use in patients with acute coronary syndromes and/or undergoing percutaneous coronary intervention. *Drugs*, 57(3):439–62.

Gobin, V., Van Steendam, K., Denys, D., and Deforce, D. L. (2014). Selective serotonin reuptake inhibitors as a novel class of immunosuppressants. *International Immunopharmacology*, 20(1):148–156.

Gobin, V., Van Steendam, K., Fevery, S., Tilleman, K., Billiau, A. D., Denys, D., and Deforce, D. L. (2013). Fluoxetine reduces murine graft-versus-host disease by induction of T cell immunosuppression. *Journal of Neuroimmune Pharmacology*, 8(4):934–943.

Gresele, P., Arnout, J., Deckmyn, H., and Vermylen, J. (1986). Mechanism of the antiplatelet action of dipyridamole in whole blood: modulation of adenosine concentration and activity. *Thrombosis and Haemostasis*, 55(1):12–18.

Griffith, M. J. (1982). Kinetics of the heparin-enhanced antithrombin III/thrombin reaction: evidence for a template model for the mechanism of action of heparin. 257(13):7360–7365.

Gross, B. S., Melford, S. K., and Watson, S. P. (1999). Evidence that phospholipase C-γ2 interacts with SLP-76, Syk, Lyn, LAT and the Fc receptor γ-chain after stimulation of the collagen receptor glycoprotein VI in human platelets. *European Journal of Biochemistry*, 263(3):612–623.

Grosse, J., Braun, A., Varga-Szabo, D., Beyersdorf, N., Schneider, B., Zeitlmann, L., Hanke, P., Schropp, P., Mühlstedt, S., Zorn, C., Huber, M., Schmittwolf, C., Jagla, W., Yu, P., Kerkau, T., Schulze, H., Nehls, M., and Nieswandt, B. (2007). An EF hand mutation in Stim1 causes premature platelet activation and bleeding in mice. *The Journal of Clinical Investigation*, 117(11):3540–3550.

Grynkiewicz, G., Poenie, M., and Tsien, R. Y. (1985). A new generation of Ca^{2+} indicators with greatly improved fluorescence properties. *Journal of Biological Chemistry*, 260(6):3440–3450.

Gurbel, P. A., Bliden, K. P., Turner, S. E., Tantry, U. S., Gesheff, M. G., Barr, T. P., Covic, L., and Kuliopulos, A. (2016). Cell-penetrating pepducin therapy targeting PAR1 in subjects with coronary artery disease. *Arteriosclerosis, Thrombosis, and Vascular Biology*, 36:189–197.

Habib, A., Fitzgerald, G. A., and Maclouf, J. (1999). Phosphorylation of the thromboxane receptor α, the predominant isoform expressed in human platelets. *Journal of Biological Chemistry*, 274(5):2645–2651.

Hackam, D. G. and Mrkobrada, M. (2012). Selective serotonin reuptake inhibitors and brain hemorrhage. *Neurology*, 79:1862–1865.

Haining, E. J., Cherpokova, D., Wolf, K., Becker, I. C., Beck, S., Eble, J. A., Stegner, D., Watson, S. P., and Nieswandt, B. (2017). CLEC 2 contributes to hemostasis independently of classical hemITAM signaling in mice. *Blood*, ():blood–2017–03–771907. Accessed: 22/10/2017.

Halai, K., Whiteford, J., Ma, B., Nourshargh, S., and Woodfin, A. (2014). ICAM-2 facilitates luminal interactions between neutrophils and endothelial cells *in vivo*. *Journal of Cell Science*, 127:620–629.

Hallback, I., Hagg, S., Eriksson, A. C., and Whiss, P. A. (2012). *In vitro* effects of serotonin and noradrenaline reuptake inhibitors on human platelet adhesion and coagulation. *Pharmacological Reports*, 64(4):979–983.

Hamberg, M., Svensson, J., and Samuelsson, B. (1975). Thromboxanes: a new group of biologically active compounds derived from prostaglandin endoperoxides. *Proceedings of the National Academy of Sciences of the United States of America*, 72(8):2994–2998.

Hancock, A. A., Bush, E. N., Stanisic, D., Kyncl, J. J., and Lin, C. T. (1988). Data normalization before statistical analysis: keeping the horse before the cart. *Trends in Pharmacological Sciences*, 9(1):29–32.

Harder, S., Klinkhardt, U., and Alvarez, J. M. (2004). Avoidance of bleeding during surgery in patients receiving anticoagulant and/or antiplatelet therapy: pharmacokinetic and pharmacodynamic considerations. *Clinical Pharmacokinetics*, 43(14):963–981.

Harper, A. G. S., Brownlow, S. L., and Sage, S. O. (2009). A role for TRPV1 in agonist-evoked activation of human platelets. *Journal of Thrombosis and Haemostasis*, 7(2):330–338.

Harrison, P. and Cramer, E. M. (1993). Platelet α-granules. *Blood Reviews*, 7(1):52–62.

Hassock, S. R., Zhu, M. X., Trost, C., Flockerzi, V., and Authi, K. S. (2002). Expression and role of TRPC proteins in human platelets: evidence that TRPC6 forms the store-independent calcium entry channel. *Blood*, 100(8):2801–2811.

Hayashi, T. and Su, T. P. (2007). Sigma-1 receptor chaperones at the ER-mitochondrion interface regulate Ca^{2+} signaling and cell survival. *Cell*, 131(3):596–610.

Heemskerk, J. W. M., Bevers, E. M., and Lindhout, T. (2002). Platelet activation and blood coagulation. *Thrombosis and Haemostasis*, 88(2):186–193.

Hergovich, N., Aigner, M., Eichler, H. G., Entlicher, J., Drucker, C., and Jilma, B. (2000). Paroxetine decreases platelet serotonin storage and platelet function in human beings. *Clinical Pharmacology and Therapeutics*, 68(4):435–442.

Herr, N., Mauler, M., Witsch, T., Stallmann, D., Schmitt, S., Mezger, J., Bode, C., and Duerschmied, D. (2014). Acute fluoxetine treatment induces slow rolling of leukocytes on endothelium in mice. *PLoS ONE*, 9(2):e88316.

Hippisley-Cox, J., Fielding, K., and Pringle, M. (1998). Depression as a risk factor for ischaemic heart disease in men: population based case-control study. *British Medical Journal*, 316:1714–1719.

Hodge, G. L., Flower, R., and Han, P. (1999). Optimal storage conditions for preserving granulocyte viability as monitored by Annexin V binding in whole blood. *Journal of Immunological Methods*, 225:27–38.

Hollopeter, G., Jantzen, H. M., Vincent, D., Li, G., England, L., Ramakrishnan, V., Yang, R. B., Nurden, P., Julius, D., and Conley, P. B. (2001). Identification of the platelet ADP receptor targeted by antithrombotic drugs. *Nature*, 409:202–207.

Horii, K., Kahn, M. L., and Herr, A. B. (2006). Structural basis for platelet collagen responses by the immune-type receptor glycoprotein VI. *Blood*, 108(3):936–943.

Hua, C. T., Gamble, J. R., and Vadas, M. A. (1998). Recruitment and activation of SHP-1 protein-tyrosine phosphatase by human platelet endothelial cell adhesion molecule-1 (PECAM-1). *Journal of Biological Chemistry*, 273(43):28332–28340.

Huang, P., Zhang, Y. H., Zheng, X. W., Liu, Y. J., Zhang, H., Fang, L., Zhang, Y. W., Yang, C., Islam, K., Wang, C., and Naranmandura, H. (2017). Phenylarsine oxide (PAO) induces apoptosis in HepG2 cells via ROS-mediated mitochondria and ER-stress dependent signaling pathways. *Metallomics*, page doi: 10.1039/c7mt00179g. [Epub ahead of print].

Hynes, R. O. (2002). Integrins: Bidirectional, allosteric signaling machines. *Cell*, 110(6):673–687.

Hyttel, J. (1977). Neurochemical characterisation of a new potent and selective serotonin uptake inhibitor: Lu 10-171. *Psychopharmacology*, 233(51):225–233.

Hyttel, J. (1982). Citalopram pharmacological profile of a specific serotonin uptake inhibitor with antidepressant activity. *Progress in Neuro-Psychopharmacology & Biological Psychiatry*, 6:277–295.

Iken, K., Chheng, S., Fargin, A., Goulet, A. C., and Kouassi, E. (1995). Serotonin upregulates mitogen stimulated B lymphocyte proliferation through 5-HT_{1A} receptors. *Cellular Immunology*, 163:1–9.

Inoue, O., Suzuki-Inoue, K., Dean, W. L., Frampton, J., and Watson, S. P. (2003). Integrin $\alpha_2\beta_1$ mediates outside-in regulation of platelet spreading on collagen through activation of Src kinases and PLCγ2. *Journal of Cell Biology*, 160(5):769–780.

Inoue, O., Suzuki-Inoue, K., McCarty, O. J. T., Moroi, M., Ruggeri, Z. M., Kunicki, T. J., Ozaki, Y., and Watson, S. P. (2006). Laminin stimulates spreading of platelets through integrin $\alpha_6\beta_1$-dependent activation of GPVI. *Blood*, 107(4):1405–1412.

Ishikawa, M., Ishiwata, K., Ishii, K., Kimura, Y., Sakata, M., Naganawa, M., Oda, K., Miyatake, R., Fujisaki, M., Shimizu, E., Shirayama, Y., Iyo, M., and Hashimoto, K. (2007). High occupancy of sigma-1 receptors in the human brain after single oral administration of fluvoxamine: a positron emission tomography study using [^{11}C]SA4503. *Biological Psychiatry*, 62(8):878–883.

Iversen, L. (2005). The monoamine hypothesis of depression. In Licinio, J. and Wong, M. L., editors, *Biology of depression: From novel insights to therapeutic strategies*, pages 71–86. Wiley-VCH, Weinheim, Germany.

Jacobsen, J. P. R., Plenge, P., Sachs, B. D., Pehrson, A. L., Cajina, M., Du, Y., Roberts, W., Rudder, M. L., Dalvi, P., Robinson, T. J., O'Neill, S. P., Khoo, K. S., Morillo, C. S., Zhang, X., and Caron, M. G. (2014). The interaction of escitalopram and R-citalopram at the human serotonin transporter investigated in the mouse. *Psychopharmacology*, 231(23):4527–4540.

Jaffe, E. A. and Weksler, B. B. (1979). Recovery of endothelial cell prostacyclin production after inhibition by low doses of aspirin. *The Journal of Clinical Investigation*, 63(3):532–535.

Jandrot-Perrus, M., Busfield, S., Lagrue, a. H., Xiong, X., Debili, N., Chickering, T., Le Couedic, J. P., Goodearl, a., Dussault, B., Fraser, C., Vainchenker, W., and Villeval, J. L. (2000). Cloning, characterization, and functional studies of human and mouse glycoprotein VI: a platelet-specific collagen receptor from the immunoglobulin superfamily. *Blood*, 96(5):1798–1807.

Janssens, F., Leenaerts, J., Diels, G., De Boeck, B., Megens, A., Langlois, X., van Rossem, K., Beetens, J., and Borgers, M. (2005). Norpiperidine imidazoazepines as a new class of potent, selective, and nonsedative H_1 antihistamines. *Journal of Medicinal Chemistry*, 48(6):2154–2166.

Jardetzky, O. (1966). Simple allosteric model for membrane pumps. *Nature*, 211:969–970.

Jarvis, G. E., Atkinson, B. T., Snell, D. C., and Watson, S. P. (2002). Distinct roles of GPVI and integrin $\alpha_2\beta_1$ in platelet shape change and aggregation induced by different collagens. *British Journal of Pharmacology*, 137(1):107–117.

Jarvis, G. E., Best, D., and Watson, S. P. (2004). Glycoprotein VI/Fc receptor γ chain-independent tyrosine phosphorylation and activation of murine platelets by collagen. *The Biochemical Journal*, 383:581–588.

Jarvis, G. E., Bihan, D., Hamaia, S., Pugh, N., Ghevaert, C., Pearce, A. C., Hughes, C. E., Watson, S. P., Ware, J., Rudd, C. E., and Farndale, R. W. (2012). A role for adhesion and degranulation-promoting adapter protein in collagen-induced platelet activation mediated via integrin $\alpha_2\beta_1$. *Journal of Thrombosis and Haemostasis*, 10(2):268–277.

Jarvis, G. E., Humphries, R. G., Robertson, M. J., and Leff, P. (2000). ADP can induce aggregation of human platelets via both P2Y1 and P2T receptors. *British Journal of Pharmacology*, 129(2):275–282.

Jarvis, G. E., Raynal, N., Langford, J. P., Onley, D. J., Andrews, A., Smethurst, P. A., and Farndale, R. W. (2008). Identification of a major GpVI-binding locus in human type III collagen. *Blood*, 111(10):4986–4996.

Joffe, P., Larsen, F. S., Pedersen, V., Ring-Larsen, H., Aaes-Jorgensen, T., and Sidhu, J. (1998). Single-dose pharmacokinetics of citalopram in patients with moderate renal insufficiency or hepatic cirrhosis compared with healthy subjects. *European Journal of Clinical Pharmacology*, 54(3):237–242.

Jokinen, J. and Nordström, P. (2009). HPA axis hyperactivity and cardiovascular mortality in mood disorder inpatients. *Journal of Affective Disorders*, 116(1-2):88–92.

Jones, K. L., Hughan, S. C., Dopheide, S. M., Farndale, R. W., Jackson, S. P., and Jackson, D. E. (2001). Platelet endothelial cell adhesion molecule-1 is a negative regulator of platelet-collagen interactions. *Blood*, 98(5):1456–1463.

Jonnakuty, C. and Gragnoli, C. (2008). What do we know about serotonin? *Journal of Cellular Physiology*, 217(2):301–306.

Judd, B. A., Myung, P. S., Obergfell, A., Myers, E. E., Cheng, A. M., Watson, S. P., Pear, W. S., Allman, D., Shattil, S. J., and Koretzky, G. A. (2002). Differential requirement for LAT and SLP-76 in GPVI versus T cell receptor signaling. *The Journal of Experimental Medicine*, 195(6):705–17.

Jung, S. M., Moroi, M., Soejima, K., Nakagaki, T., Miura, Y., Berndt, M. C., Gardiner, E. E., Howes, J. M., Pugh, N., Bihan, D., Watson, S. P., and Farndale, R. W. (2012). Constitutive dimerization of glycoprotein VI (GPVI) in resting platelets is essential for binding to

collagen and activation in flowing blood. *Journal of Biological Chemistry*, 287(35):30000–30013.

Jung, S. M., Tsuji, K., and Moroi, M. (2009). Glycoprotein (GP) VI dimer as a major collagen-binding site of native platelets: direct evidence obtained with dimeric GPVI-specific Fabs. *Journal of Thrombosis and Haemostasis*, 7:1347–1355.

Kahn, M. L., Nakanishi-Matsui, M., Shapiro, M. J., Ishihara, H., and Coughlin, S. R. (1999). Protease-activated receptors 1 and 4 mediate activation of human platelets by thrombin. *The Journal of Clinical Investigation*, 103(6):879–887.

Kahn, M. L., Zheng, Y. W., Huang, W., Bigornia, V., Zeng, D., Moff, S., Farese Jr., R. V., Tam, C., and Coughlin, S. R. (1998). A dual thrombin receptor system for platelet activation. *Nature*, 394:690–694.

Kannen, V., Marini, T., Turatti, A., Carvalho, M. C., Brandão, M. L., Jabor, V. A. P., Bonato, P. S., Ferreira, F. R., Zanette, D. L., Silva, W. A., and Garcia, S. B. (2011). Fluoxetine induces preventive and complex effects against colon cancer development in epithelial and stromal areas in rats. *Toxicology Letters*, 204:134–140.

Kato, H., Nakazawa, Y., Kurokawa, Y., Kashiwagi, H., Morikawa, Y., Morita, D., Banno, F., Honda, S., Kanakura, Y., and Tomiyama, Y. (2016). Human CalDAG-GEFI deficiency increases bleeding and delays $\alpha_{\mathrm{IIb}}\beta_3$ activation. *Blood*, 128(23):2729–2733.

Katsuki, S., Arnold, W., Mittal, C., and Murad, F. (1977). Stimulation of guanylate cyclase by sodium nitroprusside, nitroglycerin and nitric oxide in various tissue preparations and comparison to the effects of sodium azide and hydroxylamine. *Journal of Cyclic Nucleotide Research*, 3(1):23–35.

Kaumann, A. J., Parsons, A. A., and Brown, A. M. (1993). Human arterial constrictor serotonin receptors. *Cardiovascular Research*, 27(12):2094–2103.

Kawasaki, H., Springett, G. M., Toki, S., Canales, J. J., Harlan, P., Blumenstiel, J. P., Chen, E. J., Bany, I. A., Mochizuki, N., Ashbacher, A., Matsuda, M., Housman, D. E., and Graybiel, A. M. (1998). A Rap guanine nucleotide exchange factor enriched highly in the basal ganglia. *Proceedings of the National Academy of Sciences of the United States of America*, 95(22):13278–13283.

Kawashima, Y., Nagasawa, T., and Ninomiya, H. (2000). Contribution of ecto-5'-nucleotidase to the inhibition of platelet aggregation by human endothelial cells. *Blood*, 96(6):2157–2162.

Kaye, C. M., Haddock, R. E., Langley, P. F., Mellows, G., Tasker, T. C. G., Zussman, B. D., and Greb, W. H. (1989). A review of the metabolism and pharmacokinetics of paroxetine in man. *Acta Psychiatrica Scandinavica*, 80:60–75.

Kilic, F. and Rudnick, G. (2000). Oligomerization of serotonin transporter and its functional consequences. *Proceedings of the National Academy of Sciences*, 97(7):3106–3111.

Kimmel, S. E., Schelleman, H., Berlin, J. A., Oslin, D. W., Weinstein, R. B., Kinman, J. L., Sauer, W. H., and Lewis, J. D. (2011). The effect of selective serotonin re-uptake inhibitors on the risk of myocardial infarction in a cohort of patients with depression. *British Journal of Clinical Pharmacology*, 72(3):514–517.

Kimura, K., Ito, M., Amano, M., Chihara, K., Fukata, Y., Nakafuku, M., Yamamori, B., Feng, J., Nakano, T., Okawa, K., Iwamatsu, A., and Kaibuchi, K. (1996). Regulation of myosin phosphatase by Rho and Rho-associated kinase (Rho-kinase). *Science*, 273:245–248.

Klages, B., Brandt, U., Simon, M. I., Schultz, G., and Offermanns, S. (1999). Activation of G_{12}/G_{13} results in shape change and Rho/Rho-kinase-mediated myosin light chain phosphorylation in mouse platelets. *The Journal of Cell Biology*, 144(4):745–54.

Knight, C. G., Morton, L. F., Onley, D. J., Peachey, A. R., Ichinohe, T., Okuma, M., Farndale, R. W., and Barnes, M. J. (1999). Collagen-platelet interaction: Gly-Pro-Hyp is uniquely specific for platelet Gp VI and mediates platelet activation by collagen. *Cardiovascular Research*, 41:450–457.

Knight, C. G., Morton, L. F., Peachey, A. R., Tuckwell, D. S., Farndale, R. W., and Barnes, M. J. (2000). The collagen-binding A-domains of integrins $\alpha_1\beta_1$ and $\alpha_2\beta_1$ recognize the same specific amino acid sequence, GFOGER, in native (triple-helical) collagens. *Journal of Biological Chemistry*, 275(1):35–40.

Kobilka, B., Matsui, H., Kobilka, T., Yang-Feng, T., Francke, U., Caron, M., Lefkowitz, R., and Regan, J. (1987). Cloning, sequencing, and expression of the gene coding for the human platelet α_2-adrenergic receptor. *Science*, 238:650–656.

Kop, W. J., Gottdiener, J. S., Tangen, C. M., Fried, L. P., McBurnie, M. A., Walston, J., Newman, A., Hirsch, C., and Tracy, R. P. (2002). Inflammation and coagulation factors in persons > 65 years of age with symptoms of depression but without evidence of myocardial ischemia. *The American Journal of Cardiology*, 89(4):419–424.

Kragh-Sørensen, P., Overø, K. F., Petersen, O. L., Jensen, K., and Parnas, W. (1981). The kinetics of citalopram: single and multiple dose studies in man. *Acta Pharmacologica et Toxicologica*, 48(1):53–60.

Kubera, M., Grygier, B., Arteta, B., Urbańska, K., Basta-Kaim, A., Budziszewska, B., Leśkiewicz, M., Kołaczkowska, E., Maes, M., Szczepanik, M., Majewska, M., and Lasoń, W. (2009). Age-dependent stimulatory effect of desipramine and fluoxetine pretreatment on metastasis formation by B16F10 melanoma in male C57BL/6 mice. *Pharmacological Reports*, 61(6):1113–1126.

Kuo, C. Y., Wang, H. C., Kung, P. H., Lu, C. Y., Liao, C. Y., Wu, M. T., and Wu, C. C. (2014). Identification of CalDAG-GEFI as an intracellular target for the vicinal dithiol binding agent phenylarsine oxide in human platelets. *Thrombosis and Haemostasis*, 111(5):892–901.

Kushboo, S. B. and Sharma, B. (2017). Antidepressants: mechanism of action, toxicity and possible amelioration. *Journal of Applied Biotechnology & Bioengineering*, 3(5):1–13.

Lagrue-Lak-Hal, A. H., Debili, N., Kingbury, G., Lecut, C., Le Couedic, J. P., Villeval J, L., Jandrot-Perrus, M., and Vainchenker, W. (2001). Expression and function of the collagen receptor GPVI during megakaryocyte maturation. *The Journal of Biological Chemistry*, 276(18):15316–15325.

Lanzenberger, R., Kranz, G. S., Haeusler, D., Akimova, E., Savli, M., Hahn, A., Mitterhauser, M., Spindelegger, C., Philippe, C., Fink, M., Wadsak, W., Karanikas, G., and Kasper, S. (2012). Prediction of SSRI treatment response in major depression based on serotonin transporter interplay between median raphe nucleus and projection areas. *NeuroImage*, 63(2):874–881.

Larson, M. K. and Watson, S. P. (2006). Regulation of proplatelet formation and platelet release by integrin $\alpha_{\mathrm{IIb}}\beta_3$. *Blood*, 108(5):1509–1514.

Lebozec, K., Jandrot-Perrus, M., Avenard, G., Favre-Bulle, O., and Billiald, P. (2017). Design, development and characterization of ACT017, a humanized Fab that blocks platelet's glycoprotein VI function without causing bleeding risks. *MABS*, 0(0):1–14.

Lee, H. S., Lim, C. J., Puzon-McLaughlin, W., Shattil, S. J., and Ginsberg, M. H. (2009). RIAM activates integrins by linking talin to Ras GTPase membrane-targeting sequences. *Journal of Biological Chemistry*, 284(8):5119–5122.

Leeksma, C. H. and Cohen, J. A. (1956). Determination of the life span of human blood platelets using labelled diisopropylfluorophosphonate. *The Journal of Clinical Investigation*, 35(9):964–969.

Leevers, S. J., Vanhaesebroeck, B., and Waterfield, M. D. (1999). Signalling through phosphoinositide 3-kinases: the lipids take centre stage. *Current Opinion in Cell Biology*, 11(3):219–225.

Léon, C., Hechler, B., Freund, M., Eckly, A., Vial, C., Ohlmann, P., Dierich, A., Lemeur, M., Cazenave, J. P., and Gachet, C. (1999). Defective platelet aggregation and increased resistance to thrombosis in purinergic P2Y1 receptor–null mice. *The Journal of Clinical Investigation*, 104(12):1731–1737.

Leonardi, S., Tricoci, P., and Becker, R. C. (2010). Thrombin receptor antagonists for the treatment of atherothrombosis. *Drugs*, 70(14):1771–1783.

Lesch, K. P., Wolozin, B. L., Murphy, D. L., and Reiderer, P. (1993). Primary structure of the human platelet serotonin uptake site: identity with the brain serotonin transporter. *Journal of Neurochemistry*, 60(6):2319–2322.

Leysen, J. E., Niemegeers, C. J., van Nueten, J. M., and Laduron, P. M. (1982). [^{3}H]Ketanserin (R 41 468), a selective ^{3}H-ligand for serotonin$_2$ receptor binding sites: binding properties, brain distribution, and functional role. *Molecular Pharmacology*, 21:301–314.

Li, H., Lockyer, S., Concepcion, A., Gong, X., Takizawa, H., Guertin, M., Matsumoto, Y., Kambayashi, J., Tandon, N. N., and Liu, Y. (2007). The fab fragment of a novel anti-GPVI monoclonal antibody, OM4, reduces *in vivo* thrombosis without bleeding risk in rats. *Arteriosclerosis, Thrombosis, and Vascular Biology*, 27(5):1199–1205.

Lienhard, G. (1973). Enzymatic catalysis and transition-state theory. *Science*, 180:149–154.

Lin, O. A., Karim, Z. A., Vemana, H. P., Espinosa, E. V. P., and Khasawneh, F. T. (2014). The antidepressant 5-HT_{2A} receptor antagonists pizotifen and cyproheptadine inhibit serotonin-enhanced platelet function. *PLoS one*, 9(1):e87026.

Liu, F. C., Liou, J. T., Liao, H. R., Mao, C. C., Yang, P., and Day, Y. J. (2012). The anti-aggregation effects of ondansetron on platelets involve IP_3 signaling and MAP kinase pathway, but not 5-HT_3-dependent pathway. *Thrombosis Research*, 130(3):84–94.

Liu, X., Miller, M. J. S., Joshi, M. S., Sadowska-Krowicka, H., Clark, D. A., and Lancaster, J. R. (1998). Diffusion-limited reaction of nitric oxide with erythrocytes. *Journal of Biological Chemistry*, 273(30):18709–18713.

López, J. J., Redondo, P. C., Salido, G. M., Pariente, J. A., and Rosado, J. A. (2006). Two distinct Ca^{2+} compartments show differential sensitivity to thrombin, ADP and vasopressin in human platelets. *Cellular Signalling*, 18(3):373–381.

Loyau, S., Dumont, B., Ollivier, V., Boulaftali, Y., Feldman, L., Ajzenberg, N., and Jandrot-Perrus, M. (2012). Platelet glycoprotein VI dimerization, an active process inducing receptor competence, is an indicator of platelet reactivity. *Arteriosclerosis, Thrombosis, and Vascular Biology*, 32(3):778–785.

Lozano, M. L., Cook, A., Bastida, J. M., Paul, D. S., Iruin, G., Cid, A. R., Adan-Pedroso, R., González-Porras, J. R., Hernández-Rivas, J. M., Fletcher, S. J., Johnson, B., Morgan, N., Ferrer-Marin, F., Vicente, V., Sondek, J., Watson, S. P., Bergmeier, W., and Rivera, J. (2016). Novel mutations in RASGRP2, which encodes CalDAG-GEFI, abrogate Rap1 activation, causing platelet dysfunction. *Blood*, 128(9):1282–1289.

MacDonald, T. M., McMahon, A. D., Reid, I. C., Fenton, G. W., and McDevitt, D. G. (1996). Antidepressant drug use in primary care: a record linkage study in Tayside, Scotland. *British Medical Journal*, 313:860–861.

MacKenzie, A. B., Mahaut-Smith, M. P., and Sage, S. O. (1996). Activation of receptor-operated cation channels via P2X1 not P2T purinoceptors in human platelets. *Journal of Biological Chemistry*, 271(6):2879–2881.

Madsen, J., Merachtsaki, P., Davoodpour, P., Bergström, M., Långström, B., Andersen, K., Thomsen, C., Martiny, L., and Knudsen, G. M. (2003). Synthesis and biological evaluation of novel carbon-11-labelled analogues of citalopram as potential radioligands for the serotonin transporter. *Bioorganic and Medicinal Chemistry*, 11(16):3447–3456.

Mangin, P., Nonne, C., Eckly, A., Ohlmann, P., Freund, M., Nieswandt, B., Cazenave, J. P., Gachet, C., and Lanza, F. (2003). A PLCγ2-independent platelet collagen aggregation requiring functional association of GPVI and integrin $\alpha 2\beta 1$. *FEBS Letters*, 542(1-3):53–59.

Mannaioni, P. F., Bello, M. G., Raspanti, S., Gambassi, F., Mugnai, L., and Masini, E. (1993). Histamine release by human platelets. *Agents and Actions*, 38:203–205.

Mannaioni, P. F., Palmerani, B., Pistelli, A., Gambassi, F., Giannella, E., Sacchi, T. B., and Masini, E. (1990). Histamine release by platelet aggregation. *Agents and Actions*, 30:44–48.

Mannaioni, P. F., Pistelli, A., Di Bello, M. G., Gambassi, F., and Masini, E. (1992). H_1-receptor dependent increase in platelet aggregation is mediated by intracellular calcium. *Agents and Actions*, 36:402–405.

Marcus, A. J., Broekman, M. J., Drosopoulos, J. H. F., Islam, N., Alyonycheva, T. N., Safier, L. B., Hajjar, K. A., Posnett, D. N., Schoenborn, M. A., Schooley, K. A., Gayle, R. B., and Maliszewski, C. R. (1997). The endothelial cell ecto-ADPase resposible for inhibition of platelet function is CD39. *The Journal of Clinical Investigation*, 99(6):1351–1360.

Masini, E., Di Bello, M. G., Raspanti, S., Fomusi Ndisang, J., Baronti, R., Cappugi, P., and Mannaioni, P. F. (1998). The role of histamine in platelet aggregation by physiological and immunological stimuli. *Inflammation Research*, 47(5):211–220.

Masini, E., Di Bello, M. G., Raspanti, S., Sacchi, T. B., Maggi, E., and Mannaioni, P. F. (1994). Platelet aggregation and histamine release by immunological stimuli. *Immunopharmacology*, 28(1):19–29.

Maurer-Spurej, E., Pittendreigh, C., and Solomons, K. (2004). The influence of selective serotonin reuptake inhibitors on serotonin metabolism in human platelets. *Thrombosis and Haemostasis*, 91:119–128.

Mawe, G. M. and Hoffman, J. M. (2013). Serotonin signalling in the gut-functions, dysfunctions and therapeutic targets. *Nature Reviews Gastroenterology & Hepatology*, 10(8):473–486.

May, F., Hagedorn, I., Pleines, I., Bender, M., Vogtle, T., Eble, J., Elvers, M., and Nieswandt, B. (2009). CLEC-2 is an essential platelet activating receptor in hemostasis and thrombosis. *Blood*, 114(16):3464–3473.

Mazharian, A., Wang, Y. J., Mori, J., Bem, D., Finney, B., Heising, S., Gissen, P., White, J. G., Berndt, M. C., Gardiner, E. E., Nieswandt, B., Douglas, M. R., Campbell, R. D., Watson, S. P., and Senis, Y. A. (2012). Mice lacking the ITIM-containing receptor G6b-B exhibit macrothrombocytopenia and aberrant platelet function. *Science Signaling*, 5(248):ra78.

McCorvy, J. D. and Roth, B. L. (2015). Structure and function of serotonin G protein-coupled receptors. *Pharmacology & Therapeutics*, 150:129–142.

Mehta, S. R., Yusuf, S., Peters, R. J., Bertrand, M. E., Lewis, B. S., Natarajan, M. K., Malmberg, K., Rupprecht, H. J., Zhao, F., Chrolavicius, S., Copland, I., and Fox, K. A. (2001). Effects of pretreatment with clopidogrel and aspirin followed by long-term therapy in patients undergoing percutaneous coronary intervention: the PCI-CURE study. *Lancet*, 358:527–533.

Meier, C. R., Schlienger, R. G., and Jick, H. (2001). Use of selective serotonin reuptake inhibitors and risk of developing first-time acute myocardial infarction. *British Journal of Clinical Pharmacology*, 52(2):179–84.

Mercado, C. P. and Kilic, F. (2010). Molecular mechanisms of SERT in platelets: regulation of plasma serotonin levels. *Molecular interventions*, 10(4):231–41.

Milne, R. J. and Goa, K. L. (1991). Citalopram. *Drugs*, 41(3):450–477.

Milne, W. L. and Cohn, S. H. (1957). Role of Serotonin in Blood Coagulation. *American Journal of Physiology*, 189(3):470–474.

Miner, J. and Hoffhines, A. (2007). The discovery of aspirin's antithrombotic effects. *Texas Heart Institute Journal*, 34(2):179–86.

Miura, Y., Masaaki, O., Jung, S. M., and Moroi, M. (2000). Cloning and expression of the platelet-specific collagen receptor glycoprotein VI. *Thrombosis Research*, 98:301–309.

Miura, Y., Takahashi, T., Jung, S. M., and Moroi, M. (2002). Analysis of the interaction of platelet collagen receptor glycoprotein VI (GPVI) with collagen: A dimeric form of GPVI, but not the monomeric form, shows affinity to fibrous collagen. *Journal of Biological Chemistry*, 277(48):46197–46204.

Moncada, S., Higgs, E. A., and Vane, J. R. (1977). Human arterial and venous tissues generate prostacyclin (prostaglandin x), a potent inhibitor of platelet aggregation. *Lancet*, 309:18–21.

Montgomery, S. A., Loft, H., Sánchez, C., Reines, E. H., and Papp, M. (2001). Escitalopram (S-enantiomer of citalopram): clinical efficacy and onset of action predicted from a rat model. *Pharmacology & Toxicology*, 88:282–286.

Moore, N., Verdoux, H., and Fantino, B. (2005). Prospective, multicentre, randomized, double-blind study of the efficacy of escitalopram versus citalopram in outpatient treatment of major depressive disorder. *International Clinical Psychopharmacology*, 20(3):131–137.

Mori, J., Pearce, A. C., Spalton, J. C., Grygielska, B., Eble, J. A., Tomlinson, M. G., Senis, Y. A., and Watson, S. P. (2008). G6b-B inhibits constitutive and agonist-induced signaling by glycoprotein VI and CLEC-2. *Journal of Biological Chemistry*, 283(51):35419–35427.

Mori, J., Wang, Y. J., Ellison, S., Heising, S., Neel, B. G., Tremblay, M. L., Watson, S. P., and Senis, Y. A. (2012). Dominant role of the protein-tyrosine phosphatase CD148 in regulating platelet activation relative to protein-tyrosine phosphatase-1B. *Arteriosclerosis, Thrombosis, and Vascular Biology*, 32(12):2956–2965.

Moroi, M., Jung, S. M., Okuma, M., and Shinmyozut, K. (1989). A patient with platelets deficient in glycoportein VI that lack both collagen-induced aggregation and adhesion. *The Journal of Clinical Investigation*, 84:1440–1445.

Morton, L. F., Hargreaves, P. G., Farndale, R. W., Young, R. D., and Barnes, M. J. (1995). Integrin $\alpha_2\beta_1$-independent activation of platelets by simple collagen-like peptides: collagen tertiary (triple-helical) and quaternary (polymeric) structures are sufficient alone for $\alpha_2\beta_1$-independent platelet reactivity. *Biochemical Journal*, 306:337–344.

Moser, M., Legate, K. R., Zent, R., and Fassler, R. (2009). The tail of integrins, talin, and kindlins. *Science*, 324:895–899.

Mössner, R. and Lesch, K. P. (1998). Role of serotonin in the immune system and in neuroimmune interactions. *Brain, Behavior, and Immunity*, 12(4):249–271.

Mould, D. R. and Upton, R. N. (2012). Basic concepts in population modeling, simulation, and model-based drug development. *CPT: Pharmacometrics & Systems Pharmacology*, 1(9):e6.

M'Rabet, L., Coffer, P., Zwartkruis, F., Franke, B., Segal, A. W., Koenderman, L., and Bos, J. L. (1998). Activation of the small GTPase rap1 in human neutrophils. *Blood*, 92(6):2133–2140.

Musselman, D. L., Evans, D. L., and Nemeroff, C. B. (1998). The relationship of depression to cardiovascular disease. *Journal of the American Medical Association*, 55:580–592.

Musselman, D. L., Marzec, U. M., Manatunga, A., Penna, S., Reemsnyder, A., Knight, B. T., Baron, A., Hanson, S. R., and Nemeroff, C. B. (2000). Platelet reactivity in depressed patients treated with paroxetine: preliminary findings. *Archives of General Psychiatry*, 57(9):875–882.

Nagai, T., Nakamuta, S., Kuroda, K., Nakauchi, S., Nishioka, T., Takano, T., Zhang, X., Tsuboi, D., Funahashi, Y., Nakano, T., Yoshimoto, J., Kobayashi, K., Uchigashima, M., Watanabe, M., Miura, M., Nishi, A., Kobayashi, K., Yamada, K., Amano, M., and Kaibuchi, K. (2016). Phosphoproteomics of the dopamine pathway enables discovery of Rap1 activation as a reward signal *in vivo*. *Neuron*, 89(3):550–565.

Nambal, T., Oida, H., Sugimoto, Y., Kakizuka, A., Negishi, M., Ichikawa, A., and Narumiya, S. (1994). cDNA cloning of a mouse prostacyclin receptor: multiple signaling pathways and expression in thymic medulla. *Journal of Biological Chemistry*, 269(13):9986–9992.

Narita, N., Hashimoto, K., Tomitaka, S., and Minabe, Y. (1996). Interactions of selective serotonin reuptake inhibitors with subtypes of sigma receptors in rat brain. *European Journal of Pharmacology*, 307(1):117–119.

National Statistics (2017). Prescriptions dispensed to the community, statistics for England - 2006-2016: Appendix Tables. Available at: http://digital.nhs.uk/catalogue/PUB30014. Accessed: 20/09/2017. Technical report, National Statistics.

Navarro-Borelly, L., Somasundaram, A., Yamashita, M., Ren, D., Miller, R. J., and Prakriya, M. (2008). STIM1-Orai1 interactions and Orai1 conformational changes revealed by live-cell FRET microscopy. *The Journal of Physiology*, 586:5383–5401.

Neves, S. R., Ram, P. T., and Lyengr, R. (2002). G protein pathways. *Science*, 296:1636–1639.

Newman, P. J., Berndt, M. C., Gorski, J., White, G. C., Lyman, S., Paddock, C., and Muller, W. A. (1990). PECAM-1 (CD31) cloning and relation to adhesion molecules of the immunoglobin gene superfamily. *Science*, 247:1219–1222.

Nieswandt, B., Bergmeier, W., Schulte, V., Rackebrandt, K., Gessner, J. E., and Zirngibl, H. (2000). Expression and function of the mouse collagen receptor glycoprotein VI is strictly dependent on its association with the FcRγ-chain. *Journal of Biological Chemistry*, 275(31):23998–24002.

Nieswandt, B., Schulte, V., Bergmeier, W., Mokhtari-Nejad, R., Rackebrandt, K., Cazenave, J. P., Ohlmann, P., Gachet, C., and Zirngibl, H. (2001). Long-term antithrombotic protection by *in vivo* depletion of platelet glycoprotein VI in mice. *The Journal of Experimental Medicine*, 193(4):459–470.

Nieswandt, B., Varga-Szabo, D., and Elvers, M. (2009). Integrins in platelet activation. *Journal of Thrombosis and Haemostasis*, 7:206–209.

Nieswandt, B. and Watson, S. P. (2003). Platelet-collagen interaction: is GPVI the central receptor? *Blood*, 102(2):449–461.

Nishizawa, E. E. and Wynalda, D. J. (1981). Inhibitory effect of ibuprofen on platelet function. *Thrombosis Research*, 21:347–356.

Nosál, R., Drábiková, K., Jančinová, V., Petríková, M., and Fábryová, V. (2005). Antiplatelet and antiphagocyte activity of H_1-antihistamines. *Inflammation Research*, 54:19–20.

O'Callaghan, K., Kuliopulos, A., and Covic, L. (2012). Turning receptors on and off with intracellular pepducins: new insights into G-protein-coupled receptor drug development. *Journal of Biological Chemistry*, 287(16):12787–12796.

Offermanns, S. (2006). Activation of platelet function through G protein-coupled receptors. *Circulation Research*, 99(12):1293–1304.

Offermanns, S., Laugwitz, K. L., Spicher, K., and Schultz, G. (1994). G proteins of the G_{12} family are activated via thromboxane A_2 and thrombin receptors in human platelets. *Proceedings of the National Academy of Sciences of the United States of America*, 91(2):504–508.

Ohto, H., Maeda, H., Shibata, Y., Chen, R. F., Ozaki, Y., Higashihara, M., Takeuchi, A., and Tohyama, H. (1985). A novel leukocyte differentiation antigen: two monocolonal antibodies TM2 and TM3 define a 120-kd molecule present on neutrophils, monocytes, platelets and activated lymphoblasts. *Blood*, 66(4):873–881.

Olesen, O. V. and Linnet, K. (1999). Studies on the stereoselective metabolism of citalopram by human liver microsomes and cDNA-expressed cytochrome P450 enzymes. *Pharmacology*, 59(6):298–309.

Oliver, K. H., Duvernay, M. T., Hamm, H. E., and Carneiro, A. M. (2016). Loss of serotonin transporter function alters ADP-mediated glycoprotein $\alpha_{\mathrm{IIb}}\beta_3$ activation through dysregulation of the receptor. *Journal of Biological Chemistry*, 291(38):20210–20219.

Opatrny, L., Delaney, J. A. C., and Suissa, S. (2008). Gastro-intestinal haemorrhage risks of selective serotonin receptor antagonist therapy: a new look. *British Journal of Clinical Pharmacology*, 66(1):76–81.

O'Rourke, F. A., Halenda, S. P., Zavoico, G. B., and Feinstein, M. B. (1985). Inositol 1,4,5-trisphosphate releases Ca^{2+} from a Ca^{2+}-transporting membrane vesicle fraction derived from human platelets. *Journal of Biological Chemistry*, 260(4):956–962.

Owens, M. J. (2004). Selectivity of antidepressants: From the monoamine hypothesis of depression to the SSRI revolution and beyond. *Journal of Clinical Psychiatry*, 65:5–10.

Owens, M. J., Knight, D. L., and Nemeroff, C. B. (2001). Second-generation SSRIs: human monoamine transporter binding profile of escitalopram and R-fluoxetine. *Biological Psychiatry*, 50(5):345–350.

Owens, M. J., Morgan, W. N., Plott, S. J., and Nemeroff, C. B. (1997). Neurotransmitter receptor and transporter binding profile of antidepressants and their metabolites. *The Journal of Pharmacology and Experimental Therapeutics*, 283(3):1305–1322.

Palmer, D. S., Aye, M. T., Ganz, P. R., Halpenny, M., and Hashemi, S. (1994). Adenosine nucleotides and serotonin stimulate von Willebrand factor release from cultured human endothelial cells. *Thrombosis and Haemostasis*, 72(1):132–139.

Parker, N. G. and Brown, C. S. (2000). Citalopram in the treatment of depression. *Annals of Pharmacotherapy*, 34:761–771.

Parks, W. M., Hoak, J. C., and Czervionke, R. L. (1981). Comparative effect of ibuprofen on endothelial and platelet prostaglandin synthesis. *Journal of Pharmacology and Experimental Therapeutics*, 219(2):415–419.

Pasquet, J. M., Gross, B., Quek, L., Asazuma, N., Zhang, W., Sommers, C. L., Schweighoffer, E., Tybulewicz, V., Judd, B., Lee, J. R. A. N., Koretzky, G., Love, P. E., Samelson, L. E., and Watson, S. P. (1999). LAT is required for tyrosine phosphorylation of phospholipase Cγ2 and platelet activation by the collagen receptor GPVI. *Molecular and Cellular Biology*, 19(12):8326–8334.

Patil, S., Newman, D. K., and Newman, P. J. (2001). Platelet endothelial cell adhesion molecule-1 serves as an inhibitory receptor that modulates platelet responses to collagen. *Blood*, 97(6):1727–1732.

Patrono, C., Garcia Rodriguez, L. A., Landolfi, R., and Baigent, C. (2005). Low-dose aspirin for the prevention of atherothrombosis. *New England Journal of Medicine*, 353:2373–2383.

Patrono, C. and Rocca, B. (2009). Aspirin, 110 years later. *Journal of Thrombosis and Haemostasis*, 7:258–261.

Penmatsa, A., Wang, K. H., and Gouaux, E. (2013). X-ray structure of dopamine transporter elucidates antidepressant mechanism. *Nature*, 503:85–90.

Penmatsa, A., Wang, K. H., and Gouaux, E. (2015). X-ray structures of drosophila dopamine transporter in complex with nisoxetine and reboxetine. *Nature Structural & Molecular Biology*, 22(6):506–508.

Phillips, D. R. and Agin, P. P. (1977a). Platelet membrane defects in Glanzmann's thrombasthenia: evidence for decreased amounts of two major glycoproteins. *The Journal of Clinical Investigation*, 60(3):535–545.

Phillips, D. R. and Agin, P. P. (1977b). Platelet plasma membrane glycoproteins Identification of a proteolytic substrate for thrombin. *Biochemical and Biophysical Research Communications*, 75(4):940–947.

Piatt, R., Paul, D. S., Lee, R. H., McKenzie, S. E., Parise, L. V., Cowley, D. O., Cooley, B. C., and Bergmeier, W. (2016). Mice expressing low levels of CalDAG-GEFI exhibit markedly impaired platelet activation with minor impact on hemostasis. *Arteriosclerosis, Thrombosis, and Vascular Biology*, 36(9):1838–1846.

Pizzi, C., Rutjes, A. W. S., Costa, G. M., Fontana, F., Mezzetti, A., and Manzoli, L. (2011). Meta-analysis of selective serotonin reuptake inhibitors in patients with depression and coronary heart disease. *American Journal of Cardiology*, 107(7):972–979.

Plenge, P., Gether, U., and Rasmussen, S. G. (2007). Allosteric effects of R- and S-citalopram on the human 5-HT transporter: evidence for distinct high- and low-affinity binding sites. *European Journal of Pharmacology*, 567:1–9.

Poulter, N. S., Pollitt, A. Y., Owen, D. M., Gardiner, E. E., and Andrews, R. K. (2017). Clustering of glycoprotein VI (GPVI) dimers upon adhesion to collagen as a mechanism to regulate GPVI signaling in platelets. *Journal of Thrombosis and Haemostasis*, 15:549–564.

Puri, R., Minniti, C., Grana, G., Freedman, M. D., Colman, R. F., and Colman, R. W. (1992). Clopidogrel inhibits the binding of ADP analogues to the receptor mediating inhibition of platelet adenylate cyclase. *Arteriosclerosis and Thrombosis*, 12:430–436.

Pytela, R., Pierschbacher, M. D., Ginsberg, M. H., Plow, E. F., and Ruoslahti, E. (1986). Platelet membrane glycoprotein IIb/IIIa: member of a family of Arg-Gly-Asp-specific adhesion receptors. *Science*, 231:1559–1562.

Qian, Y., Melikian, H. E., Rye, D. B., Levey, A. I., and Blakely, R. D. (1995). Identification and characterization of antidepressant-sensitive serotonin transporter proteins using site-specific antibodies. *Journal of Neuroscience*, 15(2):1261–1274.

Qiao, J. l., Al-Tamini, M., Baker, R. I., Andrews, R. K., and Gardiner, E. E. (2015). The platelet Fc receptor, FcRγRIIa. *Immunological Reviews*, 268:241–252.

Qiao, J. L., Shen, Y., Gardiner, E. E., and Andrews, R. K. (2010). Proteolysis of platelet receptors in humans and other species. *Biological chemistry*, 391:893–900.

Quek, L. S., Bolen, J., and Watson, S. P. (1998). A role for Bruton's tyrosine kinase (Btk) in platelet activation by collagen. *Current Biology*, 8:1137–1141.

Rabie, T., Varga-Szabo, D., Bender, M., Pozgaj, R., Lanza, F., Saito, T., Watson, S. P., and Nieswandt, B. (2007). Diverging signaling events control the pathway of GPVI down-regulation *in vivo*. *Blood*, 110(2):529–535.

Rapport, M., Green, A., and Page, H. (1948a). Crystalline serotonin. *Science*, 108:329–330.

Rapport, M., Green, A., and Page, H. (1948b). Partial purification of the vasoconstrictor in beef serum. *Journal of Biological Chemistry*, 174:735–741.

Redondo, P. C., Rosado, J. A., Pariente, J. A., and Salido, G. M. (2005). Collaborative effect of SERCA and PMCA in cytosolic calcium homeostasis in human platelets. *Journal of Physiological Biochemistry*, 61(4):507–516.

Reilly, M. P. and Mohler, E. (2001). The role of cilostazol in the treatment of intermittent claudication. *Current Medical Research and Opinion*, 35:48–56.

Ren, J., Cook, A. A., Bergmeier, W., and Sondek, J. (2016). A negative-feedback loop regulating ERK1/2 activation and mediated by RasGPR2 phosphorylation. *Biochemical and Biophysical Research Communications*, 474(1):193–198.

Roberts, D. E., Matsuda, T., and Bose, R. (2012). Molecular and functional characterization of the human platelet Na^+/Ca^{2+} exchangers. *British Journal of Pharmacology*, 165(4):922–936.

Rocca, P., Fonzo, V., Scotta, M., Zanalda, E., and Ravizza, L. (1997). Paroxetine efficacy in the treatment of generalized anxiety disorder. *Acta psychiatrica Scandinavica*, 95(5):444–450.

Rochat, B., Amey, M., Gillet, M., Meyer, U. A., and Baumann, P. (1997). Identification of three cytochrome P450 isozymes involved in N-demethylation of citalopram enantiomers in human liver microsomes. *Pharmacogenetics and Genomics*, 7(1):1–10.

Rosado, J. A. (2011). Acidic Ca^{2+} stores in platelets. *Cell Calcium*, 50(2):168–174.

Rosenbaum, D. M., Rasmussen, S. G. F., and Kobilka, B. K. (2009). The structure and function of G-protein-coupled receptors. *Nature*, 459:356–363.

Roth, G. J. and Majerus, P. W. (1975). The mechanism of the effect of aspirin on human platelets. I. Acetylation of a particulate fraction protein. *The Journal of Clinical Investigation*, 56(3):624–632.

Roth, G. J., Stanford, N., and Majerus, P. W. (1975). Acetylation of prostaglandin synthase by aspirin. *Proceedings of the National Academy of Sciences of the United States of America*, 72(8):3073–3076.

Rudnick, G. (2006). Structure/function relationships in serotonin transporter: new insights from the structure of a bacterial transporter. In Sitte, H. H. and Freissmuth, M., editors, *Neurotransmitter Transporters. Handbook of Experimental Pharmacology*, number 175, pages 59–73. Springer-Verlag, Berlin, Germany.

Saelman, E. U., Nieuwenhuis, H. K., Hese, K. M., de Groot, P. G., Heijnen, H. F., Sage, E. H., Williams, S., McKeown, L., Gralnick, H. R., and Sixma, J. J. (1994). Platelet adhesion to collagen types I through VIII under conditions of stasis and flow is mediated by GPIa/IIa ($\alpha_2\beta_1$-integrin). *Blood*, 83(5):1244–1250.

Sakowski, S. A., Geddes, T. J., Thomas, D. M., Levi, E., Hatfield, J. S., and Kuhn, D. M. (2006). Differential tissue distribution of tryptophan hydroxylase isoforms 1 and 2 as revealed with monospecific antibodies. *Brain Research*, 1085(1):11–18.

Sakuma, I., Akaishi, Y., Fukao, M., Makita, Y., Makita, M. A., Kobayashi, T., Matsuno, K., Miyazaki, T., and Yasuda, H. (1990). Dipyridamole potentiates the anti-aggregation effect of endothelium-derived relaxing factor. *Thrombosis Research*, 12:87–90.

Sánchez (2006). The pharmacology of citalopram enantiomers: the antagonism by R-citalopram on the effect of S-citalopram. *Pharmacology & Toxicology*, 99:91–95.

Sarma, A. and Horne, M. K. (2006). Venlafaxine-induced ecchymoses and impaired platelet aggregation. *European Journal of Haematology*, 77(6):533–537.

Sauer, W. H., Berlin, J. A., and Kimmel, S. E. (2001). Selective serotonin reuptake inhibitors and myocardial infarction. *Circulation*, 104(16):1894–1898.

Savi, P., Pereillo, J. M., Uzabiaga, M. F., Combalbert, J., Picard, C., Maffrand, J. P., Pascal, M., and Herbert, J. M. (2000). Identification and biological activity of the active metabolite of clopidogrel. *Thrombosis and Haemostasis*, 84(5):891–896.

Saxena, S. P., Brandes, L. J., Becker, A. B., Simons, K. J., LaBella, F. S., and Gerrard, J. M. (2017). Histamine is an intracellular messenger mediating platelet aggregation. *Science*, 243:1596–1599.

Scarborough, R. M., Kleiman, N. S., and Phillips, D. R. (1999). Platelet glycoprotein IIb/IIIa antagonists: what are the relevant issues concerning their pharmacological and clinical use? *Circulation*, 100:437–444.

Schlienger, R. G., Fischer, L. M., Jick, H., and Meier, C. R. (2004). Current use of selective serotonin reuptake inhibitors and risk of acute myocardial infarction. *Drug Safety*, 27(14):1157–1165.

Schmaier, A. A., Zou, Z., Kazlauskas, A., Emert-Sedlak, L., Fong, K. P., Neeves, K. B., Maloney, S. F., Diamond, S. L., Kunapuli, S. P., Ware, J., Brass, L. F., Smithgall, T. E., Saksela, K., and Kahn, M. L. (2009). Molecular priming of Lyn by GPVI enables an immune receptor to adopt a hemostatic role. *Proceedings of the National Academy of Sciences of the United States of America*, 106(50):21167–21172.

Schuster, C., Fernbach, N., Rix, U., Superti-Furga, G., Holy, M., Freissmuth, M., Sitte, H. H., and Sexl, V. (2007). Selective serotonin reuptake inhibitors-A new modality for the treatment of lymphoma/leukaemia? *Biochemical Pharmacology*, 74(9):1424–1435.

Senis, Y. A., Tomlinson, M. G., Ellison, S., Mazharian, A., Lim, J., Zhao, Y., Kornerup, K. N., Auger, J. M., Thomas, S. G., Dhanjal, T., Kalia, N., Zhu, J. W., Weiss, A., and Watson, S. P. (2009). The tyrosine phosphatase CD148 is an essential positive regulator of platelet activation and thrombosis. *Blood*, 113(20):4942–4954.

Senis, Y. A., Tomlinson, M. G., García, A., Dumon, S., Heath, V. L., Herbert, J., Cobbold, S. P., Spalton, J. C., Ayman, S., Antrobus, R., Zitzmann, N., Bicknell, R., Frampton, J., Authi, K. S., Martin, A., Wakelam, M. J. O., and Watson, S. P. (2007). A comprehensive proteomics and genomics analysis reveals novel transmembrane proteins in human platelets and mouse megakaryocytes including G6b-B, a novel immunoreceptor tyrosine-based inhibitory motif protein. *Molecular & Cellular Proteomics*, 6(3):548–564.

Serafeim, A., Holder, M. J., Grafton, G., Chamba, A., Drayson, M. T., Luong, Q. T., Bunce, C. M., Gregory, C. D., Barnes, N. M., and Gordon, J. (2003). Selective serotonin reuptake inhibitors directly signal for apoptosis in biopsy-like Burkitt lymphoma cells. *Blood*, 101(8):3212–3219.

Serebruany, V. L., Glassman, A. H., Malinin, A. I., Nemeroff, C. B., Musselman, D. L., van Zyl, L. T., Finkel, M. S., Krishnan, K. R. R., Gaffney, M., Harrison, W., Califf, R. M., and O'Connor, C. M. (2003). Platelet/endothelial biomarkers in depressed patients treated with the selective serotonin reuptake inhibitor sertraline after acute coronary events: the Sertraline Antidepressant Heart Attack Randomized Trial (SADHART) platelet substudy. *Circulation*, 108(8):939–944.

Sevivas, T., Bastida, J. M., Paul, D. S., Caparros, E., Palma-Barqueros, V., Coucelo, M., Marques, D., Ferrer-Marín, F., González-Porras, J. R., Vicente, V., Hernández-Rivas, J. M., Watson, S. P., Lozano, M. L., Bergmeier, W., and Rivera, J. (2017). Identification of two novel mutations in RASGRP2 affecting platelet CalDAG-GEFI expression and function in patients with bleeding diathesis. *Platelets*, Aug 1:1-4. doi: 10.1080/09537104.2017.1336214. [Epub ahead of print].

Shen, Z., Lin, C. T., and Unkeless, J. C. (1994). Correlations among tyrosine phosphorylation of Shc, p72syk, PLC-gamma 1, and $[Ca^{2+}]_i$ flux in Fc gamma RIIA signaling. *Journal of immunology*, 152(6):3017–3023.

Shenker, A., Goldsmith, P., Unson, C. G., and Spiegel, A. M. (1991). The G protein coupled to the thromboxane A_2 receptor in human platelets is a member of the novel G_q family. *Journal of Biological Chemistry*, 266(14):9309–9313.

Smethurst, P. A., Onley, D. J., Jarvis, G. E., O'Connor, M. N., Knight, C. G., Herr, A. B., Ouwehand, W. H., and Farndale, R. W. (2006). Structural basis for the platelet-collagen interaction: The smallest motif within collagen that recognizes and activates platelet Glycoprotein VI contains two glycine-proline-hydroxyproline triplets. *Journal of Biological Chemistry*, 282(2):1296–1304.

Smyth, S. S., Mcever, R. P., Weyrich, A. S., Morrell, C. N., Hoffman, M. R., Arepally, G. M., French, P. A., Dauerman, H. L., and Becker, R. C. (2009). Platelet functions beyond hemostasis. *Journal of Thrombosis and Haemostasis*, 7:1759–1766.

Song, H. R., Jung, Y. E., Wang, H. R., Woo, Y. S., Jun, T. Y., and Bahk, W. M. (2012). Platelet count alterations associated with escitalopram, venlafaxine and bupropion in depressive patients. *Psychiatry and Clinical Neurosciences*, 66(5):457–459.

Soomro, G., Altman, D., Rajagopal, S., and Oakley-Browne, M. (2009). Selective serotonin re-uptake inhibitors (SSRIs) versus placebo for obsessive compulsive disorder (OCD). *Cochrane database of systematic reviews (Online)*, 1(1):1–65.

Sørensen, H. T., Mellemkjaer, L., Blot, W. J., Nielsen, G. L., Steffensen, F. H., McLaughlin, J. K., and Olsen, J. H. (2000). Risk of upper gastrointestinal bleeding associated with use of low-dose aspirin. *The American Journal of Gastroenterology*, 95(9):2218–2224.

Staatz, W. D., Walsh, J. J., and Santoros, S. A. (1990). The $\alpha_2\beta_1$ integrin cell surface collagen receptor binds to the α1(I)-CB3 peptide of collagen. *Journal of Biological Chemistry*, 265(9):4778–4781.

Steen, V. M., Holmsen, H., and Aarbakke, G. (1993). The platelet-stimulating effect of adrenaline through α_2-adrenergic receptors requires simultaneous activation by a true stimulatory platelet agonist. Evidence that adrenaline per se does not induce human platelet activation *in vitro*. *Thrombosis and Haemostasis*, 70(3):506–513.

Stefanini, L. and Bergmeier, W. (2010). CalDAG-GEFI and platelet activation. *Platelets*, 21(4):239–243.

Stefanini, L. and Bergmeier, W. (2016). RAP1-GTPase signaling and platelet function. *Journal of Molecular Medicine*, 94(1):13–19.

Stefanini, L., Boulaftali, Y., Ouellette, T. D., Holinstat, M., Désiré, L., Leblond, B., Andre, P., Conley, P. B., and Bergmeier, W. (2012). Rap1-Rac1 circuits potentiate platelet activation. *Arteriosclerosis, Thrombosis, and Vascular Biology*, 32(2):434–441.

Stefanini, L., Paul, D. S., Robledo, R. F., Chan, E. R., Getz, T. M., Campbell, R. A., Kechele, D. O., Casari, C., Piatt, R., Caron, K. M., Mackman, N., Weyrich, A. S., Parrott, M. C., Boulaftali, Y., Adams, M. D., Peters, L. L., and Bergmeier, W. (2015). RASA3 is a critical inhibitor of RAP1-dependent platelet activation. *The Journal of Clinical Investigation*, 125(4):1419–1432.

Stefanini, L., Roden, R. C., and Bergmeier, W. (2009). CalDAG-GEFI is at the nexus of calcium-dependent platelet activation. *Blood*, 114(12):2506–2514.

Steimer, J. L., Mallet, A., Golmard, J. L., and Boisvieux, J. F. (1984). Alternative approaches to estimation of population pharmacokinetic parameters: comparison with the nonlinear mixed-effect model. *Drug Metabolism Reviews*, 15:265–292.

Stewart, R. A. H., North, F. M., West, T. M., Sharples, K. J., Simes, R. J., Colquhoun, D. M., White, H. D., and Tonkin, A. M. (2003). Depression and cardiovascular morbidity and mortality: cause or consequence? *European Heart Journal*, 24(22):2027–2037.

Storey, R. F., Husted, S., Harrington, R. A., Heptinstall, S., Wilcox, R. G., Peters, G., Wickens, M., Emanuelsson, H., Gurbel, P., Grande, P., and Cannon, C. P. (2007). Inhibition of platelet aggregation by AZD6140, a reversible oral P2Y12 receptor antagonist, compared with clopidogrel in patients with acute coronary syndromes. *Journal of the American College of Cardiology*, 50(19):1852–1856.

Stratz, C., Trenk, D., Bhatia, H. S., Valina, C., Neumann, F. J., and Fiebich, B. L. (2008). Identification of 5-HT_3 receptors on human platelets: Increased surface immunoreactivity after activation with adenosine diphosphate (ADP) and thrombin receptor-activating peptide (TRAP). *Thrombosis and Haemostasis*, 99(4):784–786.

Strümper, D., Durieux, M. E., Hollmann, M. W., Tröster, B., den Bakker, C. G., and Marcus, M. A. E. (2003). Effects of antidepressants on function and viability of human neutrophils. *Anesthesiology*, 98(6):1356–1362.

Subramanian, H., Zahedi, R. P., Sickmann, A., Walter, U., and Gambaryan, S. (2013). Phosphorylation of CalDAG-GEFI by protein kinase A prevents Rap1b activation. *Journal of Thrombosis and Haemostasis*, 11(8):1574–1582.

Sugidachi, A., Ogawa, T., Kurihara, A., Hagihara, K., Jakubowski, J. A., Hashimoto, M., Niitsu, Y., and Asai, F. (2007). The greater *in vivo* antiplatelet effects of prasugrel as compared to clopidogrel reflect more efficient generation of its active metabolite with similar antiplatelet activity to that of clopidogrel's active metabolite. *Journal of Thrombosis and Haemostasis*, 5(7):1545–1551.

Sun, Q. H., DeLisser, H. M., Zukowski, M. M., Paddock, C., Albelda, S. M., and Newman, P. J. (1996). Individually distinct Ig homology domains in PECAM-I regulate homophilic binding and modulate receptor affinity. *Journal of Biological Chemistry*, 271(19):11090–11098.

Suzuki-Inoue, K., Fuller, G. L. J., García, Á., Eble, J. A., Pöhlmann, S., Inoue, O., Gartner, T. K., Hughan, S. C., Pearce, A. C., Laing, G. D., Theakston, R. D. G., Schweighoffer, E., Zitzmann, N., Morita, T., Tybulewicz, V. L. J., Ozaki, Y., and Watson, S. P. (2006). A novel Syk-dependent mechanism of platelet activation by the C-type lectin receptor CLEC-2. *Blood*, 107(2):542–549.

Suzuki-Inoue, K., Kato, Y., Inoue, O., Mika, K. K., Mishima, K., Yatomi, Y., Yamazaki, Y., Narimatsu, H., and Ozaki, Y. (2007). Involvement of the snake toxin receptor CLEC-2, in podoplanin-mediated platelet activation, by cancer cells. *Journal of Biological Chemistry*, 282(36):25993–26001.

Suzuki-Inoue, K., Tulasne, D., Shen, Y., Bori-sanz, T., Inoue, O., Jung, S. M., Moroi, M., Andrews, R. K., Berndt, M. C., and Watson, S. P. (2002). Association of Fyn and Lyn with the proline-rich domain of glycoprotein VI regulates intracellular signaling. *Journal of Biological Chemistry*, 277(24):21561–21566.

Takayama, H., Hosaka, Y., Nakayama, K., Shirakawa, K., Naitoh, K., Matsusue, T., Shinozaki, M., Honda, M., Yatagai, Y., Kawahara, T., Hirose, J., Yokoyama, T., Kurihara, M., and Furusako, S. (2008). A novel antiplatelet antibody therapy that induces cAMP-dependent endocytosis of the GPVI/Fc receptor γ-chain complex. *The Journal of Clinical Investigation*, 118(5):1785–1795.

Taler, M., Gil-Ad, I., Lomnitski, L., Korov, I., Baharav, E., Bar, M., Zolokov, A., and Weizman, A. (2007). Immunomodulatory effect of selective serotonin reuptake inhibitors (SSRIs) on human T lymphocyte function and gene expression. *European Neuropsychopharmacology*, 17(12):774–780.

Tamir, A., Granot, Y., and Isakov, N. (1996). Inhibition of T lymphocyte activation by cAMP is associated with down-regulation of two parallel mitogen-activated protein kinase pathways, the extracellular signal-related kinase and c-Jun N-terminal kinase. *The Journal of Immunology*, 157:1514–1522.

Tata, L. J., West, J., Smith, C., Farrington, P., Card, T., Smeeth, L., and Hubbard, R. (2005). General population based study of the impact of tricyclic and selective serotonin reuptake inhibitor antidepressants on the risk of acute myocardial infarction. *Heart*, 91(4):465–471.

Tatsumi, M., Groshan, K., Blakely, R. D., and Richelson, E. (1997). Pharmacological profile of antidepressants and related compounds at human monoamine transporters. *European Journal of Pharmacology*, 340:249–258.

Taylor, L., Vasudevan, S. R., Jones, C. I., Gibbins, J. M., Churchill, G. C., Campbell, R. D., and Coxon, C. H. (2014). Discovery of novel GPVI receptor antagonists by structure-based repurposing. *PLoS ONE*, 9(6):e101209.

Teryshnikova, S., Yan, X., and Fein, A. (1998). cGMP inhibits IP_3-induced Ca^{2+} release in intact rat megakaryocytes via cGMP- and cAMP-dependent protein kinases. *Journal of Physiology*, 512:89–96.

Thompson, N. T., Scrutton, M. C., and Wallis, R. B. (1986). Synergistic responses in human platelets. *European Journal of Biochemistry*, 161:399–408.

Tomazella, G. G., da Silva, I., Laure, H. J., Rosa, J. C., Chammas, R., Wiker, H. G., de Souza, G. A., and Greene, L. J. (2009). Proteomic analysis of total cellular proteins of human neutrophils. *Proteome Science*, 7:32.

Topiol, S., Bang-Andersen, B., Sanchez, C., Plenge, P., Loland, C. J., Juhl, K., Larsen, K., Bregnedal, P., and Bogeso, K. P. (2017). X-ray structure based evaluation of analogs of citalopram: compounds with increased affinity and selectivity compared with R-citalopram for the allosteric site (S2) on hSERT. *Bioorganic and Medicinal Chemistry Letters*, 27(3):470–478.

Traut, T. W. (1994). Physiological concentrations of purines and pyrimidines. *Molecular and Cellular Biochemistry*, 140(1):1–22.

Tricoci, P., Huang, Z., Held, C., Moliterno, D. J., Armstrong, P. W., Van de Werf, F., White, H. D., Aylward, P. E., Wallentin, L., Chen, E., Lokhnygina, Y., Pei, J., Leonardi, S., Rorick, T. L., Kilian, A. M., Jennings, L. H., Ambrosio, G., Bode, C., Cequier, A., Cornel, J. H., Diaz, R., Erkan, A., Huber, K., Hudson, M. P., Jiang, L., Jukema, J. W., Lewis, B. S., Lincoff, A. M., Montalescot, G., Nicolau, J. C., Ogawa, H., Pfisterer, M., Prieto, J. C., Ruzyllo, W., Sinnaeve, P. R., Storey, R. F., Valgimigli, M., Whellan, D. J., Widimsky, P., Strony, J., Harrington, R. a., and Mahaffey, K. W. (2012). Thrombin-receptor antagonist vorapaxar in acute coronary syndromes. *New England Journal of Medicine*, 366(1):20–33.

Tseng, Y. L., Chiang, M. L., Huang, T. F., Su, K. P., Lane, H. Y., and Lai, Y. C. (2010). A selective serotonin reuptake inhibitor, citalopram, inhibits collagen-induced platelet aggregation and activation. *Thrombosis Research*, 126(6):517–523.

Tseng, Y. L., Chiang, M. L., Lane, H. Y., Su, K. P., and Lai, Y. C. (2013). Selective serotonin reuptake inhibitors reduce P2Y12 receptor-mediated amplification of platelet aggregation. *Thrombosis Research*, 131(4):325–332.

Tsuji, M., Ezumi, Y., Arai, M., and Hiroshi, T. (1997). A novel association of Fc receptor γ-chain with glycoprotein VI and their co-expression as a collagen receptor in human platelets. *Journal of Biological Chemistry*, 272(38):23528–23531.

Turner, M., Schweighoffer, E., Colucci, F., Di Santo, J. P., and Tybulewicz, V. L. (2000). Tyrosine kinase SYK: essential functions for immunoreceptor signalling. *Immunology Today*, 21(3):148–154.

Tytgat, G. A., van den Brug, M. D., Voute, P. A., Smets, L. A., and Rutgers, M. (2002). Human megakaryocytes cultured *in vitro* accumulate serotonin but not meta-iodobenzylguanidine whereas platelets concentrate both. *Experimental Hematology*, 30(6):555–563.

Underhill, D. M. and Goodridge, H. S. (2007). The many faces of ITAMs. *Trends in Immunology*, 28(2):66–73.

Ungerer, M., Rosport, K., Bültmann, A., Piechatzek, R., Uhland, K., Schlieper, P., Gawaz, M., and Münch, G. (2011). Novel antiplatelet drug revacept (dimeric glycoprotein VI-Fc) specifically and efficiently inhibited collagen-induced platelet aggregation without affecting general hemostasis in humans. *Circulation*, 123(17):1891–1899.

Vaishnavi, S. N., Nemeroff, C. B., Plott, S. J., Rao, S. G., Kranzler, J., and Owens, M. J. (2004). Milnacipran: a comparative analysis of human monoamine uptake and transporter binding affinity. *Biological Psychiatry*, 55:320–322.

van Eeuwijk, J. M., Stegner, D., Lamb, D. J., Kraft, P., Beck, S., Thielmann, I., Kiefer, F., Walzog, B., Stoll, G., and Nieswandt, B. (2016). The novel oral Syk inhibitor, Bl1002494, protects mice from arterial thrombosis and thromboinflammatory brain infarction. *Arteriosclerosis, Thrombosis, and Vascular Biology*, 36(6):1247–1253.

van Giezen, J. J. J., Nilsson, L., Berntsson, P., Wissing, B. M., Giordanetto, F., Tomlinson, W., and Greasley, P. J. (2009). Ticagrelor binds to human P2Y12 independently from ADP but antagonizes ADP-induced receptor signaling and platelet aggregation. *Journal of Thrombosis and Haemostasis*, 7(9):1556–1565.

van Walraven, C., Mamdani, M. M., Wells, P. S., and Williams, J. I. (2001). Inhibition of serotonin reuptake by antidepressants and retrospective cohort study. *British Medical Journal*, 323:1–6.

Varga-Szabo, D., Braun, A., and Nieswandt, B. (2009). Calcium signaling in platelets. *Journal of Thrombosis and Haemostasis*, 7:1057–1066.

Vicari, A. M., Monzani, M. L., Pellegatta, F., Ronchi, P., Galli, L., and Folli, F. (1994). Platelet calcium homeostasis is abnormal in patients with severe arteriosclerosis. *Arteriosclerosis and thrombosis*, 14:1420–1425.

von Kügelgen, I. (2006). Pharmacological profiles of cloned mammalian P2Y-receptor subtypes. *Pharmacology and Therapeutics*, 110(3):415–432.

von Moltke, L. L., Greenblatt, D. J., Grassi, J. M., Granda, B. W., Venkatakrishnan, K., Duan, S. X., Fogelman, S. M., Harmatz, J. S., and Shader, R. I. (1999). Citalopram and desmethylcitalopram *in vitro*: human cytochromes mediating transformation, and cytochrome inhibitory effects. *Biological Psychiatry*, 46(6):839–849.

Vu, T. K. H., Hung, D. T., Wheaton, V. I., and Coughlin, S. R. (1991). Molecular cloning of a functional thrombin receptor reveals a novel proteolytic mechanism of receptor activation. *Cell*, 64(6):1057–1068.

Wagner, C. L., Mascelli, M. A., Neblock, D. S., Weisman, H. F., Coller, B. S., and Jordan, R. E. (1996). Analysis of GPIIb/IIIa receptor number by quantification of 7E3 binding to human platelets. *Blood*, 88(3):907–914.

Walther, D. J. and Bader, M. (2003). A unique central tryptophan hydroxylase isoform. *Biochemical Pharmacology*, 66(9):1673–1680.

Walther, D. J., Peter, J. U., Winter, S., Höltje, M., Paulmann, N., Grohmann, M., Vowinckel, J., Alamo-Bethencourt, V., Wilhelm, C. S., Ahnert-Hilger, G., and Bader, M. (2003). Serotonylation of small GTPases is a signal transduction pathway that triggers platelet α-granule release. *Cell*, 115(7):851–862.

Watanabe, D., Hashimoto, S., Ishiai, M., Matsushita, M., Baba, Y., Kishimoto, T., Kurosaki, T., and Tsukada, S. (2001). Four tyrosine residues in phospholipase C-γ2, identified as Btk-dependent phosphorylation sites, are required for B cell antigen receptor-coupled calcium signaling. *Journal of Biological Chemistry*, 276(42):38595–38601.

Westbury, S. K., Canault, M., Greene, D., Bermejo, E., Hanlon, K., Lambert, M. P., Millar, C. M., Nurden, P., Obaji, S. G., Revel-Vilk, S., Van Geet, C., Downes, K., Papadia, S., Tuna, S., Watt, C., Consortium, N. B.-R. D., Freson, K., Laffan, M. A., Ouwehand, W. H., Alessi, M.-C., Turro, E., and Mumford, A. D. (2017). Expanded repertoire of RASGRP2 variants responsible for platelet dysfunction and severe bleeding. *Blood*, 130(8):1026–1030.

Wheatcroft, J., Wakelin, D., Smith, A., Mahoney, C. R., Mawe, G., and Spiller, R. (2005). Enterochromaffin cell hyperplasia and decreased serotonin transporter in a mouse model of postinfectious bowel dysfunction. *Neurogastroenterology and Motility*, 17(6):863–870.

Wilde, J. I. and Watson, S. P. (2001). Regulation of phospholipase C γ isoforms in haematopoietic cells Why one, not the other? *Cellular Signalling*, 13:691–701.

Wilhite, D. B., Comerota, A. J., Schmieder, F. A., Throm, R. C., Gaughan, J. P., and Rao, A. K. (2003). Managing PAD with multiple platelet inhibitors: the effect of combination therapy on bleeding time. *Journal of Vascular Surgery*, 38(4):710–713.

Wilkins, E., Wilson, L., Wickramasinghe, K., Bhatnagar, P., Leal, J., Luengo-Fernandez, R., Burns, R., Rayner, M., and Townsend, N. (2017). European cardiovascular disease statistics 2017 [pdf]. Available at: http://www.ehnheart.org/cvd-statistics/cvd-statistics-2017.html. Accessed: 24/10/2017. Technical report, European Heart Network, Brussels, Belgium.

Wittchen, E. S., Worthylake, R. A., Kelly, P., Casey, P. J., Quilliam, L. A., and Burridge, K. (2005). Rap1 GTPase inhibits leukocyte transmigration by promoting endothelial barrier function. *Journal of Biological Chemistry*, 280(12):11675–11682.

Wong, P. C., Seiffert, D., Bird, J. E., Watson, C. A., Bostwick, J. S., Giancarli, M., Allegretto, N., Hua, J., Harden, D., Guay, J., Callejo, M., Miller, M. M., Lawrence, R. M., Banville, J., Guy, J., Maxwell, B. D., Priestley, E. S., Marinier, A., Wexler, R. R., Bouvier, M., Gordon, D. A., Schumacher, W. A., and Yang, J. (2017). Blockade of protease-activated receptor-4 (PAR4) provides robust antithrombotic activity with low bleeding. *Science Translational Medicine*, 9(371):1–11.

Xia, Z., DePierre, J. W., and Nässberger, L. (1996). Tricyclic antidepressants inhibit IL-6, IL-1β and TNF-α release in human blood monocytes and IL-2 and interferon-γ in T cells. *Immunopharmacology*, 34(1):27–37.

Xu, W., Tamim, H., Shapiro, S., Stang, M. R., and Collet, J.-P. (2006). Use of antidepressants and risk of colorectal cancer: a nested case-control study. *Lancet Oncology*, 7(4):301–308.

Yagasaki, Y., Numakawa, T., Kumamaru, E., Hayashi, T., Su, T. P., and Kunugi, H. (2006). Chronic antidepressants potentiate via sigma-1 receptors the brain-derived neurotrophic factor-induced signaling for glutamate release. *Journal of Biological Chemistry*, 281(18):12941–12949.

Yager, S., Forlenza, M. J., and Miller, G. E. (2010). Depression and oxidative damage to lipids. *Psychoneuroendocrinology*, 35(9):1356–1362.

Yamashita, A., Singh, S. K., Kawate, T., Jin, Y., and Gouaux, E. (2005). Crystal structure of a bacterial homologue of Na^+/Cl^--dependent neurotransmitter transporters. *Nature*, 437:215–223.

Yanaga, F., Poole, A., Asselin, J., Blake, R., Schieven, G. L., Clark, E. A., Law, C. L., and Watson, S. P. (1995). Syk interacts with tyrosine-phosphorylated proteins in human platelets activated by collagen and cross-linking of the Fcγ-IIA receptor. *The Biochemical Journal*, 311:471–478.

Yang, J., Wu, J., Kowalska, M. A., Dalvi, A., Prevost, N., O'Brien, P. J., Manning, D., Poncz, M., Lucki, I., Blendy, J. A., and Brass, L. F. (2000). Loss of signaling through the G protein, G_z, results in abnormal platelet activation and altered responses to psychoactive drugs. *Proceedings of the National Academy of Sciences of the United States of America*, 97(18):9984–9989.

Yang, M., Li, K., Ng, P. C., Chuen, C. K. Y., Lau, T. K., Cheng, Y. S., Liu, Y. S., Li, C. K., Yuen, P. M. P., James, A. E., Lee, S. M., and Fok, T. F. (2007). Promoting effects of serotonin on hematopoiesis: *ex vivo* expansion of cord blood $CD34^+$ stem/progenitor cells, proliferation of bone marrow stromal cells, and antiapoptosis. *Stem cells*, 25(7):1800–1806.

Yang, M., Srikiatkhachorn, A., Anthony, M., and Chong, B. H. (1996). Serotonin stimulates megakaryocytopoiesis via the 5-HT_2 receptor. *Blood Coagulation & Fibrinolysis*, 7(2):127–133.

Yeung, P. K., Pollak, P., Jamieson, A., Smith, G. J., and Fice, D. (2000). Determination of plasma concentrations of losartan in patients by HPLC using solid phase extraction and UV detection. *International Journal of Pharmaceutics*, 204(1-2):17–22.

Zarpellon, A., Donella-Deana, A., Folda, A., Turetta, L., Pavanetto, M., and Deana, R. (2008). Serotonin (5-HT) transport in human platelets is modulated by Src-catalysed Tyr-phosphorylation of the plasma membrane transporter SERT. *Cellular Physiology and Biochemistry*, 21(1-3):87–94.

Zhang, S. L., Yu, Y., Roos, J., Kozak, J. A., Deerinck, T. J., Ellisman, M. H., Stauderman, K. A., and Cahalan, M. D. (2005). STIM1 is a Ca^{2+} sensor that activates CRAC channels and migrates from the Ca^{2+} store to the plasma membrane. *Nature*, 437:902–905.

Zhang, W., Sloan-Lancaster, J., Kitchen, J., Trible, R. P., and Samelson, L. E. (1998). LAT: The ZAP-70 tyrosine kinase substrate that links T cell receptor to cellular activation. *Cell*, 92:83–92.

Zhang, X., Beaulieu, J., Sotnikova, D., Gainetdinov, R., and Caron, M. (2004). Tryptophan hydroxylase-2 controls brain serotonin synthesis. *Science*, 305:217–217.

Zheng, Y. M., Liu, C., Chen, H., Locke, D., Ryan, J. C., and Kahn, M. L. (2001). Expression of the platelet receptor GPVI confers signaling via the Fc receptor γ-chain in response to the snake venom convulxin but not to collagen. *Journal of Biological Chemistry*, 276(16):12999–13006.

Zhong, H., Haddjeri, N., and Sánchez, C. (2012). Escitalopram, an antidepressant with an allosteric effect at the serotonin transporter-a review of current understanding of its mechanism of action. *Psychopharmacology*, 219(1):1–13.

Zhou, F. C., Lesch, K. P., and Murphy, D. L. (2002). Serotonin uptake into dopamine neurons via dopamine transporters: a compensatory alternative. *Brain Research*, 942(1-2):109–119.

Zhu, C. B., Hewlett, W. A., Feoktistov, I., Biaggioni, I., and Blakely, R. D. (2004). Adenosine receptor, protein kinase G, and p38 mitogen-activated protein kinase-dependent up-regulation of serotonin transporters involves both transporter trafficking and activation. *Molecular Pharmacology*, 5(10):1462–1474.

Appendix A
Western blots

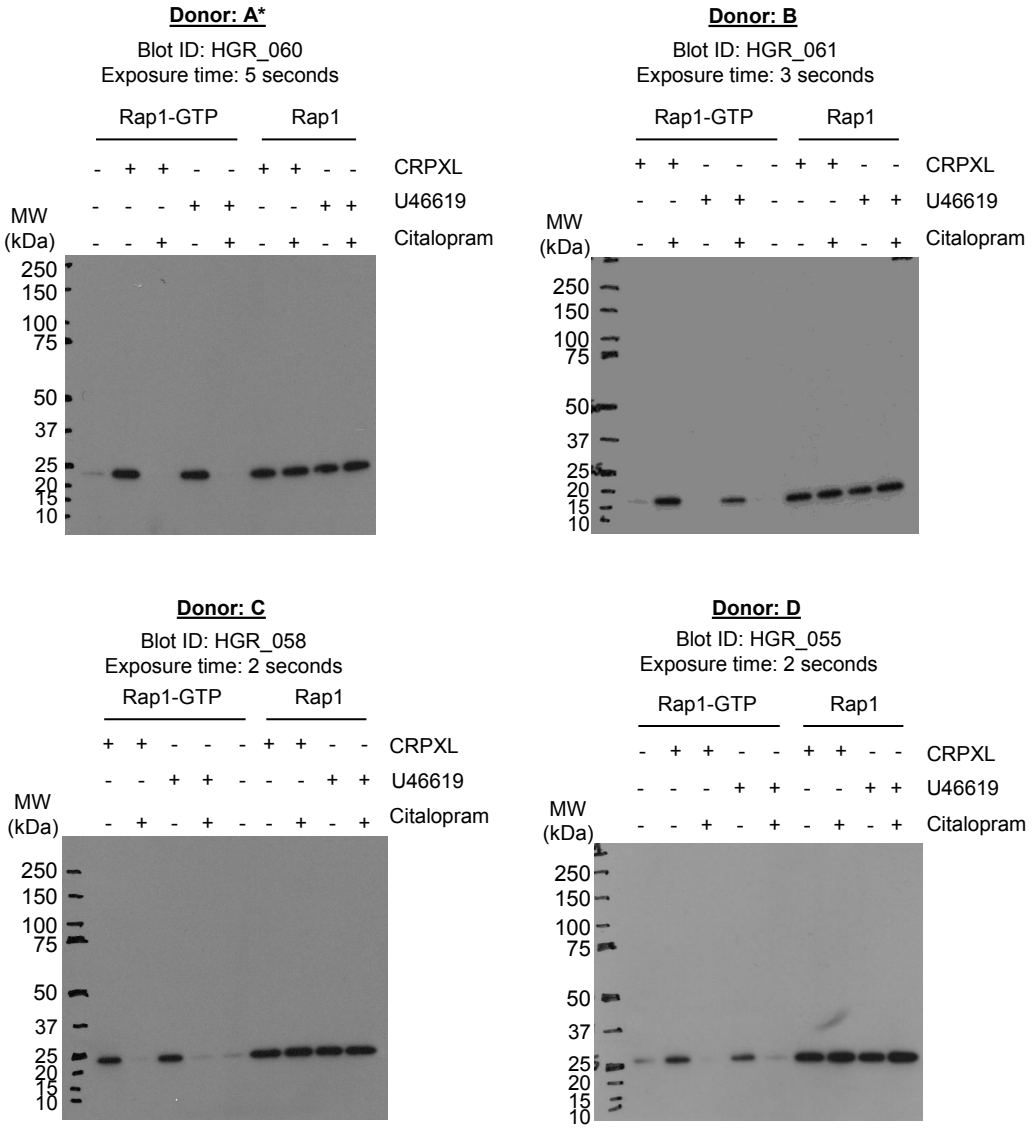

Figure. A.1 Unprocessed images of X-ray films from Western blots used to quantify Rap1-GTP and Rap1 levels from platelet lysates. Platelets were either untreated or treated with racemic citalopram (200 μM) for approximately 5 minutes, then either unstimulated or stimulated with cross-linked collagen-related peptide (CRPXL, 0.5 μg mL^{-1}) or U46619 (0.2 μM). Samples from 4 blood donors were used in total, labelled A-D. Samples were not randomised. *Indicates the blot presented in Figure 4.6. X-ray film exposure times are shown underneath each blot identification (ID).

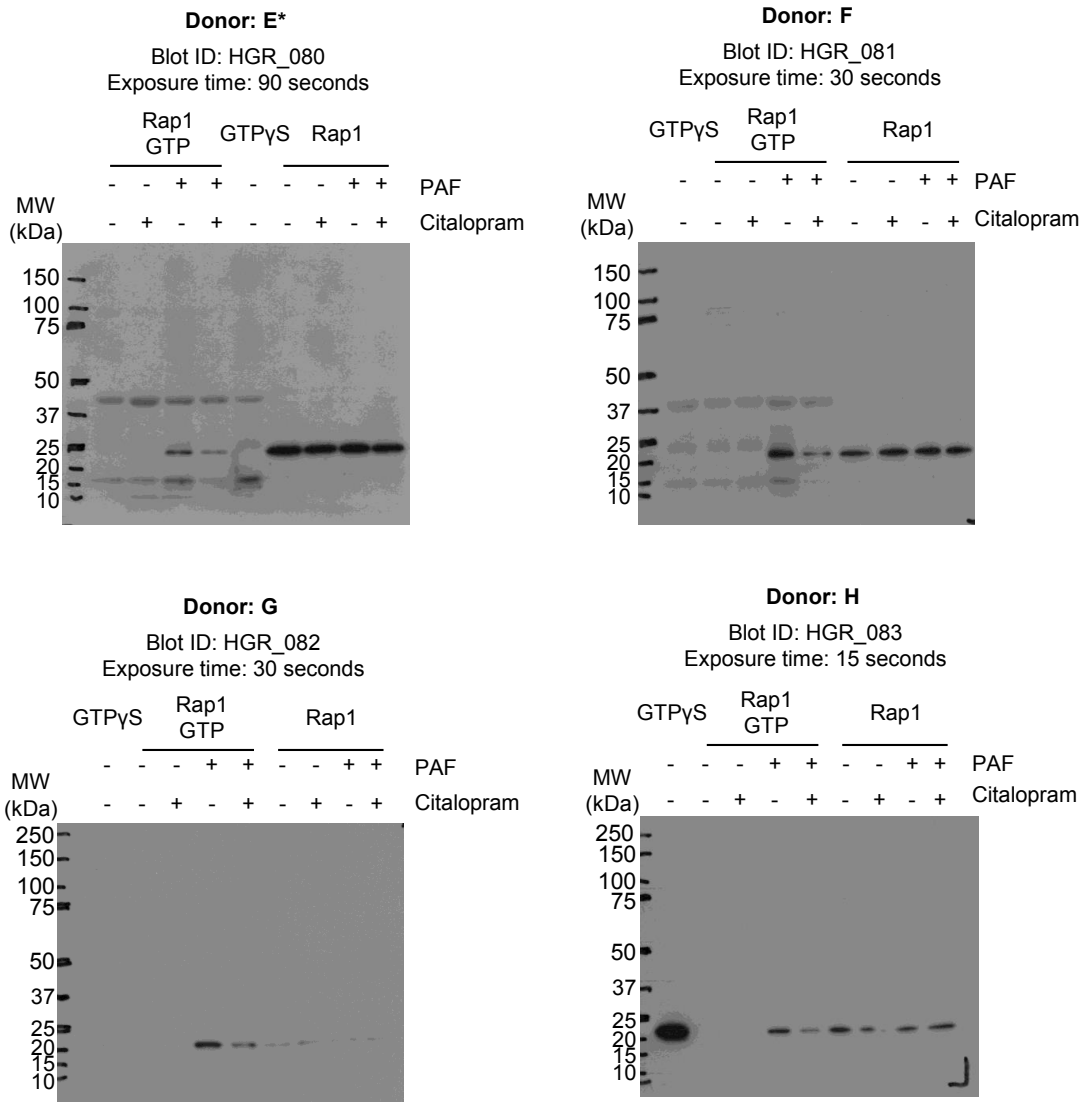

Figure. A.2 Unprocessed images of X-ray films from Western blots used to quantify Rap1-GTP and Rap1 levels from neutrophil lysates. Neutrophils were either untreated or treated with racemic citalopram (200 μM) for approximately 5 minutes, then either unstimulated or stimulated with platelet-activating factor (PAF, 1 μM). Samples from 4 blood donors were used in total, labelled E-H. For an optional positive control, lysates were incubated with GTPγS. However, due to a lack of exogenous $MgCl_2$ in samples from donors E, F & G, GTPγS-loaded samples showed low levels of binding. *Indicates the blot presented in Figure 4.7. Bands with a molecular weight of $\approx$ 40 kDa are likely to represent the GST-RalGDS-RBD fusion protein. X-ray film exposure times are those used for quantification of Rap1-GTP and differ from the exposure times used to quantify total Rap1 levels (donor E = 45 seconds, F = 60 seconds, G = 60 seconds & H = 30 seconds). Marks on the bottom right corner of Blot ID: HGR_083 indicate the outline of the polyvinylidene difluoride (PVDF) membrane.

Donor: A

Blot ID: HGR_040

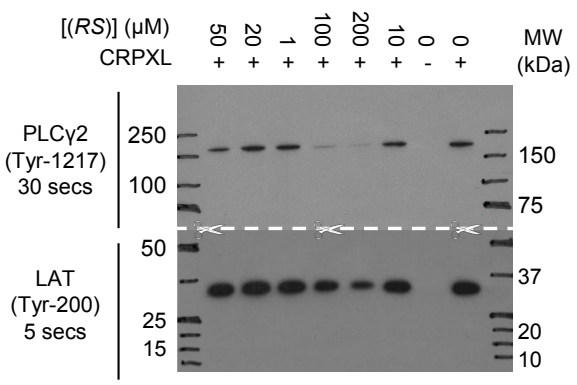

Blot ID: HGR_041

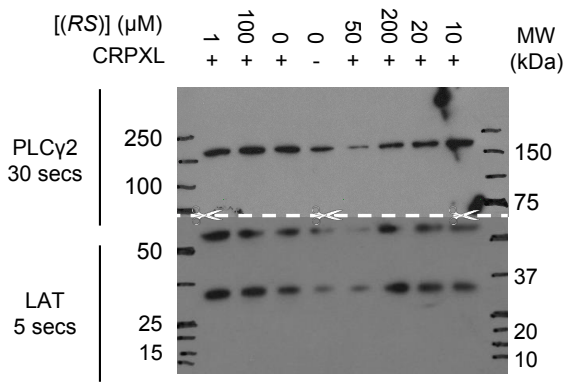

Donor: B

Blot ID: HGR_044

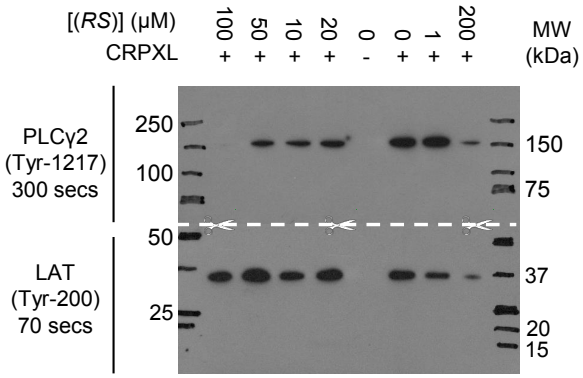

Blot ID: HGR_045

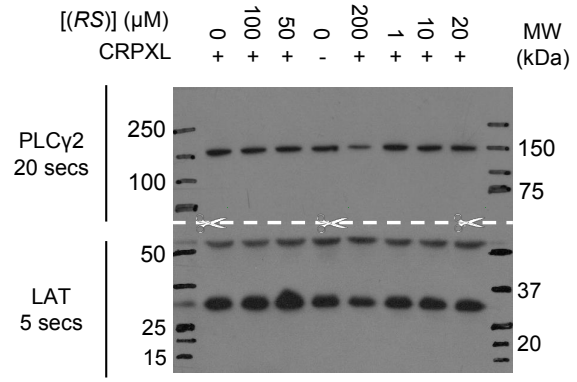

Donor: C

Blot ID: HGR_048

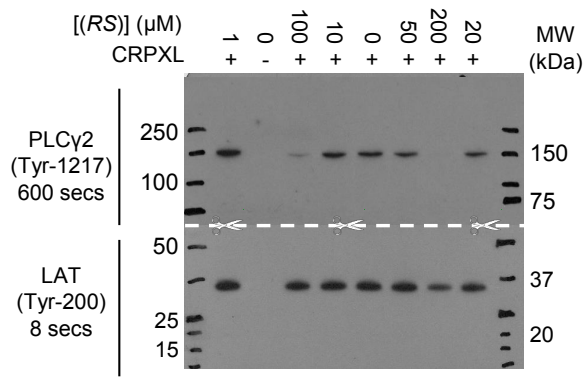

Blot ID: HGR_049

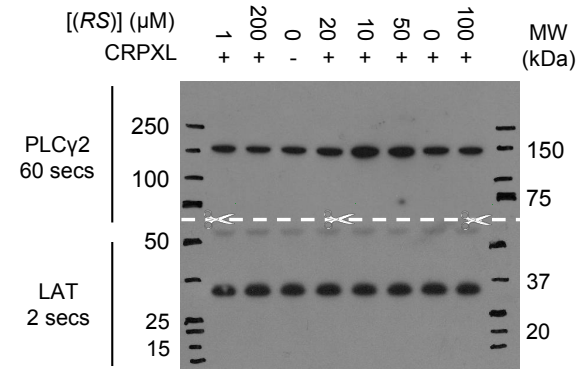

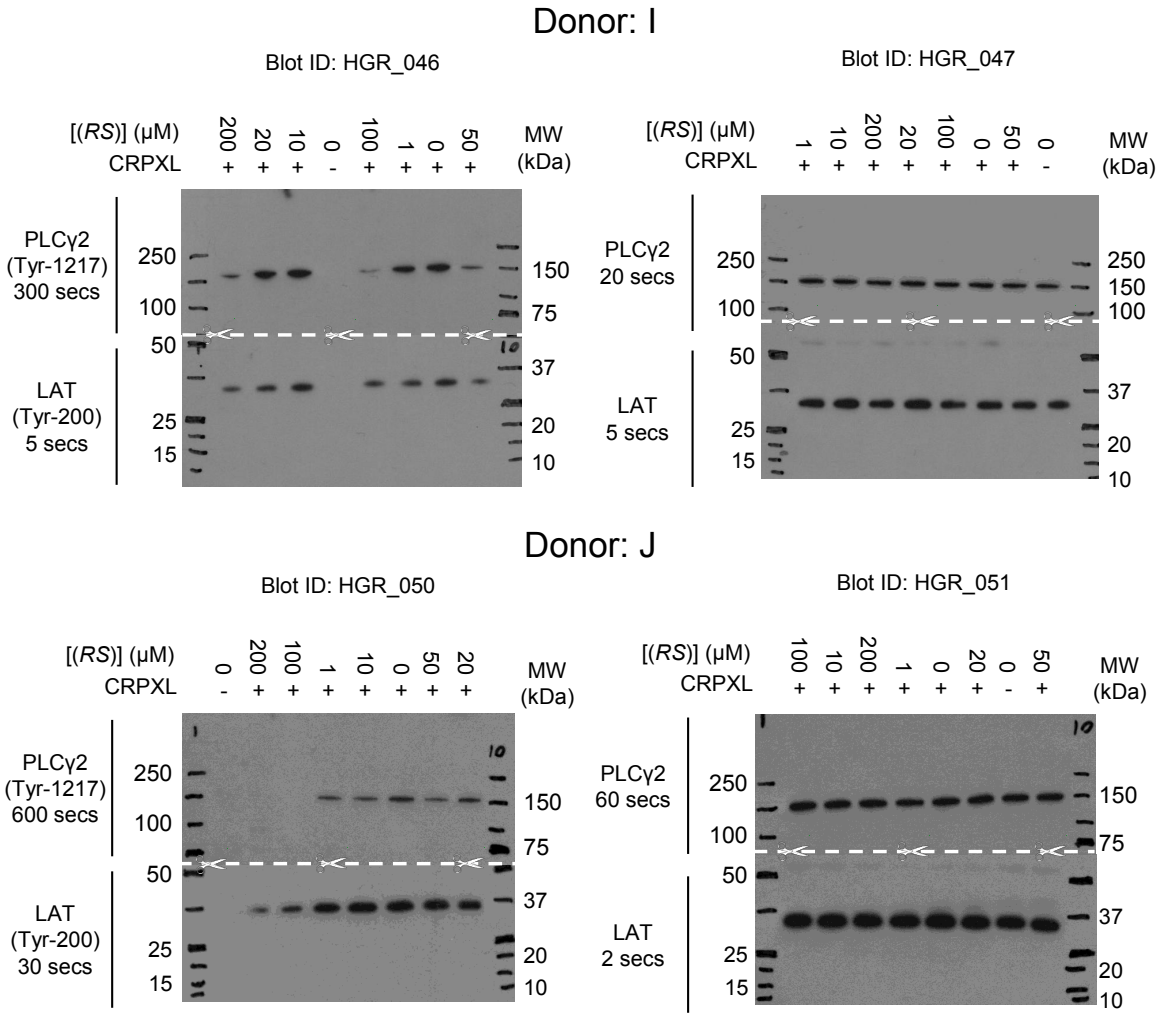

Figure. A.3 Unprocessed images of X-ray films of Western blots used for the quantification of phospho-PLCγ2 (Tyr-1217), phospho-LAT (Tyr-200), PLCγ2, and LAT. 5 blood donors were used in total, labelled A, B, C, I & J. Donors A, B and C were the same donors previously used in Figure A.1. White scissors and dashed white lines indicate where membranes were cut for subsequent blotting with different antibodies for either PLCγ2 or LAT. Samples were randomised and allocated into wells 2-9 in a blinded fashion. Different X-ray film exposure times were taken for each blot and those generating the greatest contrast are presented in this figure and were used for quantification. Exposure times (in seconds) and the primary antibody are shown on the left of each blot. [(*RS*)] indicates the concentration of racemic (*RS*)-citalopram. CRPXL = cross-linked collagen-related peptide (5 μg mL^{-1}).

Donor: A

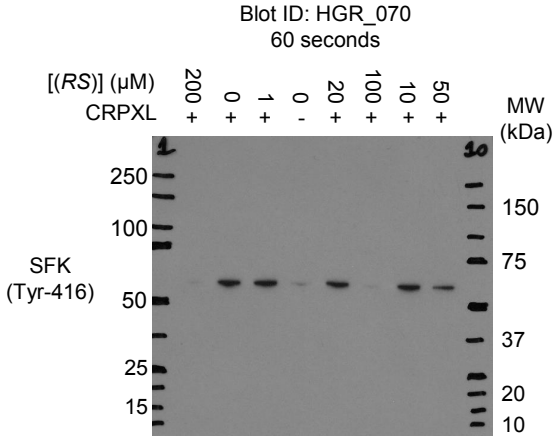

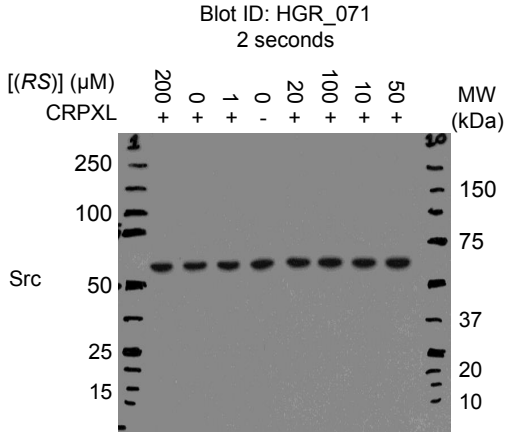

Donor: B

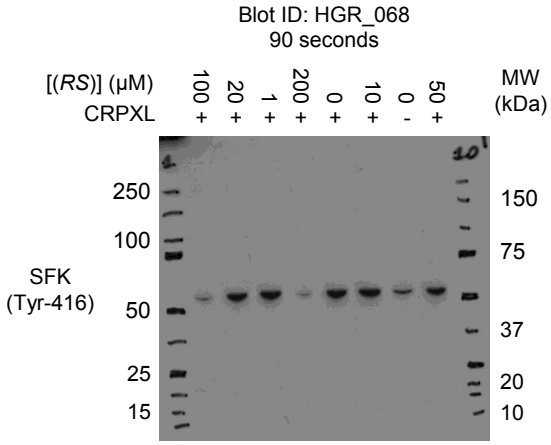

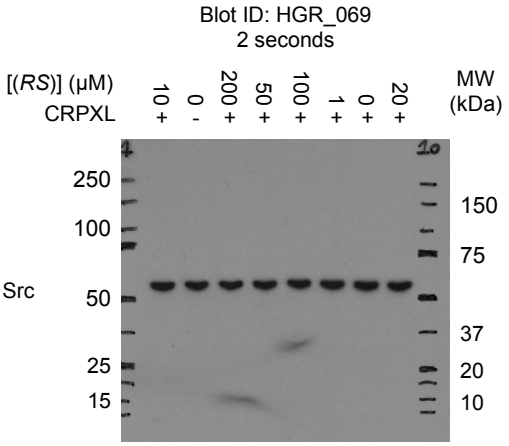

Donor: C

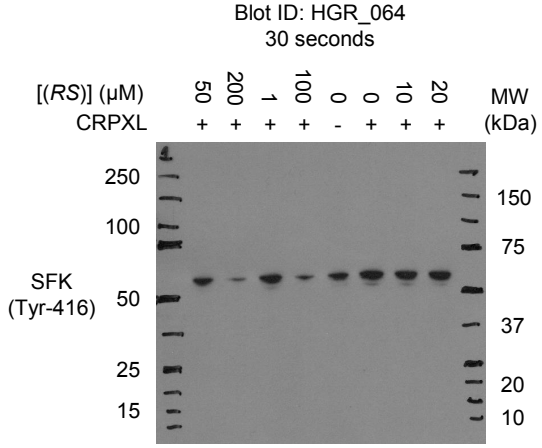

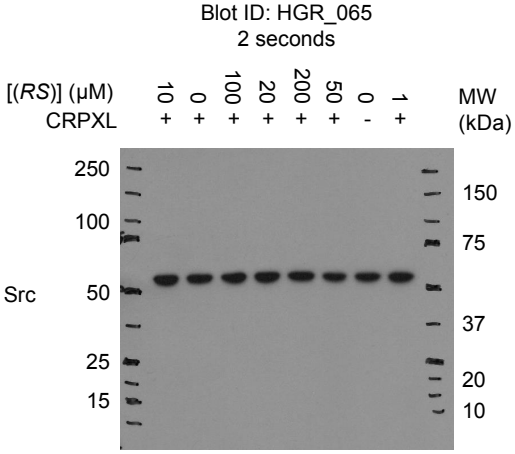

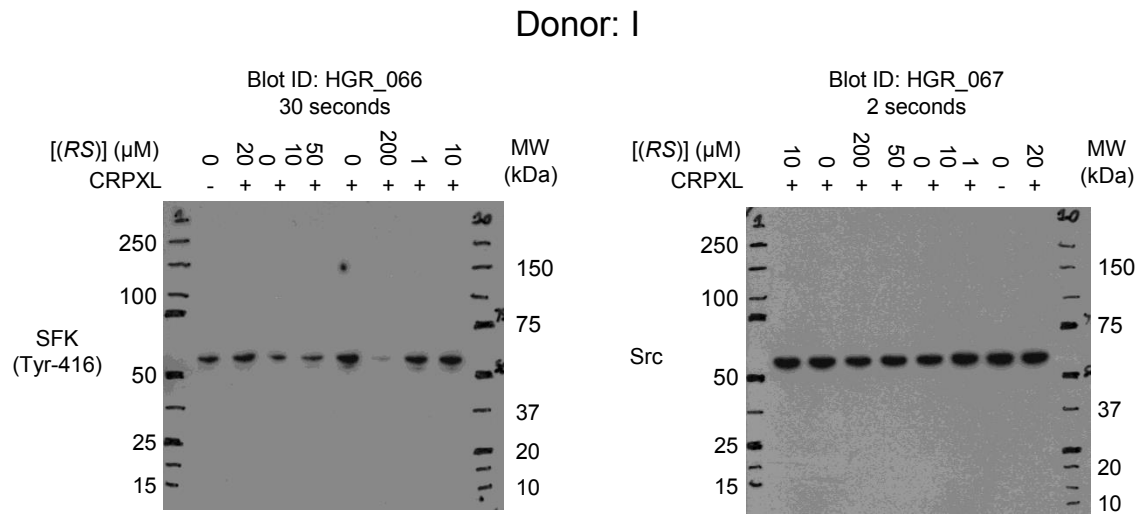

Figure. A.4 Unprocessed images of X-ray films from Western blots used to quantify phospho-Src family kinases (SFK) (Tyr-416) and Src. Samples from 4 blood donors were used in total, labelled A, B, C & I, which were the same donors previously used in Figure A.1 & A.2. No data were obtained for donor J as there was insufficient material from this donor for all conditions when the analysis was performed. Samples were randomised and allocated into wells 2-9 in a blinded fashion. Different X-ray film exposure times were taken for each blot and those generating the greatest contrast are presented in this figure and were used for quantification. Exposure times are shown underneath each blot identification (ID). The primary antibody is shown to the left of each blot. [(*RS*)] represents the concentration of racemic (*RS*)-citalopram. CRPXL = cross-linked collagen-related peptide (5 μg mL^{-1})

Appendix B
Protein sequences

CalDAG-GEFI/RASGRP2 (wild type) (UniProtKB-Q7LDG7)
MAGTLDLDKGCTVEELLRGCIEAFDDSGKVRDPQLVRMFLMMHPWYIPSSQLAAKLLHIYQQSRKDNSNSLQVKTCHLVRYWISAFPAEFDLNPELAEQIKELK
ALLDQEGNRRHSSLIDIDSVPTYKWKRQVTQRNPVGQKKRKMSLLFDHLEPMELAEHLTYLEYRSFCKILFQDYHSFVTHGCTVDNPVLERFISLFNSVSQWVQ
LMILSKPTAPQRALVITHFVHVAEKLLQLQNFNTLMAVVGGLSHSSISRLKETHSHVSPETIKLWEGLTELVTATGNYGNYRRRLAACVGFRFPILGVHLKDLV
ALQLALPDWLDPARTRLNGAKMKQLFSILEELAMVTSLRPPVQANPDLLSLLTVSLDQYQTEDELYQLSLQREPRSKSSPTSPTSCTPPPRPPVLEEWTSAAKP
KLDQALVVEHIEKMVESVFRNFDVDGDGHISQEEFQIIRGNFPYLSAFGDLDQNQDGCISREEMVSYFLRSSSVLGGRMGFVHNFQESNSLRPVACRHCKALIL
GIYKQGLKCRACGVNCHKQCKDRLSVECRRRAQSVSLEGSAPSPSPMHSHHHRAFSFSLPRPGRRGSRPPEIREEEVQTVEDGVFDIHL

CalDAG-GEFI/RASGRP2
p.(Ala552_Leu609del)
MAGTLDLDKGCTVEELLRGCIEAFDDSGKVRDPQLVRMFLMMHPWYIPSSQLAAKLLHIYQQSRKDNSNSLQVKTCHLVRYWISAFPAEFDLNPELAEQIKELK
ALLDQEGNRRHSSLIDIDSVPTYKWKRQVTQRNPVGQKKRKMSLLFDHLEPMELAEHLTYLEYRSFCKILFQDYHSFVTHGCTVDNPVLERFISLFNSVSQWVQ
LMILSKPTAPQRALVITHFVHVAEKLLQLQNFNTLMAVVGGLSHSSISRLKETHSHVSPETIKLWEGLTELVTATGNYGNYRRRLAACVGFRFPILGVHLKDLV
ALQLALPDWLDPARTRLNGAKMKQLFSILEELAMVTSLRPPVQANPDLLSLLTVSLDQYQTEDELYQLSLQREPRSKSSPTSPTSCTPPPRPPVLEEWTSAAKP
KLDQALVVEHIEKMVESVFRNFDVDGDGHISQEEFQIIRGNFPYLSAFGDLDQNQDGCISREEMVSYFLRSSSVLGGRMGFVHNFQESNSLRPVACRHCKALIL
GIYKQGLKCRACGVNCHKQCKDRLSVECRRR

CalDAG-GEFI/RASGRP2
p.(Ala552_Leu609del)
p.(Arg387_Pro404)
MAGTLDLDKGCTVEELLRGCIEAFDDSGKVRDPQLVRMFLMMHPWYIPSSQLAAKLLHIYQQSRKDNSNSLQVKTCHLVRYWISAFPAEFDLNPELAEQIKELK
ALLDQEGNRRHSSLIDIDSVPTYKWKRQVTQRNPVGQKKRKMSLLFDHLEPMELAEHLTYLEYRSFCKILFQDYHSFVTHGCTVDNPVLERFISLFNSVSQWVQ
LMILSKPTAPQRALVITHFVHVAEKLLQLQNFNTLMAVVGGLSHSSISRLKETHSHVSPETIKLWEGLTELVTATGNYGNYRRRLAACVGFRFPILGVHLKDLV
ALQLALPDWLDPARTRLNGAKMKQLFSILEELAMVTSLRPPVQANPDLLSLLTVSLDQYQTEDELYQLSLQREP_____PVLEEWTSAAKP
KLDQALVVEHIEKMVESVFRNFDVDGDGHISQEEFQIIRGNFPYLSAFGDLDQNQDGCISREEMVSYFLRSSSVLGGRMGFVHNFQESNSLRPVACRHCKALIL
GIYKQGLKCRACGVNCHKQCKDRLSVECRRR

CalDAG-GEFI/RASGRP2
p.(Ala552_Leu609del)
p.(Gly248Trp)
MAGTLDLDKGCTVEELLRGCIEAFDDSGKVRDPQLVRMFLMMHPWYIPSSQLAAKLLHIYQQSRKDNSNSLQVKTCHLVRYWISAFPAEFDLNPELAEQIKELK
ALLDQEGNRRHSSLIDIDSVPTYKWKRQVTQRNPVGQKKRKMSLLFDHLEPMELAEHLTYLEYRSFCKILFQDYHSFVTHGCTVDNPVLERFISLFNSVSQWVQ
LMILSKPTAPQRALVITHFVHVAEKLLQLQNFNTLMAVV**W**GLSHSSISRLKETHSHVSPETIKLWEGLTELVTATGNYGNYRRRLAACVGFRFPILGVHLKDLV
ALQLALPDWLDPARTRLNGAKMKQLFSILEELAMVTSLRPPVQANPDLLSLLTVSLDQYQTEDELYQLSLQREPRSKSSPTSPTSCTPPPRPPVLEEWTSAAKP
KLDQALVVEHIEKMVESVFRNFDVDGDGHISQEEFQIIRGNFPYLSAFGDLDQNQDGCISREEMVSYFLRSSSVLGGRMGFVHNFQESNSLRPVACRHCKALIL
GIYKQGLKCRACGVNCHKQCKDRLSVECRRR

Rap1B (UniProtKB-Q7LDG7)
MREYKLVVLGSGGVGKSALTVQFVQGIFVEKYDPTIEDSYRKQVEVDAQQCMLEILDTAGTEQFTAMRDLYMKNGQGFALVYSITAQSTFNDLQDLREQILRVK
DTDDVPMILVGNKCDLEDERVVGKEQGQNLARQWNNCAFLESSAKSKINVNEIFYDLVRQINRKTPVPGKARKKSSCQLL

Rap1B
p.(Lys168_Leu184del)
MREYKLVVLGSGGVGKSALTVQFVQGIFVEKYDPTIEDSYRKQVEVDAQQCMLEILDTAGTEQFTAMRDLYMKNGQGFALVYSITAQSTFNDLQDLREQILRVK
DTDDVPMILVGNKCDLEDERVVGKEQGQNLARQWNNCAFLESSAKSKINVNEIFYDLVRQINR

Figure. B.1 Protein sequences for wild type and mutated CalDAG-GEFI and Rap1B. Recombinant calcium and diacylglycerol guanine nucleotide exchange factor-1 (CalDAG-GEFI) and Ras-related protein 1B (Rap1B) were provided by Professor Wolfgang Bergmeier and Aaron Cook, from the University of North Carolina. Aaron Cook cloned CalDAG-GEFI and Rap1B from human genes into a protein expression vector p15LIC2 6xHis, which was purified in *E. coli*. The CalDAG-GEFI variants provided all contained a C-terminal truncation (p.(Ala552_Leu609del)). The C-terminal of Rap1B was also truncated (p.(Lys168_Leu184del)). According to personal communication, this truncation "removed disordered regions to improve stability during the purification process, while leaving all the functional domains intact". Catalytically inactive CalDAG-GEFI variants contained either an additional deletion (p.(Arg387_Pro404del)), or a glycine-tryptophan substitution (p.(Gly248Trp)).

Appendix C
Publications and presentations

Published Manuscripts

- **Roweth HG**, Yan R, Bedwani NH, Chauhan A, Fowler N, Watson AH, Malcor JD, Sage SO and Jarvis GE. Citalopram inhibits platelet function independently of SERT-mediated 5-HT transport. *Scientific Reports*, volume 8, Article number: 3494 (2018), doi:10.1038/s41598-018-21348-3

Manuscripts under revision or in preparation

- **Roweth HG**, Sage SO, Farndale RW and Jarvis GE. The effects of antidepressants on platelet function. Manuscript in preparation (expected submission 03/2018)
- **Roweth HG**, Sage SO, Cook A, Bergmeier W, Harper MT, Malcor JD, Jung SM, Jarvis GE. Two novel, putative mechanisms of action for citalopram-induced platelet inhibition. Manuscript in preparation (expected submission, 03/2018)

Published abstracts, posters and oral presentations

- **Roweth HG** and Jarvis GE. Mechanisms of platelet inhibition by the selective serotonin reuptake inhibitor citalopram. Poster presention (P54) at The United Kingdom Platelet Meeting, 15-16th September, 2015; Leicester, United Kingdom
- **Roweth HG** and Jarvis GE. Mechanisms of platelet inhibition by the selective serotonin reuptake inhibitor citalopram. Poster presention (179P) at Pharmacology 2015; 15-17th December, 2015; London, United Kingdom
- **Roweth HG** and Jarvis GE. The effects of antidepressants on platelet function. Poster presention (P07) at the joint British Society for Haemostasis and Thrombosis, Anticoagulation in Practice and United Kingdom Platelet Group Meeting 2016, 9-11th November, 2016; Leeds, United Kingdom
- **Roweth HG**, Fowler N, Chauhan A and Jarvis GE. Putative, novel mechanisms of action for citalopram-induced platelet inhibition. Poster presentation at the Cell Biology of Megakaryocytes and Platelets Gordon Research Seminar, 25-26th February, 2017; Tuscany, Italy
- **Roweth HG**, Fowler N, Chauhan A and Jarvis GE. Mechanisms of platelet inhibition by the selective serotonin reuptake inhibitor citalopram. Oral presentation at the Physiology, Development and Neuroscience Research Symposium, 20-21st, April 2017; Cambridge, United Kingdom

- **Roweth HG**, Fowler N, Chauhan A, Bedwani NH, Sage SO, Farndale RW and Jarvis GE. Putative, novel mechanisms of action for citalopram-induced platelet inhibition. Oral presentation (OC 45.5) at the XXVI Congress of the International Society on Thrombosis and Haemostasis, 8-13th July, 2017; Berlin, Germany
- **Roweth HG**, Yan R, Watson AH, Farndale RW and Jarvis GE. Citalopram inhibits platelet function through a SERT-independent mechanism. Poster presentation (PB 2200) at the XXVI Congress of the International Society on Thrombosis and Haemostasis, 8-13th July, 2017; Berlin, Germany